Molecular characterization of the type II secretion system of the phytopathogenic bacterium Dickeya dadantii : structural and functional studies of the interaction of OutC and OutD

Xiaohui Wang

N° d'ordre : 2012-ISAL-0010 Année 2012

Thèse
Présentée devant
L'institut national des sciences appliquées de Lyon

Caractérisation moléculaire du système de sécrétion de type II de la bactérie phytopathogène *Dickeya dadantii*: études structurales et fonctionnelles sur l'interaction entre OutC et OutD

Pour obtenir
Le grade de docteur

École doctorale: Evolution, Ecosystèmes, Microbiologie, Modélisation
Spécialité: Microbiologie Moléculaire

Par
Xiaohui WANG

Directeur de thèse: Vladimir SHEVCHIK

Soutenue le 10 Février 2012 devant la Commission d'examen

Jury :

Président	Mr P. LEJEUNE	Professeur (INSA de Lyon)
Rapporteur	Mme O. FRANCETIC	Chargée de recherche (Institut Pasteur)
Rapporteur	Mme I. ATTREE	Directeur de recherche (CNRS)
Examinateur	Mr N. BAYAN	Professeur (Université Paris Sud XI)
Directeur de thèse	Mr V. SHEVCHIK	Directeur de recherche (CNRS)

Laboratoire de recherche: UMR 5240 Microbiologie, Adaptation et Pathogénie

N° d'ordre : 2012-ISAL-0010 Année 2012

Thèse
Présentée devant
L'institut national des sciences appliquées de Lyon

Molecular characterization of the type II secretion system of the phytopathogenic bacterium *Dickeya dadantii*: structural and functional studies of the interaction of OutC and OutD

Pour obtenir
Le grade de docteur

École doctorale: Evolution, Ecosystèmes, Microbiologie, Modélisation
Spécialité: Microbiologie Moléculaire

Par
Xiaohui WANG

Directeur de thèse: Vladimir SHEVCHIK

Soutenue le 10 Février 2012 devant la Commission d'examen

Jury :

Président	Mr P. LEJEUNE	Professeur (INSA de Lyon)
Rapporteur	Mme O. FRANCETIC	Chargée de recherche (Institut Pasteur)
Rapporteur	Mme I. ATTREE	Chargée de recherche (CNRS)
Examinateur	Mr N. BAYAN	Professeur (Université Paris Sud XI)
Directeur de thèse	Mr V. SHEVCHIK	Directeur de recherche (CNRS)

Laboratoire de recherche : UMR 5240 Microbiologie, Adaptation et Pathogénie

Acknowledgements

First of all, I would like to thank the members of thesis examination committee, *Dr. Ina Attree*, *Dr. Olivera Francetic*, *Dr. Nicolas Bayan* and *Prof. Philippe Lejeune* for acting as reviewers and examiners of this thesis.

I wish to express my deep gratitude to my supervisor *Dr. Vladimir Shevchik* for giving me the opportunity to realize this thesis in France. His ideas and tremendous support had a major influence on this thesis. He encouraged and supported me with much kindness over the past three and half years. By working with him, I learned a lot of scientific and technical knowledge and I am convinced that this knowledge will help me in the future.

Dr. Nicole Cotte-Pattat, director of the UMR5240, is acknowledged for welcoming me in her laboratory. I wish to extend a special thanks to *Dr. Guy Condemine* for his academic guidance and corrections of my manuscript while to *Dr. William Nasser* and *Dr. Sylvie Reverchon* for their continuous encouragements.

I would like to thank to *Dr. Mathilde Lallemand*, *Géraldine Effantin* and *Camille Villard* for their guidence of my experiments, especially *Mathilde*, she also gave me many helps in everyday life.

I wish to express my appreciation to *Véronique Utzinger*, *Yvette Alfaro* and *Jean-Michel Prost* and *Isabelle Goncalves*. Without their help of preparing the materials, the experimental work of this thesis could not be carried out on time.

I also wish to express my appreciation to my officemates, *Camille pineau*, *Arnaud Rondelet* and *Natalia Guschinskaya*, who provided useful advices in this thesis and gave many helps, especially for the help on French language.

I also had the pleasure of becoming friends and colleagues with *Suzan Hassan*, *Ouafa Zghidi-Abouzid*, *Sana Boukerzaza-Cmaraovi*, *Xuejiao Jiang*, *Elodie Herault* and *Julien Wawrzyniak* during this period.

Last but not least, I would never forget the support and encouragement from my husband, *Chao*, as well as other members of my family, who constantly listened carefully to all of my problems, who shared my sorrow, and who motivated me in all circumstances.

This Ph.D. thesis has been supported by China Scholarship Council (CSC – UT/INSA program). The support is gratefully acknowledged.

Content

List of abbreviations

ABC ATP binding cassette
AT Autotransporter
ATP Adenosine triphosphate
Amp Ampicillin
Bam β-barrel assembly machinery
CD Circular dichroism
Cm Chloramphenicol
CMC Carboxymethyl cellulose
CP Coupling protein
CTD C-terminal domain
CuP Copper phenanthroline
EM Electron microscopy
GFP Green fluorescent protein
Gsp General secretory pathway
GST Glutathione S-transferase
HMQC Heteronuclear multiple quantum correlation
HGA Homogalacturonan
HR Homology region
HSQC Heteronuclear single quantum correlation
IA 2-Iodoacetamide
IM Inner membrane
IMP Inner membrane protein
IPTG Isopropyl-β-D-thiogalactopyranoside
Kan Kanamycin
LB Luria-Bertani
Lol Localization of outer membrane lipoprotein
LPP Lipoprotein
LPS Lipopolysaccharide
MFP Membrane fusion protein
NBD Nucleotide binding domain
NMR Nuclear magnetic resonance
NTD N-terminal domain
OM Outer membrane
OMP Outer membrane protein
PCR Polymerase chain reaction
PDZ Post synaptic density 95, Disc large protein, Zo-1
PG Peptidoglycan layer
PGA Polygalacturonate
PMF Proton motive force
PMSF Phenylmethyl-sulphonyl fluoride
POTRA Polypeptide translocation associated
PPIase Peptidyl-prolyl isomerase
PVDF Polyvinylidene fluoride
RG-I Rhamnogalacturonan-I
RG-II Rhamnogalacturonan-II
RND Nodulation and cell division
RNC Ribosome-nascent chain
SDA Secretin dynamic-associated protein
SDS-PAGE Sodium dodecyl sulfate polyacrylamide gel electrophoresis
SHS2 Strand-helix-strand-strand
SRP Signal recognition particle
Tat Twin-arginine translocation
TMS Transmembrane segment
T1SS Type I secretion system
T2SS Type II secretion system
T3SS Type III secretion system
T4P Type IV pili
T4SS Type IV secretion system
T5SS Type V secretion system
TPS Two-partner system

List of figures and tables

General introduction

Abstract

The type II secretion system (T2SS) is widely exploited by Gram-negative bacteria to secrete diverse virulence factors from the periplasm into the extra-cellular milieu. The phytopathogenic bacterium *Dickeya dadanti* (ex. *Erwinia chrysanthemi*) uses this system, named Out, to secrete several cell-wall degrading enzymes that cause soft-rot disease of many plants. The two core components of the Out system, the inner membrane protein OutC and the secretin OutD, which forms a secretion pore in the outer membrane, are involved in secretion specificity. The interaction between OutC and OutD could assure the structural and functional integrity of the secretion system by connecting the two membranes. To understand structure-function relationships between these two components and characterize their interaction sites, we applied an integrative approach involving *in vivo* cysteine scanning and disulfide cross-linking analysis, truncation analysis of OutC and OutD combined with *in vitro* GST pull-down, and structural analysis of these proteins and of their interactions by NMR. Our results indicate the presence of at least three interacting sites between the periplasmic regions of OutC and OutD and suggest a β-strand addition mechanism for these interactions. We demonstrated that one site of the HR domain of OutC can interact with two distinct sites of OutD suggesting an alternative mode of their interactions. The presence of exoproteins or/and the inner membrane components of the system OutE-L-M differently alters the affinity of the three OutC-OutD interacting sites. We suggest that successive interactions between these distinct regions of OutC and OutD may have functional importance in switching the secretion machinery between different functional states.

To study the mechanism of the targeting and assembly of the secretin OutD into the outer membrane, we exploited the interactions between OutD and two auxiliary proteins, i.e., the inner membrane protein OutB and the outer membrane lipoprotein OutS. We showed a direct interaction between the periplasmic domain of OutB and the N0 domain of OutD. Structure-function analysis of OutS-OutD complex shows that the pilotin OutS binds tightly to 18 residues close to the C-terminus of the secretin subunit causing this unstructured region to become helical on forming the complex.

This work allows us to better understand the assembly and function mechanism of the type II secretion system.

Key words: Type II secretion system, OutC, OutD, Secretin, GST pull-down, Cysteine scanning, β-strand addition.

Résumé

Le système de sécrétion de type II (T2SS) est largement exploité par les bactéries à Gram négatif pour sécréter divers facteurs de virulence depuis le périplasme vers le milieu extra-cellulaire. La bactérie phytopathogène *Dickeya dadanti* (ex. *Erwinia chrysanthemi*) utilise ce système, appelé Out, pour la sécrétion de pectinases responsable de la maladie de la pourriture molle chez de nombreuses plantes. Les deux composants essentiels du système Out, la protéine de membrane interne OutC et la sécrétine OutD, formant un pore dans la membrane externe, sont impliqués dans la spécificité de sécrétion. L'interaction entre OutC et OutD pourrait assurer l'intégrité structurelle et fonctionnelle du système de sécrétion en reliant les deux membranes. Nous avons entrepris une étude structure-fonction de ces deux composants afin d'identifier et caractériser leurs sites d'interaction et de mieux comprendre leurs rôles. Nous avons appliqué une approche intégrative impliquant une analyse *in vivo* par cystéine-scanning et pontage disulfure, une analyse *in vitro* par GST pull down et une analyse structurale d'OutC et OutD et de leurs interactions par RMN. Nos résultats indiquent la présence d'au moins trois sites d'interaction entre les régions périplasmiques d'OutC et d'OutD et suggèrent que ces interactions s'établissent par un mécanisme d'addition des brins β. Nous avons démontré qu'un site situé sur le domaine HR d'OutC pouvait interagir avec deux sites distincts d'OutD suggérant un mode d'interaction alternatif. La présence d'exoprotéines et/ou des composants de membrane interne du système OutE-L-M, modifie différemment l'affinité de ces trois sites d'interaction entre OutC et OutD. Nous proposons que ces interactions alternatives entre divers sites d'OutC et OutD pourraient refléter une succession d'étapes fonctionnelles lors du processus de sécrétion.

Pour étudier le mécanisme d'adressage et d'assemblage de la sécrétine OutD dans la membrane externe, nous avons exploité les interactions entre OutD et deux composants auxiliaires du T2SS, la protéine de la membrane interne OutB et la lipoprotéine de la membrane externe OutS. Nous avons montré une interaction directe entre le domaine périplasmique d'OutB et le domaine N0 d'OutD. Une analyse structure-fonction du complexe OutS-OutD a révélé que la pilotine OutS interagit fortement avec 18 résidus à l'extrémité C-terminale de la sécrétine, entraînant la structuration sous forme hélicoïdale de cette région initialement non structurée.

Ce travail nous permet de mieux comprendre le mécanisme d'assemblage et de fonctionnement du système de sécrétion de type II.

Mots clés: Système de sécrétion de type II, OutC, OutD, Sécrétine, GST pull-down, Cysteine-scanning, Addition des brins β.

General introduction

Secretion of various functional proteins outside of bacterial cells is an essential function directly involved in bacterial survival and pathogenesis. The secreted substrates fulfil various functions in different vital processes such as acquisition of nutrients, motility, intercellular communication and many others. Gram-negative bacteria evolved several specialized secretion systems to release these substrates into the medium or translocate them into the target host cell. Up to date, at least six distinct secretion systems (from type I to type VI) have been identified in Gram negative bacteria, which are recognizable by the characteristic of components forming the secretion machine. Pathogenic bacteria often use these systems to secrete harmful toxins, adhesins, degradative enzymes, or specialized effectors to colonize and survive within eukaryotic hosts, causing acute or chronic infections, subverting the host cell response and escaping the immune system. Studying bacterial secretion offers the possibility to design specifically drugs that can block these machineries and thus attenuate the virulence of pathogenic bacteria.

Our model organism to study the type II secretion system (T2SS) is a plant pathogenic bacterium *Dickeya dadantii* 3937. This bacterium is responsible for important economic losses since it causes diseases in many plants by secreting several cell wall degrading enzymes through the T2SS named Out (Perombelon and Kelman, 1980; Toth *et al.*, 2011).

I *Dickeya dadantii (ex. Erwina chrysanthemi)*, a phytopathogenic bacterium

I.1 Taxonomy

The phytopathogenic bacterium *Erwinia chrysanthemi* belongs to the *Enterobacteriaceae* family. Members of this family are Gram-negative bacilli, γ-proteobacteria, facultative anaerobes, nonsporing and with peritrichous flagella. The genus *Erwinia* was first established in 1917 to encompass all members of the *Enterobacteriaceae* that cause disease on plants, including both pectinolytic (e.g., *Erwina carotovora* and *Erwina chrysanthemi*) and non-pectinolytic (*Erwinia amylovora*) species. Later, Waldee (1945) proposed moving the pectinolytic *Erwinia* to a new genus, *Pectobacterium*. However, this classification had not been widely accepted until 1998 when new insights from 16S rRNA analysis led to resurrect the genus *Pectobacterium* for all pectinolytic *Erwinia* (Hauben *et al.*, 1998). Initially, the species *Erwina chrysanthemi* was assigned to the genus as a pathogen of chrysanthemum (Burkholder *et al.*, 1953). Similar

bacteria were subsequently isolated from soft rots and wilts of numerous diseased plant species and were finally gathered into a single species, *Erwinia chrysanthemi* (Skerman *et al.*, 1980). So, *Erwina chrysanthemi* (*Pectobacterium chrysanthemi*) is a complex of different bacteria. For convenience, it was subdivided into six pathovars, namely *pv. chrysanthemi*, *pv. dianthicola*, *pv. dieffenbachiae*, *pv. parthenii*, *pv. zeae* and *pv. paradisiaca* based on host specificity (Young *et al.*, 1978; Lelliott and Dickey, 1984). On the basis of 16S rRNA sequence analysis, *E. chrysanthemi pv. paradisiaca* has been renamed *Brenneria paradisiaca*, whereas the others remained cluster with members of the genus *Pectobacterium*, namely *P. chrysanthemi* (Hauben *et al.*, 1998). However, more recently, *Erwina chrysanthemi* complex has been reclassified as a novel genus, *Dickeya*, by using phenotypic characteristics, DNA-DNA hybridization, serology and 16S rRNA gene sequence analysis (Samson *et al.*, 2005). Six genomic species were delineated within the novel genus: *Dickeya chrysanthemi, Dickeya dadantii, Dickeya dianthicola, Dickeya dieffenbachiae, Dickeya paradisiaca and Dickeya zeae.* The strain *Erwinia chrysanthemi* 3937 that we used to study the mechanism of pathogenicity was reclassified as *Dickeya dadantii*. Despite of the new classification, *Erwina chrysanthemi* remains to be used in literature and in many data banks (protein and DNA) in parallel.

I.2 Hosts and disease symptoms

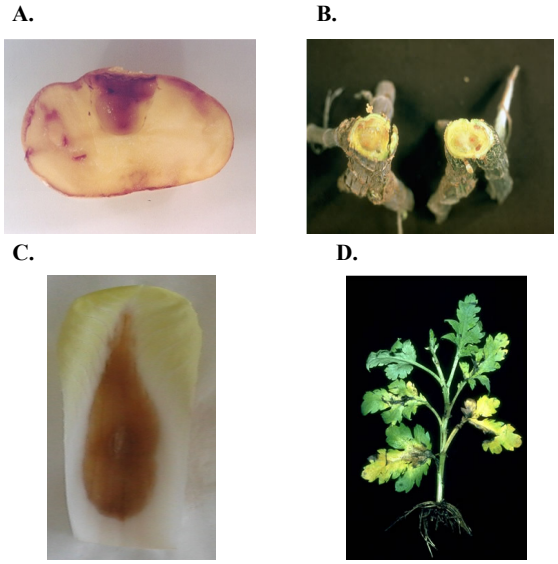

Fig. 1: Disease symptoms caused by *D. dadantii*: (A) in potato (B) in carnation (C) in chicory and (D) in chrysanthemum.

D. dadantii is frequently found in tropical and subtropical regions and has a wide variety of plant hosts, including several dicotyledonous and monocotyledonous families (Toth *et al.*, 2003). Many of these plants have great commercial importance, e.g., carnation, maize, potato, chicory and chrysanthemum. More recently, an efficient propagation of various *Dickeya* strains has been

observed in many temperate countries (including Europe) (Toth *et al*., 2011). *D. dadantii* also causes disease on certain crops and other plants in temperate regions (Toth *et al.*, 2003, 2011).

D. dadantii causes general tissue maceration, termed soft rot disease (Fig. 1). This symptom mainly results from the degradation of middle lamella of the plant cell wall caused by a set of enzymes secreted by the bacteria.

I.3 The pathogenic mechanisms of *D. dadantii*

The pathogenesis of *D. dadantii* is a multifactorial process. It encompasses the interaction between host, pathogen and the environment leading to latent and active infections. When the bacterium enters the plant, environmental conditions including free water, oxygen availability and temperature are essential for optimal disease development. Free water may allow bacterial cells to move more easily through plant tissue. Low oxygen availability may create a micro-aerobic or anaerobic environment within the plant, which has little effect on the ability of bacteria pathogen, but has a major effect on limiting oxygen-dependent defenses of the plant (Bolwell and Wojtaszek, 1997). Temperature is involved in a tight thermal regulation on the production of cell wall degrading enzymes (Nguyen *et al.*, 2002).

The bacterial cell surface structures, e.g., lipopolysaccharides (LPS), exopolysaccharides (EPS), enterobacterial common antigen (ECA) and flagella, are involved in bacterial motility and adhesion, which are necessary for successful invasion and infection of plants.

Soluble forms of iron, essential for all forms of life, are not readily available in plant or animal tissues. Under iron-limiting conditions, *D. dadantii* is able to express two high-affinity iron acquisition systems, e.g., chrysobactin and achromobactin that allow it to compete with plant for iron absorption (Franza *et al.*, 2005).

The interaction between the plant and the bacterial pathogen is dynamic and implies signal exchange between the interacting organisms. On one hand, *D. dadantii* could produce many signal factors that trigger the host defenses, e.g., oligogalacturonides (OGAs) derived from enzymatic breakdown of pectin (Norman *et al.*, 1999), pathogen-associated molecular patterns (PAMPs) such as flagellin (Zipfel *et al.*, 2004), and HrpN secreted by the type Ⅲ secretion system (Yang *et al.*, 2002). On the other hand, it can translocate into plant cells proteins that interfere with the resistance process. In fact, *D. dadantii* could inject a pathogenicity factor DspE directly into plant cells through the type Ⅲ secretion system (T3SS) which interferes with the phosphorylation cascades and suppresses the activation of plant defense genes (DebRoy *et al.*, 2004; Peng *et al*., 2006).

However, among all the pathogenicity factors of *D. dadantii*, the main factor is the secretion of various enzymes, such as pectinases, cellulases and proteases into the extracellular environment by different secretion systems. T1SS is a specific ABC transporter PrtDEF which allows secretion of four metallo-proteases (Delepelaire and Wandersman, 1990) that appear to have a relatively minor role in pathogenicity, whereas T2SS is essential for pathogenicity (Toth *et al.*, 2003). The *D. dadantii* possesses two independent T2SS, Out and Stt (Bouley *et al.*, 2001; Ferrandez and Condemine, 2008). At least 10 pectinases and one cellulase are secreted by the Out system (Kazemi-pour *et al.*, 2004). These secreted enzymes degrade the plant cell wall components and cause soft-rot disease. More recently genome sequences of *D. dadantii* 3937 revealed existence of genes and gene clusters coding for two type IV secretion system (T4SS), Type V and Type VI secretion systems (T5SS and T6SS) (Glasner *et al.*, 2011).

I.3.1 The plant cell wall

The plant cell wall is a complex macromolecular structure (Fig. 2A) that surrounds and protects the cell. It is a specific characteristic of plant essential to their survival. The cell wall is composed of polysaccharides, proteins, aromatic and aliphatic compounds. The polysaccharides are classified into three types: cellulose, hemicellulose and pectin (Caffall and Mohnen, 2009). The pectins, which are most abundant in the plant primary cell walls and the middle lamella, are group of polysaccharides that are rich in galacturonic acid (GalA) (Willats *et al.*, 2001). The pectic polysaccharides include homogalacturonan (HGA), rhamnogalacturonan-I (RG-I) and rhamnogalacturonan-II (RG-II) (Fig. 2B). These three polysaccharide domains could be covalently linked to form a pectic network throughout the primary cell wall matrix and middle lamella. HGA is a linear homopolymer of (1→4)-α-linked-D-galacturonic acid and is thought to contain 100-200 GalA residues. RG-I consists of as many as 100 repeats of the disaccharide (1→2)-α-L-rhamnose-(1→4)-α-D-galacturonic acid. RG-II has a backbone of around 9 GalA residues that are (1→4)-α-linked, and the side chains contain different sugars (mainly rhamnose, arabinose, galactose and glucuronic acid) (Willats *et al.*, 2001). Both RG-I and RG-II are thought to attach to HGA (Fig. 2B). Natural pectins present high percentages of methylesterification on the carboxyl group of galacturonate residues (from 40 to 65%). The cellulose microfibrils are linked via hemicellulosic tethers to form the cellulose-hemicellulose network, which is embedded in the pectin matrix (Fig. 2A). Cellulose is a polysaccharide consisting of a linear chain of several hundreds to over ten thousands β (1→4) linked D-glucose units. In contrast to cellulose, hemicellulose consists of several sugars, in addition to glucose, especially xylose, it also includes mannose, galactose, rhamnose and arabinose. It consists of shorter chains of about 200 sugar units.

A.

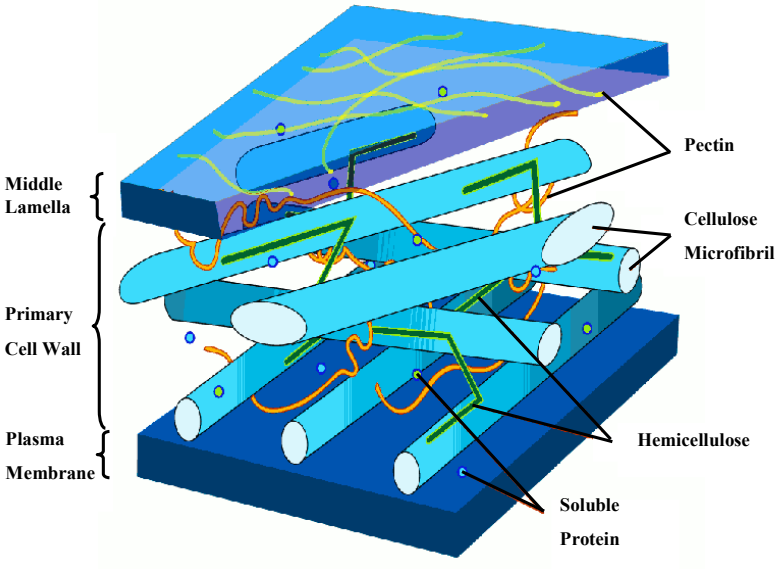

B.

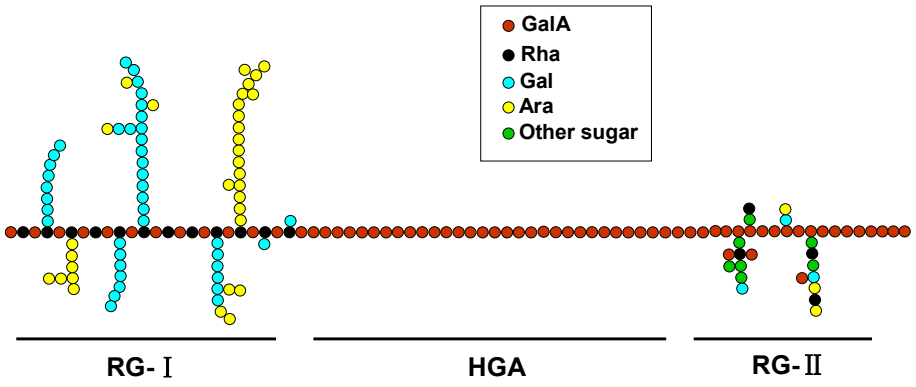

Fig. 2 The plant cell wall and the structure of pectin. (A) Schematic representation of the plant cell wall. (B) Schematic diagram of the structure of pectin. HGA: homogalacturonan; RG-I: rhamnogalacturonan I; RG-II: rhamnogalacturonan II; GalA: galacturonic acid; Rha: rhamnose; Gal: galactose; Ara: arabinose (Willats *et al.*, 2001).

I.3.2 Pectinases, the major pathogenicity factor of *D. dadantii*

D. dadantii produces diverse pectinases that play an important role in the maceration characteristic of soft-rot disease. Pectinases are classified into two groups by their site of action: the pectin esterases, responsible for the liberation of esterified group of the polymer, and depolymerases, responsible for the main chain cleavage (Robert-Baudouy *et al.*, 2000).

I.3.2.1 The pectin esterases

HGA constitutes the main chain of pectin which consists of galacturonate residues, and some

of them are modified by methyl and/or acetyl esterification (Fig. 3). The pectin esterases remove these modifications, and thus facilitate the further degradation of the polysaccharidic chain by depolymerases. *D. dadantii* 3937 produces two types of esterases: pectin methylesterases (Pem) and pectin acetylesterases (Pae). The methylesterases cleave the methyl groups of the pectin and release polygalacturonic acid (PGA) and methanol. PGA is a substrate more easily accessible to depolymerases and commercially available pectin derivative (used for bacterial growth and enzymatic assays). In *D. dadantii* 3937, the metylesterase activity is mainly due to PemA secreted by the T2SS Out (Fries *et al*., 2007) while a second isoenzyme PemB is a cell-linked outer membrane lipoprotein (Shevchik *et al.*, 1996). The acetylesterases hydrolyze O-acetyl groups in C2 and C3 of the HGA and release PGA and acetic acid. There are two acetylesterases identified in *D. dadantii* 3937: PaeY secreted by the T2SS Out, and PaeX which is mostly found in the periplasmic space (Shevchik and Hugouvieux-Cotte-Pattat, 1997; 2003).

I.3.2.2 The depolymerases

According to their mechanism of cleavage of the glycosidic bonds (β-elimination or hydrolysis), depolymerases are classified into two types: lyases (pectate lyases and pectin lyases) and hydrolyases (polygalacturonases). The preferential substrate of pectin lyases (Pnl) is high methoxyl pectins while the preferential substrate of pectate lyases (Pels) is low methoxyl pectins (PGA). The pectate lyases cleave internal glycosidic bonds in PGA via β-elimination to yield oligogalacturonates that are 4, 5-unsaturated at the nonreducing end. Polygalacturonases cleave the glycosidic bond of PGA by hydrolysis and generate saturated oligogalacturonates. The depolymerases can also differ in the random or terminal mode of attack of the polymer, endo or exo, respectively. Endo-acting enzymes would degrade the extracellular highly polymerized forms of PGA present within the plant cell wall. Exo-acting enzymes would be most efficient at producing small oligogalacturonides for intracellular transport from pectic fragments that accumulate in the periplasm.

There are 15 various pectinases identified in *D. dadantii* 3937: 10 pectate lyases (PelA, PelB, PelC, PelD, PelE, PelI, PelL, PelW, PelX and PelZ) (Robert-Baudouy *et al.*, 2000), 4 polygalacturonases (PehN, PehV, PehW and PehX) (Nasser *et al.*, 1999; Hugouvieux-Cotte-Pattat *et al.*, 2002) and one rhamnogalacturonate lyase RhiE (Laatu and Condemine, 2003). Among them, the endo-pectate lyases (PelA, PelB, PelC, PelD, PelE and PelI) are the major pectinolytic enzymes produced by *D. dadantii* and they play a crucial role in soft rot disease.

Beyond the pectinases, two cellulases, CelY and Cel5 (ex. EGZ or CelZ) are also involved in the degradation of plant cell walls by cleaving the cellulose (Py *et al.*, 1993; Zhou and Ingram,

2000). The Cel5 is an extracelluar enzyme secreted by the T2SS Out (Py *et al.*, 1993) and represents the majority of endoglucanase activity. The CelY is located in the periplasm and is less abundant (Boyer *et al.*, 1987).

The sequence of the strain *D. dadantii* 3937 reveals the existence of other pectinolytic enzymes: a pectate lyase PelN (Hassan *et al.*, in preparation), a polygalacturonase PehK (Okinaka *et al.*, 2002), two pectin lyases PnlH and PnlG homologue of *E. carotovora*, and two feruloyl esterases FaeD and FaeT (Hassan and Hugouvieux-Cotte-Pattat, 2011).

I.3.3 Enzymatic degradation of plant cell wall

The process of pectin degradation begins in the extracellular environment, then continues in the periplasm, and culminates in the cytoplasm of the bacterial cell (Fig. 3).

I.3.3.1 Extracellular pectin degradation

At least ten pectinases (PaeY, PemA, PelA, PelB, PelC, PelD, PelE, PelI, PelL and PelZ) are secreted by T2SS Out (Kazemi-Pour *et al.*, 2004) and involved in extracellular degradation of pectin.

Pectin acetylesterase PaeY (Shevchik and Hugouvieux-Cotte-Pattat, 1997) and methylesterase PemA (Laurent *et al.*, 1993) de-esterify pectin and release PGA which facilitates further degradation.

Endo-Pels (PelA, PelB, PelC, PelD, PelE, PelI, PelL and PelZ) cleave glycosidic linkages between two neighboring galacturonic acids and produce a planar product with an unsaturated bond between C4 and C5 at the nonreducing end (Fig. 3) (Robert-Baudouy *et al.*, 2000; Abbott and Boraston, 2008).

An endo-polygalacturonase PehN (Hugouvieux-Cotte-Pattat *et al.*, 2002; Abbott and Boraston, 2008), a rhamnogalactruonate lyase RhiE (Laatu and Condemine, 2003) and a cellulase CelZ (Zhou *et al.*, 1999) may be also involved in plant cell wall degradation.

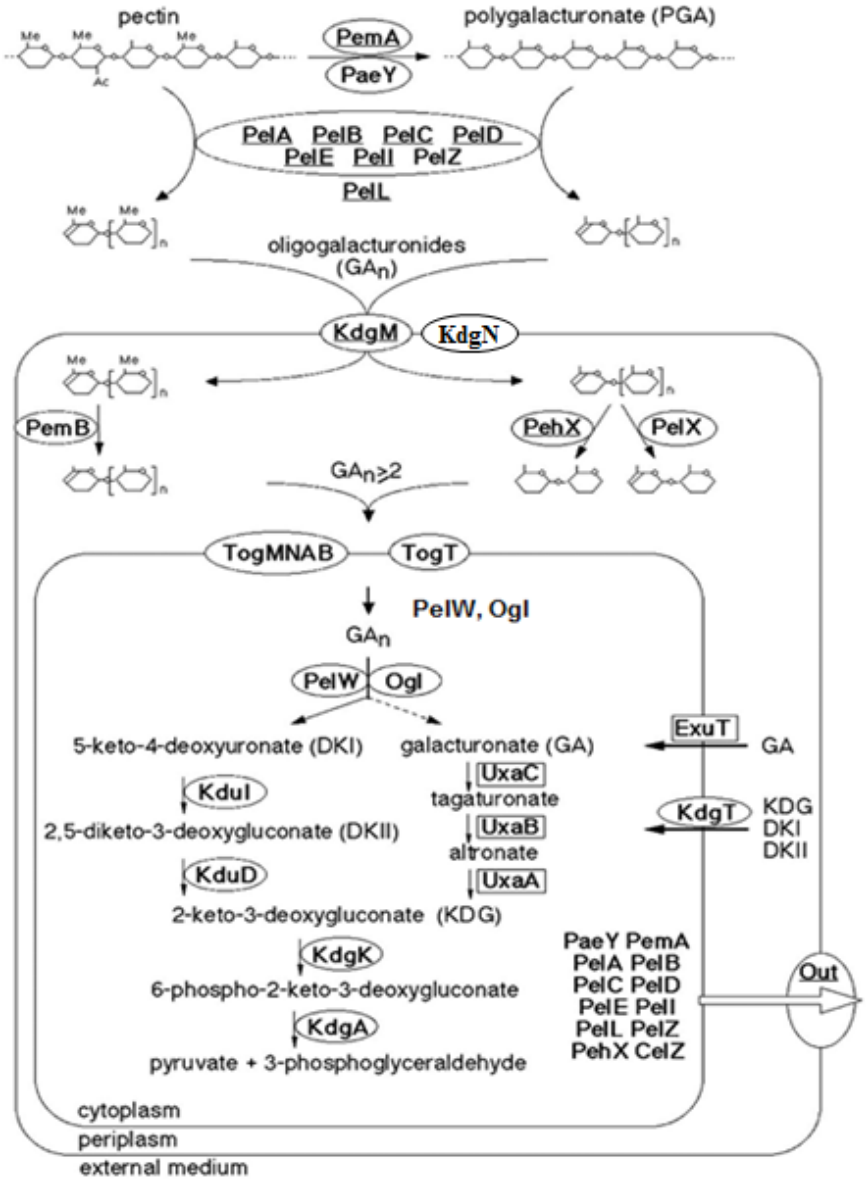

Fig. 3: Pectin catabolism in *D. dadantii* (Blot *et al.*, 2002). Extracellular pectinases (Pae- pectin acetylesterase, Pem- pectin methylesterase, Pel- pectate lyase, and Peh- polygalacturonase) degrade the pectin and the polygalacturonate (PGA) into oligogalacturonides (GAn) which then enter the cell. GAn are degraded by the periplasmic pectinases and pass through the inner membrane via one of the two transport systems, TogMNAB or TogT. GAn are then catabolized in the cytoplasm, producing pyruvate and 3-phosphoglyceraldehyde which integrate the general cellular metabolism.

Among these enzymes, the endo-Pels are considered, along with the endo-polygalacturonases, as a key factor in plant tissue maceration during soft rot infection (Pickersgill *et al.*, 1998).

Depolymerized pectic fragments are passively transported into the periplasmic space through the anion-specific oligosaccharide porins of KdgM and KdgN (Fig. 3) (Rodionov *et al.*, 2004; Condemine and Ghazi, 2007). Once transported into the periplasm, the pectic oligomers are further degraded by periplasmic pectinases into short oligomers, mainly dimers and trimers.

I.3.3.2 Periplasmic pectin degradation

Within the periplasm of *D. dadantii*, there are three major classes of pectinases:

Pectin esterases: the pectin methylesterase PemB anchored to the periplasmic face of the outer membrane (Shevchik *et al.*, 1996) and the pectin acetylesterase PaeX located in the periplasm (Shevchik and Cotte-Pattat, 2003).

An exo-pectate lyase: PelX degrades the oligogalacturonates by attacking the reducing end and yieds unsaturated digalacturonates (Shevchik *et al.*, 1999a).

Three exo-polygalacturonases: PehV, PehW and PehX, which complement the activity of the PelX, degrade the oligogalacturates by attacking their nonreducing end and release digalacturonates (Nasser *et al.*, 1999; Shevchik *et al.*, 1999a).

I.3.3.3 Intracellular transport and cytoplasmic degradation

The products of extracellular and periplasmic pectin degradation are small (di- and tri-) oligogalacturonides. These carbohydrates are subsequently transported into the cytoplasm where they are ultimately degraded by the cytoplasmic pectate lyase PelW and the oligogalacturonate lyase (Ogl) into galacturonate (GA) and 5-keto-4-deoxyuronate (DKI). These products finally degrade into pyruvate and 3-phosphoglyceraldehyde that enter the citric acid cycle and produce energy. Four distinct transporters are involved into the transport of small oligogalacturonides and monomers across the inner membrane: ExuT, KdgT, TogT and TogMNAB (Fig. 3) (Hugouvieux-Cotte-Pattat *et al.*, 2001; Abbott and Boraston, 2007). In fact, among these four independent systems, TogMNAB is the most prominent transporter during pectinolysis. In the cytoplasm, two enzymes are involved in degradation of pectic fragments: an exo-pectate lyase PelW, which degrades the short oligogalacturonates into unsatured digalacturonates; an oligogalacturonate lyase Ogl, which degrades unsaturated and saturated digalacturonates and generates galacturonate and DKI (Shevchik *et al.*, 1999b).

II Protein translocation and secretion pathways

The main pathogenicity factor of *D. dadantii* is due to the secretion of various enzymes, such as pectinases and cellulases into the extracellular environment. These secreted enzymes degrade the plant cell wall components and cause soft-rot disease. However, the bacterial cell enveloppe imposes a barrier for these proteins that are synthesized in the cytosol but function outside the cell. Various specialized transport mechanisms have evolved in Gram-negative bacteria to allow proteins to travel from the cytoplasm over the cell envelope to the exterior.

II.1 The cell envelope of Gram-negative bacteria

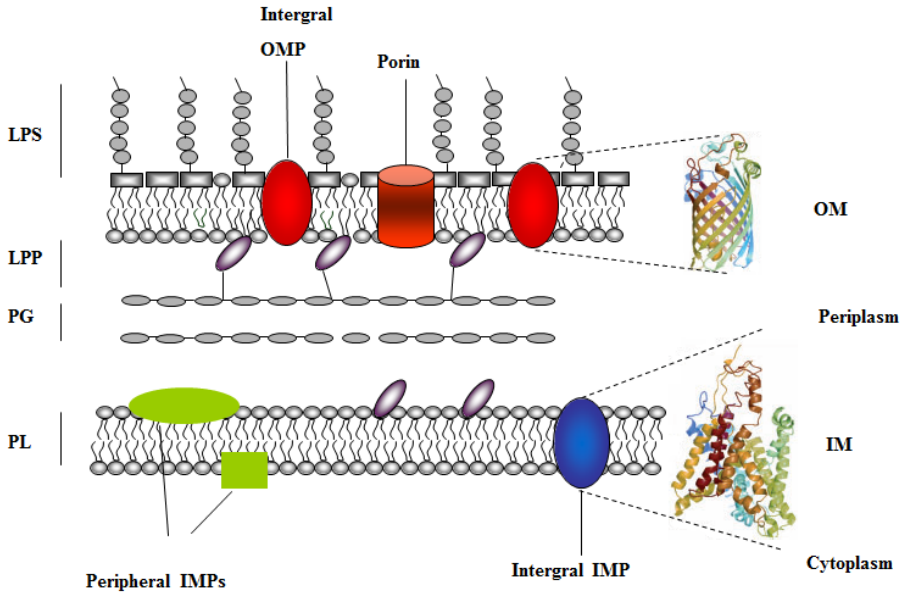

Fig. 4: Schematic representation of the Gram-negative bacterial cell envelope. The inner membrane (IM) is a symmetrical bilayer composed of phospholipids (PL). A typical structure of IM proteins (IMPs) is α-helix. The outer membrane is an asymmetrical bilayer, of which the inner leaflet is composed of PL and the outer leaflet of lipoplysaccharide (LPS). A typical structure of OM proteins (OMPs) is β-barrel. Lipoproteins (LPPs) are attached to both the inner and outer membranes. The peptidoglycan layer (PG) is located in the periplasm and is covalently attached to the outer membrane via LPPs (Tommassen, 2010).

The cell envelope of Gram-negative bacteria is composed of an inner membrane (IM) or cytoplasmic membrane (CM) and an outer membrane (OM), which are separated by the peptidoglycan-containing periplasm (Fig. 4). The IM is a symmetrical bilayer composed of phospholipids. Because of its hydrophobic nature, it is impermeable for hydrophilic compounds and also protons are unable to migrate freely over this membrane. IM proteins can be peripherally associated with the membrane by means of electrostatic and/or hydrophobic interactions or be present as integral membrane proteins spanning the phospholipids bilayer via hydrophobic α-helical segments. The OM faces the periplasm on one side and the extracellular medium on the other. This membrane is an asymmetrical bilayer composed of phospholipids in the inner leaflet and lipopolysaccharides (LPS) in the outer leaflet (Fig. 4), which renders the OM relatively resistant to detergents. The OM is semi-permeable due to the presence of channels formed by proteins, generically called “porins” (Fig. 4). These channels allow the passive diffusion of small hydrophilic molecules into the periplasm. Porins and other integral outer membrane proteins (OMPs) are characterized by the presence of amphipathic anti-parallel β-strands, which form a barrel-like structure with a hydrophobic surface facing the lipids, whereas the interior of the barrel is hydrophilic. The OM also contains lipoproteins, which are anchored

to the membrane via their lipid moiety. Between the two membranes is located a hydrophilic periplasmic compartment containing a peptidoglycan layer (Fig. 4). This is a rigid structure consisting of linear polymeric sugar chains that are covalently linked via short oligopeptides. The peptidoglycan layer is important for the cell shape and rigidity. Apart from the peptidoglycan layer, the periplasm also harbors chaperones, degradative enzymes, proteins involved in nutrient acquisition, and proteins involved in peptidoglycan synthesis.

II.2 Protein translocation across and insertion into the inner membrane

Two distinct systems are involved in the transport of proteins across the IM into the periplasm, namely the general secretion (Sec) system and the twin-arginine translocation (Tat) system (Fig. 5). In bacteria, most exported proteins are moved across IM by the Sec pathway (de Keyzer *et al.*, 2003). This system transports proteins into the periplasm in an unfolded conformation, but it can also integrate proteins into the IM. By contrast, the Tat system exports folded proteins across the IM (Berks *et al.*, 2005).

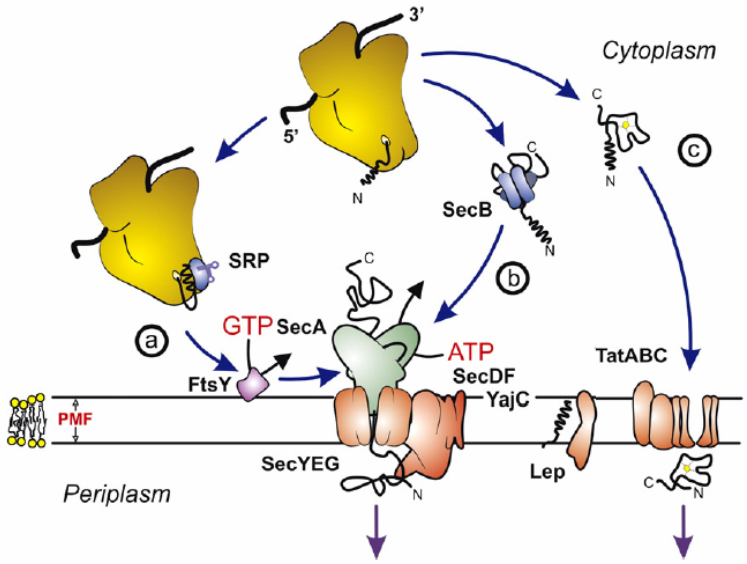

Fig. 5: Schematic overview of the *E. coli* Sec- and Tat translocases (Natale *et al.*, 2008). (a) Co-translational and (b) post-translational translocation of unfolded proteins by the Sec-translocase, and (c) Translocation of folded proteins by the Tat translocase.

II.2.1 Sec system

The Sec system consists of an IM peripherally associated ATPase SecA that acts as a molecular motor, and a translocon that constitutes the protein-conducting channel. The translocon is formed by a heterotrimeric complex, SecYEG (de Keyzer *et al.*, 2003). The translocation processes are assisted by the YidC and SecDF (YajC) complex that transiently interacts with the translocon (de Keyzer *et al.*, 2003; du Plessis *et al.*, 2011). Substrates of the

Sec systems are synthesized at ribosomes in the cytosol. To reach their destination, these proteins need to be recognized and targeted to the Sec translocase that translocates them across or inserts them into the cytoplasmic membrane.

II.2.1.1 Recognition and targeting

Substrates of Sec systems are synthesized as precursor proteins with an N-terminal signal sequence, which targets them to the translocase. A typical Sec signal sequence contains a positively charged N-terminal region (n-region), a nonpolar hydrophobic core (h-region) and a more polar C-terminal region (c-region) containing the signal peptidase cleavage site (Fig. 6).

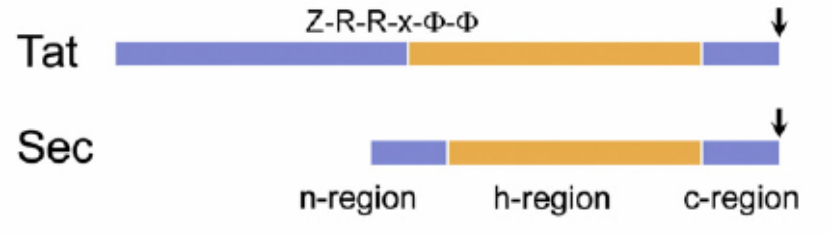

Fig. 6: Schematic comparison of typical N-terminal signal sequences from substrates of the Tat and Sec system (Natale *et al.*, 2008): n-region, a postive charged amino-terminal; h-region, an uncharged hydrophobic core; c-region, a polar carboxyl-terminal region that contains a type I signal petidase cleavage site. Z and x stand for any polar residue and Φ for hydrophobic residue.

Generally, integral membrane proteins do not have a signal sequence, and instead their hydrophobic transmembrane domains (TMDs) function as an internal signal for targeting and insertion. Two different pathways are employed for recognition and targeting of proteins to the translocation site: one employs the chaperone SecB for post-translational targeting (Fig. 5b), and the other utilizes the signal recognition particle (SRP) for co-translational targeting (Fig. 5a) (Müller *et al.*, 2001). In bacteria, the post-translational pathway is used by proteins secreted across the membrane, while co-translational pathway is mainly utilized by IM proteins (De Gier *et al.*, 1997).

SecB is a molecular chaperone that binds to newly synthesized precursor polypeptides (preproteins) and stabilizes them in an unfolded and non-aggregated state after they exit from the ribosome translation tunnel (Breukink *et al.*, 1992; Bechtluft *et al.*, 2007). Although SecB does not directly bind to the signal sequence of preproteins (Randall and Hardy; 2002), the presence of this sequence is indispensable for export (Zhou and Xu, 2005). The peptide-binding study defined a general SecB-binding motif that consists of approximately nine amino acid residues enriched in aromatic and basic residues, whereas acidic residues are strongly disfavored (Knoblauch *et al.*, 1999). SecB is a homotetramer that is organized as a dimer of dimers (Fig. 7A)

(Zhou and Xu, 2005; Natale *et al.*, 2008). Biochemical data revealed two types of preprotein binding sites in SecB tetramer: one that interacts with polypeptides with extended β-sheet stretches and another interacts with hydrophobic polypeptide regions (Randall *et al.*, 1998; Crane *et al.*, 2006). Consistent with these biochemical data, the putative peptide-binding groove in crystal structure of SecB tetramer seems to contain two subsites that are involved in recognition of distinct features in the preprotein. One subsite is a deep cleft lined with mostly conserved aromatic residues that may recognize the hydrophobic and aromatic regions of the polypeptides, while the other subsite forms a shallow open groove with a hydrophobic surface that might be involved in the binding of β-pleated sheets (Fig. 7B) (Natale *et al.*, 2008; Zhou and Xu, 2005). Subsequently, SecB directs the bound preprotein into the translocation pathway via its specific interaction with membrane-bound SecA (Randall and Henzl, 2010).

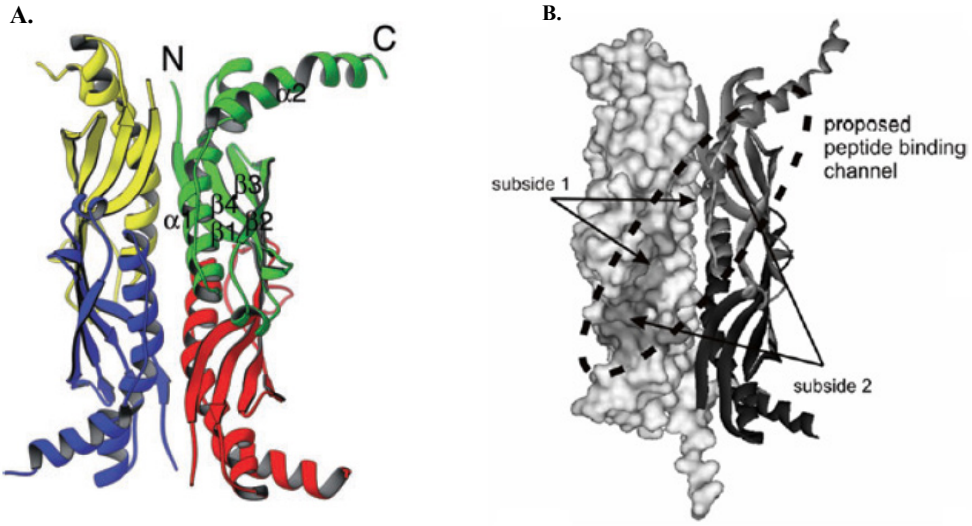

Fig. 7: The structure of SecB homo-tetramer (A) and the peptide-binding groove within the SecB molecule (B). The homo-tetramer (A) is organized as a dimer of dimers. Each subunit is colored differently; one dimer consists of the green and red subunits while the other consists of the blue and yellow subunits. The unfolded preprotein would bind to a channel consisting of two subsites (1 and 2) (B) (Natale *et al.*, 2008; Zhou and Xu, 2005).

Preproteins with very hydrophobic signal peptides and most IMPs are targeted to Sec system by SRP in a co-translational manner. In fact, unlike in eukaryotes, translational arrest was not been observed in Gram-negative bacteria. However, it was suggested that the shorter traffic distances and the faster translocation rates in bacteria overcome the need for translation arrest (Driessen and Nouwen, 2008). The *E. coli* SRP is composed of a complex of a 4.5S RNA and a 48 kDa GTPase P48 or Ffh (for fifty-four homolog) that interacts specifically with the signal sequence or hydrophobic TMSs of nascent proteins (Driessen and Nouwen, 2008). SRP also binds to the ribosomal large subunit near its exit gate (Schaffitzel *et al.*, 2006) and brings the

ribosome-nascent chain (RNC) complex to the membrane through its interaction with FtsY (SRP receptor). FtsY binds to membrane via the anionic phospholipids but also binds directly to the SecYEG channel (Angelini *et al.*, 2006; Kuhn *et al.*, 2011). Both Ffh and FtsY are GTP-binding proteins and are capable of GTP hydrolysis, which is activated by the interaction of these two proteins (Egea *et al.*, 2004). Upon GTP hydrolysis by both SRP and its receptor, the RNC-SRP-FtsY complex dissociates, and the released RNC complex is transferred to the translocase (see, for review, du Plessis *et al.*, 2011).

II.2.1.2 Mechansim and structural insights in preprotein translocation

The SRP and SecB-mediated targeting routes converge at the translocase. SecA couples with the stepwise translocation of preprotein across the SecYEG channel in the bacterial IM.

(1) SecA, an ATPase dependent motor protein

SecA is a soluble protein that localizes to both the cytosol and the IM. It functions as an ATPase dependent motor protein. It binds to the membrane via low- and high-affinity interaction with anionic phospholipids and the SecYEG complex, respectively (Du Plessis *et al.*, 2011). It interacts with nearly all other components involved in protein translocation, and its ATP hydrolysis activity is suppressed in its resting state, whereas it is stimulated by its binding to the membrane or interaction with acidic phospholipids and more strikingly in the presence of SecYEG and preproteins (Kusters and Driessen, 2011). It is believed that SecA undergoes large conformational changes to drive protein translocation. The crystal structure of SecA from various organisms have been solved (Hunt *et al.*, 2002; Sharma *et al.*, 2003; Osborne *et al.*, 2004; Vassylyev *et al.*, 2006; Papanikolau *et al.*, 2007). Most of these structures display SecA packed as a dimer (Fig. 8) with an antiparallel orientation except for the *T. thermophilus* SecA that was crystallized as a parallel dimer (Vassylyev *et al.*, 2006). The SecA protomer can be subdivided into several structural subdomains (reviewed by Kusters and Driessen, 2011 and du Plessis *et al.*, 2011), i.e., nucleotide-binding folds 1 and 2 (NBF1 and NBF2), the preprotein cross-linking domain (PPXD), the α-helical scaffold domain (HSD), the α-helical wing domain (HWD) and the C-terminal linker (CTL). The actual motor function of SecA is performed by the "DEAD motor" core that consists of NBF1 and NBF2. The interface between these two domains forms the nucleotide binding site. ATP can be bound to the interface and hydrolyzed to induce the conformational changes necessary for preprotein translocation. The PPXD domain can be cross-linked to the leader and mature domain of preprotein. The HSD domain contacts all other domains of SecA and therefore likely plays an important role in the catalytic cycle of SecA. The HWD domain seems to be flexible and loosely linked with the rest of the molecule. The CTL

domain has been shown to be involved in lipid binding, in Zn^{2+} and in SecB binding. Recently, it was shown that the amino terminus of SecA was also involved in the SecB binding (Randall *et al.*, 2010).

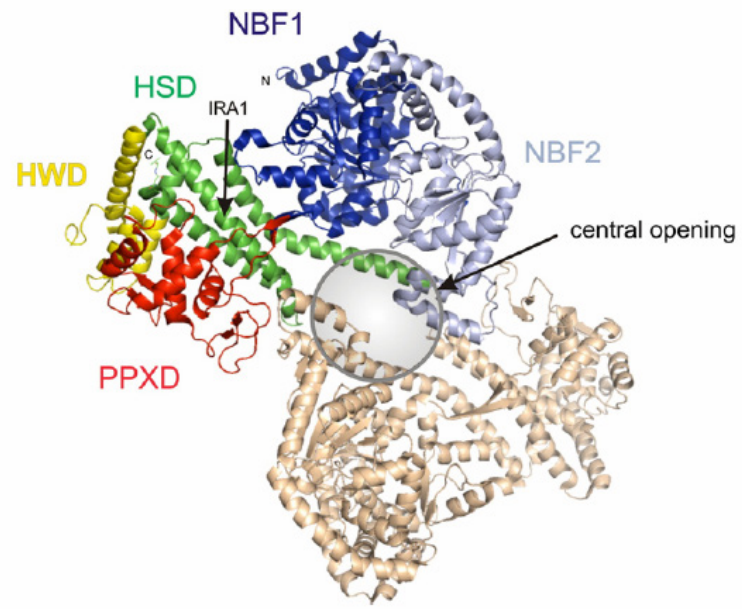

Fig. 8: Crystal structure of SecA dimer with an antiparallel orientation of *M. tuberculosis*. A central pore at the centre of the dimer is indicated by a circle. The different domains of SecA are represented by different colors: dark blue and light blue represent the nucleotide binding folds 1 and 2 (NBF1 and NBF2), respectively. The preprotein cross-linking domain (PPXD) is shown in red, while α -helical scaffold domain (HSD) is shown in green, the α-helical wing domain (HWD) is shown in yellow, and the C-terminal linker domain (CTL) was not resolved in this structure (du Plessis *et al.*, 2011).

(2) SecYEG complex, the protein-conducting channel

The pore of the translocase is formed by a complex of the SecY, SecE and SecG proteins. The heterotrimeric organization of the translocation pore is conserved throughout the three kingdoms of life (de Keyzer *et al.*, 2003). Among the three components, SecY is the central component of translocon, in which a polypeptide-conducting channel is formed. SecY has 10 transmembrane segments (TM1-TM10), six cytosolic regions (C1-C6) and five periplasmic regions (P1-P5). It interacts independently with SecE and SecG to form a heterotrimeric SecYEG complex. The interaction of SecE and SecY protects SecY from degradation by the membrane-bound protease FtsH (Kihara *et al.*, 1995) that is involved in the degradation of unassembled membrane protein complexes. SecE is a 14 kDa integral membrane protein. In *E. coli*, SecE consists of three transmembrane segments (TMSs) while the homologue Sec61γ has only one TMS (Kusters and Driessen, 2011). Cysteine-scanning mutagenesis studies identified contacts between SecE TMS3

and SecY TMS 2, 7 and 10 (Kaufmann *et al.*, 1999; Veenendaal *et al.*, 2001, 2002). Despite its small size, SecE is essential for viability and translocation, while SecG, a small protein of ~12kDa containing two TMS, is not essential for viability or translocation. It was hypothesized that SecG facilitates the binding and insertion of SecA into the translocon by undergoing transient topological inversions during protein translocation (Nagamori *et al.*, 2002). However, another study showed that a topologically fixed SecG was fully functional in protein translocation (van der Sluis *et al.*, 2006). Cysteine-scanning mutagenesis showed that SecG is in close proximity to C3 and TMS4 of SecY (van der Sluis *et al.*, 2006). To date, no evidence has been found for a physical interaction between SecE and SecG.

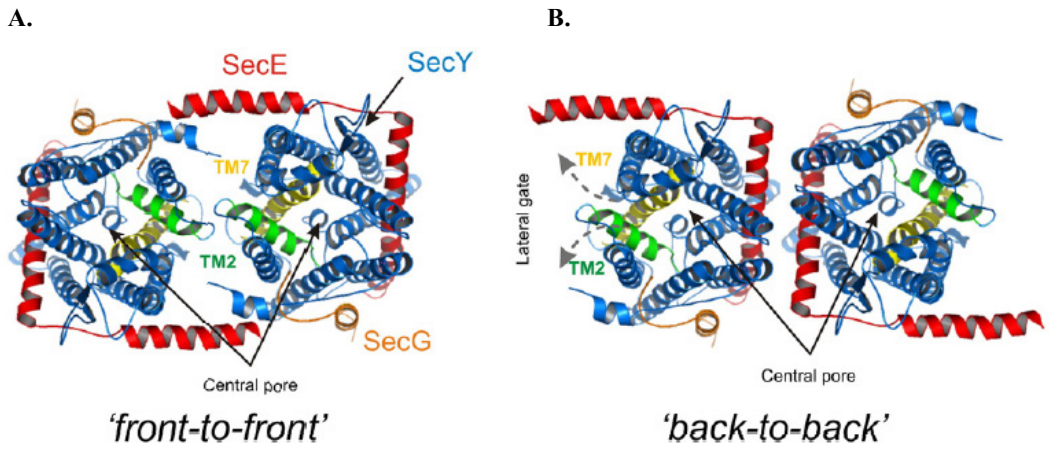

Fig. 9: Models proposed for the dimer of the SecYEG. (A) The front-to-front model with the lateral gates formed by TM2 (green) and TM7 (yellow) of SecY opposing each other. SecE (red) braces the two translocons on each side. (B) The back-to-back arrangement for two SecYEG translocons. In this instance, the two translocons are aligned with the large TM of SecE. Both translocons can act independently of each other for membrane protein insertion and protein translocation. Indicated are the locations of the central pores as well as the TM2/TM7 lateral gate (du Plessis *et al.*, 2011).

A number of studies demonstrated the oliogomeric states of SecYEG, such as dimers, trimers, or tetramers (Manting *et al.*, 2000; Tziatzios *et al.*, 2004; Mitra *et al.*, 2005). Interestingly, a structural analysis suggested that monomeric SecA-SecYEG is sufficient for translocation (Zimmer *et al.*, 2008). There is evidence that an interacting partner (ribosome or SecA) as well as simple integration into the lipid bilayer induces dimerization/oligomerization of SecYEG (Matra *et al.*, 2005; Scheuring *et al.*, 2005). Currently, two models are proposed for the orientation of the dimeric translocon: the 'front-to-front' and 'back-to-back' orientation (Fig. 9) (du Plessis *et al.*, 2011). In the 'front-to-front' orientation, the lateral gates of the two SecYEG complexes are facing each other (Fig. 9A), while in the 'back-to-back' orentation, the two SecYEG complexes are contacted via the TMS of SecE that embraces the SecY subunits as a clamp. However, the functional relevance of these two orientations remains puzzle (du Plessis *et*

al., 2011).

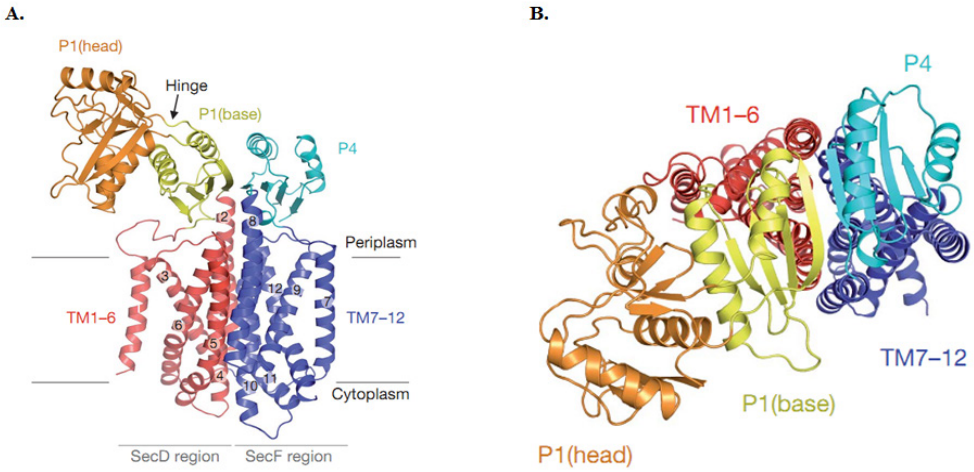

Fig. 10: Structures of *T. thermophilus* SecDF (Tsukazaki *et al.*, 2011). (A) The crystal structure of full-length SecDF viewed from the membrane side and (B) the periplasmic side.

The SecYEG complex can also associate transiently with another heterotrimeric membrane protein complex YidCSecDF (YajC) which stimulates preprotein translocation (Nouwen and Driessen, 2002). Although YajC associates with SecDF, it is not essential for functionality, but cells lacking SecD and SecF are cold sensitive, which prevents growth, and are severely defective in protein translocation (Driessen and Nouwen, 2008). However, the SecDF is not needed for translocation per se. The role of SecDF has remained unclear, although it is proposed to function in later stages of translocation and in membrane protein biogenesis (Driessen and Nouwen, 2008; du Plessis *et al.*, 2011). Recently, the crystal structure of *T. thermophilus* SecDF revealed a pseudo-symmetrical, 12-helix transmembrane domain belonging to the resistance nodulation and cell division (RND) superfamily and two major periplasmic domains, P1 and P4 (Fig. 10) (Tsukazaki *et al.*, 2011). They proposed that SecDF functions as a membrane integrated chaperone, powered by proton motive force (PMF) to achieve ATP-independent protein translocation. This function depends on the ability of the periplasmic P1 domain to interact with a substrate and to undergo a structural transition.

YidC is functionally and structurally homologous to Oxa1 in mitochondria and Alb3 in chloroplasts (Samuelson *et al.*, 2000; Kuhn *et al.*, 2003). It facilitates the insertion of a subset of membrane proteins via the translocon (Kol *et al.*, 2009; du Plessis *et al.*, 2011). YidC is also able to act as an insertase on its own (Serek *et al.*, 2004; Dalbey *et al.*, 2011).

(3) Mechanism of protein translocation

It is believed that multiple rounds of ATP binding and hydrolysis lead to the stepwise translocation of the preprotein (Fig. 11) (Facey and Kuhn, 2010). The preprotein is targeted by

SecB or SRP to the tranlocon. The translocation starts with the binding of ATP to SecA. A hairpin loop of the signal sequence with the early mature protein region is inserted into the translocation pore. This step can also be stimulated by the PMF, which likely affects the orientation of the signal sequence within the channel or the conformation of the SecY protein and facilitate opening of the lateral gate region (Facey and Kuhn, 2010). ATP hydrolysis results in a dissociation of SecA from the preprotein and weakens the SecA-SecYEG binding affinity. SecA is then likely released from the translocon but may rebind to the partially translocated preprotein trapped in the SecYEG pore and thereby causing a translocation of about 5 kDa of preprotein through the pore (Facey and Kuhn, 2010). Repeated cycles of ATP binding and hydrolysis, as well as polypeptide binding and release, result in the stepwise translocation of the polypeptide across the membrane (Fig. 11).

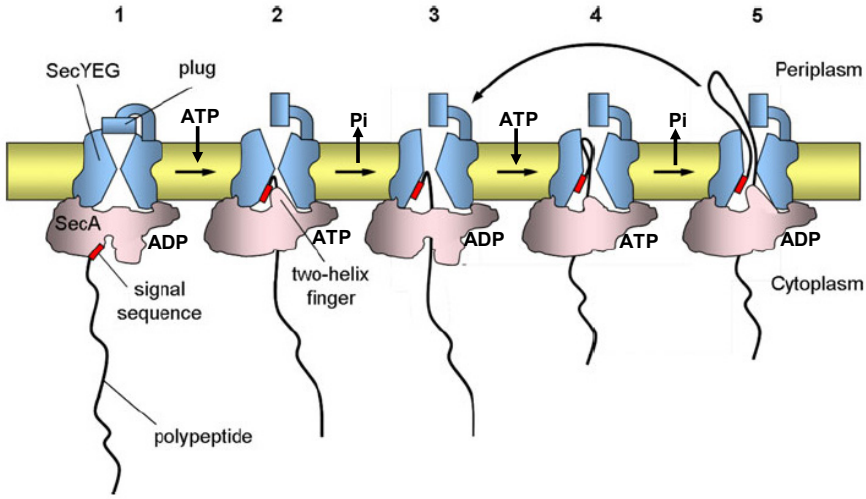

Fig. 11: The model for the different steps of Sec-mediated protein translocation (Facey and Kuhn, 2010). These steps are coupled to ATP hydrolysis cycles and steps 3-5 are repeated until the polypeptide is fully translocated.

Once the preprotein has been transported into periplasm, the N-terminal signal sequences of precursors are cleaved by the type II signal peptidase for lipoproteins and the type I for the others (Dev and Ray, 1984; Tuteja, 2005)

II.2.2 Protein insertion in the inner membrane

Most IMPs insert into the membrane via the Sec system (du Plessis *et al.*, 2011; Dalbey *et al.*, 2011). They are synthesized without a cleavable signal sequence but with hydrophobic TMS required for targeting and insertion into IM. Indeed, SRP recognizes and binds to a hydrophobic segment of a membrane protein as it emerges from the ribosome at the membrane face and target the complex to its receptor FtsY located at the membrane. After GTP hydrolysis, the IMPs are transferred to the SecYEG translocation channel, and SRP and FtsY dissociate from each other.

Both translocase SecYEG and insertase YidC are required to insert newly synthesized proteins into membrane (Dalbey *et al.*, 2011). SecYEG typically mediates the insertion of proteins into the membrane and the lateral partitioning of the TMSs into the lipid phase (Fig. 12a). The insertase YidC, suggested to play a direct role during the insertion of Sec-independent substrates, is responsible for inserting small proteins into the membrane (Fig. 12c) (Winterfeld *et al.*, 2009; Dalbey *et al.*, 2011). YidC can also function as an integrase and cooperate with the Sec translocase to mediate membrane protein insertion (Fig. 12b). In some cases, YidC inserts the N-terminal domain of protein, SecYEG then promotes the insertion of the C-terminal region of the protein (Fig. 12d). The topology of membrane proteins is established during its insertion step and obeys the positive-inside rule (von Heijne, 2006; Dalbey *et al.*, 2011).

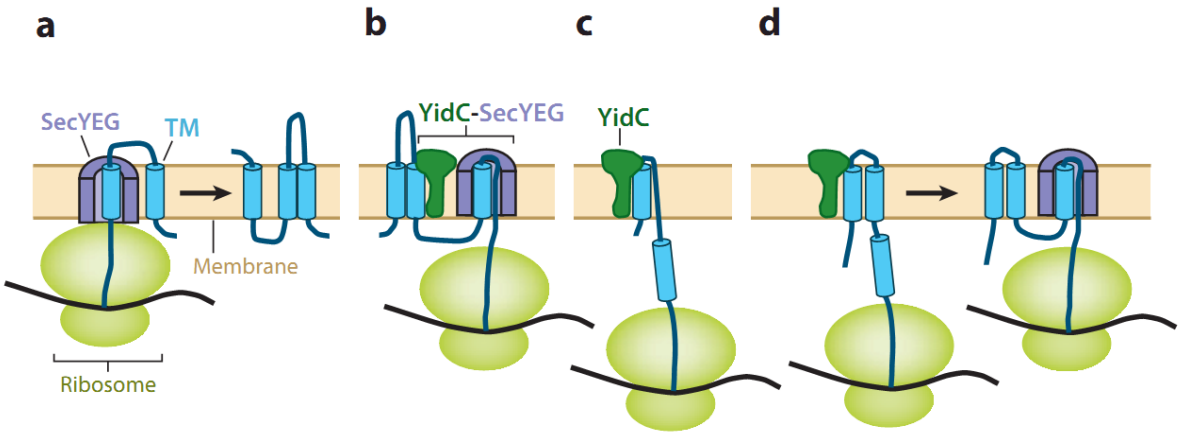

Fig. 12: The machineries involved in inner membrane proteins insertion (Dalbey *et al.*, 2011). (a) SecYEG mediates the insertion of proteins into the membrane. (b) YidC and SecYEG function together to insert and integrate membrane proteins. (c) YidC acts as an independent insertase. (d) YidC and SecYEG work sequentially to insert membrane proteins.

II.2.3 Tat system

The Tat system is found in the cytoplasmic membranes of many eubacteria, some Archaea, and the chloroplasts and mitochondria of plants (Müller, 2005). In bacteria, the Tat system mediates export of periplasmic proteins in folded conformation (Müller, 2005). Tat translocases consist of two or three membrane integrated subunits, i.e., TatA and TatC or TatA, TatB and TatC that together form a receptor and a protein conducting machinery for Tat substrates (Natale *et al.*, 2008). The energy for translocation is provided by the proton motive force (PMF) (Müller, 2005).

II.2.3.1 Tat substrates

Generally, Tat substrates bear N-terminal signal sequences that resemble the overall organization of Sec signal sequences. They also contain a positively charged n-region, a

hydrophobic h-region and a short polar c-region with the peptidase cleavage site (Fig. 6). However, there are some differences between Sec and Tat signals (Natale *et al.*, 2008):

i) Tat signal sequence is characterized by the consensus motif Z-R-R-x-Φ-Φ at the interface of the N- and H-regions and a replacements of one or both arginine residues which are highly conserved markedly decrease the transport efficiency;
ii) bacterial Tat signal sequences are usually longer than their Sec counterparts;
iii) h-region of Sec signal sequences are more hydrophobic than those of Tat signal peptides due to more glycine and threonine residues;
iv) c-region of Tat signals often contains basic residues while Sec signals are almost never charged in c-region, which are support to function as a Sec-avoidance motif.

Tullman-Ercek *et al.* (2007) showed that Tat specificity depends both on the overall charge of the c-region and the N-terminal section of the mature protein. Some Tat substrates of *E. coli* do not have a Tat signal sequence of their own. They are transported in multimeric complexes together with protein containing a Tat signal sequence by a so-called “hitchhiker mechanism” (Rodrigue *et al.*, 1999).

The Tat system exports proteins that are folded prior to transport and somehow senses and rejects unfolded substrates, suggesting that the Tat machinery might have an innate ‘quality control’ activity that confers the ability to recognize the folded state of a substrate protein (Robinson *et al.*, 2011). This is particularly important for the Tat substrates required cofactor insertion. In *E. coli*, about 6% of all secreted protein are predicted to be Tat-dependent and the majority are cofactor-containing redox proteins including hydrogenases, formate dehydrogenases, trimethylamine N-oxide (TMAO) reductase, dimethyl sulfhoxide (DMSO) reductase and nitrate reductases (Palmer *et al.*, 2005; Lee *et al.*, 2006), all of which function in anaerobic respiration. It was suggested that the signal sequence plays a certain role in cofactor assembly of a Tat substrate, either by interaction with an accessory protein or by specific protein-protein interaction with unfolded portion of the mature protein sequence (Berks *et al.*, 2005).

In addition to cofactor-containing proteins, in *E. coli*, there are also Tat substrates which lack cofactors, such as Sulf I and the periplasmic amidases AmiA and AmiC (Berks *et al.*, 2005), indicating that co-factor assembly is not the only reason for Tat dependent transport.

The Tat system also allows integration of certain IMPs. Targeting to the IM requires both the hydrophobic C-terminal transmembrane helices (C-tail) and the N-terminal Tat signal peptide (Hatzixanthis *et al.*, 2003). In addition, Tat system was also shown to be involved in the targeting of pre-folded or fast-folding lipoproteins (Shruthi *et al.*, 2010).

II.2.3.1 Tat translocase

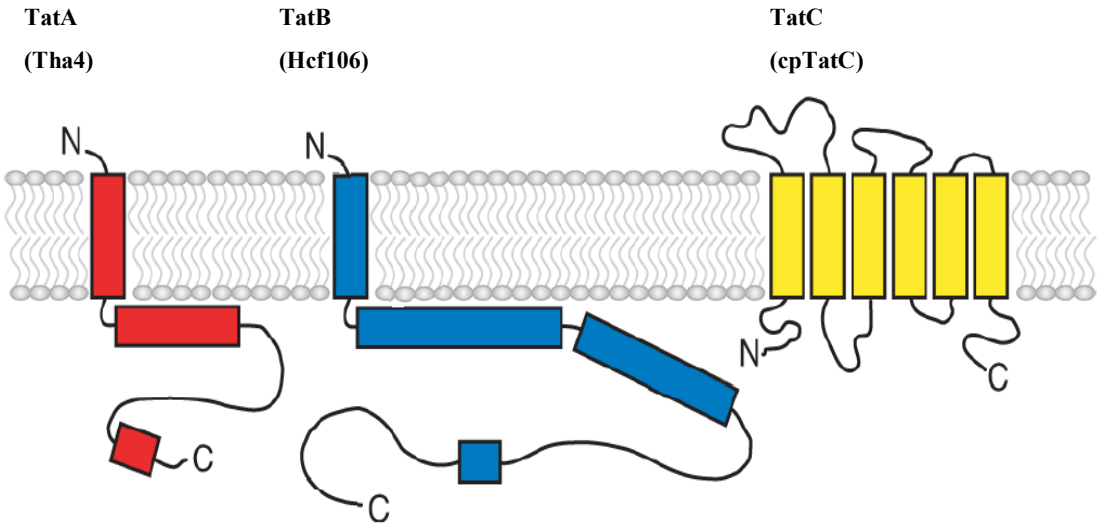

Fig. 13: The predicted topology of the *E. coli* Tat components. Predicted helical regions are shown as boxes. (Lee *et al.*, 2006)

The Tat system of *E. coli* consists of three individual IMPs: TatA, TatB and TatC (Fig. 13). The orthologues in the thylakoidal membrane of chloroplasts are termed Tha4, Hcf106 and cpTatC, respectively (Lee *et al.*, 2006). TatC is the largest and most highly conserved component consisting of 258 amino acids. It contains six predicted transmembrane helices with both N- and C-teminus located on the cytoplasmic side of the membrane (Fig. 13) (Lee *et al.*, 2006). It is generally accepted that the TatC protein alone, or in a complex with TatB, forms the initial recognition site for a Tat signal sequence (Alami *et al.*, 2003). However, the precise signal sequence-binding site of TatC has not yet been identified, it seems that the entire N-terminal half of TatC is involved in recognition (Holzapfel *et al.*, 2007), with the first cytosolic loop of TatC being of particular importance (Kreutzenbeck *et al.*, 2007; Strauch and Georgiou, 2007). Both TatA and TatB have a similar topology, with an N-terminal transmembrane α-helix that is linked by a hinge region to an extended amphipathic helix followed by an unstructured C-terminal tail (Fig. 13) (Lee *et al.*, 2006).

In Gram-negative bacteria, two separate complexes are found at a steady state: a TatABC complex and homo-oligomeric TatA complex (Lee *et al.*, 2006; Robinson *et al.*, 2011). Within the TatABC complex, TatB and TatC form a functional unit with a ratio 1:1 (Oates *et al.*, 2005; Orriss *et al.*, 2007). The TatBC plays important roles in substrate binding but the role of TatA in the complex is unclear. However, the complex appears to be less stable in the absence of TatA (Dabney-Smith *et al.*, 2006; Behrendt *et al.*, 2007). Further analysis revealed that the major binding site for folded substrates is formed by TatB (Maurer *et al.*, 2010). The TatA complexes have very unusual properties: they are remarkably heterogeneous and range in size from 50 kDa

to well over 500 kDa. TatA forms different size homo-oligomeric complexes in the membrane, which suggests that TatA forms a size-fitting protein-conducting channel (McDevitt *et al.*, 2006; Greene *et al.*, 2007). The functionally essential regions of TatA are located within the cytoplasmic region and the hinge region (Hicks *et al.*, 2003; 2005). Since the TatABC and TatA complexes show little or no propensity to associate after isolation, it is generally accepted that, at the steady state, the Tat system comprises two distinct complexes, one containing TatABC and the other containing only TatA (Robinson *et al.*, 2011).

II.2.3.2 Translation mechanism

The bacterial and the thylakoidal Tat systems transport fully folded proteins across the IM into the periplasm of bacteria and across the thylakoid membrane into the luminal space of the chloroplast, respectively. Tat transport is somehow triggered by PMF. The translocation process can be divided into two separate stages: firstly, targeting and binding of the substrates to the TatBC receptor complex, and secondly, PMF dependent recruitment of the TatA complex to form the fully assembled and active Tat translocase. Several models have been proposed to explain the transport mechanism. Most of the models supposed that TatA complex form a hydrophilic channel through which the passenger domain of the Tat substrate is transported across the membrane (Sargent *et al.*, 2001; Alami *et al.*, 2003). However, Dabney-Smith *et al.* (2006) suggest that the TatA-recruitment does not depend on the substrates size, which is not consistent with the hypothesis of preformed TatA pores. Thus, another non-pore model is proposed (Fig. 14) (Natale *et al.*, 2008). Prior to the contact with the Tat translocase, Tat substrates seem target to the membrane via an unassisted insertion of the signal sequence into the lipid bilayer. The region of the twin-arginine motif in Tat substrate signal sequences binds to the TatBC complex (Fig. 14A). Upon substrate binding and in the presence of PMF, TatA is recruited to the TatBC-substrate ternary complex (Fig. 14B). Multiple hydrophobic TMDs of TatA assemble near the bound Tat substrate. This may destabilize the membrane bilayer. The interaction between TatA and Tat substrates may induce the conformational change in TatBC (Fig. 14C), which pulls the Tat substrate across membrane weakened by TatA (Fig. 14D). In the moment of releasing of the Tat substrate, a transient hole may be formed which could account for the large proton flux accompanying Tat substrate (Fig. 14E). After transport, the membrane has to be sealed immediately, TatA disassembles from TatBC and Tat substrate is released from the membrane by a cleavage of type I or type II signal sequences peptidases (Fig. 14F).

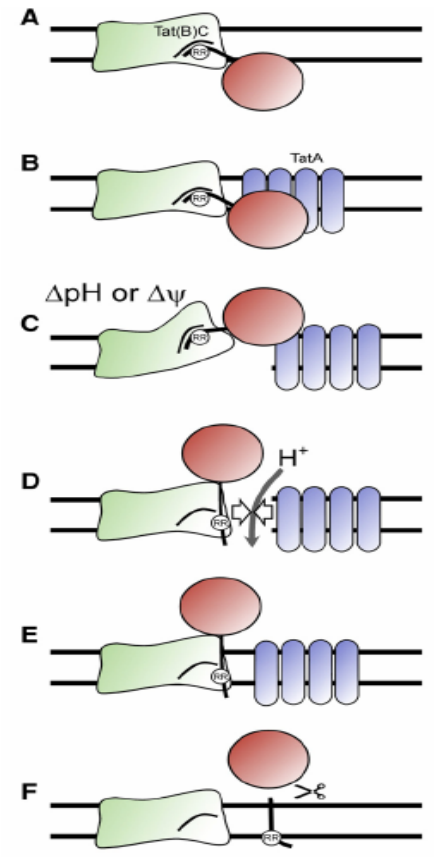

Fig. 14: Model for the membrane passage of Tat substrates (Natale *et al.*, 2008). A) Binding of Tat substrates with Tat(B)C complex. B) Recruitment of TatA. C) Conformational change of Tat(B)C and transport of the substrate through the membrane which is weakened by TatA. D) Flux of proton. E) Seal of the membrane hole. F) Disassembly of TatA form TatBC and release of substrate by a cleavage peptidase.

II.3 Protein folding and maturation in the periplasm

Once transported over the IM into the periplasm by the Sec or by the Tat system, the proteins residing in or transiting through the periplasm are folded into their native-conformation in periplasm. In the periplasm of *E. coli*, three groups of factors might facilitate their folding (Mogensen and Otzen, 2005) (Fig. 15), i.e., proteases, molecular chaperones and folding catalysts. Indeed, this categorization is not strict, since many of the proteins display several activities (Fig. 15). For example, DegP is a protease that degrades unfolded or misfolded proteins in the periplasm but also has chaperone activity, and peptidyl-prolyl isomerases (PPlases) SurA and FkpA act also as chaperones. The molecular chaperones are proteins that assist the non-covalent folding or unfolding of target proteins. In *E. coli*, several chaperones, i.e., DegP, Skp and SurA assist in the maturation of OMPs (Sklar *et al.*, 2007b). Two types of folding catalysts are found in the periplasm, namely protein disulphide isomerases and *cis-trans* PPlases. The former catalyze the formation and rearrangement of disulfide bonds, which promotes the oxidative folding of secreted proteins, while the latter catalyse the *cis-trans* isomerization of peptide bonds. The disulphide isomerases DsbA and DsbC function together with the IMPs DsbB and DsbD. DsbA and DsbB catalyze the introduction of disulfide bonds into folding

proteins, whereas DsbC and DsbD provide a proofreading system for the restoration of misfolded proteins with non-native disulfide bonds (Nakamoto and Bardwell, 2004; Mogensen and Otzen, 2005; Inaba, 2009). DsbC of *D. dadantii* is also involved in catalyzing the formation of disulfide bonds in the secretion of pectate lyases (Shevchik *et al*., 1995)

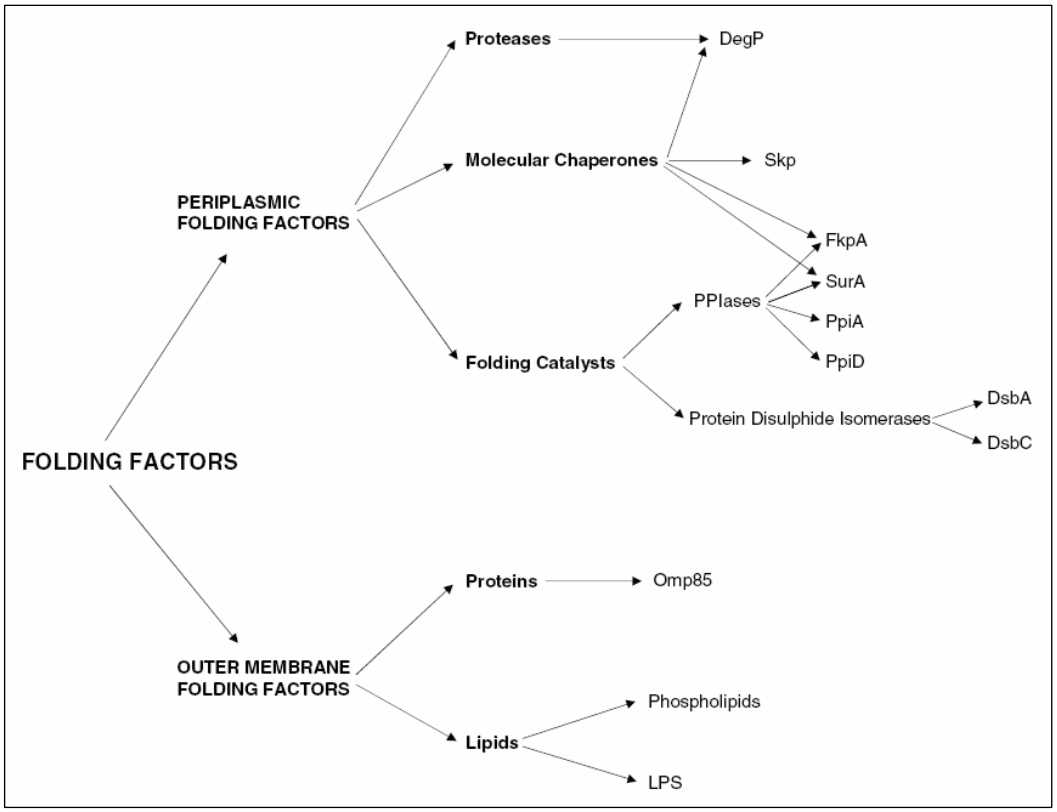

Fig. 15: The periplasmic and outer membrane folding factors (Mogensen and Otzen, 2005). In the periplasm of *E. coli*, three groups of proteins might assist in protein folding: protease, molecular chaperones and folding catalysts. In the OM of *E. coli*, both proteinaceous and lipidic components may assist in OMP folding.

II.4 Lipoproteins

Bacterial lipoproteins are anchored to the IM or OM via an N-terminal lipid moiety N-acyl-diacyl-glyceryl cysteine. Lipidation and folding of these proteins occur after their translocation over the IM via the Sec system or in some case by the Tat system (Gralnick *et al*., 2006). Prior to cleavage of the signal sequence, a diacylglycerol group is transfered by enzymes Lgt from phosphatidylglycerol to the sulfhydryl group of the cysteine located at the N-terminal of lipoproteins (Sankaran and Wu, 1994). After cleavage of the signal sequence by type II signal peptidase, the free α-amino group of the cysteine is acylated by the enzyme Lnt (Sankaran and Wu, 1994), yielding the mature lipoprotein.

In *E. coli*, lipoproteins are sorted to the IM or OM depending on the lipoprotein-sorting signal located at position 2 of mature lipoprotein. An aspartate at this position retains the lipoprotein in

the IM, whereas the absence of this IM retention signal results in transport to OM by Lol system (Tokuda and Matsuyama, 2004, Lewenza *et al.*, 2006). However, in *P. aeruginosa*, +3 and +4 positions were identified as sorting residues. A lysine and serine residue at +3 and +4, respectively, retained the protein in the IM, whereas a leucine and isoleucine resulted in translocation to the OM (Narita and Tokuda, 2007; Tanaka *et al.*, 2007).

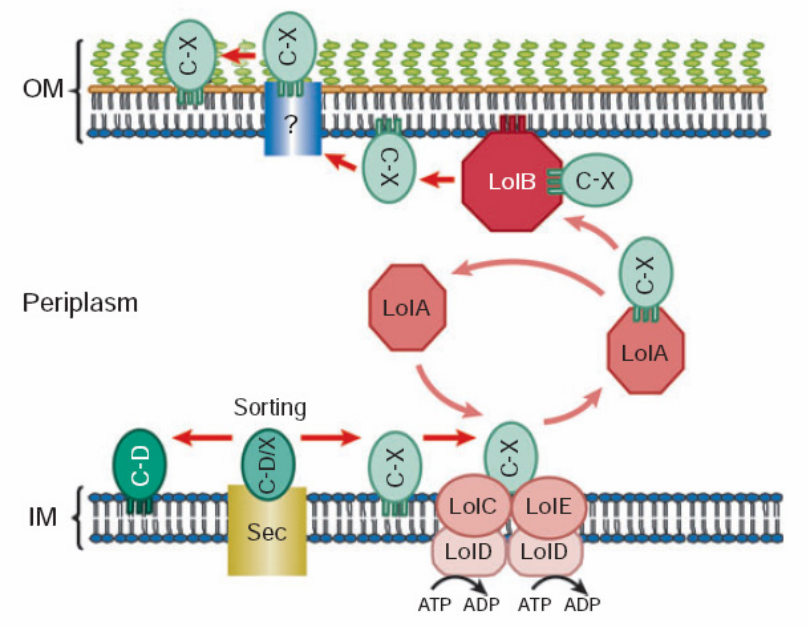

Fig. 16: Model for lipoprotein transport through the bacterial cell envelope (Bos *et al.*, 2007). After their transport via the Sec system and subsequent lipidation at the N-terminal cysteine (C), lipoproteins with an aspartate (D) at the +2 (C-D) retain in the IM. Lipoproteins with another amino acid at the +2 position (X) are destined for the OM. Energy from ATP hydrolysis by LolD is transferred to LolC and LolE and utilized to open the hydrophobic LolA cavity to accommodate the lipoprotein. When the LolA-lipoprotein complex interacts with the OM receptor LolB, the lipoprotein is transferred to LolB and inserted into the OM. Further transport to the outer leaflet of the OM, if applicable, occurs through unknown mechanisms.

The Lol system comprises an IM ATP-binding cassette (ABC) transporter LolCDE complex, a periplasmic carrier protein LolA and an OM receptor protein LolB. The model (Fig. 16) (Bos *et al.*, 2007) states that lipoproteins destined for the OM interact with the LolCE, and the binding results in an increase in the affinity of LolD for ATP. Upon hydrolysis of ATP, the lipoprotein is released from LolCE to the periplasmic chaperone LolA (Ito *et al.*, 2006). LolA chaperones OM lipoproteins across the periplasm and delivers them to LolB, which causes lipoprotein releasing from LolA and integration of the lipoprotein into the inner leaflet of the OM (Bos *et al.*, 2007). In some bacteria, cell surface-exposed lipoproteins also are present. However, whether the transport over the OM occurs through an extension of the Lol system or by an unrelated transport system is unclear. For example, in *K. oxytoca*, cell surface-exposed lipoprotein pullulanase contains an aspartate at position +2, indicating that it is not transported by Lol system. Indeed, it

requires the T2SS named Pul for transport (Pugsley, 1993). In *N. meningitidis*, the cell surface-exposed lipoproteins LbpB and TbpB could be transported form the IM to OM by the Lol system. However, no component of the Lol system is involved in the translocation of the surface-exposed lipoprotein from the periplasmic side of the OM to the cell surface. In addition, the sequenced genomes do not reveal the presence of a type II secretion apparatus (Van Ulsen and Tommassen, 2006). They may be transported to the cell surface via an extension of the Lol system.

II.5 Integral outer membrane proteins

There are two major types of proteins in the OM, lipoproteins and integral OMPs. These two types of proteins require different systems for folding and insertion into the OM. Integral β-barrel OMPs need the SurA and Skp-DegP pathways to transport nascent OMPs across the periplasmic space to the OM (Sklar *et al.*, 2007b). It is well kown that integral OMPs require Bam complex for folding and insertion into the OM (Werner and Misra, 2005; Wu *et al.*, 2005; Doerrler and Raetz, 2005, Malinverni *et al.*, 2006; Sklar *et al.*, 2007a). One known exception is secretin PulD. It has been shown that Bam complex is not required for insertion of PulD into the OM (Collin *et al.*, 2007; Guilvout *et al.*, 2008). Recently, Collin *et al.* (2011) showed that PulD is sorted via the lipoprotein-specific Lol pathway.

Bam complex is composed of five proteins: BamA (formerly YaeT in *E. coli* and Omp85 in *N. meningitidis*) and four accessory lipoproteins, BamB (YfgL), BamC (NlpB), BamD (YfiO) and BamE (SmpA) (Wu *et al.*, 2005; Vuong *et al.*, 2008; Knowles *et al.*, 2009). BamA is found in all Gram-negative bacteria and folds into two distinct domains: an N-terminal soluble domain assembled from five POTRA (polypeptide translocation associated) domains and a C-terminal *trans*-membrane domain assumed to fold as a β-barrel (Misra, 2007). It was proposed that the first two POTRA domains are involved in interaction with OMPs. The POTRA-OMP interactions may be mediated through β-augmentation, in which a β-strand of POTRA is augmented by the addition of a β-strand from the substrates (Kim *et al.*, 2007; Knowles *et al.*, 2008). The C-terminal phenylalanine of substrates seems to be important for the recognition of BamA (Robert *et al.*, 2006). Indeed, the importance of having five POTRA domains in all BamA remains unclear. Several studies suggested that POTRA domains also act as a scaffold for the binding of accessory factors and the number of POTRA domains correlate with the correct substrate folding (Kim *et al.*, 2007; Bos *et al.*, 2007; Knowles *et al.*, 2008).

The accessory lipoproteins BamBCDE are less conserved since not all of them are present in every Bam complex (Gatsos *et al.*, 2008; Volokhina *et al.*, 2009; Anwari *et al.*, 2010). Among them, BamD seems to be the only essential lipoprotein (Sklar *et al.*, 2007a; Fardini *et al.*, 2009;

Volokhina *et al.*, 2009). Recently, the 3D structure of BamB, BamD and BamE became available (Heuck *et al.*, 2011; Sandoval *et al.*, 2011; Kim and Paetzel, 2011). It was suggested that the C-terminal domain of BamD provides a scaffold for interaction with Bam components, while the N-terminal domain is involved in interaction with the substrates (Sandoval *et al.*, 2011). BamB, a nonessential component of the Bam complex, could simultaneously bind to BamA and prefolded β-barrel proteins, thereby enhancing the folding and membrane insertion capacity of the Bam complex (Heuck *et al.*, 2011). The functional significance of the BamC and BamE remain to be elucidated.

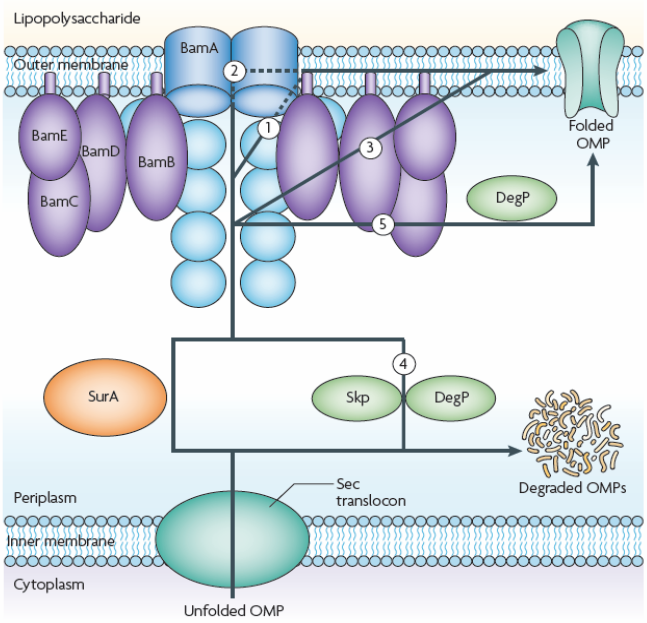

Fig. 17: Models proposed for outer membrane proteins (OMPs) biogenesis in *E. coli* (Knowles *et al.*, 2009). OMPs destined for the β-barrel assembly machinery (Bam) complex are transported across the IM by the Sec system. Following export, the nascent OMPs are recruited by two proposed chaperone pathways, the SurA and the Skp-DegP pathways, and are transported through the periplasm to the OM. Five models are proposed: 1) the pore-folding model; 2) the complex pore-folding model; 3) the barrel-folding model; 4) the chaperone -folding model; 5) the accessory -folding model.

Several models were proposed to explain how BamA facilitates assembly and insertion of the β-barrel OMPs (Fig. 17) (Knowles *et al.*, 2009): i) pore-folding model, the Bam complex functions as a single monomeric complex and incorporates the nascent OMP into the β-barrel pore, the POTRA and/or accessory components thread the OMP into the pore; ii) the complex pore-folding model, the central pore is formed by a multimeric Bam complex, the release of folded OMP into the membrane occurs owing to the opening of the oligomeric assembly and the periplasmic components help folding and deposit the protein directly into the membrane; iii) the barrel-folding model, the BamA provides a template for OMP barrel folding in the vicinity of the

membrane; iv) the chaperone folding model, the periplasmic chaperones, in particular DegP, fold the nascent OMPs and protect them from degradation, and the Bam complex only function in the insertion into the membrane; v) the accessory folding model, the Bam complex only functions to fold the nascent OMP, and the folded OMP is then released to DegP in a quality-control mechanism to remove misfolded OMPs. The folded OMPs are then inserted into the OM probably facilitated either by DegP or by an additional periplasmic factor.

II.6 Protein secretion systems in Gram-negative bacteria

Gram-negative bacteria have evolved several secretion systems to deliver extracellular proteins across the bacterial cell envelope into the external medium or directly into the target cell. The secreted proteins fulfil various functions, e.g., acquisition of nutrients, motility and intercellular communication. Moreover, pathogenic bacteria use these systems to secrete harmful toxins, adhesins, degradative enzymes and other secreted effectors to help the colonization of host organism. There are six secretion systems, from type I to type VI (T1SS to T6SS), which have been identified in Gram-negative bacteria to date (Desvaux *et al.*, 2009; Bleves *et al.*, 2010; Filloux, 2011). These secretion systems can be classified into two categories: i) the Sec or Tat independent pathways, including T1SS, T3SS; T4SS and T6SS (Holland *et al.*, 2005; Gerlach and Hensel, 2007; Durand *et al.*, 2009). They transport secreted proteins from the bacterial cytoplasm out of the cells in one-step; ii) the Sec or Tat dependent pathways, including T2SS and T5SS. The secretion by these systems is a two-step process. In the two later cases, the substrates are synthesized with a N-terminal signal peptide, which are recognized by the Sec or Tat translocons and are translocated across the IM (Voulhoux *et al.*, 2001; Chevalier *et al.*, 2004). Subsequently, the mature proteins (without the N-terminal peptide) are targeted to one of these two secretion systems that mediate their transport through the OM. The main structural and functional features of T1SS, T3SS, T4SS, T5SS and T6SS will be summarized briefly in the following sections. Since *D. dadantii* T2SS is the subject of this thesis, this system will be addressed in more details in a special section.

II.6.1 Type I secretion system (T1SS)

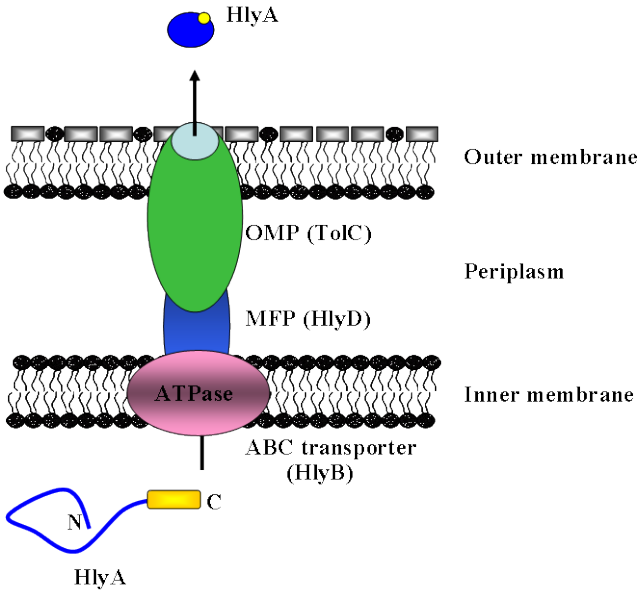

Fig. 18: Model of the T1SS (Delepelaire, 2004). The T1SS consists of an IM protein, ABC transporter, an OM protein, OMP and membrane fusion protein, MFP. The secretion signal (colored in yellow) is located at the C-terminus of unfolded secreted protein and is not cleaved during secretion.

The type I secretion system (T1SS) belongs to a large family of ATP-binding cassette (ABC) transporters involved in export (ABC exporter or effluxer)/import (ABC importer) of various substrates across bacterial cell membrane. The T1SS is widespread in Gram-negative bacteria and transports unfolded proteins of various sizes, including pore-forming hemolysins (HlyA), adenylate cyclases, lipases, proteases, surface layers and hemophores (HasA), from the cytoplasm to the extracellular medium in one step (Delepelaire, 2004). This system is a heterotrimeric complex consisting of an ABC transporter, a channel forming outer membrane protein (OMP) and a membrane fusion protein (MFP) connecting the above two proteins (Fig. 18). It has been shown that T1SS-secreted proteins have a C-terminal secretion signal and this signal interacts with the ABC protein (Blight and Holland, 1994). However, several studies pointed out that additional domains may be involved in the interaction with the secretion complex. Firstly, efficient secretion of heterologous proteins fused to *E. coli* HlyA or *D. dadantii* PrtB requires C-terminal fragments much larger than the minimal secretion signals (Létoffé and Wandersman, 1992; Palacios *et al.*, 2001). Secondly, hemophore (residues, 1-174) without its C-terminal signal retains its capacity to interact with HasD (ABC protein) and induce the assembly of the tripartite complex (Cescau *et al.*, 2007). Recently, Masi and Wandersman (2010) identified multiple regions distributed along HasA (residues, 1-174) as additional HasD binding sites.

II.6.1.1 ABC protein, the motor of the system

ABC protein binds and hydrolyses ATP, and uses the energy to drive the transport of secreted proteins across membranes. It is suggested that ABC protein functions as homodimers (Fetsch and Davidson, 2002; Zaitseva *et al.*, 2005ab) and is also responsible for substrate recognition and specificity. ABC exporter comprises four domains: two transmembrane domains (TMDs) and two cytosolic nucleotide-binding domains (NBDs). The NBD is formed by various conserved motifs such as the Walker A and B motifs, the C-loop or ABC signature motif, the Q- and Pro-loop, and the D- and H-loops (Higgins and Linton, 2004), while TMD displays very little sequence homology. The homodimerization through TMDs form the substrate translocation pathway, while the NBDs control the conformation of the TMDs through ATP-induced dimerization and hydrolysis-induced separation (Zaitseva *et al.*, 2006, Procko *et al.*, 2009; Gyimesi *et al.*, 2011) (Fig. 19). The export process is driven by ATP binding and/or hydrolysis at the NBD. Without nucleotide, the NBDs are apart or open. Unpon binding of ATP, both NBDs close to form a tight dimer with two ATPase active sites at the interface (Hollenstein *et al.*, 2007). When the NBDs are open, the substrate-binding cavity formed by the TMDs faces inwards the cytosolic NBDs. When the NBDs bound to ATP and closed, the substrate-binding cavity faces outwards (Fig. 19) (Procko *et al.*, 2009). Both ABC exporter and importer probably use the same basic mechanism.

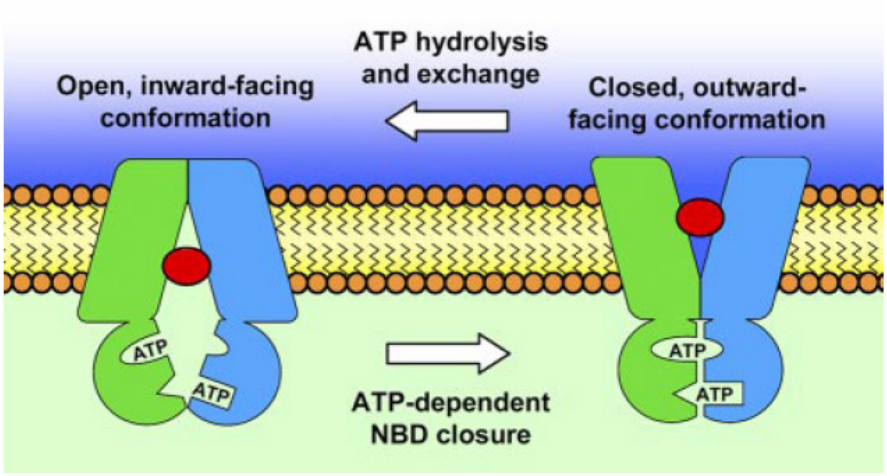

Fig. 19: Mechanism of a typical ABC transporter (Procko *et al.*, 2009). Binding of ATP triggers the formation of dimer and moves the coupling helices closer together and flips the TMDs to an outward-facing conformaiton. Hydrolysis of ATP revert the TMDs to adopt an inward-facing conformation.

II.6.1.2 Membrane fusion protein (MFP)

MFP or adaptor proteins span across the periplasm bridging the two membrane components (ABC transporter/OMP). The crystal structure of several proteins of MFP family have been

solved and revealed that they consist of a membrane-proximal (MP) domain, a β-barrel domain, a lipoyl domain, and an α-hairpin domain (Akama *et al.*, 2004; Mikolosko *et al.*, 2006; Symmons *et al.*, 2009; Yum *et al.*, 2009). The α-hairpin domain was suggested to be involved in interaction with OMP TolC, while the other domains are related to interaction with IMP (Lobedanz *et al.*, 2007; Symmons *et al.*, 2009). Furthermore, Xu *et al.* (2010) revealed that the conserved residues located at the tip region of the α-hairpin of MacA (MPF in efflux pump MacAB-TolC) play an essential role in the binding of TolC, which support the idea of tip-to-tip binding between MacA and TolC (Yum *et al.*, 2009; Xu *et al.*, 2009, 2010).

II.6.1.3 Outer membrane protein (OMP)/TolC

The OMP forms the exit pore for both the ABC transport pathway and the drug efflux pumps. The 3D structures of three OMPs, i.e., TolC, OprM and VceC from *E. coli*, *P. aeruginosa* and *V. cholerae*, respectively, have been solved (Koronakis *et al.*, 2000; Akama *et al.*, 2004; Federici *et al.*, 2005). Despite very little sequence similarity, they are structurally conserved. Take TolC as an example, it adopts a trimeric structure organized into two barrels (Fig. 20). A 12-stranded, 40 Å-long β-barrel inserts into the OM to form an open pore of 30 Å in diameter. The unusual α-helical barrel, 100 Å in length, protrudes into the periplasm. The tip of the TolC periplasmic entrance interacts with the apex of AcrB (Xu *et al.*, 2010). TolC is open to the outside medium but is closed by densely packed α-helical coiled coils, inner H7/H8, and outer H3/H4 at its periplasmic entrance. Opening of the periplasmic entrance is therefore the key to the function of TolC.

An allosteric mechanism has been proposed for TolC opening (Koronakis *et al.*, 2000). This mechanism envisages that the inner coiled-coils α-helices (H7 and H8) undergo an iris-like movement to realign with the outer coiled-coils (H3 and H4), thereby enlarging the pore in a "twist-to-open" transition (Koronakis *et al.*, 2000; Andersen *et al.*, 2002). Recently, the crystal structure of two open states of TolC, $TolC^{RS}$ (370 pS, represents the conductance of membrane) and $TolC^{YFRS}$ (1,000 pS) have been solved, which presents sequential snapshots of the transition to advanced opening (Pei *et al.*, 2011). They supposed that disruption of the interprotomer links is the key to movements at the periplasmic tip (Pei *et al.*, 2011). In the moderated conductance state of $TolC^{RS}$ (370 pS compared with the 80 pS of $TolC^{WT}$), disruption of the bonds of Arg^{367}-Asp^{153} and Arg^{367}-Thr^{152} causes inner helix H7 at the periplasmic tip to undergo a significant twist and expansion around H8. The magnitude of twist and expansion is similar in the advanced open-state $TolC^{YFRS}$ (1,000 pS), with interprotomer distances of 18.9Å ($TolC^{RS}$) and 21.3 Å ($TolC^{YFRS}$).

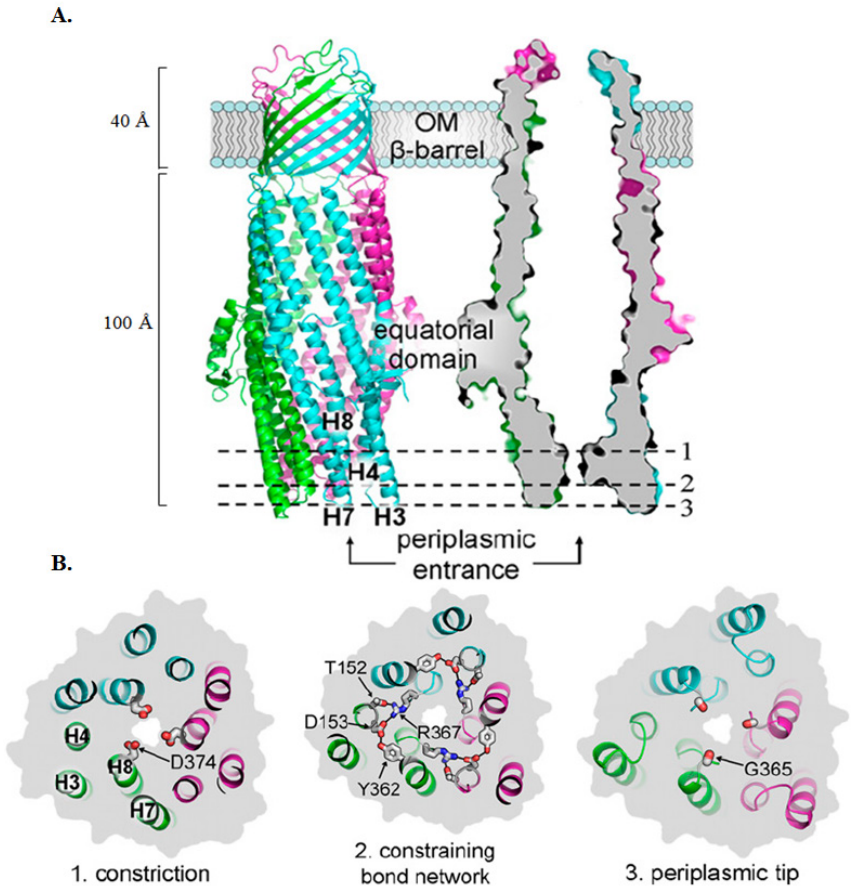

Fig. 20: Structural overview of the TolC periplasmic entrance (Pei *et al.*, 2011). (A) Side view of the resting closed state of trimeric TolC. The individual protomers are colored blue, magenta, and green. The outer membrane embedded β barrel is open to the extracellular medium, but the coiled coils taper to close the periplasmic entrance of the α-helical barrel. H3, H4, H7 and H8 are the periplasmic α-helices that rearrange during the openning of TolC. Dashed lines indicate cross-sections through TolC, at the levels of the following: 1, the narrowest constriction of the pore formed by a ring of Asp^{374} residues; 2, the constraining bond network; and 3, the periplasmic tip. (B) Cross-sections indicated by dashed lines in A, viewed through the pore toward the equatorial domain and OM β barrel. The gray backgroud outlines the surface representation.

II.6.2 Type III secretion system (T3SS)

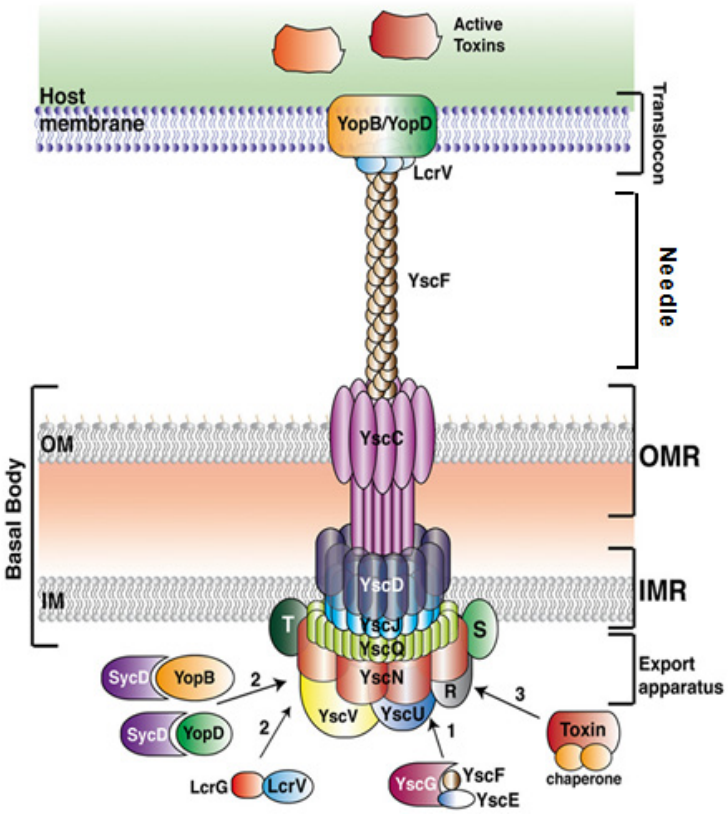

Fig. 21: Schematic diagram of the T3SS of *Yersinia spp* (Izoré *et al.*, 2011). The system is composed of three major parts: the basal body, the needle and the translocon. The basal body is a multi-ring structure that anchors the system to the two bacterial membranes. Upon its formation, the needle protein potentially travels through the ring (step 1) and self-polymerizes on the outside of the bacterium. Subsequently, translocon proteins (step 2) are secreted, and finally, toxins/effectors are injected into the eukaryotic cytoplasm (step 3).

The type III secretion system (T3SS) is used by various Gram-negative bacteria, especially those involved in animal and plant pathogenesis, e.g., *Yersinia, Shigella, Salmonella, Pseudomonas,* enteropathogenic and enterohemorrhagic *Escherichia coli* (EPEC, EHEC) and *Erwinia,* to inject effector proteins directly into the eukaryotic host cell cytoplasm (Moraes *et al.*, 2008; Worrall *et al.*, 2010). The T3S machinery, also known as the injectisome or needle complex, is genetically, structurally and functionally related to bacterial flagella (Blocker *et al*, 2003; Erhardt *et al.*, 2010). One of the differences between the two systems is that the T3SS apparatus contains an OM multimeric protein complex, formed by the protein called secretin. The T3SSs are composed of at least 20 different proteins. However, the core of injectisome proteins, whose sequence are conserved in all known examples, do not exceed nine proteins (Cornelis, 2006). These proteins assemble into three major parts (Fig. 21), including a basal body of the system, a hollow needle-like structure and a 'translocon' (Izoré *et al.*, 2011; Matteï *et al.*, 2011). The assembly of the needle complex occurs in an orderly manner, in which the base

substructure is assembled followed by the assembly of the inner rod and needle substructure (Diepold *et al.*, 2010).

II.6.2.1 The basal body of the T3SS

The basal structure of the injectisome includes a pair of rings in the inner and outer membranes, joined together by a rod. The IM ring (IMR) is proposed to be the first ring to be assembled within the base (Kimbrough and Miller, 2002). However, Diepold *et al.* (2010), by studying the *Yersinia* Ysc system, showed that the formation of the OM ring (OMR) precede that of the IMR. The IMR consists of two proteins (YscJ/MxiJ/PrgK and YscD/MxiG/PrgH in *Yersinia*, *Shigella*, and *Salmonella* spp, respectively) that oligomerize to form two concentric rings of different diameters (Fig. 22). The OMR, associated with the OM and the peptidoglycan layer, is a 12-14-mer of the YscC that belongs to subfamily of secretins (Tamano *et al.*, 2000; Blocker *et al.*, 2001; Burghout *et al.*, 2004b). The proper location and insertion of secretins into the OM require the assistance of a protein of the YscW family, called pilotin (Burghout *et al.*, 2004a). In recent reconstructions of *Salmonella* and *Shigella* needle complexes, the secretin protrudes into the periplasmic space, forming a "neck" region that is potentially formed by its N-terminus and directly contacts the IMR (Fig. 22) (Hodgkinson *et al.*, 2009; Schraidt *et al.*, 2010; Schraid and Marlovits, 2011). This observation was confirmed by experiments in which the crystal structure of the soluble N-terminal domain of EscC (the *E. coli* secretin) was docked into the *S. typhimurium* T3SS electron density map (Spreter *et al.*, 2009). The reconstructuion of the *S. flexneri* needle complex indicates a 12-fold symmetry for the OM secretin-containing region and 24-fold symmetry for the IM region (Fig. 22A) (Hodgkinson *et al.*, 2009). However, a recent high-resolution reconstruction of the *S. typhimurium* needle complex revealed a 15-fold symmetry for the secretin and a 24-fold symmetry for the IM ring, which yields a three-fold symmetry for the overall complex (Fig. 22B) (Schraid and Marlovits, 2011).

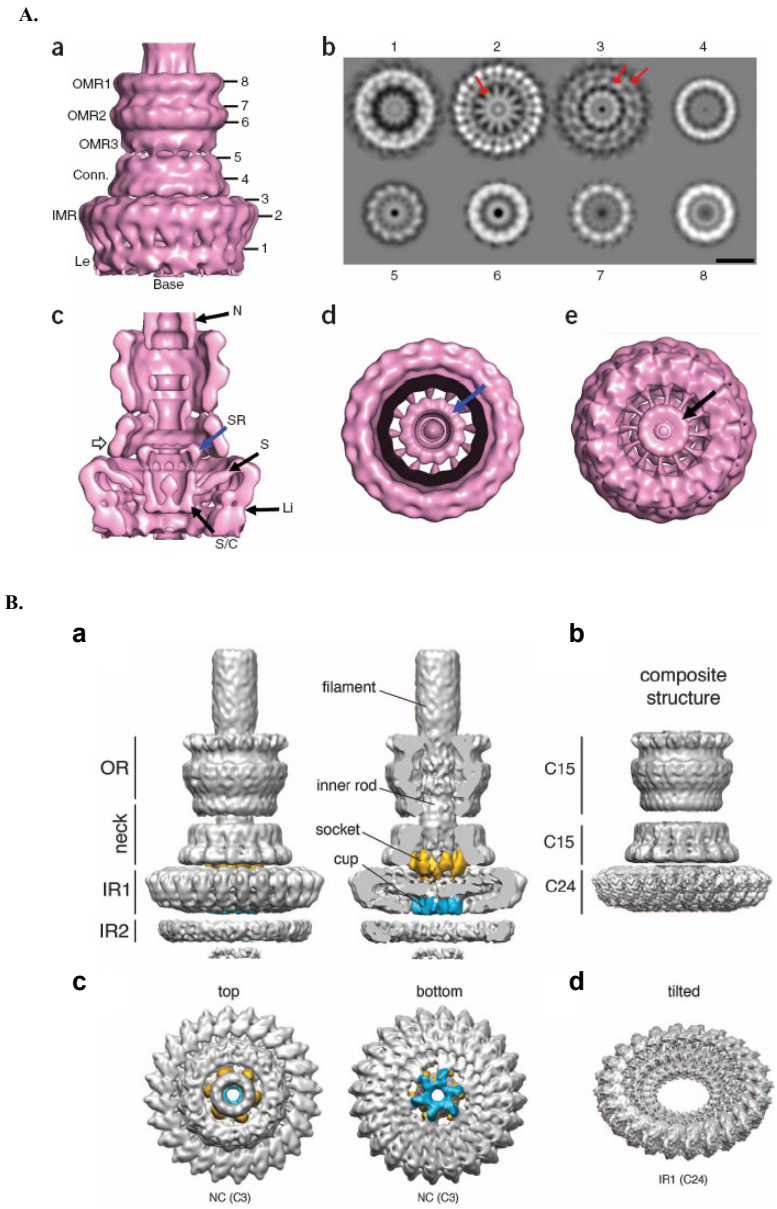

Fig.22: Three-dimension reconstruction of the *S. flexneri* (A) (Hodgkinson *et al.*, 2009) and *S. typhimurium* (B) (Schraid and Marlovits, 2011) needle complex (NC). (A. a) Surface representation. (A. b) Slices through the 3D reconstructions at the linker (1), IMR shoulder (2), shoulder-connector transition (3), connector (4), connector-OMR3 transition (5), OMR2 (6), OMR2-OMR1 transition (7) and OMR1 (8). (A. c) Longitudinal cutaway map. The hollow arrow on the left side of connector indicates the point at which the structure is cut to give the view in d. (A. d) The top view surface (view from outside the cell) and (A. e) The bottom view surface (view from the cytoplasm). (B) Applying symmetries to substructures of different components of the NC, that is, a 24-fold for the IR1 and a 15-fold for the neck and OR, led to higher resolutions. (B. a) Surface representation and (B. c) top and bottom view of *S. typhimurium* NC. (B. d) Tilted view (45°) of IR1 after symmetrization (C24) revealed structural details to subnanometer resolution.

Subsequent to assembly of the basal body, this structure must be rendered competent for secretion by 'export apparatus' which involves five membrane embedded proteins and several cytoplasmic membrane associated proteins (Fig. 21) (Izoré *et al.*, 2011). Although all of the

components of the 'export apparatus' are essential for T3SS, it is unknown whether these membrane proteins exert a common function or even if they exist as a single complex within the bacterial envelope. One of the components of the 'export apparatus', YscU in *Yersinia* was found to work as a substrate specificity switch (Sorg *et al.*, 2007). This protein and its homologues possess N-terminal transmembrane domain and a long cytoplasmic C-terminal domain that undergoes auto-cleavage. YscU cleavage is required to acquire the conformation allowing recognition of translocators. The ATPase is implicated in chaperone/substrate recognition and subsequent dissociation and unfolding of substrates. This process utilizes ATP hydrolysis to energize effector secretion but also depends on PMF (Worrall *et al.*, 2011; Izoré *et al.*, 2011).

II.6.2.2 The needle formation and regulation

Once the basal body is in place, the T3SS needle is synthesized. The T3SS needle is formed by a single small protein of the YscF/PrgI/MxiH family that is synthesized in the cytoplasm and polymerized only after secretion to the surface. It was found that the monomeric forms of needle proteins are not stable. Thus, within the bacterial cytoplasm, the needle-forming protein must be stabilized by their cognate chaperones to prevent its self-assembly or degradation. For example, in *P. aeruginosa*, the needle protein PscF is maintained in its monomeric form within the bacterial cytoplasm by a bimolecular chaperone, PscE-PscG (Plé *et al.*, 2010). Once the needle proteins are secreted to the surface, the needle is built by several hundred subunits that polymerize into an approximately 60 nm in length and 8 nm in diameter (with internal diameter 2-2.5 nm) structure. The length of the needle is highly regulated. It was proposed that YscP protein, which could act as a molecular ruler, determines the length of the *Yersinia* T3SS needle (Journet *et al.*, 2003; Wagner *et al.*, 2009). Wagner *et al.* (2009) further showed that the needle length correlates with the helical content of the ruler part of YscP. The polymerization of protomer into T3SS needles is spontaneous but requires a conformational change in the C-terminal helix of the protein to a β-sheet (Poyraz *et al.* 2010).

After the needle complex is fully assembled, the secretion machine switches substrate specificity, becoming competent for the secretion of translocon components and effector proteins.

II.6.2.3 The translocon

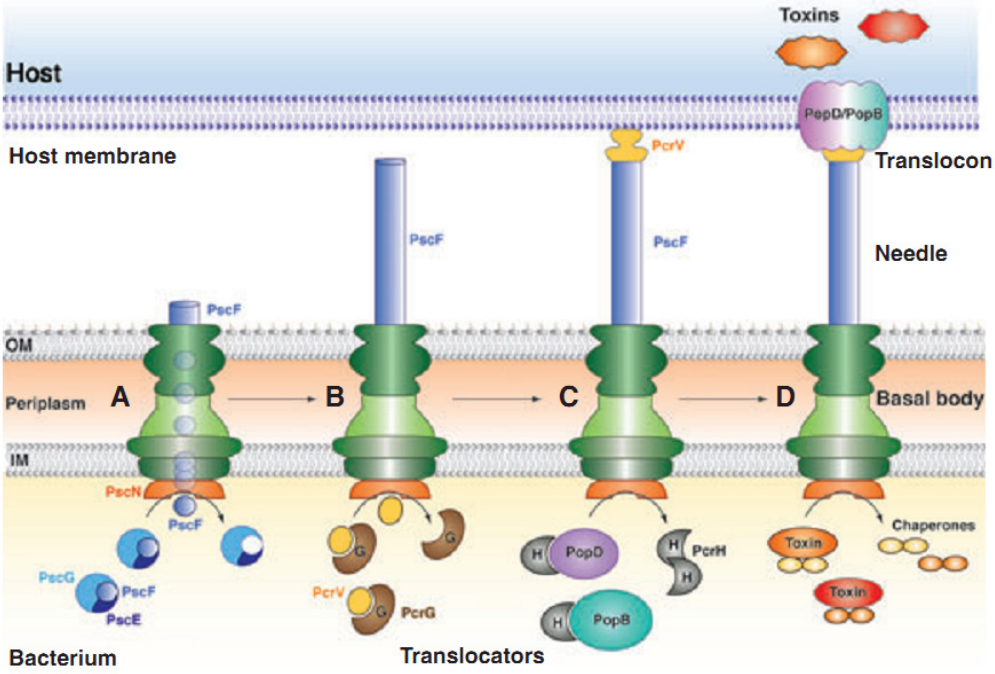

Fig. 23: Schematic diagram illustrating needle and translocon formation, as well as toxin secretion steps in the T3SS of *P. aeruginosa* (Matteï *et al.*, 2011). (A) Once the base rings (green) are in place, the needle protein PscF is released from its chaperones (PcsG and PscE) and polymerizes to form the T3SS needle. (B) The hydropilic translocator PcrV (V antigen) is released from its cytoplasmic partner (PscG) and forms the cap of the PscF needle. (C) Two hydrophobic translocator proteins PopB and PopD release PcrH. (D) Upon formation of the Pop translocon on the eukaryotic membrane, toxins produced in the bacterial cytoplasm release their cognate chaperones and are injected through the translocon pore and into the target cytoplasm.

The translocon is a proteinaceous pore-forming complex that inserts directly into the host cellular membrane. It is composed of one hydrophilic and two hydrophobic translocator proteins. Two hydrophobic translocators (PopB/PopD and YopB/YopD in *Pseudomonas* and *Yersinia*, respectively) form the pore itself within the host cell membrane, while the hydrophilic protein (PcrV and LcrV, respectively) form a tip connecting the distal end of the needle to the membrane spanning translocon (Goure *et al.*, 2005; Mueller *et al.*, 2008). These components are dispensable for secretion but are essential for the injection of type III effectors into the target cytoplasm. Therefore, the translocon components are considered to be the first substrates secreted by the T3SS needle upon cell contact. Before secretion, all three translocon components remain associated with their respective chaperones and are stored in the cytoplasm (Fig. 23) (Matteï *et al.*, 2011). In the bacterial cytoplasm, the two hydrophobic translocators are associated with a common chaperone that shares a considerable sequence identity even in distant species. Upon cell contact, the chaperones are released and the unfolded translocators presumably travel through the interior of needle. Once having reached outmost extremity of the conduit, they are

refolded and oligomerized to form the translocation pore (Fig. 23). Indeed, several studies have analyzed the structure of the pore by different methods (Ide *et al.*, 2001; Dacheux *et al.*, 2001; Schoehn *et al.*, 2003). The pore size was estimated between 3.0 and 5.0 nm. An equimolar mix of the two translocators PopB and PopD of the *P. aeruginosa* T3SS *in vitro* led to the formation of ring structures, suggesting that PopB and PopD oligomerize to form ring-like complexes (Faudry *et al.*, 2006).

II.6.2.4 The assembly of the system and protein secretion

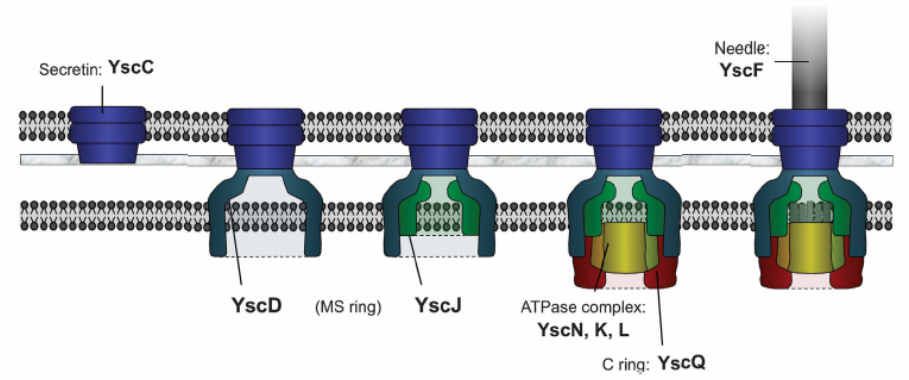

Fig. 24: Model of assembly of the *Yersinia* injectisome (Diepold *et al.*, 2010). Formation of the injectisome is initiated by formation of the secretin ring in the OM. Next, YscD attaches to YscC, which allows the subsequent completion of the membrane and supramembrane (MS) ring by attachment of YscJ. After the formation of the membrane ring structures, the ATPase-C ring complex, consisting of YscN, K, L, and Q assembles at the cytoplasmic side of the injectisome. Afterwards, the needle consisting of YscF and LcrV can be assembled.

The assembly of the T3SS apparatus appears to be a conserved, tightly regulated and inducible process. Recently, it was shown that the assembly of the injectisome starts with the formation of the stable secretin ring in the OM, and proceeds inwards through discrete attachment steps of YscD and YscJ at the IM. After the formation of the membrane rings, the components of the cytosolic ATPase-C ring complex assemble at the cytosolic side of the injectisome. Afterwards, the needle and translocon can be assembled (Fig. 23 and 24) (Diepold *et al.*, 2010; Matteï *et al.*, 2011). However, Wagner *et al.* (2010) showed that the assembly process is initiated by the deployment of a subset of the conserved IMP components of the export apparatus. Upon assembly completion, the T3SS switches into a state that can be termed as 'standby' mode. The switch from a standby mode to active injection may be triggered by the contact with the host cell membrane (Enninga and Rosenshine, 2009). The needle could transmit a signal back to the bacterium by altering its helical state or changing in the packing of the needle (Kenjale *et al.*, 2005; Deane *et al.*, 2006). The cytoplasmic face of the T3SS reconginzes the effectors and initates the transport. The signal leading to substrate recognition has been proposed to be

encoded either in the N-terminal peptide or in the 5'-signal in its mRNA (Blaylock *et al.*, 2008; Arnold *et al.*, 2010). Chaperone dependent processes might also serve as additional signal or signal enhancer.

II.6.3 Type IV secretion system (T4SS)

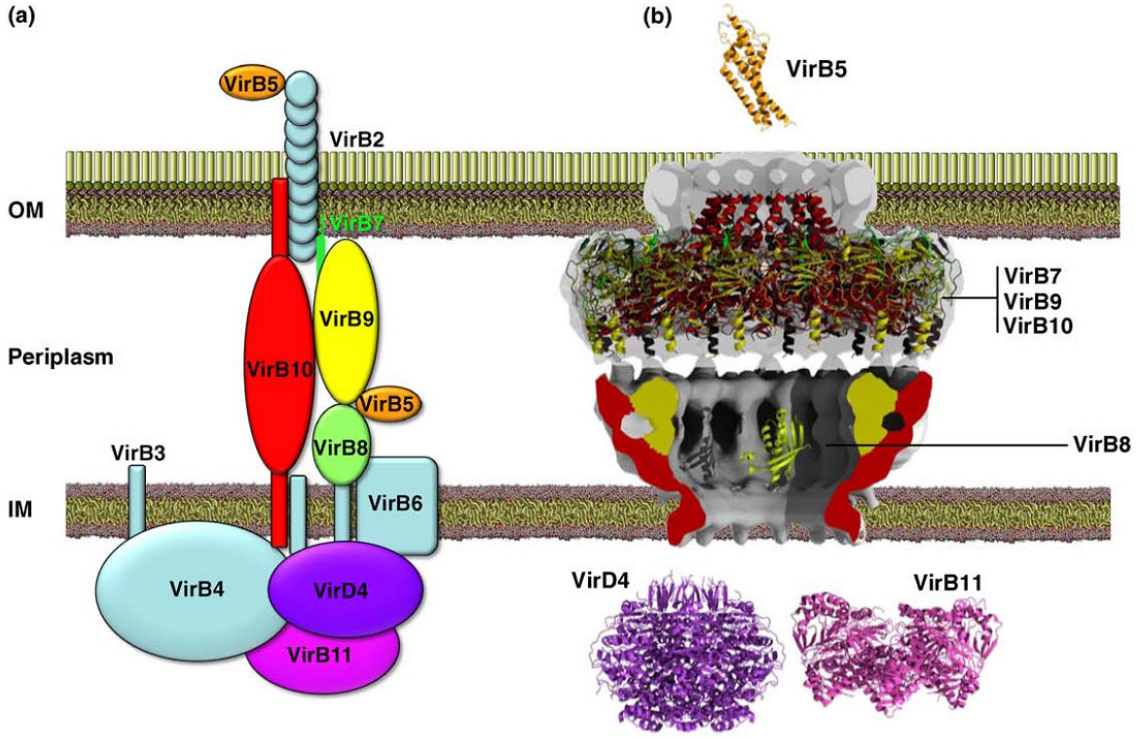

Fig. 25: Secretion pathway and structure of the T4SS (Waksman and Fronzes, 2010). (a) The T4SS composition and assembly. The components are represented according to their proposed localization. Most (but not all) of the interactions that have been confirmed biochemically are indicated by the physical proximity of the schematic representations of each protein. (b) T4SS component structures. The atomic structures are shown in ribbon representation. They include full-length VirB5 (in orange), the VirB8 periplasmic domain (in light green), full-length VirB11 (in violet), the VirD4 soluble domain (in magenta) and the T4S OM complex comprising full-length VirB7 (in green) and the VirB9 CTD (in yellow) and VirB10 CTD (in red). The structure of the core complex determined using cryo-EM and single particle analysis is rendered as a cut-out volume (in grey). The core complex is composed of the full-length VirB7, VirB9 and VirB10 proteins.

The T4SSs are widely distributed among Gram-negative and-positive bacteria and fulfil a wide variety of fuction, such as mediating the conjugative transfer of plasmids and other mobile DNA elements to bacterial recipient cells, or delivering protein or DNA substrates to eukaryotic target cell. Another type of T4SSs mediates DNA uptake (transformation) or release, thereby promoting further genetic exchanges (Wallden *et al.*, 2010; Waksman and Fronzes, 2010). Although different T4SSs have different functions, they share the same central components and probably assemble and function in a similar manner. In Gram-negative bacteria, many T4SSs are

similar to the *A. tumefaciens* VirB-VirD T4SS (Fig. 25), which is one of the best-studied T4SSs. This system comprises 12 proteins named VirB1 to VirB11 and VirD4 (Christie *et al.*, 2005). These proteins can be grouped according to their functions and/or cellular locations: an extracellular pilus composed of a major (VirB2) and a minor (VirB5) subunit; three ATPases located at the IM, i.e., VirB4, VirB11, and VirD4; an IM channel formed by VirB6, VirB8, and the NTDs of VirB9 and VirB10; an OM complex composed of VirB7, the CTDs of VirB9 and VirB10 (Chandran *et al.*, 2009; Waksman and Fronzes, 2010).

II.6.3.1 Structure of the core complex

The structure of T4SS core complex from the conjugative pKM101 plasmid has been determined (Fronzes *et al.*, 2009). This structure showed that VirB7, VirB9 and VirB10 homologues form a tightly associated 'core complex' that is inserted in both the inner and outer membranes. The core complex is a cylindrical structure of 185 Å in diameter and 185 Å in length containing two layer termed O (outer) and I (inner) linked by thin stretches of density (Fig. 25b and Fig. 26) (Fronzes *et al.*, 2009).

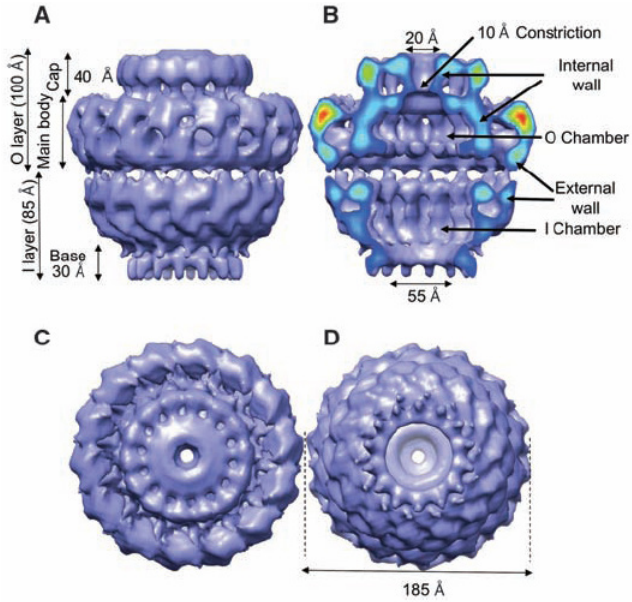

Fig. 26: Cryo-EM structure of the TraN/VirB7, TraO/VirB9, and TraF/ VirB10C-ST core complex (Fronzes *et al.*, 2009). (A) Side view. (B) Cut-away side view. Electron density is color-coded from red to blue to indicate regions of strong to weaker density, respectively. (C) Top view (view from outside the cell). (D) Bottom view (view from the cytoplasm).

Each layer forms a double-walled ring-like structure that defines hollow chambers inside the complex. The I layer is anchored in the IM and resembles a cup with a cytoplasmic opening of 55 Å in diameter. It consists of the N-terminal domains (NTDs) of the VirB9 and VirB10 homologues. The O layer consists of a main body and a narrower cap defining a 10 Å-diameter

hole. It is inserted into the OM and is composed of the VirB7 homologue, the C-terminal domains (CTD) of VirB9 and CTD of VirB10 homologues.

II.6.3.2 Structure of the outer-membrane complex

Crystal structure of the T4SS OM complex containing the entire O layer has been solved recently (Chandran *et al.*, 2009). In this structure, the O layer has two parts (Fig. 27), i.e., the main body and the cap. The cap is made of a hydrophobic ring of two-helix bundles contributed by 14 CTDs of TraF/VirB10 defining a 32 Å channel. The main body is made of the rest of CTDs of TraF/VirB10, TraO/VirB9 and TraN/VirB7. It has a 172 Å diameter. When the complex is viewed from the extracellular milieu, the VirB10 CTD forms an inner ring surrounded by the VirB9-VirB7 complex. The VirB7 forms spokes that radially cross the entire assembly. Because VirB10 homologues span the entire space between two membranes and are inserted in both, they are suggested to play regulatory roles, probably sensing conformational changes due to substrate binding in the cytosol and relaying them to regulate OM channel opening and closing (Wallden *et al.*, 2010; Waksman *et al.*, 2010). Indeed, Banta *et al.* (2011) recently showed that a VirB10 mutation disrupts a gating mechanism in the core chamber, which confirmed the role of VirB10 in regulating passage of secretion substrates across the OM.

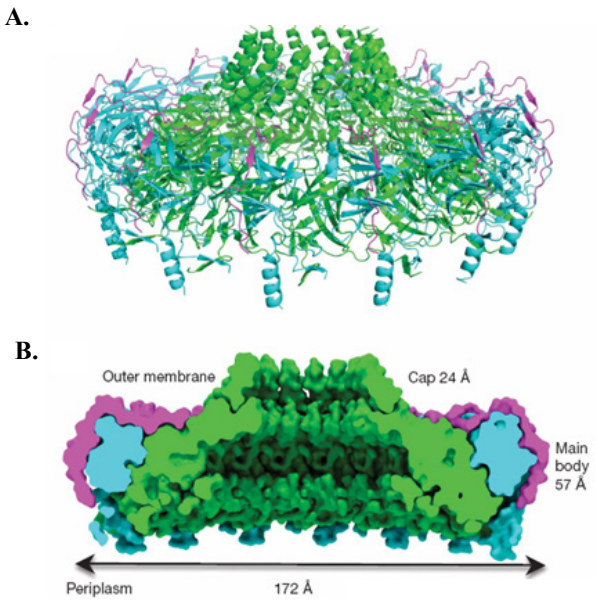

Fig. 27: The T4S system outer-membrane complex (Chandran *et al.*, 2009). Ribbon diagram (A) and space-filling cut-away (B) of the tetradecameric complex. $TraF_{CT}$/$VirB10_{CT}$, $TraO_{CT}$/$VirB9_{CT}$ and TraN/VirB7 subunits are colored green, cyan and magenta, respectively. In (B), dimensions and labelling of the various parts of the complex are provided.

II.6.3.3 Structure of the inner-membrane complex

The NTDs of VirB9 and VirB10 constitute the I layer of the T4SS core complex which is

inserted in the IM via the VirB10 N-terminal transmembrane segment. It was suggested that two membrane proteins VirB6 and VirB8 are also involved in formation of the IM pore. VirB6 is probably a central component of the IM channel. It is a polytopic IM protein with a periplasmic N terminus, five TMS and a cytoplasmic CTD (Jakubowski *et al.*, 2004). VirB8 is a bitopic IM protein consisting of an N-terminal TMS and a large periplasmic CTD (Terradot *et al.*, 2005). Both VirB6 and VirB8 were shown to directly contact the substrate during secretion in *A. tumefaciens* (Cascales and Christie, 2004).

II.6.3.4 The cytoplasmic ATPase

Three ATPases, VirB4, VirB11 and VirD4, energize the system for apparatus assembly and substrate translocation through the channel. VirB4 is one of the less characterized with no crystal structure solved to date. Various oligomerization states of this protein have been reported (Rabel *et al.*, 2003; Arechaga *et al.*, 2008; Durand *et al.*, 2010). However, ATPase activity has only been reported for hexameric forms (Arechaga *et al.*, 2008; Durand *et al.*, 2010), indicating that VirB4 functions as a hexamer, similarly to VirB11 and VirD4.

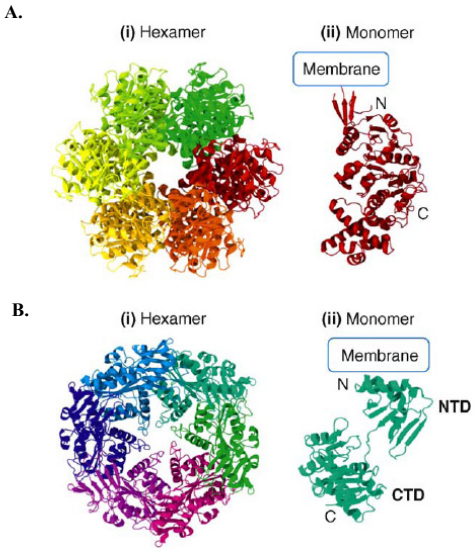

Fig. 28: Crystal structure of the T4SS ATPases VirD4 and VirB11. (A) The hexameric (i) and monomeric (ii) crystal structures of *E. coli* VirD4 homologue TrwB (Gomis-Rüth *et al.*, 2001). (B) the *H. pylori* VirB11 homologue Hp0525 (Savvides *et al.*, 2003). CTD, C-terminal domain; NTD, N-terminal domain.

VirB11 belongs to a family of ATPases termed 'traffic ATPase', which are associated with Gram-negative bacterial typeII, type III, type IV and typeVI secretion systems (Fronzes *et al.*, 2009). VirB11 homolgues are hexameric peripheral IM proteins (Krause *et al.*, 2000). The crystal structure of *H. pylori* VirB11 homologue (HP0525) revealed that each monomer consists of two domains formed by the N- and C-terminal halves of the protein (Fig. 28B) (Yeo *et al.*, 2000; Savvides *et al.*, 2003). The nucleotide-binding site is at the interface between the two domains.

In the hexamer, the NTD and CTD form two separate rings defining a chamber of ~50 Å in diameter (Fig. 28B).

The ATPase VirD4 functions as coupling protein (CP) in DNA-transferring systems, coupling DNA substrate processing and translocation, and as substrate receptor in effector translocation systems where it recruits substrates to the T4SS for secretion (Wallden *et al.*, 2010). CPs are anchored in the bacterial IM by their N-terminal membrane helix. The crystal structure of a soluble fragment of T4SS CP, namely TrwB, revealed a globular hexameric assembly composed of two distinct domains with a ~20 Å-wide channel in the middle (Gomis-Rüth *et al.*, 2001) (Fig. 28A). It was suggested that TrwB might operate as a motor, pumping DNA through its central channel using the energy derived from ATP hydrolysis (Tato *et al.*, 2007). Substrates recognition occurs through specific interactions between the CPs and signal sequences harbored by their substrates (Waksman and Fronzes, 2010). For the DNA substrate, signal sequences were carried by relaxase components of DNA transfer intermediates. For effector proteins, secretion signals have been initially positioned near the C termini and presumed to consist of clusters of hydrophobic or positive charged residues (Schulein *et al*., 2005). Howerever, recent findings suggested that the substrate recognition is mediated by a combination of C-terminal signal, additional intrinsic motifs, and other cellular factors, e.g., chaperones and accessory proteins (Alvarez-Martinez and Christie, 2009).

II.6.3.5 The pilus

VirB2 and VirB5 form pilus structure extending from the extracellular surface. The pilus might be used as a conduit for substrates or for adhesion (Waksman and Fronzes, 2010). The VirB2 of *A. tumefaciens* forms the major pilus component and is cyclized via an intramolecular covalent head-to-tail peptide bond (Eisenbrandt *et al.*, 1999). No structural information for VirB2-like proteins is available. However, a crystal structure is available for the minor pilus component VirB5 homologue in pKM101 TraC (Yeo *et al.*, 2003). The structure reveals a three-helix bundle flanked by a smaller globular part (Fig. 25b). VirB5 was shown to localize at the tip of the T pilus (Aly and Baron, 2007) and to play a role in adhesion and host recognition (Yeo *et al.*, 2003).

II.6.4 Type V secretion system (T5SS)

The T5SS comprises the most wide-spread and simplest secretion system in Gram-negative bacteria (Hodak and Jacob-Dubuisson, 2007). This system allows secretion of proteins across the OM via a transmembrane pore formed by a β-barrel structure without any need of energy (Yen *et al.*, 2002; Desvaux *et al.*, 2004). The T5SSs are subdivided into two branches, i.e.,

autotransporter (Type Va) and two-partner secretion pathway (Type Vb) (Jacob-Dubuisson *et al.*, 2004; Cotter *et al.*, 2005). Proteins secreted via these systems have similarities in their primary structures composed of three domains (Fig. 29) (Hodak and Jacob-Dubuisson, 2007): i) the N-terminal signal sequence for IM translocation; ii) the functional passenger domain; and iii) the C-terminal translocation unit.

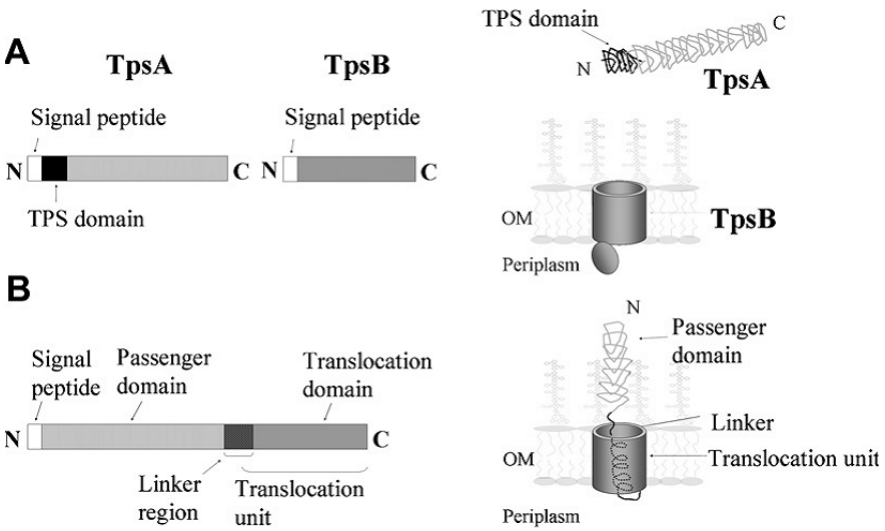

Fig. 29: Proteins composing the two-partner system (TPS) (A) and autotransporter (AT) (B) (Hodak and Jacob-Dubuisson, 2007). (A) TpsA proteins are the secreted components containing the conserved N-terminal, ~250-residue-long TPS domain, followed by a long region forming essentially β-strands. The TpsB transporter is composed of a C-terminal β-barrel and an N-terminal periplasmic region containing a POTRA domain. (B) The AT proteins contian an N-terminal passenger domain rich in β-strands, similarly to TpsA proteins, and a C-terminal β-barrel. A linker region forming an α-helix separates the two domains.

II.6.4.1 Autotransporter protein secretion (AT)

The ATs typically consist of a 20-400-kDa passenger domain that possesses the effector functions and a 10-30-kDa β-domain facilitating translocation across the OM (Dautin and Bernstein, 2007). The ATs can be classified into two groups, i.e., classical AT and trimeric AT (Cotter *et al.*, 2005). The differences between classical AT and trimeric AT are that (Cotter *et al.*, 2005; van Ulsen, 2011; Lyskowski *et al.*, 2011):

i) the C-terminal translocator domain of the classical AT is monomeric whereas the trimeric AT is trimeric (Fig. 30);

ii) the structure of the passengers is rather different, the passenger domain of classical ATs generally form a right-handed β helical structure, while different folds have been observed in various trimeric ATs passenger domains (Fig. 31).

iii) the passenger domain is released from the translocator domain into the extracellular

milieu by a proteolytic cleavage in most classical ATs,, whereas in trimeric ATs, all passenger domain studied so far remain covalently attached to their β barrel membrane anchor.

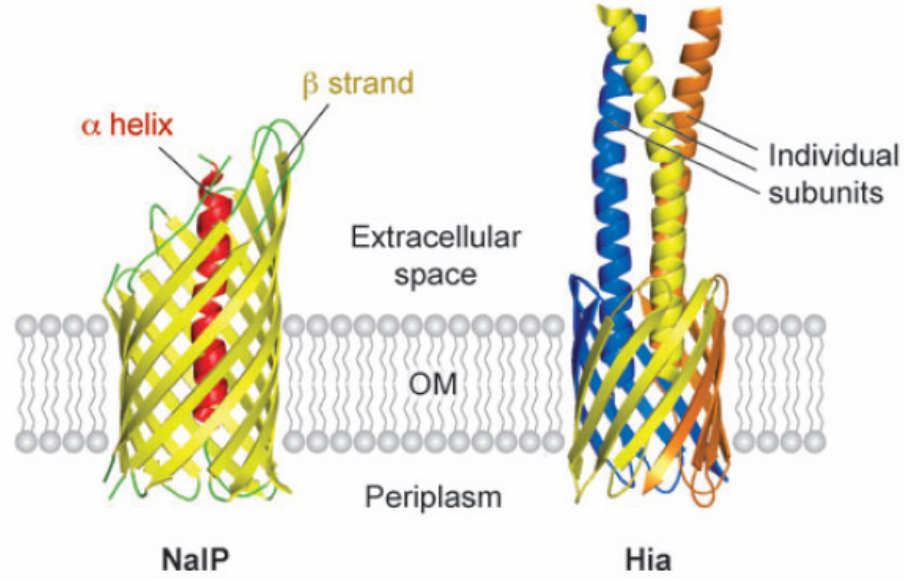

Fig. 30: Crystal structures of C-terminal fragments of the classical autotransporter NalP (Oomen *et al.*, 2004) and the trimeric autotransporter Hia (Meng *et al.*, 2006). In the NalP structure, β strands are colored yellow and α helix is colored red. In the Hia structure, individual subunits are colored blue, yellow, and orange.

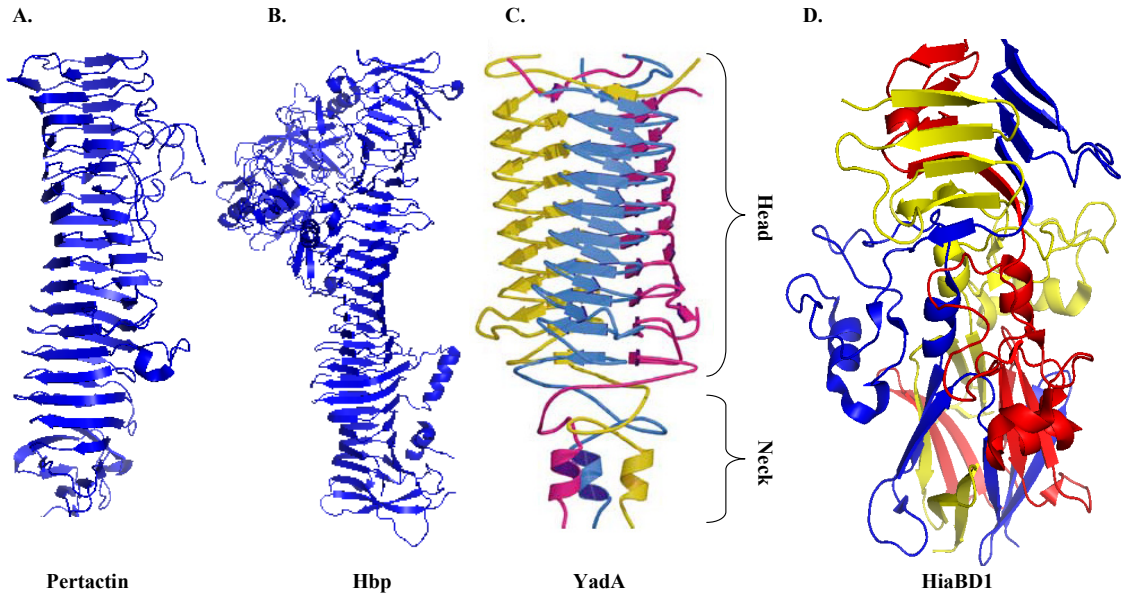

Fig. 31: The crystal structure of different autotransporter (AT) passenger domains. (A) Pertactin passenger domain reveals 16-turn-β helix fold (Emsley *et al.*, 1996). (B) A remarkable pertactin-like 24-turn β helical structure of Hemoglobin protease Hbp passenger domain (Otto *et al.*, 2005). (C) The trimeric crystal structure of the *Y. enterocolitica* collagen binding (YadA) passenger domain (Nummelin *et al.*, 2004) and (D) *H. influenzae* Hia adhesion binding domain (HiaBD1) (Yeo *et al.*, 2004).

Despite these aforementioned differences, the mechanism of ATs is generally assumed to be

the same for both classical ATs and trimeric ATs. All AT proteins are synthesized as pre-pro-proteins and exported across the IM via a Sec-dependent process, initiated by its N-terminal signal sequence, and finally released in the periplasm in a pro-protein form. Once in the periplasm, it was originally supposed that ATs mediate their own transport across OM. However, recent research suggests that they are chaperoned by certain periplasmic proteins, such as SurA and DegP to the Bam (Omp85) complex located in the OM which may assist in translocation (van Ulsen, 2011; Lazar Adler *et al.*, 2011). Indeed, several ATs have been shown to interact directly with the periplasmic chaperones including SurA and DegP (Ieva and Bernstein, 2009; Ruiz-Perez *et al.*, 2009) and Bam complex (Sauri *et al.*, 2009; Lehr *et al.*, 2010). BamA forms a 16-stranded β barrel with a pore size of ~2.5 nm which is significantly larger than the AT β barrel (~1.2 nm). This would allow for translocation of partially folded ATs. However, the mechanism by which the passenger domain is translocated across the OM remains to be elucidated. Three models have been proposed to explain the autotransportation mechanism (Fig. 32) (Hodak and Jacob-Dubuisson, 2007; Dautin and Bernstein, 2007; Lyskowski *et al.*, 2011), i.e., i) haripin model, in which translocation might be initiated by the formation of a hairpin at the C-terminus of the passenger domain that is maintained while proximal segments of the polypeptide are threaded through the pore in a linear fashion; ii) Omp85/YaeT (Bam complex) assisted secretion model, in which the transport of the passenger domain across the OM and the integration of the β domain into the OM are catalyzed by the Bam complex; iii) multimeric model, in which the passenger domain folds at least partially in the periplasm and is then transported across the OM through a large channel created by the oligomerization of the β domain.

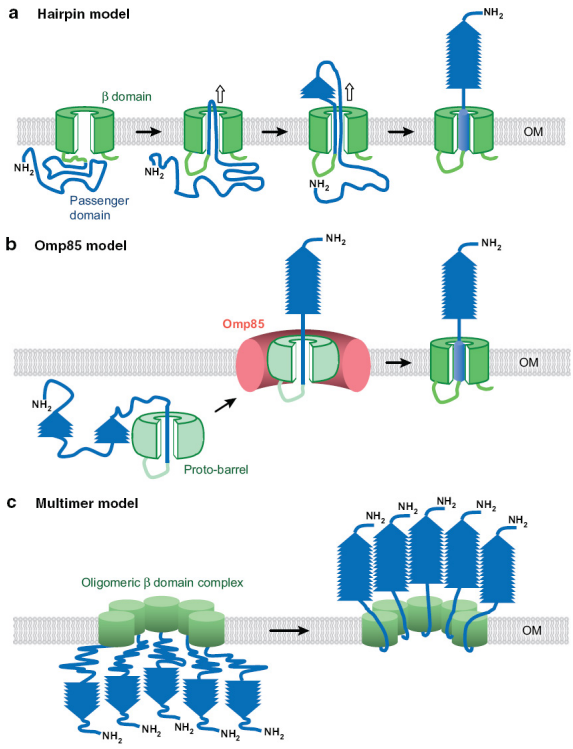

Fig. 32: Models for the autotransport mechanism (Dautin and Bernstein, 2007). (a) The hairpin model, (b) the Omp85 model and (c) the multimer model. The passenger domain (blue), the β barrel (dark green) and Omp85 (pink) are colored differently.

II.6.4.2 The two-partner system (TPS)

Although the TPS resembles the AT in several aspects, for example, exoproteins contain all the information for translocation through cell envelope, translocation of exoproteins across the OM via a transmembrane pore formed by a β-barrel, there are fundamental differences in the mechanism of secretion. Unlike AT, the passenger domain and the pore forming β-domain of TPS are encoded by two separate genes, refered as member of TpsA and TpsB families, respectively (Fig. 29A) (Hodak and Jacob-Dubuisson, 2007). Most of the TpsA proteins share two common features, i.e., an N-terminal conserved region containing ～300 residues, termed the "TPS domain" and stretches of repeated sequences that have been predicted to form β-helical structures (Junker *et al.*, 2006; Kajava and Steven, 2006). The crystal structure of two TpsA proteins, fiamentous hemagglutinin adhesin FHA and *H. influenzae* adhesin HMW1, revealed that the TPS domain folds into a β-helix (Fig. 33A) (Clantin *et al.*, 2004; Yeo *et al.*, 2007). TpsB transporters specifically recognize their cognate TpsA partners in the periplasm and mediate their translocation across the OM through a hydrophilic channel. TpsB belongs to the Omp85 (BamA)/TpsB superfamily involved in assembly of proteins into, or translocation across the OM (Delattre *et al.*, 2011). All the members of this superfamily share a similar organization, with one to seven POTRA domains followed by a C-terminal TM β barrel. The FHA/FhaC pair of

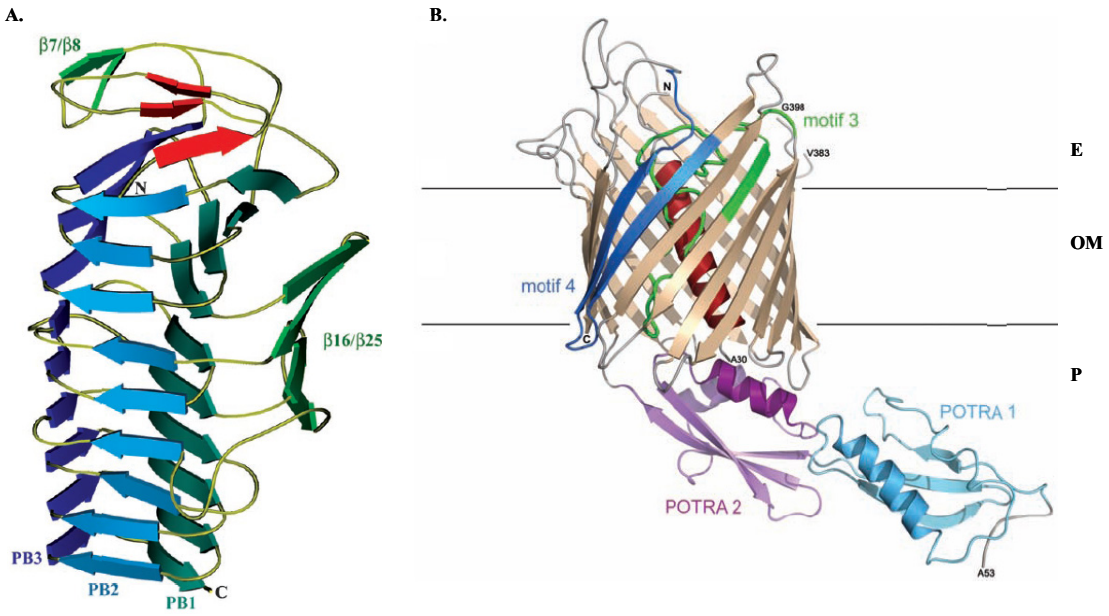

Fig. 33: Crystal structures of TPS domain of fiamentous hemagglutinin FHA (A) and FhaC (B). (A) Ribbon representation of the overall structure of Fha30. The helix β-sheets PB1, PB2 and PB3, the β-hairpin β7/β8, and the β-sheet β16/β25 are shown (Clantin *et al.*, 2004). (B) Ribbon representation of FhaC viewed from the membrane plane. Putative position of OM boundary is indicated with horizontal lines, with the extracellular side (E) at the top and the periplasm (P) at the bottom. The α helix H1 is colored red, POTRA 1 light blue, POTRA 2 purple. (Clantin *et al.*, 2007).

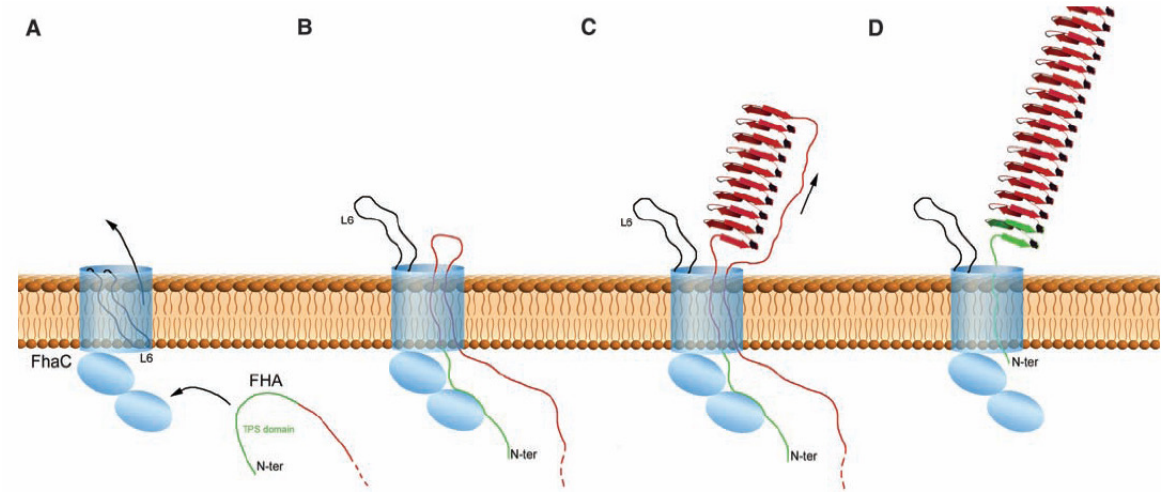

Fig. 34: Proposed model of FHA transport across the outer membrane (Clantin *et al.*, 2007). (A) The TPS domain of FHA in an extended conformation interacts with POTRA1 of FhaC. (B) The channel opens after conformational changes of loop L6, and translocation initiates, with FHA adopting transiently an extended β hairpin structure. (C) FHA progressively folds and elongates into its β-helical fold. (D) After the C terminus of FHA has reached the surface, the TPS domain dissociates from POTRA 1 and is translocated. The folding of the TPS domain caps the N terminus of the FHA β helix.

B. pertussis represents a paradigm model TPS system. The crystal structure of FhaC revealed a 16 β-barrel that is occluded by an N-terminal α-helix and a hairpin-like loop, along with a periplasmic module composed of two POTRA domains (Fig. 33B) (Clantin *et al.*, 2007). According to the FhaC structure and functional experiments, Clantin *et al.* (2007) proposed a model for FHA transport across the OM (Fig. 34). FHA is exported across the IM in a Sec-dependent manner and transits through the periplasm in an extended conformation. It was shown that DegP chaperones the extended FHA polypeptide in the periplasm (Baud *et al.*, 2009). The N-terminal TPS domain of FHA initially interacts in an extended conformation with the FhaC POTRA1 domain in the periplasm. This interaction would then bring the region corresponding to the first repeats of the central β-helical domain of FhaC in proximity to the tip of loop L6. Conformational changes in FhaC would then expel loop L6 out of the β-barrel, opening a larger channel for FHA translocation. FHA folds progressively at the bacterial surface into a long β-helix. Recently, Delattre *et al.* (2011) showed that both POTRAs are involved in FHA recognition. When the TPS domain of FHA emerges in the periplasm, it is initially attracted to FhaC's POTRA1 by electrostatic interactions. In a second step, extended segments of FHA interact with the edges of the POTRA domain by β augmentation. POTRA2 positions FHA in a favourable manner for translocation.

II.6.5 Type VI secretion system (T6SS)

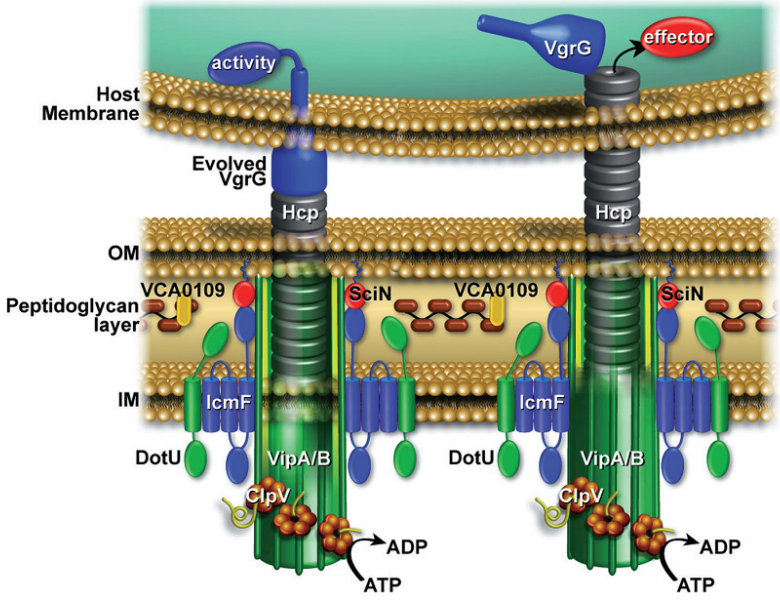

Fig. 35: Structure and function of the T6SS (Bönemann *et al.*, 2010). VipA/VipB tubules are suggested to act as tail sheath proteins by engulfing Hcp tubes. A pilus-like structure formed by Hcp and VgrG, punctrues the lipid bilayer of target cells. The role of T6SSs in bacterial virulence is either based on the exposure of evolved VgrG-linked effector domains (left part) or the delivery of effector proteins to cytosol of target cells (right part).

The recently identified T6SS is a widely distributed protein export machine. It is capable of cell-contact-dependent targeting of effector proteins between Gram-negative bacterial cells (Pukatzki *et al.*, 2009; Schwarz *et al.*, 2010). This system not only functions in pathogenesis, but also was found to plays a role in biofilm formation and killing of other bacterial cells (Enos-Berlage *et al.*, 2005; Jani and Cotter, 2010; Zheng *et al.*, 2011). T6SS gene clusters contain from 15 to more than 20 genes and secrete substrates lacking N-terminal hydrophobic signal sequences (Bingle *et al.*, 2008; Bönemann *et al.*, 2010). The proteins encoded by T6SS gene clusters are assembled into a multi-component apparatus (Fig. 35) (Cascales, 2008; Pukatzki *et al.*, 2009; Bönemann *et al.*, 2010). Bioinformatic analysis has identified a core of 13 genes that may constitute the minimal member needed to produce a functional apparatus (Boyer *et al.*, 2009).

T6SS core components include two IM components, IcmF (intracellular multiplication protein F) and DotU/IcmH orthologs (Zheng *et al.*, 2007), an AAA+ (ATPases associated with various cellular activites) family ATPase called ClpV (Bönemann *et al.*, 2010). ClpV associates with several other conserved T6SS proteins and its ATPase activity has been reported to be essential for T6SS function. In most T6SSs, hemolysin co-regulated protein (Hcp) and valine-glycine repeat protein G (VgrG) are both exported by T6SS and required for the function of the T6SS machine (Leiman *et al.*, 2009; Hachani *et al.*, 2011). However, how T6SS machines assembles and the mechanism by which effectors are delivered via the secretory apparatus have remained elusive. Current models of the T6SS derive from the observation that several of its components share structural homology to bacteriophage T4 proteins (Pukatzki *et al.*, 2007; Leiman *et al.*, 2009; Bönemann *et al.*, 2010), it has been proposed that target cell recognition and effector delivery occur in a process analogous to bacteriophage entry (Fig. 36) (Kanamaru, 2009; Bönemann *et al.*, 2010). Indeed, the structure of Hcp and VgrG provide evidence for an evolutionary relationship between T6SSs and the cell-puncturing machinery of bacteriophage. The crystal structure of Hcp revealed the formation of hexameric rings (Mougous *et al.*, 2006), which readily polymerize in solution to form nanotubes with external and internal diameters of 85 Å and 40 Å, respectively and are up to 100 nm long (Mougous *et al.*, 2006; Jobichen *et al.*, 2010). This structure shows an evolutionary relationship to the T4 tail tube protein gp19 (Leiman *et al.*, 2009). VgrG proteins show structural similarities to the spike complex of the T4 bacteriophage, which is composed of the $(gp27)_3$-$(gp5)_3$ complex. This complex is used by phage to puncture the bacterial cell surface, which allows to inject DNA into the cytoplasm (Pukatzki *et al.*, 2007; Leiman *et al.*, 2009). VgrG may form a trimeric 'needle' at the distal end of a tail tube-like structure formed by the polymerisation of hexameric rings of Hcp (Pukatzki *et al.*, 2009).

However, because the triple β-helix of VgrG is too narrow to function as a protein channel, it might dissociate from the Hcp tubule after it has punctured the target cell membrane (Bönemann *et al.*, 2010). In addition, some VgrGs carrying an additional C-terminal extension may act as genuine effectors. These VgrGs have been named 'evolved VgrGs' (Pukatzki *et al.*, 2009). Recently, another T6SS component HsiF (Lossi *et al.,* 2011) shows similarity to a T4 phage protein gp25, which was proposed to have lysozyme activity. However, lysozyme activity for HsiF proteins was not detectable. Several other components of T6SS are also characterized. The IM proteins IcmF interacts with the IM protein DotU/IcmH and the lipoprotein SciN that is tethered to the OM and is exposed to the periplasm (Sexton *et al.*, 2004; Aschtgen *et al.*, 2008). This IcmF-DotU/IcmH-SciN complex might form the core of a transmembrane-spanning structure (Bönemann *et al.*, 2010). The cytoplasmic domain of IcmF has a conserved Walker A motif implicated in nucleotide binding and hydrolysis. Thus, IcmF may be involved in energizing of T6SS (Ma *et al.*, 2009b).

Based on the overall similarities in architecture between VipA and VipB tubules and the viral tail sheath structure, it was proposed that contraction of VipA/VipB tubules could energize the injection of putative Hcp tubules with the VgrG tip on top into target cells (Fig. 36). ClpV might be required to export VipA and VipB subunits into the periplasm, followed by VipA/VipB tubule reformation and engulfment of the Hcp tube (Fig. 36B). Alternatively, it might need to remove cytosolic VipA/VipB tubules that do not harbor an engulfed Hcp tube (Fig. 36C).

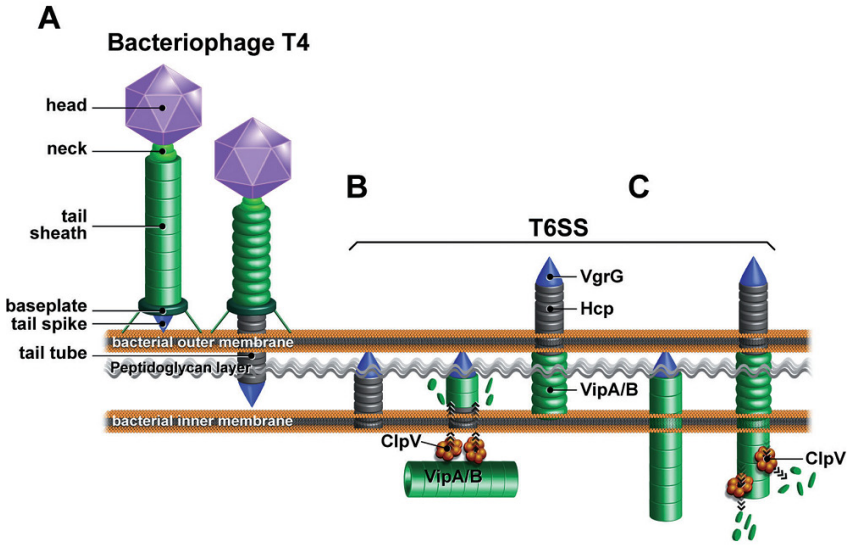

Fig. 36: Potential similarities in the injection mechanisms of tailed bacteriophage and T6SS (Bönemann *et al.*, 2010). (A) Contraction of the T4 tail sheath structure upon contact with host cells provides the energy to push the tail needle through the OM of target cells. Contraction of VipA/VipB tubules is suggested to have a similar function leading to the export of Hcp and VgrG. (B and C) Putative roles of the ClpV in causing contraction of periplasmic VipA/VipBs.

III Type II secretion system (T2SS)

The T2SS was first discovered in *Klebsiella oxytoca*. This system, called the Pul system, is required for secretion of the starch-hydrolyzing lipoprotein, pullulanase PulA (D'Enfert *et al.*, 1987). This system have then been demonstrated in numerous other Gram-negative bacteria, including human pathogens such as *Vibrio cholerae* (Eps) and *Pseudomonas aeruginosa* (Xcp), fish pathogens such as *Aeromonas hydrophila* (Exe) and plant pathogens such as *Erwinia chrysanthemi*, *Erwinia carotovora* (Out) and *Xantomonas campestris* (Xps) (Cianciotto *et al.*, 2005). In these bacteria, the T2SSs secrete important virulence factors directly involved in the pathogenesis. Sequencing of bacterial genomes has identified T2S-like genes in numerous other species (Cianciotto, 2005). This system is highly conserved in various Gram-negative bacteria and notably among human and plant pathogens where this machinery is often a major virulence factor (Cianciotto, 2005).

III.1 Genetic organization of the T2SS

The number of genes identified as being essential for theT2SS, also referred to as Gsp (general secretory pathway), varies from 12 to 16 dependent on species (Filloux, 2004). The homologous genes and gene products have been designated in most species by letters A to O and S. However, in *Pseudomonas*, the letters P to Z and A have been used instead. *gsp* genes are often organized into one or two operons including the most conserved genes *gsp*C to *M* and *O* coding for essential core components (Fig. 37). Some other *gsp* genes, coding for accessory components presented in only certain T2SSs, such as *gspAB*, *gspN* and *gspS,* are often located separately from the core *gsp* genes (Fig. 37). Generally, the T2SSs exhibit a similar genetic organization. However, in some species, the genetic organization varies. The *gspC* and *gspD* genes of *P. aeruginosa* form an operon that is divergent from the operon containing the *gspE-M* genes (de Groot., 2001) (Fig. 37). In *X. campestris*, *gspCD* genes were found to be localized next to *gspM* at the end of the *gsp* operon (Fig. 37). Mutations in core *gsp* genes prevent secretion and result in the accumulation of the exoproteins in the periplasm. Thus, the products of all core *gsp* genes are essential for formation of the function T2S machinery.

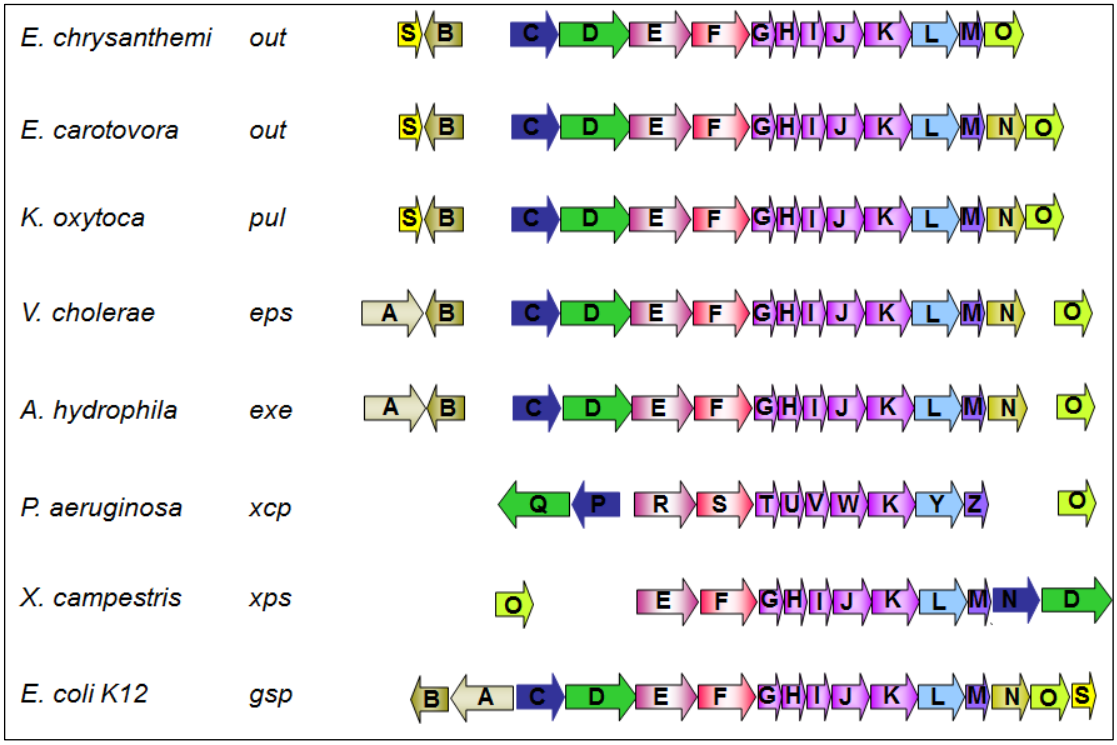

Fig. 37: Genetic organization of the T2SS. The homologue genes coding for T2SS components are represented by the same color (Filloux, 2004).

III.2 Structural organization and function of the T2SS

Secretion by the T2SS is a two-step process (Fig. 38). The proteins to be secreted (exoproteins) are firstly synthesized with an N-terminal cleavable signal sequence. These precursors are targeted and transported through the IM via the Sec (in unfolded state) or Tat (in folded state) translocon (Johnson *et al.*, 2006; Filloux, 2011). The signal peptide is then cleaved by an appropriate leader peptidase and the mature proteins are released into the periplasm. Once in the periplasm, the exoproteins are folded before being recognized by the secretion machine and translocated across the OM by the T2SS.

The T2S machinery also named secreton, is a multiprotein complex that spans both the IM and OM of bacteria (Johnson *et al.*, 2006). It is composed of 12 core components. The OM secretin GspD forms a secretion pore. A cytoplasmic ATPase GspE, along with the IM proteins GspF, L, M form an IM platform. The major (GspG) and minor (GspH, I, J, K) form a pilus-like fiber. The IM protein GspC may play as a linker by connecting the two sub-secreton complexes, the IM platform GspE-F-L-M and the OM secretin complex. The pre-pseudopilin peptidase/methylase GspO processes the pseudopilins prior to their integration into the apparatus (Cianciotto, 2005; Johnson *et al.*, 2006). Beyond these core components, there are some accessory components presented in only some species, including the pilotin GspS, GspN, GspA and GspB.

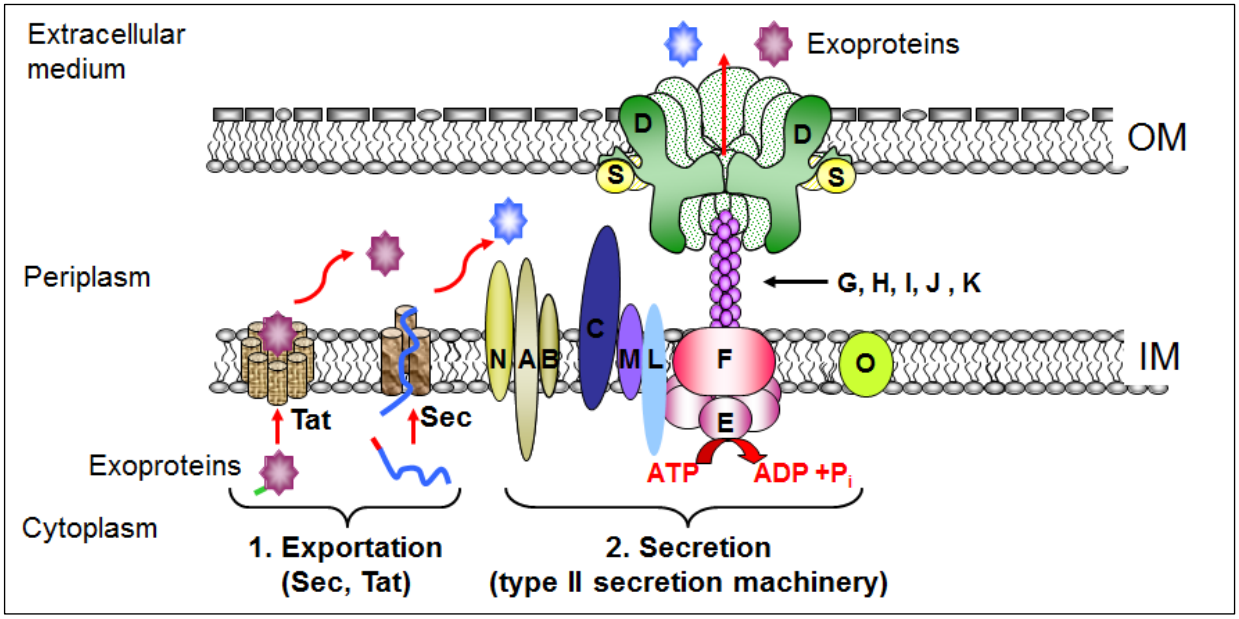

Fig. 38: Model of structural organization of the T2SS. 1. Sec or Tat systems promote export of exoproteins through the inner membrane (IM). 2. T2SS transports exoproteins across the outer membrane (OM).

III.3 Description of the different parts of theT2S secreton

III.3.1 The secretin GspD: the channel of the machinery

The OM protein GspD belongs to the secretin family. Secretins form large homomultimeric protein complexes in the OM of Gram-negative bacteria that are crucial for translocation of proteins and assembled fibers across the OM. The secretins are involved in the T2SS, T3SS, the type IV pili system (T4PS) and the filamentous bacteriophage assembly (Korotkov *et al.*, 2011a).

III.3.1.1 The T2SS secretin, GspD

Sequence comparisons and further functional and structural studies showed that the secretin GspD consists of two main regions: a conserved C-terminal domain and a variable N-terminal domain (Fig. 39A) (Genin and Boucher *et al.*, 1994; Nouwen *et al.*, 2000; Korotkov *et al.*, 2011a). In addition, some secretins contain a small S-domain (30-70 amino acids) near the secretin C-terminus (Fig. 39A) to which a secrtin-specific pilotin binds (Nouwen *et al.*, 1999; Guilvout *et al.*, 2011). The conserved C-terminal domain contains several putative transmembrane β-strands and forms a β-barrel in a multimeric state that makes the actual channel in the OM. Indeed, the C-domain of the GspD homologue XcpQ from *P. aeruginosa* was predicted to contain 13 putative transmembrane β-strands (equivalent to 50% of the XcpQ C domain) (Bitter *et al.*, 1998). However, circular dichroism (CD) indicated that only 25% of the PulD C domain could have β-strand configuration, which suggests that a large part of C domain is not organized in a classical OM β-barrel structure and, therefore, is probably not embedded in

the membrane (Chami *et al.*, 2005).

The N-terminal domain of GspD extends into the periplasm and could be implicated in interaction with other T2SS components, and/or with secreted proteins. The structural study (Korotkov *et al.*, 2009a) showed that the N-terminal domain of the secretin GspD from enterotoxigenic *Escherichina coli* (ETEC) consists of four subdomains (N0 to N3). The crystal structure of the first three N-terminal domains N0-N1-N2 showed that these three periplasmic domains are arranged into two lobes (Fig. 39B): a compact N-terminal lobe containing the N0 and N1 subdomains, and a second lobe containing the N2 subdomain (Korotkov *et al.*, 2009a). In the structure, the N0 subdomain interacts with the N1 subdomain via an antiparallel pair of β strands involving β3 of N0 and β6 of N1. Their interface residues are hydrophobic throughout the T2SS GspD family, which suggests that the compact N0-N1 lobe of peri-GspD is most likely a common feature in T2SSs. The N0 subdomain is composed of two α helices flanked on one side by a mixed three-stranded β sheet and on the other by a two stranded antiparallel sheet (Fig. 39B) (Korotkov *et al.*, 2009a). This fold is similar to the signaling domain of TonB-dependent receptors (Brillet *et al.*, 2007; Ferguson *et al.*, 2007). TonB-dependent receptors are bacterial OM proteins that bind and transport ferric chelates, called siderophores, vitamin B_{12}, nickel complexes and carbohydrates (Noinaj *et al.*, 2010). The transport requires energy in the form of PMF and an IM complex TonB-ExbB-ExbD, to transduce this energy to the OM. This process involves the interaction between TonB box of the OM receptor and TonB of the IM complex. Superimposition of the TonB-dependent OM receptor FpvA signaling domain onto the N0 domain of ETEC-GspD showed that an extra β strand could be bound by the N0 domain in a fashion similar to the interaction between the TonB box and the signaling domain (Fig. 40) (Korotkov *et al.* 2009a). In the structure of ETEC-GspD, the β2 of N0 is accessible and not blocked by the tight interactions between the N0 and N1 subdomains. Thus, the authors suggested that β2 of N0 might interact with a β strand from another protein during the functioning of the T2SS.

The N1 and N2 subdomains consist of two or three α helices and a three-stranded β-sheets (Fig. 38B). This structure is similar to the eukaryotic type I KH (hnRNP K homology, named for the human heterogeneous nuclear ribonucleoprotein K) domain that is typically involved in binding RNA and DNA (Valverde *et al.*, 2008). This fold is also present in ring-forming proteins of the T3SS (Spreter *et al.*, 2009). The N3 subdomain was suggested to have a structure similar to that of the N1 and N2 subdomains (Korotkov *et al.*, 2009a). The crystal structure of two N-terminal domains (N0 and N1) of the secretin EscC from the EPEC T3SS reveals that they adopt folds similar to those observed in the N0 and N1 domains of the EPEC GspD T2SS secretin (Fig.

39C) (Spreter *et al.*, 2009). However, the mutual orientation of these domains in the T2SS and T3SS secretins is unexpectedly different. It is unknown whether these structural differences simply indicate the different organization in these two secretins or represent different conformations of a flexible unit adopted by both secretins during secretion or assembly (Korotkov *et al.*, 2011a).

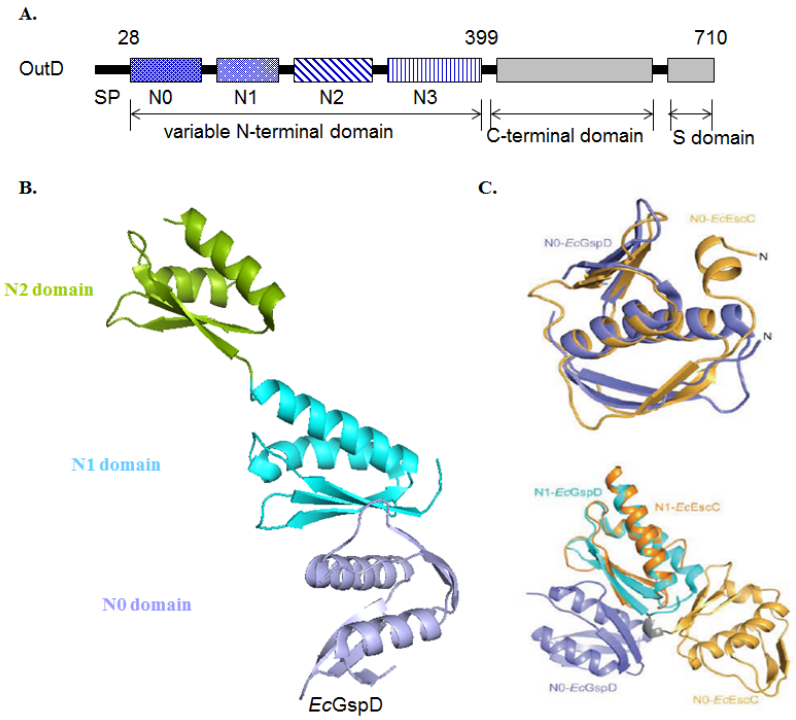

Fig. 39: Schematic representation of *D. dadantii* T2SS secretin OutD (A) and crystal structure of N0-N1-N2 domains of ETEC T2SS secretin GspD (B) (Korotkov *et al.*, 2009a) and comparison of N0 and N1 domains of ETEC T2SS secretin GspD and EPEC T3SS secretin EscC (C) (Reichow *et al.*, 2010). SP, signal peptide.

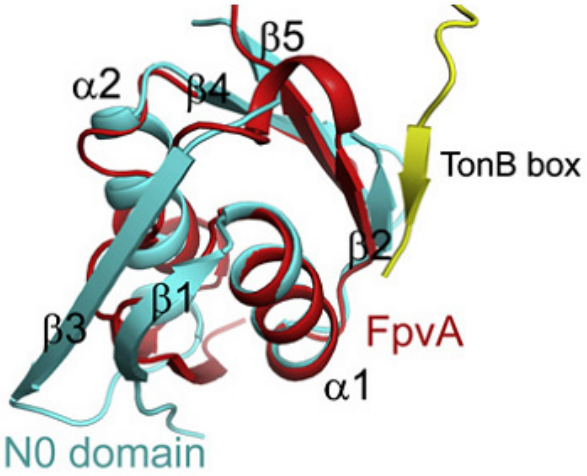

Fig. 40: Comparison of peri-GspD N0 subdomain with TonB-dependent OM receptor FpvA from *P. aeruginosa* (Korotkov *et al.*, 2009a). The N0 subdomain (cyan) superimposed onto the signaling domain (red) of the FpvA. TonB box residues of FpvA are shown in yellow.

III.3.1.2 Channel formed by the secretin GspD homomultimeric complex

Eelectron microscopy (EM) studies revealed that 12-14 identical secretins form toroidal complexes with a central cavity that ranges from 50 to 90 Å in diameter dependent on the species (Bitter *et al.*, 1998; Nouwen *et al.*, 2000; Burghout *et al.*, 2004). As a channel of this size in the OM would cause leakage of periplasmic proteins, so the opening and closing of the secretion channel should be tightly regulated. EM analysis of the T2SS secretin PulD from *K. oxytoca* (Nouwen *et al.*, 2000) and cryo-EM of the secretin pIV from the filamentous bacteriophage assembly system (Opalka *et al.*, 2003) revealed a central channel plug. The N terminus of secretins seems to fold back into the cavity formed by the C terminus and plugs the channel (Nouwen *et al.*, 2000). However, the following cryo-EM studies of PulD indicated that the C-domain probably forms the plug that occludes the channel (Chami *et al.*, 2005). 3D reconstruction of PulD shows a cylindrical dodecameric arrangement of secretin subunits with two rings. An open ring (‘saucer’ appearance) is present in the outer leaflet of the OM, with weak connections to a second ring (‘cup’ appearance) in the periplasm and the inner leaflet of the OM (Fig. 41). The periplasmic entrance of the cylinder is wide open, but a continuous density closes off the periplasmic part of the structure from the OM region (Fig. 41). Chami *et al.* (2005) suggested that docking of secreted proteins might displace the centrally located plug, thus creating a continuous channel through which the proteins can be secreted. Indeed, the secreted protein PelB of *D. dadantii* binds directly to GspD during secretion (Shevchik *et al.*, 1997). Moreover, recently, both surface plasmon resonance (SPR) and EM studies have shown that the periplasmic domain of ETEC GspD and *V. cholerae* GspD interact with the B-pentamer of heat-labile enterotoxin (LT) and the B-pentamer of cholera toxin (CT), respectively (Reichow *et al.*, 2010, 2011). However, the interactions between secreted proteins and secretin are not sufficient to cause the pore opening since the addition of pullulanase to the mixture liposome/PulD did not change the channel conductivity (Nouwen *et al.*, 1999). In addition, various studies have shown interaction between secretin and other proteins, such as GspG (Lee *et al.*, 2005), GspK-GspI-GspJ complex (Reichow *et al.*, 2010), GspC (Korotkov *et al.*, 2006; Login *et al.*, 2010) and GspB (Condemine and Shevchik, 2000; Ast *et al.* 2002; Strozen *et al.*, 2011). These interactions may be also directly or undirectly involved in the pore opening control. To date, how the pore opening remains puzzled.

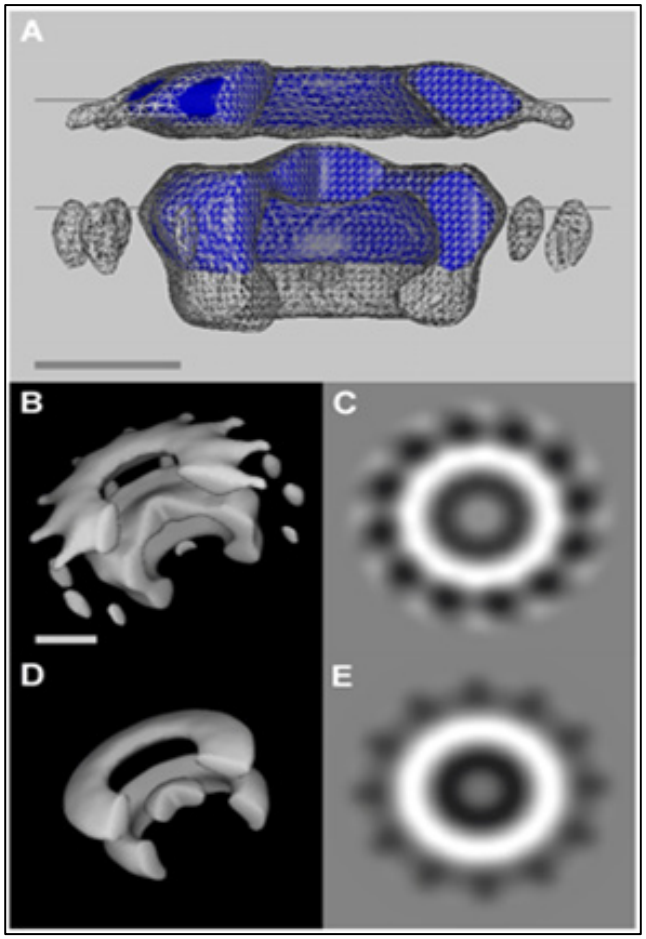

Fig. 41: 3D reconstruction of the *K. oxytoca* secretin PulD (Chami *et al.*, 2005). (A) The intact complex (white mesh) and the digested fragment (blue). The C domain is represented by blue; the N and S domains are represented by gray. The top perspective view of the native PulD complex (B) and the bottom perspective view of trypsin-resistant PulD complex (D) are shown. The corresponding axial back-projection is shown in (C) and (E), respectively.

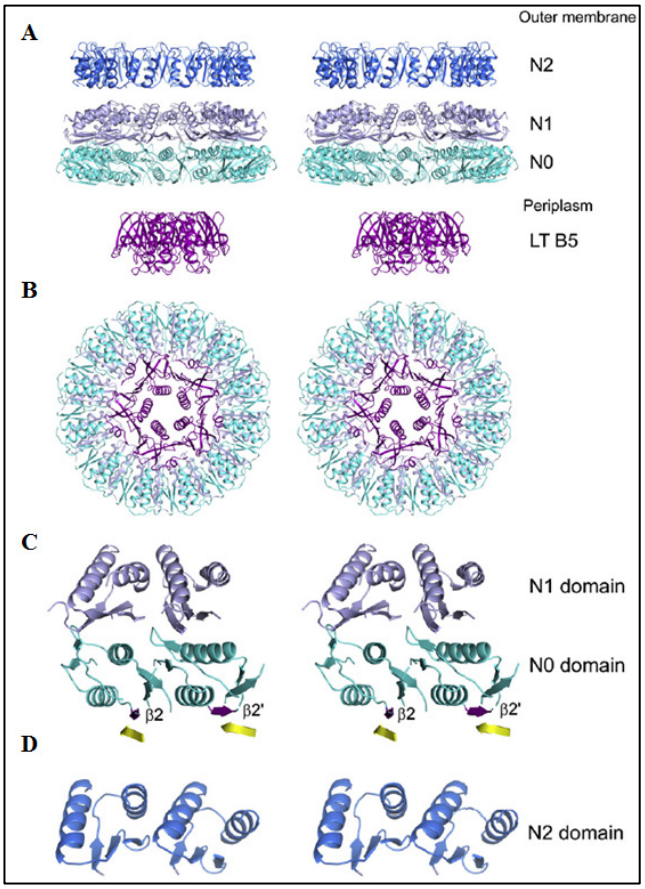

Fig. 42: Modeled cylindrical arrangements of periplasmic GspD domains (Korotkov *et al.*, 2009a). (A) The models of dodecameric N0-N1 ring and N2 ring. The structure of heat-labile enterotoxin (LT B5) is shown for size comparison. (B) Bottom view of the C12 ring of the N0-N1 subdomains with the LT B5 toxin structure. (C) Stereo figure of the N0:N1 interface viewed perpendicular to the C12 symmetry axis in the ETEC GspD model shown in (A). (D) Stereo figure of the subunit interface viewed parallel to the C12 symmetry axis in the ETEC GspD ring of N2 domains shown in (B).

Based on the crystal structure, Korotkov *et al.* (2009a) modeled cylindrical arrangements of periplasmic GspD domains. Although they did not obtain a plausible model using the entire peri-GspD structure, both the N0-N1 and N2 lobe produced models that showed that they form an assembly with cyclic C12 symmetry (Fig. 42). In the N0-N1 ring, β4 from one N0 subdomain approaches β1 of a neighboring N0 subdomain resulting in the formation of an extended β sheet (Fig. 42C), while helix α1 of one N1 subdomain approaches helix α5 of a neighboring N1 subdomain in a manner similar to the corresponding helices in the rings of N2 subdomain. The inner diameter of N0 ring (~70 Å) is sufficient to allow entry of molecules like the CT and LT AB5 enterotoxins (~ 64 Å), while the N1 ring (~ 46 Å) seems to be too narrow for passage of the folded B pentamer (Fig. 42A). The authors suggested that the pentamer might be transiently unfolded to interact with strand β2 of the N0 subdomain, thereby permitting a passage of the pentamer through the N1 and N2 rings. Alternatively, the secretin undergoes conformational changes during translocation of proteins. This might widen the N1 ring (Korotkov *et al.*, 2009).

Recently, a number of EM studies on secretins from various export systems have been published (Hodgkinson *et al.*, 2009; Reichow *et al.*, 2010; Jain *et al.*, 2011; Burkhardt *et al.*, 2011). It is now recognized that features common to all secretins include a cylindrical arrangement of 12-15 subunits, a large periplasmic vestibule with a wide opening at one end and a periplasmic gate at the other (Korotkov *et al.*, 2011a). The very recent cryo-EM study on the T2SS secretin EspD from *V. cholerae* (*Vc*GspD) showed an assembly of ~155 Å in diameter and ~200 Å in length, with a largely unobstructed periplasmic vestibule (Fig. 43) (Reichow *et al.*, 2010). The opening to the periplasmic vestibule is ~75 Å in diameter, and the channel was narrowed to ~55 Å in internal diameter by a constriction (Fig. 43). The periplasmic vestibule from the extracellular chamber of the channel was sealed off by the periplasmic gate. Following the periplasmic gate, the extracellular domain appears as a chamber of ~100 Å in diameter. Reichow *et al.* (2010) have placed the dodecameric ring models composed of N0-N1, of N2 and of N3 in the density map of *Vc*GspD. The N0-N1 ring fits into the widest area at the bottom of the periplasmic part of the secretin, and the N2 and N3 rings can be positioned directly above the N0-N1 ring in the map. In addition, the N3 ring fits to the constriction site of the cryo-EM map (Fig. 44A). They also placed the structure of the cholera toxin heterohexamer AB_5 into the *Vc*GspD secretin density (Fig. 44B). The AB_5 structure (~65 Å) fits well within the ~75 Å-wide vestibule created by the N0-N2 subdomains, without any steric hindrance. However, the AB_5 cannot fit through the constriction formed by N3 (~55 Å in diameter) without a major conformational change in the secretin (Fig. 44B). A recent study showed that CT B5 binds in the lower part of the periplasmic vestibule of the secretin *Vc*GspD, just below the channel

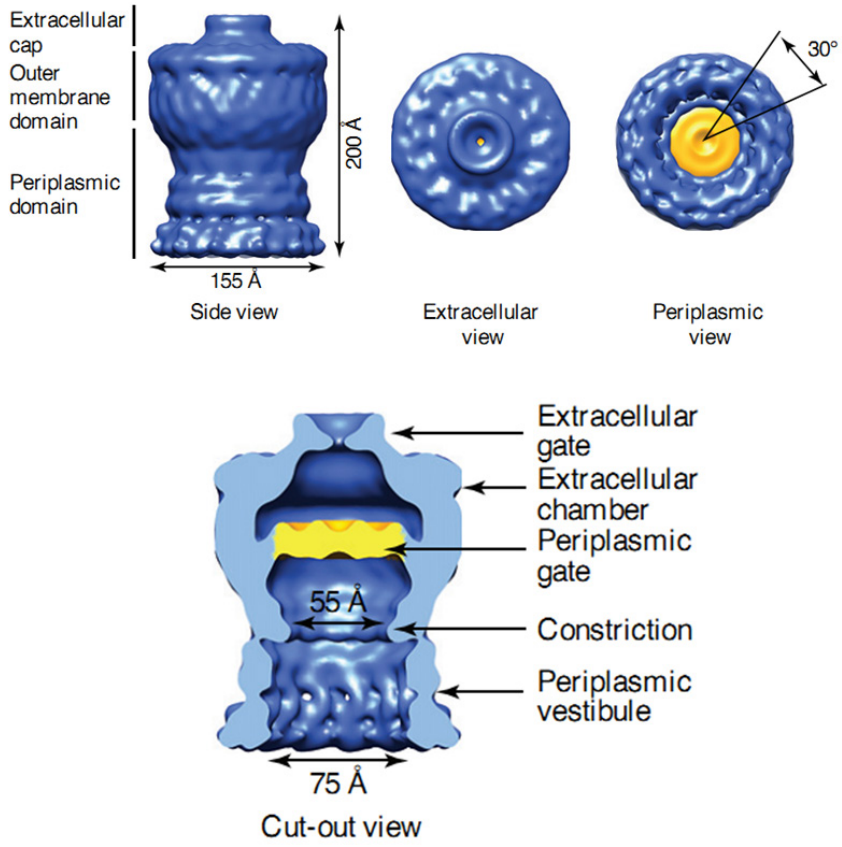

Fig. 43: Cryo-EM reconstruction of *V. cholerae* T2SS secretin GspD (Reichow *et al.*, 2010). In side view, three domains are identified from bottom to top as the periplasmic domain, the outer membrane domain and the extracellular cap. In slice view, the channel contains an extracellular gate, an extracellular chamber, a periplasmic gate and a perplasmic vestibule with a constriction.

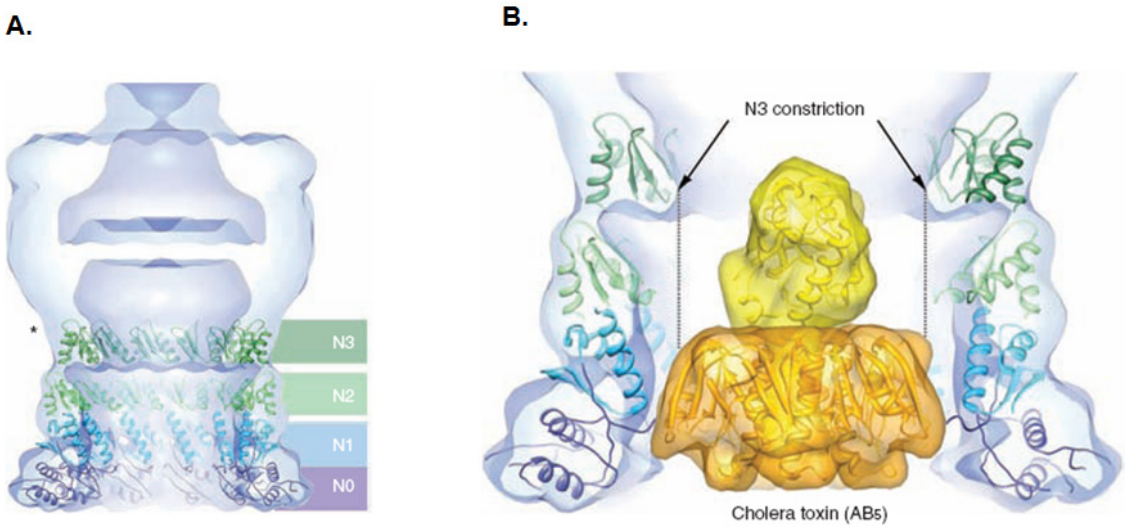

Fig. 44: Fitting models (Reichow *et al.*, 2010). (A) Fitting of 12-fold symmetric ring models of the *Vc*GspD N-terminal periplasmic domains (N0-N3) into the *Vc*GspD density map. (B) Fitting of the cholera toxin AB_5 heterohexamer (A subunit, yellow; B subunits, gold) into the *Vc*GspD periplasmic vestibule.

constriction (Reichow *et al.*, 2011). It was proposed that during the process of secretion, the secreted proteins interact with the secretin constriction. This interaction could provide the trigger that causes large conformational changes in the T2SS secretin, which results in opening of the periplasmic gate (Reichow *et al.*, 2011).

III.3.1.3 The secretin multimerization and insertion into the OM

The general OM assembly factor Omp85/YaeT (BamA) may be one of the factors that facilitate secretin insertion and multimerization (Voulhoux *et al.*, 2003). Indeed, the absence of Omp85 prevents *N. meningitidies* secretin PilQ multimerization and decreases the amount of PilQ detected on the surface by immunofluorescence (Voulhoux *et al.*, 2003). However, a study of *K. oxytoca* secretin showed that PulD multimerization and membrane insertion are independent of BamA (YaeT) (Collin *et al.*, 2007).

In certain T2SSs, lipoprotein pilot GspS is necessary for the correct targeting and insertion of the secretin into the OM (Shevchik and Condemine, 1998; Guilvout *et al.*, 2006). In *D. dadantii*, pilotin OutS has been shown to bind to the C-terminal 62 residue of the secretin OutD (Shevchik and Condemine, 1998). Recently, Nickerson *et al.* (2011) identified the 28 C-terminal residues of the S domain as a minimal binding site that is sufficient for OM targeting of PulD *in vivo*. The region upstream of this binding site is not required for targeting or multimerization, but is needed for secretin function in T2SS. In the absence of pilotin or S domain of secretin, the secretin miss-locates to the IM (Guilvout *et al.*, 2006, 2011). *In vitro* studies showed that secretin PulD does not require PulS for multimerization or membrane insertion and PulD multimerization occurs very quickly without PulS (Guilvout *et al.*, 2008). The PulD multimers would be too large to diffuse through the peptidoglycan (Demchick and Koch, 1996). Thus, PulS binds to S domain of PulD to protect PulD monomers from degradation and to target them to OM via the conserved OM lipoprotein-specific Lol pathway (Collin *et al.*, 2011). Some secretins are lipoproteins per se, and they do not depend on separate pilotins for correct OM targeting. For example, $GspD^{HxcQ}$, the lipoprotein secretin from the second T2SS of *P. aeruginosa*, was showed to be self-piloted to the OM via its N-terminal lipid anchor (Viarre *et al.*, 2009).

In some other bacteria T2SSs, secretin assembly requires other auxiliary factors, for example, the GspA and GspB complex has been shown to be required for correct localization and multimerization of the secretin GspD multimer in the OM of *A. hydrophila* (Ast *et al*, 2002, Strozen *et al.*, 2011).

III.3.2 The pseudopilins and prepilin peptidase

Five proteins of T2SS, i.e., GspG,-H,-I,-J and -K, share sequence homology with pilin subunits of type IV pili and are called pseudopilins. These pseudopilins assemble a pilus-like structure, called pseudopilus, spanning the periplasmic compartment and/or acting as a piston to push the secreted protein through the OM pore (Hazes and Frost, 2008; Reichow *et al.*, 2011). Both the T2S pseudopilins and the type IV pilins are synthesized as precursors, which are processed by a specific prepilin petidase (Filloux, 2004; Johnson *et al.*, 2006).

III.3.2.1 GspO, a specialised prepilin peptidase/methylase

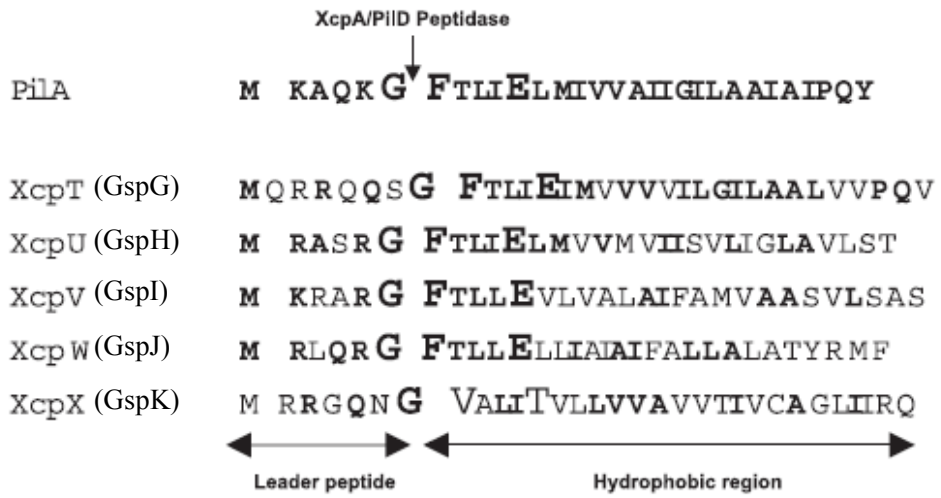

Fig. 45: Sequence alignment of the N-terminal domains of the PilA pilin subunit of type IV pili and pseudopilins of the Xcp-type II secretory pathway from *P. aeruginosa*. XcpT,-U, -V, -W and -X are more generally named GspG, -H, -I, -J and -K, respectively. The residues in the pseudopilins that are identical to those in the PilA sequence are shown in bold. Here R and K, and also I and L, are treated as 'identical' residues. The conserved G1, F+1 and E+5 residues are shown in uppercase. The position of the leader sequence cleavage site is indicated with an arrow. The leader peptide and the hydrophobic region are shown (Filloux, 2004).

The precursors of pseudopilins contain a conserved N-terminal leader peptide composed of six or seven residues followed by a hydrophobic domain of about 20 residues (Fig. 45) (Filloux, 2004). This leader peptide is recognized and processed by the prepilin peptidase/methylase PilD/GspO and the liberated N-terminus is further methylated. This modification is also catalyzed by the prepilin peptidase, which is thus a bifunctional enzyme (Filloux, 2004; Johnson *et al.*, 2006). The topology study of prepilin peptidase OutO from *D. dadantii* demonstrated that GspO is polytopic IM protein with eight transmembrane segments (Reeves *et al.*, 1994). The first cytoplasmic loop of this protein is large and contains a tetracysteine consensus motif, C-X-X-C ___X21___C-X-X-C. However, this motif does not seem to be required for peptidase activity

(LaPointe *et al.*, 2000). The sole residue required for peptidase activity is aspartate located in the second and third cytoplasmic loop. Thus, GspO is a bifunctional aspartic acid protease that cleaves the leader peptides of pseudopilin subunits and N-methylates the newly generated N-terminus (Johnson *et al.*, 2006). The processing site is located immediately before the hydrophobic region after a highly conserved glycine residue (G-1) (Fig. 45). Then, the mature pseudopilin subunits are helically packed via interactions between their hydrophobic N-terminal domains and are assembled into pseudopilus. A conserved glutamate residue within the hydrophobic domain (E+5) could play a key role in the assembly process of pilin and pseudopilin subunits (Aas *et al.*, 2007; Campos *et al.*, 2010).

III.3.2.2 The pseudopilus: the piston of the machinery

Except for GspK, the pseudopilins have an N-terminus similar to type IV pilins (G(F/M)XXXE) followed by 15-20 hydrophobic amino acids (Fig. 45). GspK is considered to be atypical because it lacks the phenylalaine (+1) and glutamate (+5) residues (Fig. 45) (Filloux, 2004) and has a higher molecular weight (>30kDa) than classical pilins and pseudopilins (15-30 kDa) (Bleves *et al.*, 1998). In addition, in most T2SS GspK has a pair of cysteine residues that form a disulfide bridge (Pugsley *et al.*, 2001; Korotkov and Hol, 2008), whereas other pseudopilins are cysteine-free. The relative *in vivo* stoichiometry between pseudopilins has been estimated in *P. aeruginosa* to be 16 (GspG):1(GspH):1(GspI):4(GspJ). Thus, GspG is considered as the major pseudopilin and the others GspH-GspK are the minor pseudopilins (Durand *et al.*, 2009).

(1) The major pseudopilin GspG

GspG is cotranslocationally inserted into the IM using the SRP/Sec pathway and does not require any components of the T2SS IM platform to be targeted into the IM (Francetic *et al.*, 2007; Arts *et al.*, 2007). Given the strong conservation of their N-terminal sequences, it is likely that other (pseudo)pilins also use the SRP/Sec pathway (Francetic *et al.*, 2007). Following insertion into the IM, GspG was suggested to be processed by the prepilin peptidase GspO. It has been speculated that this process causes a conformational change of GspG, which enables GspG to interact with other components of the T2SS (Gray *et al.*, 2011). The IM components suggested to act as a platform for the assembly of the subunits into a (pseudo)pilus-like structure, using the energy provided by the ATPase GspE. Indeed, upon overexpression, both GspG homologs from the *K. oxytoca* (PulG) and *P. aeruginosa* (XcpT) could be assembled in a multifibrillar structure (pseudopilus), crossing the bacterial cell envelop and exposed on the cell surface (Sauvonnet *et al.*, 2000; Durand *et al.*, 2003, 2005). Although these pseudopili obtained by overproduction of

pseudopilins cannot be considered as physiologically relevant structures, they reveal that GspG pseudopilins have a propensity to pack into helical complexes reminiscent of type IV pilus. None of the other four pseudopilins have been shown to form a pseudopilus, which suggests that the assembly of such a structure is a unique property of GspG (Durand *et al.*, 2005). The structures of the soluble domain of PulG and XcpT, GspG homologs from *K. oxytoca* and *P. aeruginosa* have been solved, respectively (Köhler *et al.*, 2004; Alphonse *et al.*, 2010). Both structures globally present the same features as the type IV pilins. All type IV pilins share a common fold with an extended N-terminal hydrophobic α-helix, a four-stranded anti-parallel β-sheet and a variable domain called the αβ-loop containing a disulfide bridge (Fig. 46). However, GspG lacks a highly variable αβ-loop region and do not have disulfide bridge stabilizing the protein fold. Recently, Korotkov *et al.* (2009b) showed that the major pseudopilin GspG binds to calcium ion to obtain sufficient stability necessary for its function. However, the major pseudopilin HxcT of the second T2SS of *P. aeruginosa* is unable to assemble a hyper-pseudopilus, which suggests different pseudopilus architecture (Durand *et al.*, 2011).

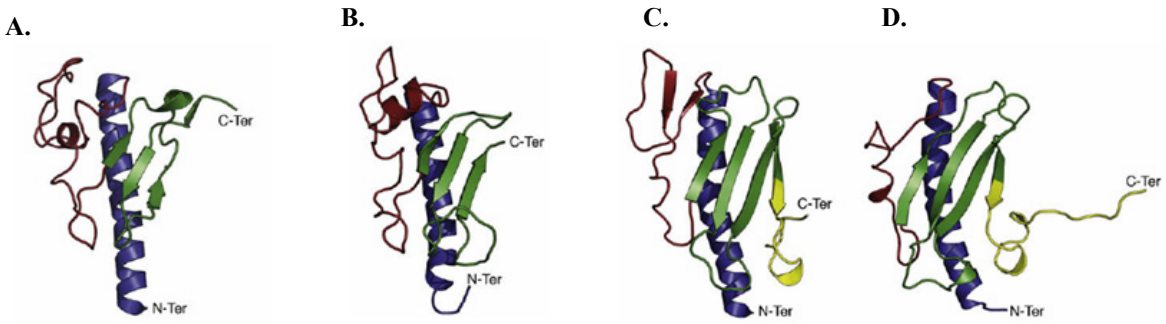

Fig. 46: Comparison of major pseudopilins with type IV pilins. (A) The soluble domain of the pseudopilin PulG from *K. oxytoca* and the soluble domain of the pseudopilin XcpT from *P. aeruginosa* (B), (C) the soluble domain of the pilin PilA from *P. aeruginosa* strain PAK and (D) the soluble domain of the pilin PilA from *P. aeruginosa* strain K122-4. The N-terminal α-helices are colored in blue, β-sheet of the α/β roll in green and the αβ-loop in red. In yellow are indicated the 'D' domain of the pilin structures (Alphonse *et al.*, 2010).

The formation of an extracellular pseudopilus blocks protein secretion, which suggests that the overproduced pseudopilus cross the OM via the secretin channel and thus disturb the release of secreted protein through the same channel at the same time (Durand *et al.*, 2003). Consequently, it is supposed that in physiological conditions, the pseudopilus formed by the pseudopilins should be retained in the periplasm. The length of T2SS pseudopilus might be controlled by the incorporation of minor pseudopilin subunits. Indeed, it was demonstrated that GspK constrols the pilus elongation since the pilus length was found to vary conversely to the concentration of GspK subunits (Durand *et al.*, 2005). GspK was also found to interact with GspG and induce disassembly of the pseudopilus. Results obtained with *K. oxytoca* and *P. aeruginosa* pseudopilins

suggested that GspI plays a major role at the initiation step of GspG assembly. Alternatively, it may anchor the T2SS pilus to the cell envelop (Sauvonnet *et al.*, 2000; Vignon *et al.*, 2003; Durand *et al.*, 2005). GspI may be loacted at the basis of the pseudopilus, in connection with IM components of the machinery. However, more recent studies suggest that GspI together with GspJ and GspK could constitute the tip of the pseudopilus (Korotkov and Hol, 2008).

(2) The minor pseudopilins GspHIJK

The crystal structure of the N-terminally truncated variant of EpsH, a GspH homolog from *V. cholerae*, comprises an N-terminal α-helix and C-terminal β-sheet consistent with the type IVa pilin fold (Fig. 47) (Yanez *et al.*, 2008b). However, structural comparisons revealed major differences between the minor pseudopilin EpsH and the major pseudopilin GspG from *K. oxytoca*. EpsH contains a large β-sheet in the variable domain, where GspG contains an α-helix. Importantly, EpsH contains at its surface a hydrophobic crevice between its variable and conserved β-sheets, wherein a majority of the conserved residues within the EpsH family are clustered. In addition, the authors proposed a tentative model of a T2SS pseudopilus with EpsH at its tip, the conserved crevice faces away from the helix axis and may be involved in the interaction with one or more other T2SS proteins.

The crystal structure of a complex formed by the *V. vulnificus* GspI and GspJ (EpsI and EpsJ) represents the first atomic resolution structure of a complex of two different pseudopilin components from the T2SS (Yanez *et al.*, 2008a). It gives the evidence that the two minor pseudopilins EpsI and EpsJ interact directly with each other. In the crystal structure, EpsI comprises of one N-terminal α-helix followed by four anti-parallel β-strands arranged with one β-sheet (Fig. 48A). EpsJ consists of one N-terminal α-helix followed by ten β-strands, of which nine occur within two β-sheets, plus a short β2' strand which is not part of a β-sheet (Fig. 48A). The interface between EpsI and EpsJ is highly conserved with a large number of hydrophobic residues involved in heterodimer formation. In addition, the arrangement of EpsI and EpsJ in the heterodimer would correspond to a right-handed helice, characteristic for proteins assembled into a pseudopilus. The recently solved nanobody-aided structure of the EpsI:EpsJ complex confirmed this viewpoint (Lam *et al.*, 2009). The main progress in the understanding of the assembly of pseudopilins into the pseudopilus is achieved by the crystal structure of the GspK-GspI-GspJ complex from enterotoxigenic *E. coli* (ETEC) (Korotkov and Hol, 2008). GspK consists of two domains, a pilin domain and a unique α-domain (Fig. 47). The former domain has the characteristic components of the pilin fold: an N-terminal α-helix, a short 'variable' segment and a four-stranded C-terminal antiparallel β-sheet. GspK, GspI and GspJ form a stable

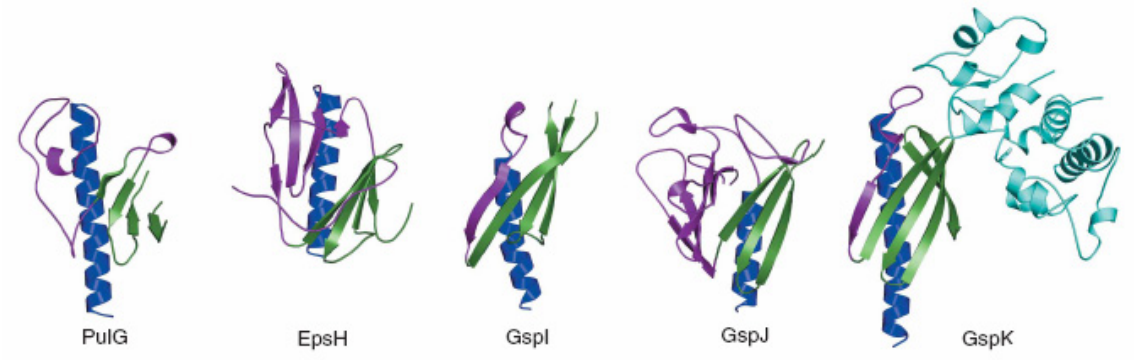

Fig. 47: The crystal structures of pseudopilins (Korotkov and Hol, 2008). The N-terminal a-helices are represented in blue, the conserved β-sheet is in green, the variable region is in purple and the α-domain of GspK is in light blue. Above, ribbon diagrams of the individual structures of GspI, GspJ and GspK from ETEC, the structures of the major pseudopilin GspG from *K. oxytoca* and the minor pseudopilin GspH from *V. cholerae*. All structures are shown in similar orientations based on superposition of the shared C-terminal β-sheet (green).

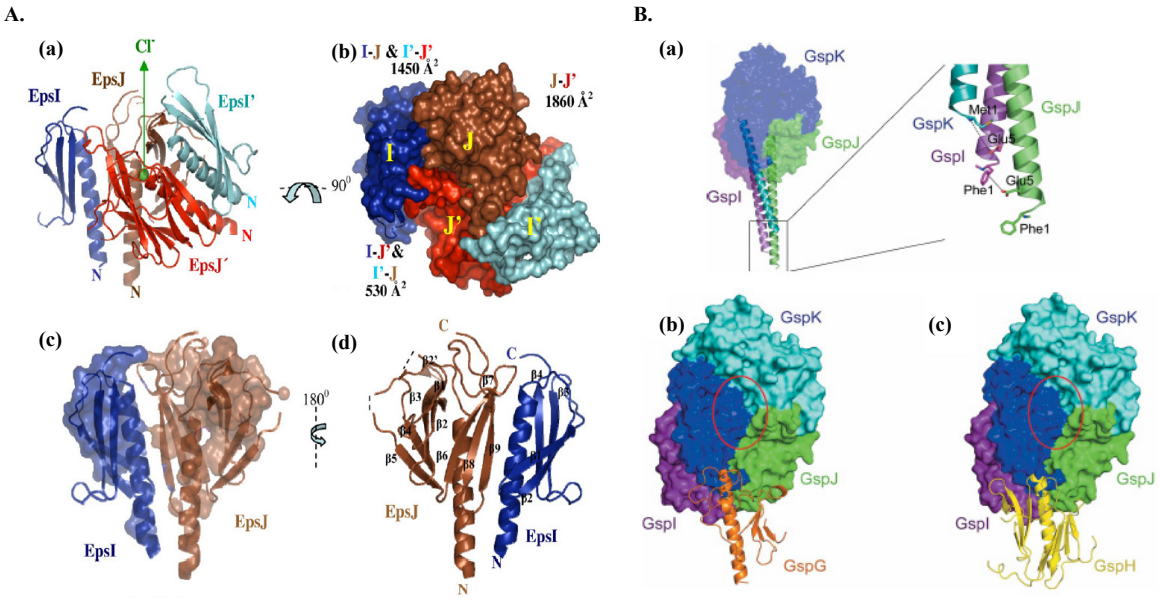

Fig. 48: The crystal structure of pseudopilin complexes. (A) The crystal structure of the *V. vulnificus* EpsI: EpsJ complex (Yanez *et al.*, 2008a). a) A ribbon diagram of one *Vv*EpsI$_2$: EpsJ$_2$ heterotetramer. *Vv*EpsI, blue; *Vv*EpsI', cyan; *Vv*EpsJ, brown; and *Vv*EpsJ', red. One chloride ion, located between *Vv*EpsJ and *Vv*EpsJ', is shown in green. b) A 'top' view of one *Vv*EpsI$_2$:EpsJ$_2$ heterotetramer with buried accessible surfaces of the intersubunit contacts indicated. c) A close-up view of one *Vv*EpsI: EpsJ heterodimer, in the same orientation as the heterotetramer shown in (a), with *Vv*EpsI colored dark blue and *Vv*EpsJ colored brown. d) The *Vv*EpsI: EpsJ heterodimer shown in (c) rotated by 180°. (B) The crystal structure of the ETEC GspK-GspI-GspJ complex (Korotkov and Hol, 2008). a) The modeled N-terminal a-helical extensions of GspK (blue), GspI (violet) and GspJ (green). The observed heterotrimer crystal structure is shown in surface representation and modeled α-helices are shown as cartoons. The insert shows that residues GspJ-Glu5 and GspI-Phe1, and also GspI-Glu5 and GspK-Met1, are in close proximity when the a-helices are extended. (b) The complex of GspK-GspI-GspJ by downward addition of GspG (orange) or GspH (yelleow) (c).

quasihelical heterotrimer. The N-terminal α-helices of the three subunits interact with each other in the center of the complex (Fig. 48B), in a fashion that is very similar to the models of the type IV pilus fibers (Köhler *et al.*, 2004; Craig *et al.*, 2006). GspK is able to form a stable complex with the pseudopilins GspI and GspJ, which suggests that GspK may participate in several interactions with other pseudopilins during pseudopilus assembly and/or function since it has been already demonstrated to interact with the major pseudopilin GspG (Durand *et al.*, 2005). The GspK-GspI-GspJ heterotrimer seems to be at the tip of the pseudopilus, with GspK and GspJ positioned in such a way that no additional pseudopilin subunit can be added 'upward'.

III.3.2.3 Assembly mode of the pseudopilus

It seems that two distinct complexes contribute to the pseudopilus structure: the pseudopilus core formed by the homomultimerization of the major pseudopilin through interaction between hydrophobic domains and a tip heteromeric complex formed by at least three of the minor pseudopilins. EM and modeling image analysis of the PulG-containing pseudopilus suggested that pseudopilus is most likely assembles into a left-handed helical pilus with the long N-terminal α-helix of each subunit packing into the core of the pilus structure (Köhler *et al.*, 2004). However, Campos *et al.* (2010, 2011) recently proposed that the overall organization of T2SS pilus is right-handed, consistent with protomer organization in gonococcal T4P structure (Craig *et al.*, 2006). Based on the high-resolution structure of the PulG monomer completed by modeling and the scanning transmission electron microscopy (STEM) analysis of single PulG filaments, Campos *et al.* (2010) proposed a one-start helix T2S pilus assembly model validated by cysteine cross-linking and charge inversion experiments (Fig. 49). In this model, each protomer (P) interacts directly with three upper (P_{+1}, P_{+3}, P_{+4}) and three lower (P_{-1}, P_{-3}, P_{-4}) protomers in the filament, through hydrophobic (P_{-1} and P_{+1}) and electrostatic (all six) interaction. In the first step, the protomer P is tethered to the nascent filament via electrostatic interactions with protomer P_{+1} (Asp^{48}-Arg^{87}, Glu^{44}-Arg^{88}, and Glu^{5}-Phe^{1}). The hydrophobic patch on protomer P_{+3} and P_{+4} exposed to aqueous environment (Fig. 49A, B and D) could contribute to these contacts or be masked by an assembly factor (PulF/L/M). Upon insertion, Lys^{35} and Lys^{28} of protomer P could interact with Glu^{5} of P_{+3}, which stabilizes the P_{+3} in its final state (Fig. 48B, C, and E) and promotes the most frequently modeled TMS arrangement.

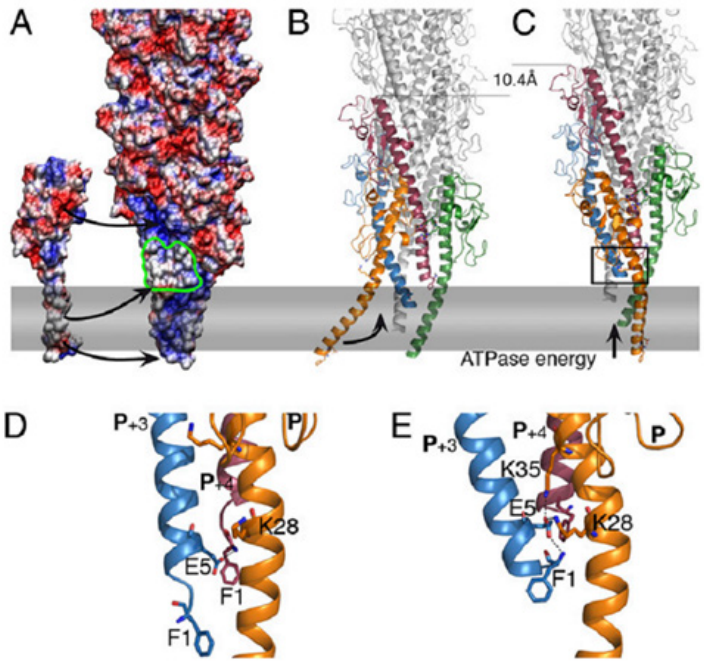

Fig. 49: The pseudopilus assembly model (Campos *et al.*, 2010). (A) Electrostatic envelop of the pilus and PulG monomer, inserted in the membrane (gray rectangle). Arrows indicate the PulG tethering via Asp^{48}-Arg^{87} and Glu^{44}-Arg^{88} salt bridges, the hydrophobic patch (outlined in green), and Glu^{5}. (B) Ribbon view of the pilus and the incoming protomer. (C) The incoming protomer (P) incorporation is associated with the membrane extraction of the P_{+1}, driving by the PulE ATPase, adding 10.4Å to the pilus. (D and E) Zoom views of the rectangle in C showing two alternative interaction of Glu^{5} of P_{+3} with Phe^{1} of P_{+4} (D) of Lys^{35} and Lys^{28} of P, stabilizing the pilus in its optimal state (E).

The minor pseudopilins in the GspJ-I-K tip also are arranged in a right-handed helix (Forest, 2008). Recently, Douzi *et al.* (2009) revealed an additional interaction between GspH and GspJ, which suggested the existence of a quaternary complex (GspH-GspI-GspJ-GspK) at the tip of the pseudopilus. During the pseudopilus biogenesis, GspH may be located at the base of the minor pseudopolins complex and could form the hinge between the tip complex and the core pseudopilus formed by the GspG. Indeed, several studies favor a linker position for GspH:

1)Yanez *et al.* (2008b) suggested to place GspH at the tip of the GspG pseudopilus with its specific conserved crevice by docking experiments;

2) GspH was shown to interact with pseudopilins GspG and GspJ (Kuo *et al.*, 2005; Douzi *et al.*, 2009). GspI is the central component and initiator of pseudopilus formation by interacting with both GspJ and GspK with two different interaction sites. GspH then enters the ternary complex GspJ-GspI-GspK via its interaction with GspJ. The tip quaternary complex is then able to accommodate the major pseudopilin GspG via a hydrophobic interaction with GspH.

The elongation of the pseudopilus might be arrested by contact of the tip complex with the

secretin. Indeed, it was shown by SPR that the trimeric pseudopilus tip complex GspK-GspI-GspJ interacts with the periplasmic domain of secretin (Reichow *et al.*, 2010). In addition, it was shown that both minor pseudopilin GspJ (Douet *et al.*, 2004) and major pseudopilin GspG (Gray *et al.*, 2011) interact with GspL. This indicates that energy transduced by GspL may be required to extract the N-terminal hydrophobic α-helix of both the major and minor pseudopilins from the IM while the pseudopilus is formed in the periplasmic compartment.

III.3.3 GspE-F-L-M: the inner membrane complex

GspE, GspF, GspL and GspM constitute a complex in the IM that is presumably used as a platform for assembling and anchoring the pseudopilus to the IM (Py *et al.*, 2001). Moreover, the IM platform is assumed to either initiate the signal transduction for gating the pore or to generate and transmit the energy that is necessary for protein secretion via conformational changes.

III.3.3.1 The motor GspE

GspE belongs to the large superfamily of 'typeII/IV secretion NTPases', or 'secretion superfamily ATPases'. This superfamily involves the ATPases, which function in multiple macromolecular transport system, such as T2SS and T4SS, type IV pilus (T4P) assembly, DNA uptake, and archeal flagellae assembly systems (Planet *et al.*, 2001; Peabody *et al.*, 2003; Craig *et al.*, 2004). The ATPases belonging to the T2SS and T4P share the following features: i) a Walker A box with the P-loop GX4GK(S/T) that is used to bind NTP; ii) an atypical Walker B box which is thought to be the determinant for nucleoside recognition; iii) the Aspartate box located between the Walker A box and Walker B box, may be involved in the formation and stabilization of the nucleoside-binding fold by interacting with Mg^{2+}; iv) a conserved Histidine box for which no function has yet been assigned; v) a tetracysteine motif, which is reminiscent of a zinc-binding domain, appears to be essential for function (Possot *et al.*,1997).

GspE are multi-domain proteins (Fig. 50A), which contain domains N1 to C2. Domain N0 is only present in a few homologs including XpsE and XcpR in *X. campestris* and *P. aeruginosa*, respectively. The crystal structure of an N-terminally truncated version of GspEΔ90 and N1 subdomain of GspE (N1-EpsE) in complex with the cytoplasmic domian of GspL (cyto-EpsL) from *V. cholerae* have been solved, respectively (Robien *et al.*, 2003; Abendroth *et al.*, 2005). The former structure revealed an organization in two major domains for the monomer, i.e., the N2 domain and the complete C-terminal domain with its three subdomains C1, CM and C2 (Fig. 50B) (Robien *et al.*, 2003), while the latter showed that GspE and GspL form a hetero-tetramer, in which GspL is the central dimer and GspE binds on the periphery (Fig. 50C) (Abendroth *et al.*, 2005). The N2 and C domains are separated by a linker of 15 amino-acid residues. The C1

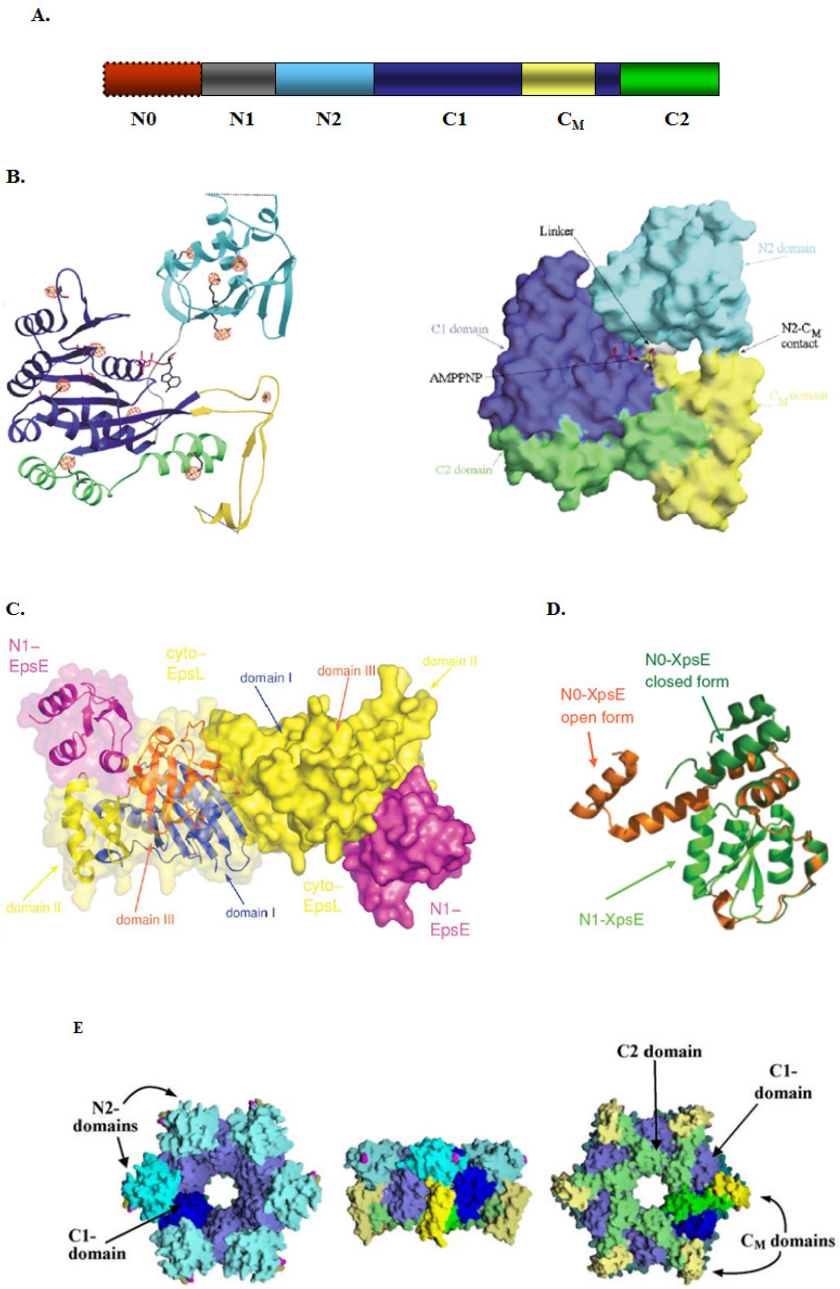

Fig. 50: GspE domain organization and crystal structures. (A) Schematic representation of domain structure of GspE with the subdomains N0 (red), N1 (gray), N2 (cyan), C1 (dark blue), C_M (yellow) and C2 (green). The N0 subdomain is restricted to a subset of GspE family member. (B) Crystal structure of N-terminally truncated version of GspEΔ90 monomer from *V. cholerae* (Robien *et al.*, 2003). The position of a bound molecule of AMPPNP (non-hydrolysable analog of ATP) is shown. (C) Crystal structure of the N1 subdomain of GspE (N1-EpsE) in complex with the cytoplasmic domain of GspL (cyto-EpsL) from *V. cholerae* (Abendroth *et al.*, 2005). (D) Superposition of the two structures of GspE N0-N1 from *X. campestris* with domain N1 colored light green and domain N0 in its closed and open conformations colored in dark green and orange, respectively (Chen *et al.*, 2005). (E) Hexameric ring model of EpsE. View from the proposed membrane-facing side (left), side view (middle), and the cytoplasmic face (right) of the hexameric ring model of EpsE (Robien *et al.*, 2003).

domain contains all four conserved boxes that characterize traffic ATPases from the T2SS and T4P assembly machinery, i.e., the Walker A, Walker B, Asp and His boxes. The small C_M subdomain is a hairpin-like meandering loop with a conserved tetracysteine motif that binds a metal cation near the sharply bent proximal end of the loop. The C2 subdomain is spatially interposed between the C1 and C_M subdomains (Robien *et al.*, 2003). Another crystal structure of the N-terminal domain of GspE from *X. campestris* was reported in two conformational forms, i.e., open form and closed form (Fig. 50D) (Chen *et al.*, 2005). GspE family proteins have been shown to form hexameric rings (Fig. 50E and 51) (Robien *et al.*, 2003; Shiue *et al.*, 2006). Moreover, Patrick *et al.* (2011) modeled GspE as a hexameric ring with C2 symmetry. ATP binding triggers the oligomerization of GspE as well as its association with N-terminal domain of GspL (Shiue *et al.*, 2006) (Fig. 51). Indeed, a double-mutant GspE mutated at K331 and R504, which is defective in ATP binding, no longer oligomerized in the presence of Mg-AMPPNP (non-hydrolysable analog of ATP), nor did it associate with GspL. Unlike the GspE (K331M, R504A) double-mutant, single mutation in GspE at K331 in Walker A motif causes reduction in its ATPase activity by 17-fold without significantly influencing its interaction with GspL, which indicates that GspE-GspL association precedes ATP hydrolysis (Fig. 51). Acidic phospholipids, specifically cardiolipin, together with cytoplasmic domain of GspL, synergistically stimulated both the oligomerization and intrinsic ATPase activity (Camberg *et al.*, 2007). Further analysis showed that residues at the C-terminus of GspL cytoplasmic domain adjacent to the predicted transmembrane helix interfered with the cardiolipin-stimulated ATPase activity of GspE. This suggests that the membrane proximal region of the cytoplasmic domain of GspL may participate in fine-tuning the interaction of GspE with phospholipids and thereby regulate its oligomerization and ATPase activity (Camberg *et al.*, 2007).

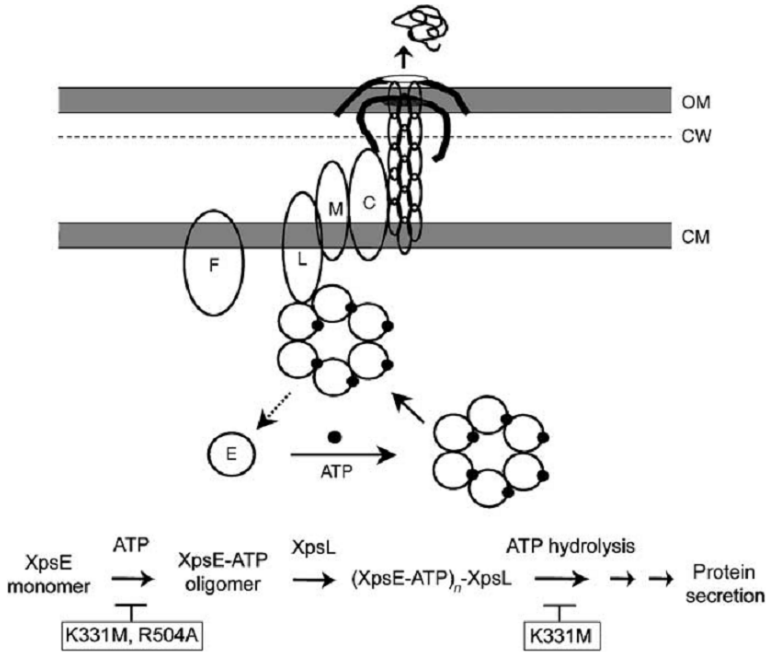

Fig. 51: Model depicting sequence of events in T2SS initiated by ATP binding to GspE (Shiue *et al.*, 2006). Steps blocked by mutant GspE are indicated by mutated residue(s) in boxes. Filled circles depict ATP.

Shiue *et al.* (2007) identified R286 as a key residue in GspE. This residue plays a pivotal role in coupling ATP hydrolysis to protein translocation. Mutation of R286 to Ala caused the basal GspE ATPase activity elevated. However, the mutant GspE (R286A) is non-functional in protein secretion via T2SS (Shiue *et al.*, 2007). Detailed analyses indicated that GspE (R286A) lost the ability of the coordinating N- and C-domains of GspE. The authors proposed that R286 serves as a sensor for different states of the nucleotide. Once mutated, the 'sensor' function of R286 is broken. Thus, the structural alteration resulted from the ATP binding or ATP binding-induced oligomerization could not propagate to the N-domain of GspE as judged by lack of conformation change at N-domain required for its association with the N-domain of GspL. Thus, GspE lost the ability to associate with the cytoplasmic membrane via GspL. Consequently, ATP hydrolysis by GspE was uncoupled from protein secretion. Recently, Patrick *et al.* (2011) showed that several other conserved arginines are essential for ATP hydrolysis. Replacements of these arginines abrogate the T2S process due to reduction of the ATPase activity but do not have any measurable effect on ATP binding or oligmerization of GspE. Similarly, some additional mutations within the intersubunit interface disrupt the function of GspE, indicating that a precise arrangement of residues from different subunits around the active site is essential for the action of GspE (Patrick *et al.,* 2011).

In brief, GspE is active as an oligomer, likely a hexamer. The binding, hydrolysis and release of nucleotide cause GspE to undergo dynamic structural changes, thus converting chemical

energy to mechanical work, ultimately resulting in extracellular secretion. GspE associates with the T2SS through interaction with the N-terminal domains of GspL and GspF (Py *et al*., 2001; Arts *et al.*, 2007a).

III.3.3.2 GspF, L and M: the platform stabilizers

(1) GspF

GspF is a polytopic integral IMP. It consists of a small periplasmic loop and two larger cytoplasmic domains connected by three transmembrane segments. The N-terminal domain is located in the cytoplasm whereas the C-terminus is located in the periplasm ((Thomas *et al.*, 1997; Arts *et al.*, 2007a). Using a yeast two-hybrid system, Py *et al.* (2001) revealed that the cytoplasmic N-terminal domain of OutF interacts with OutE and the cytoplasmic domain of OutL. Furthermore, OutL was required for the formation of OutE-OutF complex whereas the OutE-OutL complex formation is independent of OutF. This leads to the suggestion that GspE and GspL might first interact together and then associate with the GspF. XcpS, a GspF homolog of *P. aeruginosa*, was found unstable in the absence of other Xcp components, but could be stabilized by co-expression of the XcpR (GspE) and XcpY (GspL) components of the machinery (Arts *et al.*, 2007a), which indicates an interaction between these three proteins. The cytoplasmic loop located at the C-terminal part of XcpS was shown to be involved in the stabilization by XcpR and XcpY. These results suggest that the two cytoplasmic domains of GspF could participate in the interaction with GspE and GspL and contribute to the stability of the IM complex.

Recently solved crystal structure of the N-terminal cytoplasmic domain of EpsF (cyto-EpsF) (GspF of *V. cholerae*) showed that it adopts an all-helical fold with six helices forming two layers (Fig. 52) (Abendroth *et al.*, 2009a). Two cyto-EpsF domains form a tight dimer and contain two symmetry-equivalent calcium sites (Fig. 52). *In vivo* cross-linking experiments further support for dimer formation of cyto-EpsF (Abendroth *et al.*, 2009a). Sequence analysis of the GspF family suggests that the second cytoplasmic domain of members of this family adopts the same conformation as the first cytoplasmic domain.

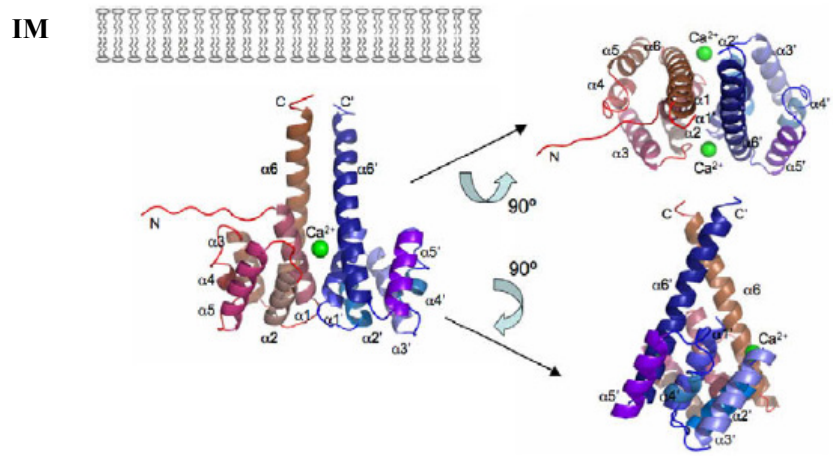

Fig. 52: The dimer of N-terminal cytoplasmic domain of EpsF (cyto1-EpsF$^{56-171}$) from *V. cholerae* (Abendroth *et al.*, 2009a). Each cyto-EpsF$^{56-171}$ subunit consists of a six-helix bundle. The dimer is shown in three different orientations, green spheres indicate calcium ions in the dimer interface.

(2) GspL and GspM

GspL is a bitopic IM protein. It consists of a large cytoplasmic domain, a single transmebrane helix and a small periplasmic domain (Fig. 53). The crystal structure of the cytoplasmic domain of the GspL *V. cholerae*, cyto-EpsL, unexpectedly revealed structural homology with the actin-like ATPase superfamily (Fig. 54) (Abendroth *et al.*, 2004a). Cyto-EpsL consists of three β-rich domains with domains I and III corresponding to the conserved domains 1A and 2A of the actin-like ATPases. However, cyto-EpsL is incapable of forming actin-like filaments because it misses the non-conserved domains 1B and 2B of the actin-like proteins (Fig. 54). Moreover, cyto-EpsL has an additional domain II, which has a SHS2 (strand-helix-strand-strand) topology. This topology is only observed for domain 1C of the cell division protein FtsA, where it likely participates in intermolecular interactions that result in recruitment of other proteins essential for cell division (Rico *et al.*, 2004; Johnson *et al.*, 2006). Structural homology and sequence conservation suggested that domain II of cyto-EpsL is also involved in protein-protein interactions. Indeed, the crystal structure of N1 subdomain of EpsE in complex with cyto-EpsL shows that domains II and III of cyto-EpsL are involved in the interaction with the N1 subdomain of EpsE and the majority of the protein-protein interface involves domain II of cyto-EpL (Fig. 50C) (Abendroth *et al.*, 2005). Contrary to the actin-like ATPase, no nucleotide-binding site was found in cyto-EpsL by sequence analysis of structural homologues of the superfamily or in the crystal structure (Abendroth *et al.*, 2004a). Instead, EpsL together with acidic phospholipids synergistically stimulated both the oligomerization and intrinsic ATPase activity of EpsE (Shiue *et al.*, 2006; Camberg *et al.*, 2007).

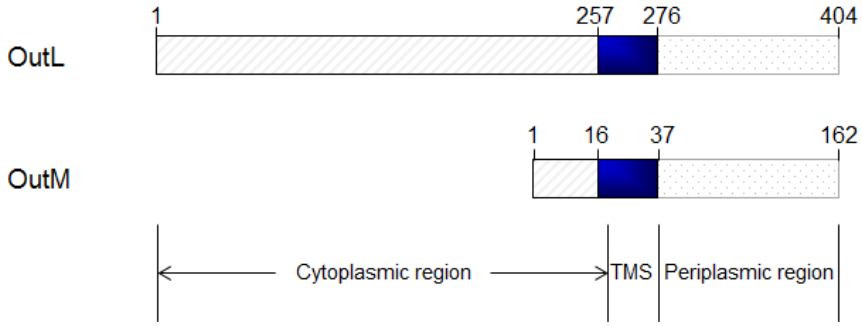

Fig. 53: Schematic representation of GspL and GspM from *D. dadantii*.

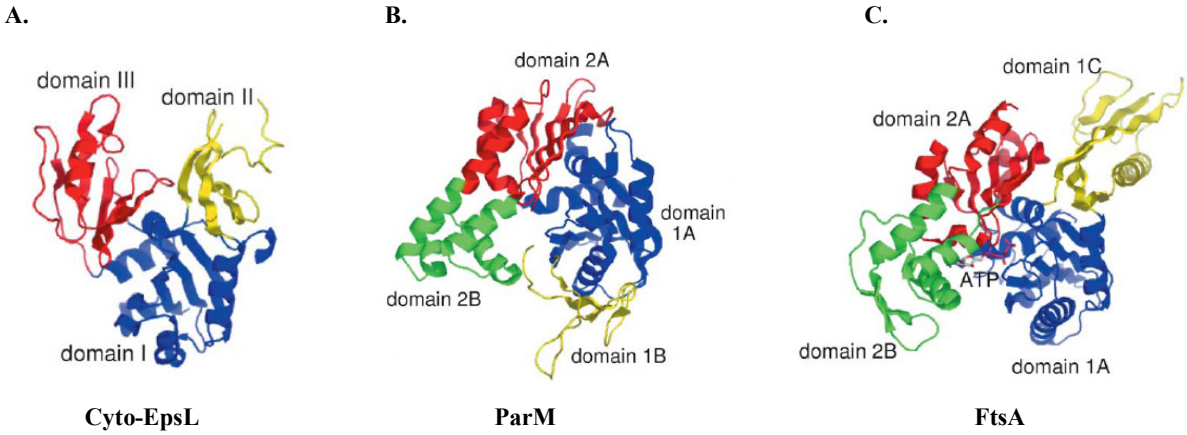

Fig. 54: Crystal structure of cyto-EpsL and the closest structural homologues ParM and FtsA of cyto-EpsL (Abendroth *et al.*, 2004a). (A) The structure of cyto-EpsL consists of three β-rich domains I, II and III. The corresponding domains are the same color in the homologues. (B) ParM has the typical actin-like fold with the four domains 1A, 1B, 2A and 2B. Domains 1A and 2A share the RNaseH fold. (C) FtsA differs from the typical actin-like fold in that it is missing domain 1B, but having a unique domain 1C instead. Cyto-EpsL contains the RNaseH like domains I and III. It is missing the variable domains 1B and 2B, but has an additional domain II, which, in spite of considerable size differences, is structurally and topologically related to domain 1C of FtsA.

Many studies have shed light on the GspL dimer formation. The yeast two-hybrid studies on the periplasmic domain of *E. chrysanthemi* GspL revealed that this domain interacts with itself (Py *et al.*, 1999). With a similar approach, Douet *et al.* (2004) suggested that both the cytoplasmic and the periplasmic domains of *E. chrysanthemi* OutL are involved in the formation of dimer. The crystal structure of cyto-EpsL revealed a homodimer interface (Fig. 55A) (Abendroth *et al.*, 2004a). In agreement with of this, the X-ray structure of N1-EpsE and cyto-EpsL complex showed that the cyto-EpsL is dimeric and forms a heterotetramer with the N1-EpsE (Abendroth *et al.*, 2005). Recently, the structure of the periplasmic domain of GspL from *V. parahaemolyticus* (*Vp* peri-EpsL) was solved (Abendroth *et al.*, 2009b). Each *Vp* peri-EpsL chain folds as a compact globular unit and consists of two α-helices and four β-strands forming

an anti-parallel β-sheet (Fig. 55B). This is an unusual variant of the ferredoxin-like fold, observed for the first time in peri-EpsM (Abendroth *et al.*, 2004b) (Described below). The *Vp* peri-EpsL was found to form a dimer in solution and in crystals. The dimer interface is made up by residues from the N-terminal helices $^{c}\alpha1$ and $^{c}\alpha1'$ and the N-terminal strands $^{c}\beta A$ and $^{c}\beta A'$ (Fig. 55B) (Abendroth *et al.*, 2009b). The interface residues of the *Vp* peri-EpsL dimer are well conserved in the GspL family, suggesting conservation of the dimer too. Therefore, the dimer interface might spread out over the cytoplasmic, the periplasmic and membrane domains and all contributions might be required simultaneously for a stable dimerization.

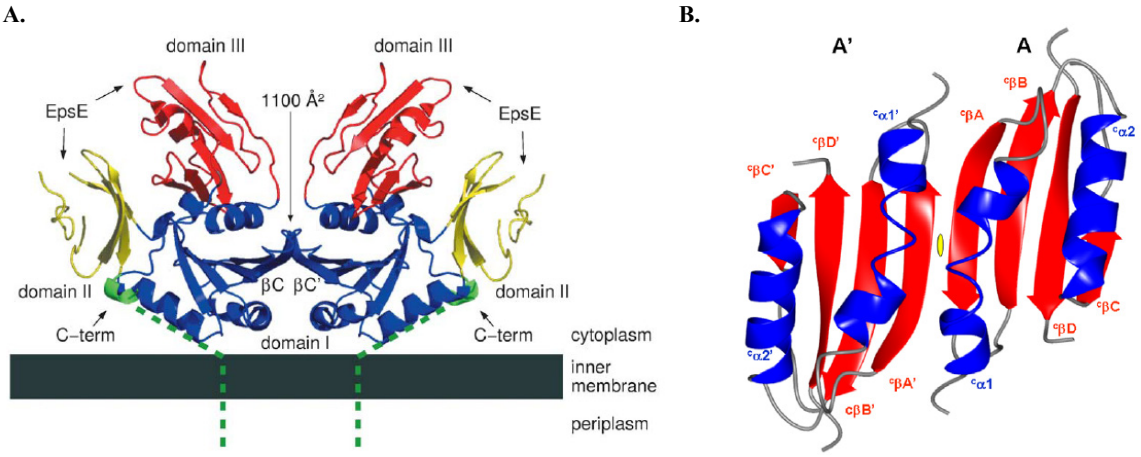

Fig. 55: The crystallographic dimer of GspL. (A) The dimer of cyto-EpsL. The dimer interface, transmembrane helices (green dots) and the putative EpsE-binding region are indicated (Abendroth *et al.*, 2004a). (B) The *Vp* peri-EpsL dimer in the crystal. The subunits A' and A are positioned left and right, respectively. The anti-parallel four-stranded β-sheet per subunit is extended to form an eight-stranded anti-parallel β-sheet in the dimer (Abendroth *et al.*, 2009b).

GspM is a small IMP with a short cytoplasmic segment, one transmembrane helix and a periplasmic C-domain (Fig. 53). The crystal structure of the periplasmic domain of GspM from *V. cholerae* (EpsM, residue 44-165) has been solved (Abendroth *et al.*, 2004b). It adopts a novel variation of the ferredoxin-like fold. Monomeric EpsM consists of two compact contiguous αββ-subdomains forming a sandwich of two α-helices and a four-stranded β-sheet (Fig. 56A), while in the "classic" ferredoxin fold, the arrangement of secondary structure elements along the polypeptide chain is βαβ-βαβ (Fig. 56B).

Both full-length EpsM (Sandkvist *et al.*, 1999) and the soluble periplasmic domain are capable of forming dimer (Abendroth *et al.*, 2004b). This suggests that neither the transmembrane domain nor the short cytoplasmic N-terminus is required for homodimerization. However, it remains to be confirmed that the full-length protein forms the same dimer interface as the periplasmic domain. Most of dimer interface of the crystal dimer formed by residues from helix

α2. A deep cleft with a polar rim and a hydrophobic bottom, made by conserved residues, are located between the two monomers. Additional electron density was found in the clef between the subunits (Abendroth *et al.*, 2004b), suggesting that this region might serve as a binding site for an unknown ligand or protein partner. Further experimental analysis mapped the region involved in EpsM dimerization to its C-terminal region between amino acids 100 and 135, thus confirming the X-ray crystal structure model (Johnson *et al.*, 2007).

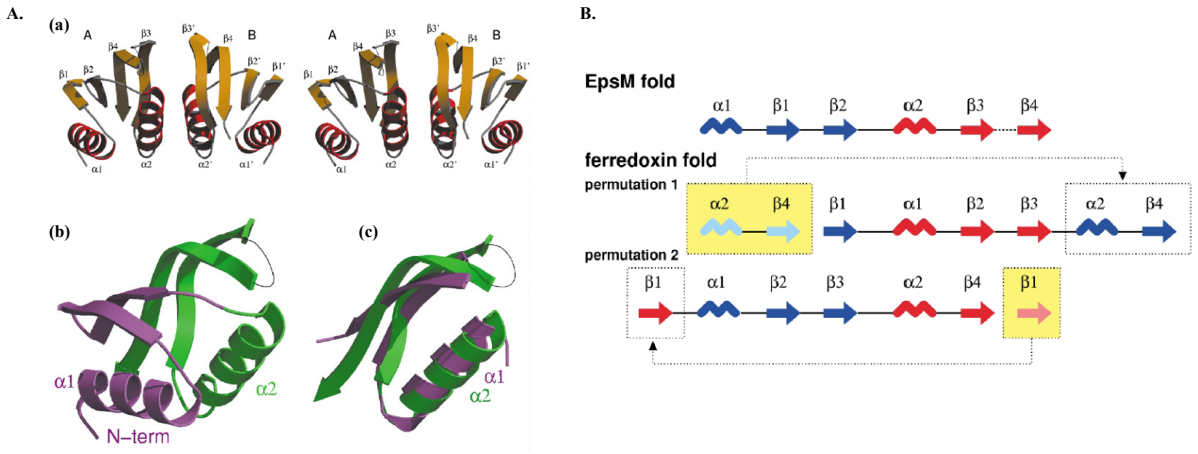

Fig. 56: The structure of the periplasmic domain of EpsM from *V. cholerae* (A) and comparison of the EpsM and ferredoxin folds (B) (Abendroth *et al.*, 2004b). (A) The structure of the dimer (a). Each EpsM consists of a sandwich of a four-stranded antiparallel β-sheet and two helices. Helices α2 and α2* mediate most of the intermolecular contacts, the putative ligand-binding groove is located between β3 and β3*. (b) The monomer consists of two αββ-subdomains, which have a very similar structure. (c) The superposition of the two subdomains in the same orientation as of the green subdomain in (b). (B) Comparison of the EpsM and ferredoxin folds. Structurally corresponding secondary structure elements have the same color and the secondary structure elements after virtual transformation are in lighter colors.

As aforementioned, the overall folds of the preplasmic regions of GspM and GspL are similar and consist of a permutation of ferredoxin-like fold. However, their roles in secretion process are not elucidated. Several investigations demonstrated that GspL and GspM play an important role in the stabilization of the IM platform. GspL and GspM of *V. cholerae* were found to form a stable binary complex and protected each other from proteolytic degradation when produced in *E. coli*, indicating that these two proteins interact with each other *in vivo* (Sandvist *et al.*, 1999). Similar results were obtained in *P. aeruginosa* and *K. oxytoca* (Michel *et al.*, 1998; Possot *et al.*, 2000). Studies in yeast-two hybrid system showed that the periplasmic domain of OutM and OutL from *E. chrysanthemi* interact with each other (Py *et al.*, 2001; Douet *et al.* 2004).

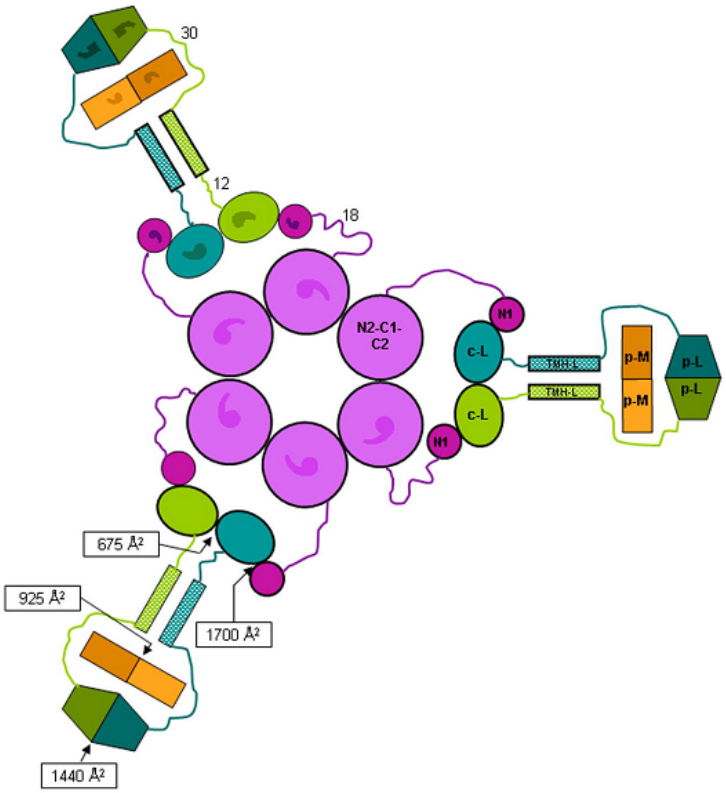

Fig.57: A possible architecture of the T2SS IM GspE: GspL subcomplex (Abendroth *et al.*, 2009b). The view is from the cytoplasm outwards with the cytoplasm in the center and the periplasm at the periphery. The hexamer of full-length of GspE (purple) and the three dimers of cyto-GspL (shades of green per dimer) shown in the center are in the cytoplasm. Predicted TM helices of GspL are shown as hatched rods, located in the IM. On the outside are depicted three peri-GspL dimers in the periplasm (in darker shades of green). A tentative position of the peri-GspM dimer is depicted in light and darker yellow.

Based on the results on GspE, L, M of T2SS, Abendroth *et al.* (2009b) proposed architecture of the T2SS IM complex (Fig. 57). The cyto-GspL and N1-GspE form heterotetramer. Each heterotetramer is linked to two adjacent N2-C1-C2 domains of GspE in the hexamer. The TM helices of GspL in each heterotetramer cross the IM and the periplasmic domains of GspL form dimers.

GspL was also shown to interact with minor pseudopilin GspJ (Douet *et al.*, 2004). Recently, *in vivo* cross-linking study showed an interaction between GspL and the major pseudopilin GspG (Gray *et al.*, 2011). Previous studies have shown that GspL interacts with GspE. Together with these results, Gray *et al.* (2011) proposed that GspL may function as a scaffold to link GspG and GspE and thereby transduces the energy generated by ATP hydrolysis to support secretion.

III.3.4 Connection between IM and OM sub-complexes: GspC

Most of the proteins composing the T2SS are associated with or integrated in the IM, except for GspD and GspS, which are located in the OM. This suggests that the certain components of

the T2SS ensure a permanent or transient junction between the two cellular membrane to allow for a structural integrity of the secretion machinery. It has been suggested that the IM protein GspC may connect the two sub-complexes, the IM platform consisting of GspE-F-L-M and the OM secretin pore formed by GspD by interacting with both the secretin GspD and the two IM components GspL and GspM.

GspC is a bitopic IM protein that appears to be one of the least conserved component of all the core components of the T2SS (Gérard-Vincent *et al.*, 2002). It consists of a short cytoplasmic N-terminal cytoplasmic sequence, a single membrane-spanning helix (TMS), followed by a large hydrophilic region which protrudes into the periplasm (Fig. 58). The periplasmic region contains a so-called homology region (HR) and a PDZ domain near their C termini in the majority of GspC. In some GspC family members, the PDZ domain is absent or replaced by a coiled-coil (CC) domain (Gérard-Vincent *et al.*, 2002; Peabody *et al.*, 2003).

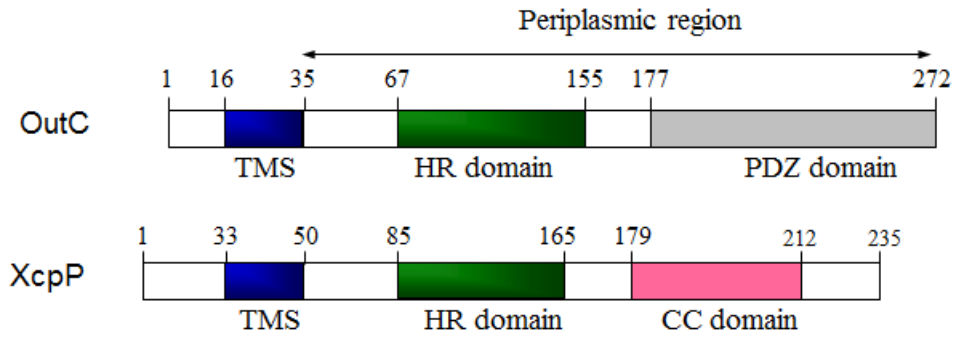

Fig. 58: Schematic representation of the OutC and XcpP domains. The positions are according to Login *et al.* (2010) and Gérard-Vincent *et al.* (2002).

The PDZ domains are named after the three eukaryotic proteins in which they were first found: PSD-95 (a 95 kDa protein involved in signaling at the post-synaptic density), DLG (the *Drosophila melanogaster* Discs large protein) and ZO-1 (the zonula occludens 1 protein involved in maintenance of epithelial polarity) (Hung and Sheng, 2002). These domains have also been referred to as DHR (Discs large homology repeat) domains or GLGF repeats (after the highly conserved four-residue GLGF sequence within the domain). They are small globular modules of about 80-100 amino acid residues consisting of six β-strands (βA- βF) and two α-helices (αA and αB) (Fig. 59) (Harris and Lim, 2001). The PDZ domains function as protein-protein interaction modules and typically recognize the short (about five residues long) extreme C-termini of target proteins (Jelen *et al.*, 2003). Peptide ligands bind in an extended groove between strand βB and helix αB thus serving as an additional antiparallel β-stranded within the PDZ domain (Fig. 59A). This mechanism is referred to as β-strand addition (Remaut and Waksman, 2006). The highly conserved GLGF motif is located within the loop connecting

strands βA and βB. It is involved in hydrogen bond formation with the carboxyl group of the C-terminal residues of the interacting peptide (Harris and Lim, 2001). Certain PDZ domains associate with partner proteins via internal protein sequence that structurally mimics the C-terminus (Brenman *et al.*, 1996). For instance, the PDZ domain of neuronal nitric oxide synthase (nNOS) specifically interacts with PDZ domains of PSD-95 and syntrophin (Brenman *et al.*, 1996). A stable β-hairpin (called the β-finger) of the nNOS PDZ domain appeared to be responsible for binding to PDZ domains in a fashion similar to that of peptides despite the absence of a carboxy-terminal carboxylate moiety (Fig. 59B) (Hillier *et al.*, 1999).

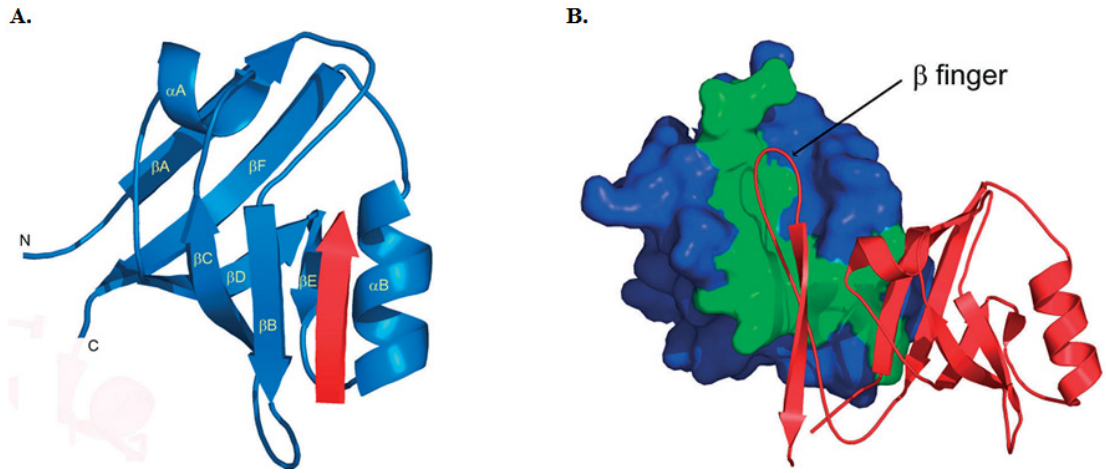

Fig. 59: Structure of the PDZ domain bound to peptide and internal peptide motif. (A) Ribbon representation of the PDZ domain of PSD95 (blue) with KQTSV peptide forming antiparallel β-sheet with βB strand (red arrow). (B) Complex of the syntrophin PDZ domain (shown as blue and green solvent-accessible surface representation) and nNOS PDZ domain (shown as red ribbon representation with β-finger indicated) (Jelen *et al.*, 2003).

The PDZ domain of GspC appears to be involved in interaction with certain exoproteins and therefore determines the secretion specificity, as shown by swapping the PDZ domains of OutC from *E. chrysanthemi* and *E. carotovora* which switches the specificity of the secretion system (Bouley *et al.*, 2001). The crystal structures of two variants of the PDZ domain of EpsC, a short (residues 219-305; called s-PDZ-C) and a long (residue 201-305; called also l-PDZ-C), have been solved (Korotkov *et al.*, 2006). The structure of the s-PDZ-C of EpsC has the typical PDZ domain fold with six characteristic β-strands (βA- βF) flanked by helices αA and αB (Fig. 60A). While the structure of the l-PDZ-C of EpsC has a unique feature that is not present in any other PDZ domain of known structure. The chain of l-PDZ-C starts with the long helix α1 followed by a kink and the shorter helix α2 (Fig. 60B). This N-terminal extension together with helix αA forms a well-ordered helical sub-domain in the structure of l-PDZ-C. Both variant structures show that the PDZ domain of EpsC adopts a more open form than in previously reported

structures. In addition, no members of the GspC family contain a GLGF motif preceding strand βA. These indicate that the PDZ domain of this bacterial protein binds proteins in a manner which is altogether different from that seen in any other PDZ domain so far (Korotkov *et al.*, 2006). The fact that two variant crystal structures show a significant movement of αB, may reflect the occurrence of conformational changes in EpsC upon protein binding and release when the T2SS performs its intricate function (Fig. 60C) (Korotkov *et al.*, 2006).

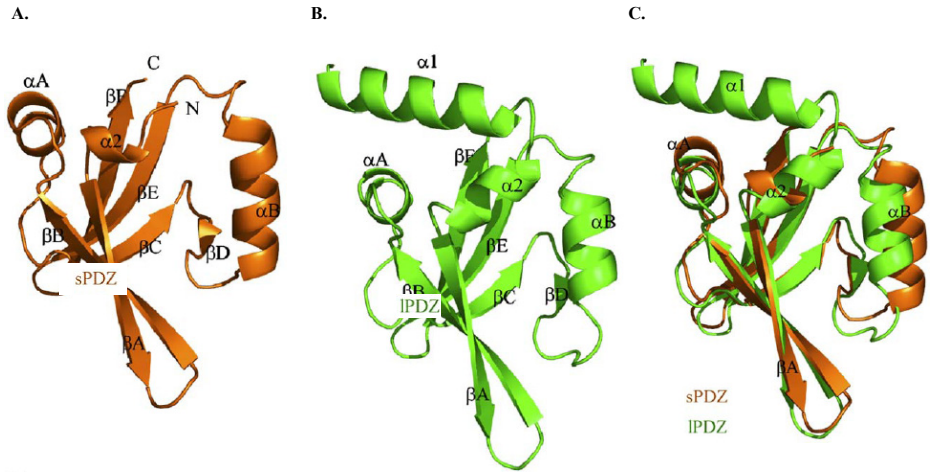

Fig. 60: The structure of the PDZ domain of EpsC from *V. cholerae* (Korotkov *et al.*, 2006). (A) The structure of the short version of the PDZ domain of EpsC (s-PDZ-C), spanning residues 219 to 305. (B) The structure of the long version of the PDZ domain of Eps-C (l-PDZ-C), ranging from residue 201 to 305. (C) The superposition of the two PDZ-C structures.

The coiled-coil domains are composed of two or more α helices arranged in parallel or antiparallel manner and usually implicated in protein-protein interactions (Burkhard *et al.*, 2001). It has been suggested that both the coiled-coil and PDZ domains are involved in homomultimerization of GspC components in a non-specific maner (Gérard-Vincent *et al.*, 2002). Certain GspC, such as XphA, which is much shorter and possesses neither a PDZ nor coiled-coil domain, is still a functional protein (Michel *et al.*, 2007). This is consistent with the previous results that lack of the C-terminal coiled-coil domain in XcpP (GspC of *P. aeruginosa*) does not prevent the protein from assembling into a functional T2SS (Gérard-Vincent *et al.*, 2002) and deleting the PDZ domain of OutC of *E. chrysanthemi* results in a partially functional protein (Bouley *et al.*, 2001).

Studies of GspC of *P. aeruginosa* and *X. campestris* showed that substitution of the N-terminal region, either with the first TMS of TetA or with a signal peptide, completely abolished protein function (Bleves *et al.*, 1999; Lee *et al.*, 2004). This indicates that the TMS of GspC not only functions anchor, but also implicates in the functionality of the protein. This was further confirmed by Login and Shevchik (2006). They showed that the TMS of OutC is more than just

a membrane anchor. It mediates an efficient self-association necessary for protein function. Site-directed mutagenesis of the TMS revealed that cooperative interactions between three polar residues, Gln^{29}, Arg^{15}, and Arg^{36}, located at the same helical face provide adequate stability for OutC self-assembly (Login and Shevchik, 2006). The disruption of OutC TMS self-association resulted in a loss of protein activity *in vivo*. However, studies with the PulC (GspC of *K. oxytoca*) suggested that the TMS of this protein could be replaced with a lipid anchor, without a loss of functionality (Possot *et al.*, 1999). Thus, the exact function and necessity of the TMS may differ between bacterial backgrounds.

Little is known about structural properties of the HR domain. Recently, in collaboration with Prof. Pickersgill from London University, the 3D structure of HR domain of OutC was solved. It revealed a structure that similar to PilP of T4P (Golovanov *et al.*, 2006). The protein adopts a beta-sandwich type fold with two beta sheets, each composed by 3 antiparallel strands, stacked on each other (Gu *et al.*, 2012b). A short 3_{10} helix is formed at the N-terminus, which is also found in the only other β-sandwich -type fold protein PilP (Golovanov *et al.*, 2006). The exact function of this domain is still unclear. The HR domain of GspC of *V. cholerae* was shown to be engaged in interactions with the periplasmic domain of the secretin EpsD (Korotkov *et al.*, 2006). This result is in agreement with previous studies suggesting that GspC could interact with the OM secretin (Bleves *et al.*, 1999; Lee *et al.*, 2000; Possot *et al.*, 1999). Recently, we showed that a short peptide of the HR domain of OutC (OutCsip) interacts *in vitro* with two distinct sites of OutD: N0 and N2-N3' subdomains (Login *et al.*, 2010).

In conclusion, Studies on the GspC from various bacterial species have revealed that this protein is most likely performing multiple functions in the T2SS, Namely:

i) it was shown that the the periplasmic region of GspC proximal to the TMS interacts with the GspL-M hetero-multimer and thus GspC may be part of a larger IM sub-complex consisting of GspC-F-L-M (Possot *et al.*, 2000; Robert *et al.*, 2002, 2005; Tsai *et al.*, 2002; Lee *et al.*, 2004);

ii) several studies point out interactions between GspC and the OM secretin GspD (Lindeberg *et al.*, 1996; Possot *et al.*, 2000; Rober *et al.*, 2005; Korotkov *et al.*, 2006), furthermore, our recent studies showed that a short peptide of the HR domain of OutC (OutCsip) interacts *in vitro* with two distinct sites of OutD: N0 and N2-N3' subdomains (Login *et al.*, 2010);

iii) deletion and domain exchange studies of GspC and GspD proteins from *Erwinia* indicated that both the PDZ domain of GspC and the N-terminal domain of GspD are

involved in the secretion specificity of the T2SS (Bouley *et al.*, 2001);

iv) cross-linking analysis revealed an association of the major pseudopilin GspG with the GspC in functional strains of *X. campestris pv.campestris* (Lee *et al.*, 2005).

Thus, GspC is thought to link three subcomplexes, namely the secretin GspD in the outer membrane, the pseudopilins and the IM platform and allows to form an integral T2S apparatus.

III.3.5 Auxiliary proteins GspN, GspA and GspB

GspN is a bitopic IM protein. It has been identified in many bacteria, e.g., in *K. oxytoca, V. cholerae, E. carotovora,* but not in *D. dadantii*. Non-polar PulN mutant of the T2SS of *K. oxytoca* reconstructed in *E. coli* remained functional (Possot *et al.*, 2000).

GspA and GspB proteins are not present in all the species carrying a T2SS, indicating that the role of GspAB is not indispensable to assembly of the T2SS. For example, a recent study showed that GspAB present in both *Aeromonas* and *Vibrio* and is essential for formation of a functional T2SS in *Aeromonas* but is dispensable in *Vibrio* (Strozen *et al.*, 2011). GspA is a membrane protein with a conserved ATP binding site which suggested to be a traffic ATPase (Schoenhofen *et al.*, 2005), whereas GspB has a sequence similar to that of TonB which associates with the IM and is required to transduce IM energy to OM TonB-dependent receptors. This suggested the involvement of GspB in an energy-transducing process. It was demonstrated that GspA and GspB form a complex within the cytoplasmic membrane and such complex from *A. hydrophila* (ExeA/ExeB) may help the translocation of the ExeD secretin from the IM to the OM (Ast *et al.*, 2002; Strozen *et al.*, 2011). Indeed, in the abesence of ExeAB, ExeD remains in the IM as a monomer. Interestingly, the periplasmic domain of ExeA was found to contain a putative peptidoglycan-binding motif and the interaction with peptidoglycan may help achieve such a function (Howard *et al.*, 2006). Moreover, this inteaction caused the periplasmic ExeA domain to form a large multimers, possibly a ring-like structure (presumable also containing ExeB) on petidoglycan (Li and Howard, 2010). Such ring could act as a scaffold to direct the assembly of the secretin through ExeA-D and/or ExeB-D interaction. Indeed, GspB homolog OutB was found to be required for the secretion in *E. chrysanthemi* and interact with secretin OutD. The two proteins are also characterized by a mutual stabilization (Condemine and Shevchik, 2000). However, contrary to the essential role of GspAB in assembly of the secretin and secretion of T2SS substrates in *Aeromonas* species, GspB is not required for pullulanase secretion, at least when the T2SS of *K. oxytoca* were reconstructed in *E. coli* (Possot *et al.*, 2000). In *vibrio*, mutation of *gspA* (which also apparently inactivated *gspB*) did not prevent secretion of T2SS substrates. However, a significant reduction in the amount of assembled secretin multimer were

detected in the absence of GspAB (Strozen *et al.*, 2011). The precise function of GspAB play in the T2SS secretion remains to be elucidated.

III.4 Cell location of the T2SS components

Fluorescence microscopy of living *V. cholerae* cells revealed that green fluorescent protein (GFP) chimeras of GspM (EpsM) and GspL (EpsL) localized predominantly to one of the poles of the *V. cholerae* cell (Scott *et al.*, 2001). Moreover, EpsM was found to have all the information needed to be localized at the pole of the cell because when expressed in *E. coli*, EpsM can localize to the pole in the absence of other T2SS components. Interestingly, EpsL was associated with the cell pole only upon co-expression with EpsM. These results indicate that not all the proteins of T2SS contain the information required for polar targeting. And the assembly of the machinery is an ordered event with a cascade protein-protein interaction in which the GspM protein may determine the membrane location of the machinery, recruiting the GspL component, which in turn brings GspE into association with the membrane. Coherent with the polar location of GspM and GspL, this study also revealed a polar secretion of the *V. cholerae* toxins (Scott *et al.*, 2001). However, Buddelmeijer *et al*. (2006) showed that both GFP-PulL and GFP-PulM (GspL and GspM of *K. oxytoca*) localized circumferentially in the *E. coli* cell envelope, with occasional brighter foci when other secreton factor were present. Furthermore, overproduction of GFP-PulM or GFP-PulL results in their polar localization. These results suggest that polar accumulation may be due to overproduction of the proteins and do not represent the normal location of GspM and GspL. Coherent with the non-polar localzation of the *K. oxytoca* T2SS components, Buddelmeijer *et al*. (2009) further showed that chromosome-encoded PulD-mCherry (PulD fused to a monomeric red fluorescent protein) formed fluorescent foci on the periphery of the cell in the presence of high levels of its cognate chaperone, the pilotin PulS. Recently, Lybarger *et al.* (2009) showed that fluorescently tagged, chromosomally expressed GspC and GspM of *V. cholerae* form discrete foci along the lengths of the cells (Lybarer *et al.*, 2009). Furthermore, they showed that those fluorescent foci in both chromosomal GFP-GspC- and GFP-GspM-expressing strains of *V. cholerae* disperse upon deletion of *gspD*, suggesting that GspD is crucial for proper localization of the IM proteins GspC and GspM and perhaps their assembly into the T2S complex (Lybarer *et al.*, 2009).

III.5 Exoprotein recognition

Secrection by the T2SS is a two-step process. Exoproteins bearing singal peptide are firstly recognised either by the Sec or the Tat system and translocated across the IM. Then they are folded in the periplasm and become the substrates for the T2SS. The T2SS could distinguish its

substrates from other periplasmic proteins and translocted them through OM. However, little is known how the T2S apparatus recognizes T2S substrates and no obvious amino acid sequence motif has been identified in T2S substrates as a notable secretion signal. Indeed, proteins secreted by the same bacterium often do not share any obvious sequence homology. This process may be based on the recognition of a structural secretion motif by some of the Gsp components.

III.5.1 Species-specific recognition of exoproteins

T2SS is often well conserved between various Gram-negative bacteria. However, T2SS-dependent exoproteins from one specie can not be generally secreted via the T2SS of antother specie. For example, the *K. oxytoca* Pul system cannot secrete *P. aeruginosa* or *E. chrysanthemi* proteins (de Groot *et al.*, 1991; He *et al.*, 1991a), whereas, *P. aeruginosa* can not secrete pullulanase (de Groot *et al.*, 1991). Heterologous secretion has been observed only in certain closely related organisms. For example, the bacteria *P. alcaligenes* and *P. aeruginosa* could secrete exoproteins of each other (de Groot *et al.*, 2001). *E. chrysanthemi* and *E. carotovra* use the T2SS (Out system) whose individual components share a high degree of sequence conservation, to secrete similar Pels. However, the *E. chrysanthemi* T2SS fails to secrete Pel1 from *E. carotovora* even though Pel1 possesses 71% indentity to *E. chrysanthemi* PelC (Lindeberg *et al.*, 1998). Two pectate lyases, PelI of *E. chrysanthemi* and Pel-3 of *E. carotovora*, share 67% identity. When PelI and Pel-3 were expressed from plasmids in *E. carotovora*, they were secreted with a similar efficiency. However, when expressed in *E. chrysanthemi*, PelI was secreted but Pel-3 was not. This indicates that the Out systems of *E.carotovora* and *E. chrysanthemi* differ on their capacity to distinguish between the secretion substrates (Bouley *et al*., 2001). Heat-labile enterotoxin (LT) from ETEC and cholera toxin (CT) from *V. cholerae* are very similar in structure, they share 83% sequence identity in the mature B subunit. Despite the high degree of homology between LTB and CTB, it was shown that mutations affect their secretion differently in distinct T2SS, indicating that each substrate has evolved closely with its T2SS to enable its secretion (Mudrak and Kuehn, 2010). In conclusion, these results suggested a different level of T2SS species-specifity. Exoprotein recognition process may depend on the presence of a secretion motif within the secreted protein. However, comparisons of the sequences of the diverse proteins which are secreted by T2SS did not reveal an obvious common linear motif in various T2S substrates. The fact that Gsp-dependent exoproteins are translocated across the OM in a folded conformation led to suggest that a three-dimensional “structural motif” may exist in T2SS substrates.

III.5.2 Folding and secretion motif of exoproteins

Several studies suggested that T2SS exoproteins are translocated across the OM in a folded conformation.The studies with *V. cholerae* and *A. hydrophila* have shown that the B pentamer of the cholera toxin is formed in the periplasm before secretion while aerolysin is secreted as a dimer (Hirst and Holmgren, 1987). The studies with *E. chrysanthemi* cellulase and pectate lyases and *K. oxytoca* pullulanase have shown that the disulfide bond formation is a prerequisite for T2SS-dependent secretion (Pugsley, 1992; Bortoli-German *et al.*, 1994; Shevchik *et al.*, 1995). The lipase of *P. aeruginosa* was not secreted in a mutant strain devoid of the oxidoreductase DsbA, indicating the importance of the disulfide bond formation to the secretion of the enzyme (Urban *et al.*, 2001). Therefore, the secretion motif may be formed and presented to the secretory apparatus on the folding of the exoprotein. This motif probably involve distal regions brought into close proximity by the folding of the protein.

Many studies have attempted to identify the structural motif presented as secretion signal in T2SS substrates. Two non-adjacent regions in the *K. oxytoca* pullulanase, A (close to the signal peptide) and B (in the C-terminal region), together direct the secretion of PulA-BlaM and PulA-CelZ hybrid proteins (Sauvonnet and Pugsley, 1996). Furthermore, Francetic and Pugsley (2005) showed that A and B fused to the PelB signal peptide (sp) can also promote secretion of BlaM and CelZ but not that of nuclease NucB or several other reporter proteins. PelBsp-PulA, a nonacylated variant of PulA made by replacing the lipoprotein signal peptide (sp) with the signal peptide of pectate lyase PelB from *E. chrysanthemi*, was efficiently secreted into the medium. However, the deletion of most of region A or all of region B, either individually or together, had only a minor effect on PelBsp-PulA secretion. These led to identify an additional PulA region (region C) that could contain part of the PulA secretion signal or be important for its correct presentation (Francetic and Pugsley, 2005). Indeed, the deletion of region C abolished PelBsp-PulA secretion without dramatically affecting its stability, and PelBsp-PulA-NucB chimeras were secreted only if the PulA-NucB fusion point was located downstream from region C (Francetic and Pugsley, 2005). Studies of cellulase Cel5 from *E. chrysanthemi* suggested that, prior to secretion, a folded form of the cellulose-binding domain (CBD) interacts physically with the catalytic domain, resulting in a transient secretion-specific conformation (Chapon *et al.*, 2000). Furthermore, Chapon *et al.* (2001) suggested that the catalytic domain ought to fold into a wild-type conformation before Cel5 is secreted. Since a mutation of R57H, which is located at the heart of the catalytic domain of Cel5, exhibits distinct but close conformation from the wild-type, is not secreted, indicating the strong constraints that secretion exerts upon folding. In polygalacturonase PehA of *E. carotovora* , two regions, one close to the C-terminus between

residues 342 and 369 and another between residues 84 and 135 in the large central loop were required together to promote secretion, indicating that these two regions include a targeting motif (Palomäki *et al.*, 2002). These two motifs are structurally dissimilar, which suggests that there are two distinct recognition regions in the T2SS. In PelC of *E. chrysanthemi*, a single C-terminal region composed of loops was considered to be involved in a targeting motif whereas two helical regions, which were also reported to be required for secretion, were suggested to be necessary for the proper positioning of the loop region (Lindeberg *et al.*, 1998).

As reported above, the secretion motif may be composed of different parts of the polypetide chain which are brought together during protein folding. However, the nature of the conformational signal has not yet been elucidated even though the 3D structure of several T2S-dependent exoproteins have been solved. There is evidence that these proteins are rich in β-sheet content (Sandkvist, 2001b). For example, studies on *P. aeruginosa* showed that exotoxin A 60-120 region appeared to be rich in anti-parallel β-sheet (Lu and Lory, 1996). Several 3D structures of the proteins, i.e., PelC, PelE, Cel5, PelA, Pel9A and PelI secreted by *E. chrysanthemi* T2SS Out, showed that they are all rich in β-sheet (Yoder *et al.*, 1993, Lietzke *et al.*, 1994; Chapon *et al.*, 2001; Thomas *et al.*, 2002; Jenkins *et al.*, 2004; Creze *et al.*, 2008). However, the putative secretion motif of PelC seems to be composed of loops (Lindeberg *et al.*, 1998). In addition, one of putative PehA targeting motif, the A region, is composed of two large loop structure (Palomäki *et al.*, 2002). Thus, nature of the secretion motif in the proteins secreted by the T2SS remains to be identified.

III.5.3 Secretion specificity and GspC/GspD

Several studies have shown that two components of the secreton GspC/GspD are not individually exchangeable, even between closely related species such as *P. aeruginosa* and *P. alcaligenes* XcpP/XcpQ (de Groot *et al.*, 2001), or *E. chrysanthemi* and *E. carotovora* OutC/OutD (Lindeberg *et al.*, 1996). These indicated that GspC and GspD could be involved in the specific recognition of the exoproteins. Indeed, the pectate lyase PelB of *E. chrysanthemi* but not PelC of *E. carotovora* was demonstrated to interact with the N-terminal domain of OutD (Shevchik *et al.*, 1997). Recently, surface plasmon resonance (SPR) studies showed that the periplasmic domain of ETEC GspD interacts with the B-pentamer of heat-labile enterotoxin (Reichow *et al.*, 2010) while EM showed that the B-pentamer of cholera toxin bound within the *V. cholerae* GspD periplasmic vestibule (Reichow *et al.*, 2011). The N-terminus is the most variable region of the secretin, consistent with the notion of specificity for recognition of the exoproteins. Bouley *et al.* (2001) have shown that both the PDZ domain of OutC and the N-

terminal domain of OutD are required for specific recognition of secreted proteins. And the proteins secreted by *E. chrysanthemi* Out system could be divided into three main groups:

i) most of the pectate lyases, for example, PelB, C, D, E and PelL, whose secretion is dependent on the presence of the PDZ domain of OutC and the N-terminal domain of OutD;

ii) Cel5, that is secreted in a PDZ-independent manner but require the presence of the N-terminal domain of OutD for secretion;

iii) PemA and PelI, whose secretion is PDZ-independent and is mediated as much by OutD of *E. chrysanthemi* as by OutD of *E. carotovora*.

Thus, Bouley *et al.* (2001) proposed that diverse exoproteins possess a variable number of targeting signals which are recognized by different regions of OutC and OutD.

III.6 Comparison between the T2SS and the type IV pili

The type IV pili (T4P) are cell surface filament that traverses the OM of Gram-negative bacteria and contribute to prokaryotic cell survival and pathogenesis. These polar filaments are composed of thousands of copies of pilin and are 5-8 nm in diameter and up to several micrometers long (Chiang *et al.*, 2005; Nudleman *et al.*, 2006). T4P serve remarkably diverse functions, including bacterial motility, adhesion, microcolony and biofilm formation, DNA uptake during natural transformation, phage transduction (reviewed in Craig *et al.*, 2004 and Pelicic, 2008). It was also shown that the contribution of T4P to virulence was related to its direct involvement in the secretion of toxins (Hager *et al.*, 2006; Han *et al.*, 2007). Based on length and sequence of the pilin subunit, T4P can be further classified into two subclasses, termed T4aP and T4bP (Craig and Li, 2008). Pilins of T4aP have short leader peptides (less than 10 aa) and a characteristic length of about 150-160 aa. T4aP are involved in adherence, twitching motility and a form of flagellar-independent surface motility involved in dissemination from the point of attachment. Pilins of T4bP have long leader peptides (about 15-30 aa) and are either long (180-200 aa) or surprisingly short (only about 40-50 aa). T4bP are found predominantly in enteric pathogens, function in adhesion and bacterial aggregation (Ayers *et al.*, 2010). Systematic genetic studies showed that the proteins associated with T4bP are more diverse than their T4aP counterparts (Pelicic, 2008). Even so, a conserved core of proteins, common to both T4aP and T4bP is identified (Figs. 61B and 61C), namely: i) one or several pilin proteins; ii) a specific peptidase that processes the prepilins and prepilin-like proteins; iii) an ATPase that powers T4P assembly; iv) an OM secretin responsible for mediating the passage of the pilus fiber across the OM; v) IM complex that is critical for the assembly of functional machinery.

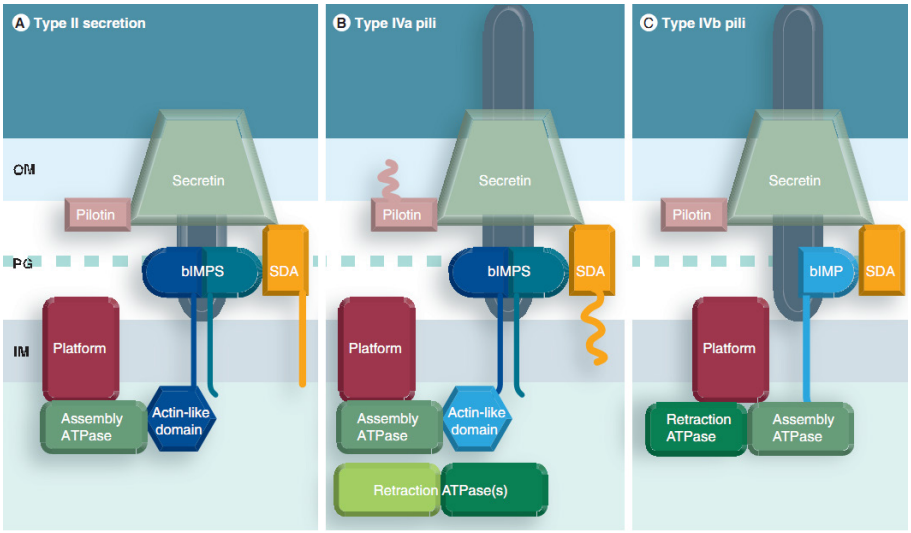

Fig. 61: T2S and T4P system architectures (Ayers *et al.*, 2010). They have a similar organization, consisting of inner and outer membrane subcomplexes. Proteins predicted to have similar structures are represented with similar colors. OM subcomplexes consist of a dodecameric secretin with its associated pilotin. The SDA (secretin dynamic-associated protein) mediates secretin function and also links the OM components with those in the IM. IM subcomplexes typically consist of the platform protein, one or more bIMPs (bitopic inner membrane protein), the ATPase(s) and, in the T2S/T4aP system, a cytoplasmic protein with an actin-like fold.

The T2SS and T4P, especially T4aP, share a number of protein homologs that are predicted, or have been demonstrated, to localize and function in a similar manner (Fig. 61). Most strikingly, T2SS requires the presence of proteins that are highly homologous to type 4 pilins (Bose *et al.*, 2002). In both systems, the prepilins or prepilin-like proteins are processed by a homologous type 4 prepilin peptidase. In addition, both systems have an OM protein, known as the secretin, that has been demonstrated to multimerize and form an OM channel through which proteins can pass during the extracellular translocation step. Both systems also have at least one ATPase, together with conserved polytopic IM protein, named GspE/PilB and GspF/PilC, in T2SS and T4P respectively. These proteins are thought to assure extrusion of growing (pseudo)pilus from the IM (Py *et al.*, 2001; Morand *et al.*, 2004). They have an IM complex composed of several conserved proteins that are critical for the assembly of functional machinery (Sampaleanu *et al.*, 2009). However, some secreton components that are needed for T2SS assembly appear to be absent from the T4P system (Table. 1). Additionally, certain components are only present in T4P systems (Table. 1). These observations probably reflect the ancient separation during divergent evolution of the T2S and T4P systems. Nevertheless, the comparison between T2S and T4P systems, especially with current research findings, will help us to better understand the assembly and function mechanism of the two systems.

Table. 1: Nomenclature used for Gsp and Xcp T2SSs, Pil T4aP in Gram-negative bacteria *P. aeruginosa* (Hazes and Frost, 2008; Ayer *et al*., 2010).

T2SS		Type IV pili	Comment
Gsp	Xcp	Pil	
GspG	XcpT	PilA	Major (pseudo)pilin
GspH	XcpU	PilE	Minor (pseudo)pilin. Not essential
GspI	XcpV	PilV	Minor (pseudo)pilin. Essential for secretion and pilus assembly
GspJ	XcpW	PilW	Minor (pseudo)pilin. Essential for secretion, not pilus assembly
GspK	XcpX	PilX	Minor (pseudo)pilin. Inhibits pilus extension, lacks Glu5
GspO	XcpA	PilD	Prepilin peptidase/N-methylase
GspD	XcpQ	PilQ	OM. Secretin. Conduit for pili and substrates
GspE	XcpR	PilB	Cytoplasmic. Hexameric ATPase. Energizes transport
GspL	XcpY	PilM/N	IM sub-complex component
GspM	XcpZ	PilO	IM sub-complex component
GspF	XcpS	PilC	Transmembrane protein
GspC	XcpP	-	IM. Connects IM sub-complex and OM sub-complex
GspA	-	-	IM. Unknown function
GspB	-	-	IM. Unknown function
GspN	-	-	IM. Unknown function
GspS	-	PilP	OM. Pilotin, binds and stabilizes GspD
-	-	PilT	Hexameric ATPase. Energizes retraction
-	-	PilU	Hexameric ATPase. Energizes retraction
-	-	FimT	Minor pseudopilin. Not essential
-	-	FimU	Minor pseudopilin.

III.6.1 The secretin

The secretin family is conserved in different secretion and export systems (Fig. 62) and is known to form oligomeric ring-like structures in the OM of Gram-negative bacteria. It consists of a variable N-terminal domain that resides in the periplasm and a conserved C-terminal domain that inserts in the OM where it forms a pore conduit for pili or secreted proteins (see the Chapter III.3.1.2, the secretins of T2SS). The micromolecular complexes formed by several secretins from T2SS, T3SS, T4P and filamentous phage extrusion systems have been studied by EM analysis (Reichow *et al.*, 2010; Hodgkinson *et al.*, 2009; Jian *et al.*, 2011; Opalka *et al.*, 2003). Recently, atomic resolution structures of periplasmic domain of secretins from T2SS and T3SS have been solved (see Chapter III.3.1.1, page 55) (Korotkov *et al.*, 2009a; Spreter *et al.*, 2009)

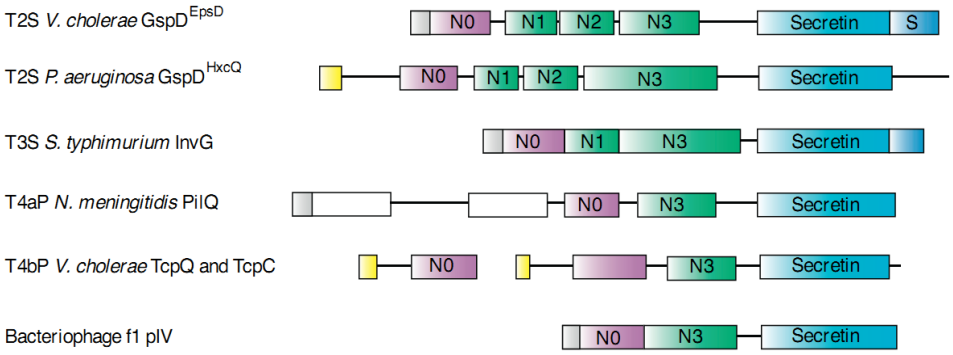

Fig. 62: Domain composition of secretins in different systems. The N-terminal signal sequences recognized and cleaved by a signal peptidase are represented by gray and prolipoprotein signal peptidases are represented by yellow. The homologous domains are represented by the same colors, N0: purple, N1-N2-N3: light green, Secretin domain: blue, pilotin-interaction domain (S domain): dark blue and unknown topology domains: white (Korotkov *et al.*, 2011a).

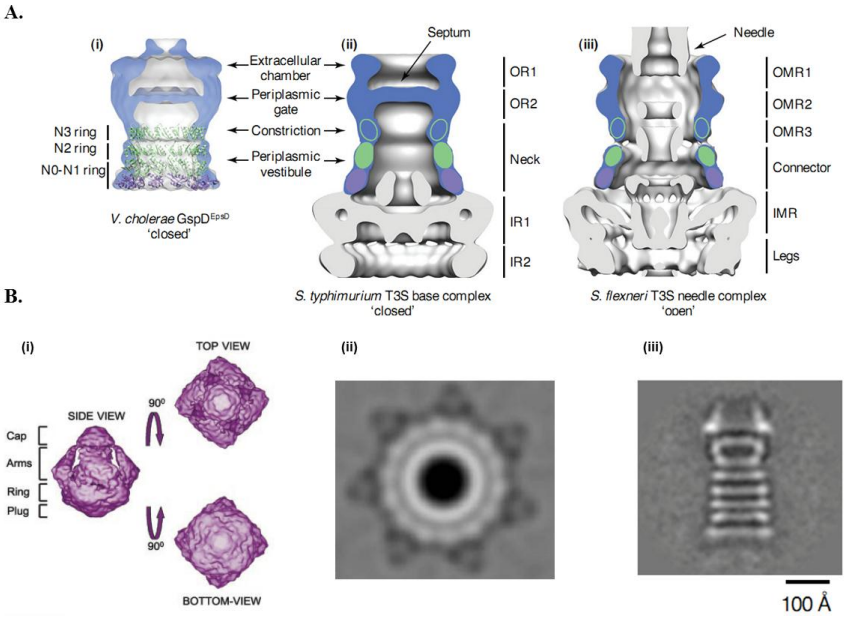

Fig. 63: Electron microscopy structures of secretins. (A) Cryo-EM reconstruction of T2SS secretin (i) (Reichow *et al.*, 2010) and T3SS secretin (ii, iii) (Hodgkinson *et al.*, 2009). (B) EM structures of PilQ secretins from *N. meningitidis* (i) (Collins *et al.*, 2004), *N. gonorrhoeae* (ii) (Jain *et al.*, 2011) *and T. thermophilus* (iii) (Burkhardt *et al.*, 2011).

Although some differences in symmetry and nature of the constriction or plug were found, they share a similar basic overall structure (Fig. 63) (Ayers *et al.*, 2010; Korotkov *et al.*, 2011a). For example, the crystal structures of the N-terminal domains (N0-N1-N2) of the T2SS secretin GspD from ETEC and the periplasmic domains (N0-N1) of the T3SS secretin EscC from EPEC revealed that the two N-terminal domains N0-N1 from two systems adopt a similar fold, although the mutual orientation of these domains with respect to each other is unexpectedly different (Fig. 39C) (Korotkov *et al.*, 2009a; Spreter *et al.*, 2009). Recent cryo-EM structure of

the secretin GspD from the *V. cholera* T2SS revealed a multimeric channel of 12-fold symmetry with a periplasmic gate in its closed state (Fig. 43) (page 60) (Reichow *et al.*, 2010). Similar results were initially observed through transmission EM studies of the T4aP secretin PilQ (Collins *et al.*, 2001, 2003). However, subsequent cryo-EM and 2D crystal analyses suggested that the T4aP secretin adopts fourfold symmetry that is closed at both ends but lacks the periplasmic gate found in reconstructions of the secretins from other secretion systems (Fig. 63B, i) (Collins *et al.*, 2004). Very recent transmission EM analysis of the T4P secretin PilQ from *N. gonorrhoeae* showed a double ring structure with a 14-fold symmetry for the central ring, which consists of PilQ (Fig. 63B, ii) (Jain *et al.*, 2011). Another recent study revealed a PilQ complex with a width of 15 nm and a length of 34 nm consisting of an extraordinary stable "cone" and "cup" structure and five ring structures with a large central channel (Fig. 63B, iii), which differs from all T2SS, T3SS and T4P secretin complexes known to date (Burkhardt *et al.,* 2011). The authors suggested that the 500 residue long N-terminal aa form a complex structure comprising of five staged ring systems spanning the periplasmic space (Burkhardt *et al.,* 2011). This model is coherent with those of the secretins from the T2SS and T3SS. The ring models generated by using the crystal structures of the periplasmic domains of the secretins from the T2SS (N0-N1-N2) and T3SS (N0-N1), suggested that the N-terminus of secretins could mediate the formation of periplasmic rings (Korotkov *et al.*, 2009a; Spreter *et al.*, 2009).

Top view of secretins from various export systems showed ring-like structures ranging from 12-20 nm in diameter, with large central channels ranging from 5-10 nm in diameter (Burkhardt *et al.*, 2011; Reichow *et al.*, 2010; Collins *et al.*, 2004). To maintain the integrity of the OM, secretins need to be gated. It was suggested that the interactions between the secretin and other components of the T2S/T4P machinery are involved in the gating of the secretin. Indeed, the IM lipoprotein PilP of the *Neisseria* T4aP and the IM protein GspC of the T2SS have been shown to interact with their respective secretins (Balasingham *et al.*, 2007; Login *et al.*, 2010). This group of proteins that is also involved in the IM complexes, was recently suggested to be designated as 'secretin dynamic-associated' (SDA) proteins (Ayers *et al.*, 2010). In the T4bP, a putative SDA protein BfpU has also been shown to interact with the N-terminal domain of the cognate secretin (Daniel *et al.*, 2006). A recent study on the bacteriophage secretin pIV identified two gate regions within the C-terminal secretin domain, called GATE1 and GATE2. Amino acid substitutions in these regions resulted in a leaky channel phenotype (Spagnuolo *et al.*, 2010). Several mutations resulted in a similar phenotype have also been identified in the N3 domain that corresponds to the periplasmic constriction site in *Vc*GspD structure. This was consistent with the notion that this domain may be involved in triggering the opening of the periplasmic gate of the secretin

complexes (Reichow *et al.*, 2010, 2011).

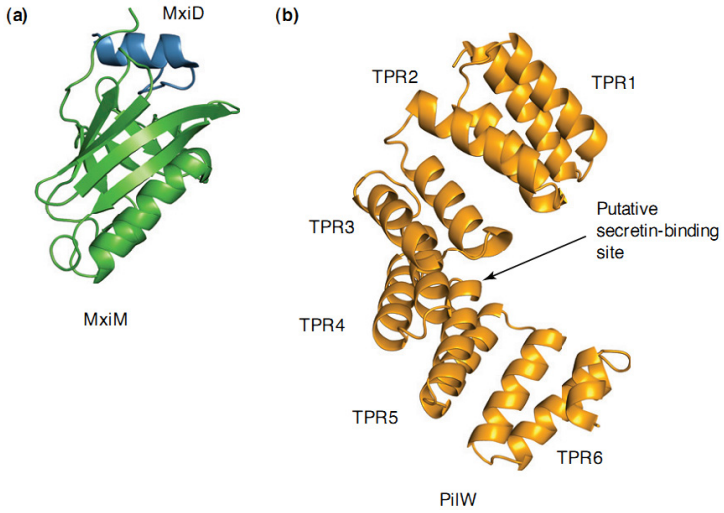

Fig. 64: Structures of pilotins. (a) The structure of the *S. flexneri* T3SS pilotin MxiM (green) in complex with the C-terminal fragment of the secretin MxiD (dark blue) (Okon *et al.*, 2008). (b) The structure of the *N. meningitidis* T4PS pilotin PilW (orange) is composed of six TPR motifs arranged as a superhelix (Trindade *et al.*, 2008).

In many cases, the assembly of secretins is assisted by a specific small OM lipoprotein, pilotin. In T4P, the pilotin PilF from *P. aeruginosa* is required for the OM targeting and multimerization of T4aP secretin PilQ (Watson *et al.*, 1996b). Homologous pilotins PilW from *N. meningitidis* and Tgl from *M. xanthus* appear to be required for multimerization of the cognate secretins, but not for their targeting to the OM (Carbonnelle *et al.*, 2005; Nudleman *et al.*, 2006). Recent structure data showed that unlike the T3SS pilotin MxiM from *S. flexneri*, which adopts a conical shape β-barrel structure interrupted by an α-helix (Fig. 64a) (Okon *et al.*, 2008), T4aP pilotins are composed of six tetratricopeptide repeats (TPRs) arranged as a super-helix (Fig. 64b) (Koo *et al.*, 2008; Trindade *et al.*, 2008). The concave surfaces on the structures were suggested as potential binding sites for the T4aP secretin whereas the hydrophobic cleft at the top of the β-barrel of MxiM serves as binding site for either lipids or the C-terminal domain of of MixD. However, unlike T2SS and T3SS secretins, T4P secretins lack the C-terminal pilotin binding domain, S-domain (Fig. 62). It is still unknown which part of T4aP secretin interacts with a pilotin.

III.6.2 The (pseudo)pilins

The pseudopilus and pilus are essential components of both T2SS and T4P, respectively. One major (pseudo)pilin and several minor (pseudo)pilins are involved in the assembly of (pseudo)pilus. However, in both systems, the (pseudo)pilus itself is composed mainly by major (pseudo)pilin subunits while the precise roles of the minor (pseudo)pilins remain to be

investigated. For example, the major T4aP pilin PilA (in *P. aeruginosa*) or PilE (in *Neisseria spp.*) homopolymerizes to form the pilus fiber, whereas the minor pilins PilE, PilV, PilW, PilX, FimT-U (in *P. aeruginosa*) or PilH, PilI, PilJ, PilK, PilX (in *Neisseria spp.*) contribute to pilus assembly in ways that are still poorly understood (Hazes and Frost, 2008). Recent study in *P. aeruginosa* suggested that the minor pilins PilV, PilW and PilE may be required for the formation of one or more subcomplexes that allow FimU and PilX to promote pilus assembly and stimulate the opening of the secretin pore (Giltner *et al.*, 2010). This indicates that at least certain minor pilins could play a role in the initiation but not termination, of pilus assembly. FimT, unlike the other minor pilins, does not have significant role in pilus assembly. Giltner *et al.* (2010) also demonstrated that the minor pilins are incorporated not simply at the tips of new pili, but also throughout growing pili, which suggests that the minor pilins and major pilin together form the pilus fiber. In the T2SS, the pseudopilus core is formed by the homomultimerization of the major pseudopilin GspG through interactions between hydrophobic domains. A tip heteromeric complex is formed by at least three of the minor pseudopilins. The minor pseudopilin GspI may be invovled in initiation of peseudopilus formation while GspK may control pilus elongation (see Chapter III.3.2.2).

The pilins are synthesized as precursors, prepilins, which typically have a conserved hydrophotic N-terminal sequence in an extended α-helix containing a leader sequence with putative prepilin peptidase GspO/PilD cleavage and methylation sites (Fig. 45, page 62). Processing and methylation of pilins by peptidase require three highly conserved residues: Gly (-1), Phe (+1) and Glu (+5) (Strom and Lory, 1993). The prepilins are co-translationally targeted by the signal recognition particle to the Sec machinery and remain in the IM as bitopic proteins due to their hydrophobic N-terminal α-helix (Pelicic, 2008). After processed by peptidase, pilins could be extracted from the IM and added to the base of the growing pilus. The mechanism of this process remains poorly understood. An IM complex coupled to a cytoplasmic ATPase is needed for this process. In the T2SS, cytoplasmic ATPase GspE may probably drive both extension and retraction. In the T4aP, cytoplasmic ATPase PilB may energize pilus extension while two additional ATPase, PilT and PilU play a role in pilus retraction, since inactivation of either gene results in a hyperpiliated phenotype (Hazes and Frost, 2008).

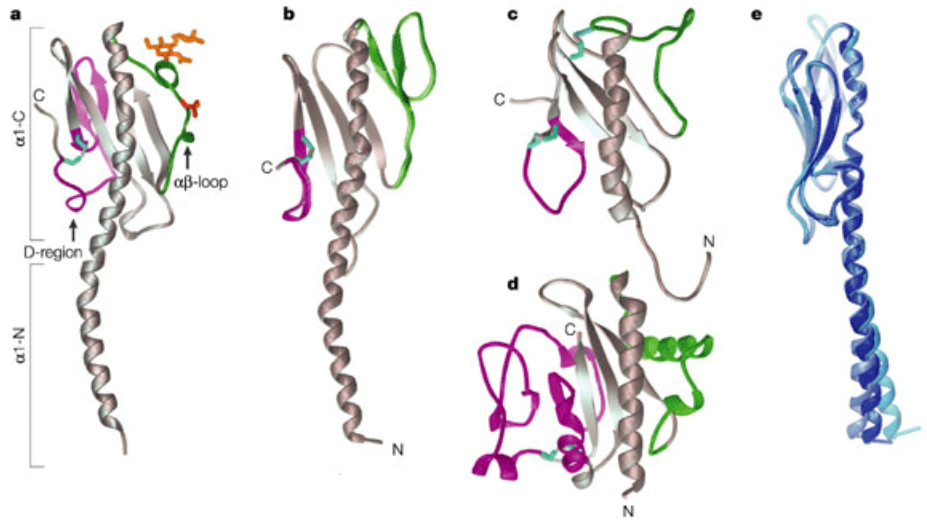

Fig. 65: Crystal structures of the type IV pilins. **(**a) Full-length PilE structure of *N. gonorrhoeae*. (b) Full-length PilA structure of *P. aeruginosa K*. (c) Soluble domain structure of *P. aeruginosa* K122-4 PilA. (d) Soluble domain structure of major pilin TcpA of *V. cholera* T4bP. (e) Superposition of the three independent full-length PilA structures shows flexibility in α1-N (Craig *et al.*, 2004).

The architecture of T2SS and T4P pilus is that subunits assemble through interactions between the conserved N-terminal α-helix of the pilins, which form a hydrophobic core in the filament. Meanwhile the less conserved C-terminal globular domains provide specific subunit-subunit interfaces and define the exposed surface of the pilus to provide functional variability (Craig *et al.*, 2004). Several high resolution structures of T4P and T2SS pilin subunits have been determined by X-ray crystallography and NMR, which provides a molecular basis for overall (pseudo)pilus assembly and functionality (see chapter III.3.2.3). The T4P pilins share a common fold with an extended N-terminal α1-helix, a globular domain, an αβ-loop and D-region (Fig. 65a). The α1 mediates pilus assembly by forming a hydrophobic helical bundle in the filament core. The protruding half of α1, α1-N is primarily hydrophobic, whereas the buried half, α1-C is amphipathic. The hydrophobic face of α1-C interacts with the globular head domain while the hydrophilic face is exposed on the surface of the protein. Due to the presence of two helix-disrupting residues: a glycine or proline at position 22 and a proline at position 42, which introduce subtle kinks in the α-helix, the α1 of the full-length GC and PAK pilin structures have an S-shaped curve (Figs. 65a and 65b). Indeed, the proline at position 22 is highly conserved in major pseudopilins from the T2SS and also introduce kink in the α-helix. Campos *et al.* (2010) showed that PulG^{P22A} mutant was significantly less piliated than the wild type, which suggested that the kink induced by Pro is an important structural element facilitating the α-helix bundle packing.

The superposition of three independent structures of pilins revealed the flexibility in α1. When

the α1-C portions of three structures are superimposed, the positions of N-termini diverge by 10 Å (Fig. 65e) (Craig *et al.* 2004). The α1 structures of the T4b pilins may be less curved than in T4a pilins because of lacking residues proline or glycine at positions 22 and 42.

The dominant features of the globular heads domain are the N-terminal α1-helix, α1-C, and a four- (T4P) or three- (major pseudopilin GspG, minor pseudopilins GspH, GspI and GspJ) stranded anti-parallel β-sheet (Alphone *et al.*, 2010) (Figs. 65 and 47). The αβ-loop and D-region flank the β-sheet of the T4P pilins (Fig. 65a). The αβ-loop connects the N-terminal α-helix to the β-sheet. In the T4P, the D-region is bound by the two conserved C-terminal cysteines, which forms a disulfide bridge that is essential for pilus assembly (Kirn *et al.*, 2000).

III.6.3 The inner membrane complex

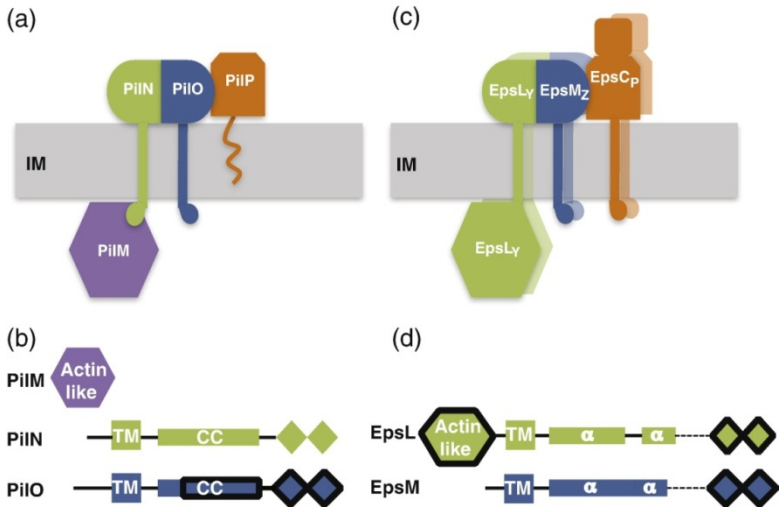

Fig. 66: Comparison of the T4P and T2S IM sub-complexes (Sampaleanu *et al.*, 2009). (a) and (b) represent the models while (b) and (d) represent the schematic domain organization of the IM sub-complexes found in T4P (a and b) and T2S (c and d). Similar proteins are rendered in the same color. The ferredoxin-like fold is shown as a pair of diamonds. Domains for which structures are available are surrounded by thick outlines while regions predicted to be unstructured are shown with broken lines.

Protein interaction studies in both the T2S and the T4P systems have led to the identification of IM complexes, GspL/M/C and PilM/N/O/P, respectively, which are critical for the assembly of the respective systems (Py *et al.*, 2001; Ayers *et al.*, 2009). Since these components do not share any sequence similarity, it was thought that they could play specific functions within each of these systems (Filloux, 2004; Hazes and Frost, 2008). However, the recent structural studies revealed a structural similarity between these components, suggesting that they could play similar roles in (pseudo)pilus assembly (Sampaleanu *et al.*, 2009; Karuppiah and Derrick, 2011). It was suggested that the T4P PilM/N/O/P complex is homologous to GspL/M/C in the T2SS (Fig. 66). Additionally, a detailed analysis of PilM/N/O and their ortholog, GspL/M,

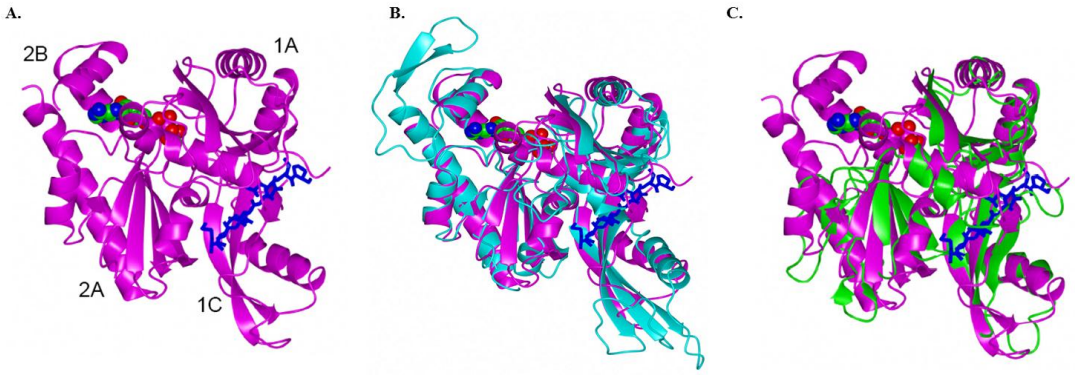

Fig. 67: Structure of *T. thermophiles* PilM and comparison with other bacterial actin-like proteins. (A). Structure of PilM (magenta) overlaid with the PilN peptide (blue) and ATP. (B) Superposition of of PilM and ligands with FtsA (cyan) and EpsL (green) (C) (Karupphiah and Derrick, 2011).

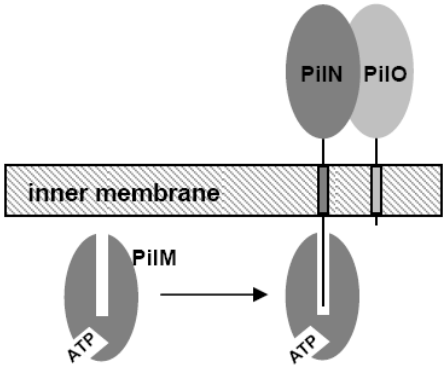

Fig. 68: Model for the interaction of PilM with PilN and PilO (Karupphiah and Derrick, 2011).

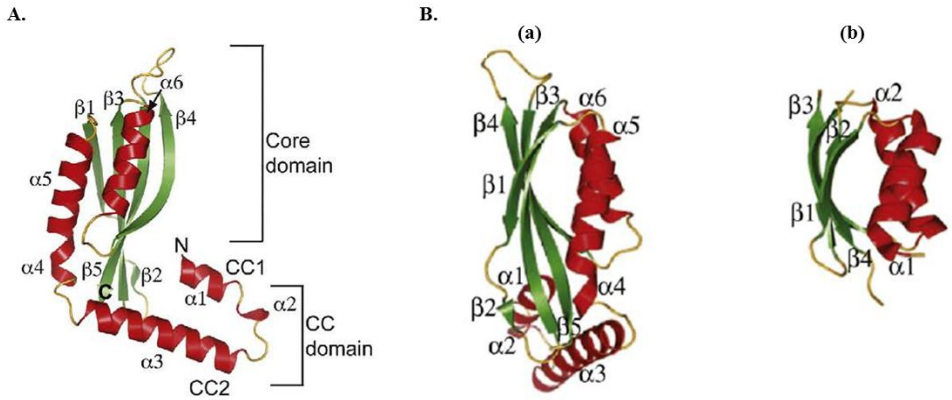

Fig. 69: Crystal structure of *P. aeruginosa* $PilO_{\Delta 68}$ (A) and comparison of the ferredoxin-like folds (B) in monomer of PilO (a) and EpsM (b) (Sampaleanu *et al.*, 2009). (A) The PilO periplasmic domain consists of two N-terminal coiled coils (CC domain) and a C-terminal ferredoxin-like domain (Core domain). (B) The ferredoxin-like domain is similar to that adopted by the T2SS protein EpsM.

in the *V. cholerae* T2SS revealed significant similarities in their secondary structures and three-dimensional folds (Fig. 66) (Sampaleanu *et al.*, 2009). PilM is a cytoplasmic protein with an actin-like fold. The crystal structure of PilM could be divided into two subdomains, 1A/C and

2A/B (Fig. 67A) (Karupphiah and Derrick, 2011), according to a previous designation for FtsA (Van de Ent *et al.*, 2000). The cytoplasmic domain of the T2SS protein GspL aligns well with the PilM structure (Fig. 67C; rmsd backbone atoms 2.8 Å). And the periplasmic portion of GspL exhibits the similar fold as PilN. The PilN peptide binds in a narrow channel between the 1A and 1C subdomains while ATP is bound in a deep cleft on the PilM surface, with the triphosphate moiety buried more deeply than the ribose and adenine rings. According to these results, Karuppiah and Derrick (2011) proposed a model for the interactions of PilM and PilN and PilO (Fig. 68). PilM would first bind ATP, and then the PilM-ATP binary complex would associate with the N-terminus of PilN. The structure of the PilO periplasmic domain consists of two N-terminal coiled coils (CC domain) and a C-terminal ferredoxin-like domain that is similar to that adopted by the T2SS protein GspM (Fig. 69) (Sampaleanu *et al.*, 2009; Abendroth *et al.*, 2004). Thus, these recent structural studies revealed the similar structural organization of soluble domains of PilM/N/O and GspL/M, respectively. More, these results suggested that the bitopic GspL could be equivalent to PilM (cytoplasmic) fused to PilN (periplasmic).

The *in vivo* mutual stability data offered the first indication that PilN/O may interact (Ayers *et al.*, 2009). Sampaleanu *et al.* (2009) provided evidence for a direct interaction between them *in vitro*. The authors showed that PilO may assist in the proper folding of PilN and that the periplasmic domain of PilN and PilO interact to form a stable heterodimer.

PilP is predicted to be a lipoprotein with its lipid attachment site at Cys16, which anchors it to the IM (Balasingham *et al.*, 2007). PilP is thought to be a part of the IM complex of T4P and has been initially assigned as pilotin since it stabilizes the secretin PilQ complex (Drake *et al.*, 1997). However, subsequent studies suggested that it was inappropriate to define PilP as pilotin since PilP was not required for PilQ stability (Balasingham *et al.*, 2007). Moreover, the reduced amounts of PilQ (monomer and complex) in the *pilP* deletion mutant were merely due to the fact that *pilP* and *pilQ* genes are cotranscribed. Thus, PilP may fulfil some other roles. Indeed, it is important for pilus biogenesis. In addition, the structure of PilP is very different from that of the pilotin MxiM from the T3SS (Golovanov *et al.*, 2006) and the pilotin OutS from the T2SS (Gu *et al.*, 2012a, accepted). The structure of PilP from *Neisseriae* revealed a novel β-sandwich structure, made up of a single 3_{10}-helix and seven β-strands (Golovanov *et al.*, 2006). Although the lipoprotein PilP was not clearly needed to stabilize the secretin PilQ complex, the N- and C-terminal regions of PilP have been shown to interact with the central portion of the PilQ monomer (Balasingham *et al.*, 2007). Recently, Ayers *et al.* (2009) showed that loss of any one of PilM/N/O/P has a negative impact on the stability of the other gene products, which indicated the interactions between them. These observations suggest that PilP on one hand, interacts with

IM proteins PilN or PilO, and on the other hand, interacts with the OM secretin PilQ, and thus connects the IM and OM subcomplexes, similar to the putative function of GspC. Furthermore, our recent structure analysis of the HR domain of GspC revealed a fold similar to PilP, indicating that these two proteins could play similar functions within the T2SS and T4P, respectively (see results section, Gu *et al.*, 2012b).

Objective of this thesis

The type II secretion system (T2SS) is widely employed by pathogenic Gram-negative bacteria to secrete toxins and lytic enzymes facilitating host invasion. The phytopathogen *Dickeya dadanti* (ex. *Erwinia chrysanthemi*) uses this system, named Out, to secrete several cell-wall degrading enzymes and to cause soft-rot disease of many plants. The T2SS consists of 12-15 proteins that build together a multiprotein complex spanning the entire cell envelope. Currently, how the individual components assemble to form functional machinery and how exoproteins are transported across the OM are still unclear. The OM pore formed by the secretin GspD is thought to allow translocation of folded exoproteins. Gating of this pore should be tightly regulated. Notably, the IM component GspC, interacts with the secretin GspD and could be involved in the gating of the OM secretin pore. It seems therefore that GspC and GspD interaction plays a crucial role in structural and functional integrity of the secretion machinery by connecting the IM components of the T2SS to the OM secretin pore. Functional and structural characterization of these two components and molecular analysis of their interactions are necessary to better understand the assembly and function of the T2SS. Certain previous studies investigated the putative interactions between GspC and GspD. However, which regions and residues are involved in these interactions and how these two proteins interact within a functional T2SS are still unclear. Therefore, molecular and functional analysis of these protein-protein interactions is the main objective of this thesis. This study will allow to better understand the assembly and function of this nano-machine.

Previous results of our laboratory (the thesis of Dr. F. Login) have shown that the N-terminal domain of OutD (aa 28-285) interacts with the non-PDZ periplasmic region of OutC (corresponding mainly to HR) by an *in vitro* GST pull-down assay and by NMR spectroscopy. The first task of this thesis is to identify the minimal regions involved in OutC-OutD interaction using *in vitro* copurification. The results of this study have been published in the article: “A 20-residue peptide of the inner membrane protein OutC mediates interaction with two distinct sites of the outer membrane secretin OutD and is essential for the functional type II secretion system in *Erwinia chrysanthemi*” (Login *et al.*, 2010) in *Molecular Microbiology* and will be presented in Chapter I.

To better understand molecular mechanisms that govern OutC-OutD interactions, very recently, the structural analysis of OutC and of OutC-OutD interactions was performed by NMR in collaboration with Prof. Pickersgill from Queen Mary University of London. This pioneer

structural analysis (3D structures of neither HR nor GspC-GspD complex were not yet available for other T2SS) opens a new possibility to exploit the T2SS and provides us with an excellent guideline for the functional analysis of the system. In Chapter II, we therefore used alanine and cysteine substitutions and disulfide cross-linking to examine the predictions on the structure of HR domain of OutC and the $OutC^{HR}$-$OutD^{N0}$ complex *in vivo*. This work constitutes a part of the article titled "Solution structure of homology region (HR) domain of the type II secretion system" (Gu *et al*., 2012b) in *Journal of Biological and Chemistry*.

To probe the putative HR/OutD interfaces in the functional secretion system and to assess the biological relevance of the HR/N0 interface indicated by recent crystal structure of $GspC^{HR}$-$GspD^{N0-N1}$ complex (Korotkov *et al*., 2011b), we performed *in vivo* cysteine-scanning mutagenesis and disulfide cross-linking analysis to search for residues that are directly involved in OutC-OutD interaction and are important for the protein function. The results will be presented in Chapter III and in the form of the article: "Cysteine scanning mutagenesis and disulfide mapping analysis of the arrangement of GspC and GspD protomers within the T2SS" (Wang *et al*., accepted).

Targeting and proper assembly of the secretin into the OM often require accessory proteins. The pilotin GspS and the IM protein GspB play such a role towards a cognate secretin. To unravel the molecular mechanism of GspS action and its interaction with the secretin, we undertook a structural and functional analysis of the pilotin OutS. This work will be presented in Chapter IV, as a part of the manuscript: "Structural and functional insights into the pilot-secretin complex of the type II secretion system" (Gu *et al.*, 2012a). Several studies suggested the interaction between the secretin OutD and IM protein OutB. However, there was no direct evidence for this interaction. In Chapter V, we examined the interaction between OutD and OutB.

Lastly, we tried to construct the protein derivatives of OutC and OutD suitable for NMR, crystallography and X-ray analysis. The results will be presented in Chapter VI.

Materials and methods

I Bacterial strains and growth conditions

I.1 Bacterial strains

E. coli strains NM522 (Δ (*lac-proAB*) Δ (*mcrB-hsdSM*) *5 supE thi*, (F' *proAB lacI*^{q}, *lacZ*Δ*M15*) and BL21 (DE3) (*F*$^-$ *dcm*$^-$ *ompT rB*$^-$ *mB*$^-$ *Ion*$^-$ *λ* (DE3)) were used for general cloning and protein production purposes, respectively. *D. dadantii* strains constructed and used are listed in Table. 2.

I.2 Growth conditions and conservation

The bacteria were usually grown in rich medium LB (10 g·l^{-1} tryptone, 5 g·l^{-1} Yeast extract and 10 g·l^{-1} NaCl, pH 7) or minimal medium M63 (13.6 g·l^{-1} KH_2PO_4, 2 g·l^{-1} $(NH_4)_2SO_4$, 0.2 g·l^{-1} $MgSO_4$, 0.5 mg·l^{-1} $FeSO_4$ supplied with 2 g·l^{-1} glycerol, pH 7.2). The solid media were realized by adding agar at 15 g·l^{-1}. The cultures were grown under aeration with shaking at 150 rpm or 120 rpm at 30 °C for *E. coli* and 28 °C for *D. dadantii*. If necessary, arabinose and IPTG were added at 0.03% and 1 mM, respectively. Antibiotics were used at the following final concentrations: ampicillin, 150 μg·ml^{-1}, kanamycin, 100 μg·ml^{-1}, chloramphenicol, 50 μg·ml^{-1}.

For conservation, the bacteria cells were grown in rich medium Luria-Bertani (LB) overnight. For *D. dadantii*, glycerol was added to a final concentration of 40% and the cells were conserved at -80°C. For *E. coli*, glycerol was added to a final concentration of 20% and the cells were conserved at -20°C.

II Genetic and molecular biology methods

II.1 Plasmids construction and DNA manipulations

Plasmids and primers used in the study are listed in appropriate chapters. DNA cloning and manipulation were performed using standard methods. Site-directed mutagenesis was performed using the QuickChange kit (Stratagene). The nucleotide sequences of mutant and amplified genes were checked (Cogenics). Plasmids were introduced by the $CaCl_2$ procedure into *E. coli* (Sambrook *et al.*, 1989) or by electroporation into *D. dadantii* (Enderle and Farwell, 1998).

II.2 Preparation of the stock of φEC2 bacteriophage

The φEC2 phage lysate was prepared from the donor bacteria in exponential growth phase

(OD_{600} of approximately 1). This culture was infected by φEC2 phage stock (0.2 ml bacteria + 0.2 ml bacteriophage). After 20 min of adsorption at room temperature (without agitation), 5 ml of soft agar (0.4% in LB medium), which was melt and maintained in liquid state, was added into the bacteria phage mixture. The mixture was then poured on plates LCG (solid medium GL + glucose + CaCl2). After overnight incubation at 30°C, phage lysates were harvested by scraping the top layer after adding 5 ml of LB. The retained cells were lysed by adding chloroform. The mixture was vortexed until homogeneous, agar and cell debris were removed by centrifugation (10 min, 8000 g) and the phage stocks were stored at 4°C.

II.3 Transduction

Transduction is a mechanism for transfer of bacterial DNA from one cell to another by using a virus (bacteriophage) as a vector.

0.2 ml of phage stock was added to 0.2 ml of overnight grown culture. After incubation for 20 min at room temperature without agitation, the mixture was supplemented with 0.8 ml of LB and grown at 30°C for 2-3 h for the expression of transduced genes of resistance to antibiotics usually used as markers for transduction. The cells were then spread on the plate containing an appropriate antibiotic and grown at 30°C for 48 h.

II.4 Construction of *D. dadantii* mutant strains

The *D. dadantii* mutant strains carrying single cysteine substitution on chromosome were constructed by exchange-eviction mutagenesis (Ried *et al.*, 1987). The *nptI-sacB-sacR* cartridge that confers kanamycin (Kan) resistance and sucrose sensitivity was inserted into a PstI site of *outC*, cloned on a plasmid and then introduced into the chromosome by gene exchange recombination. The resulting mutant strain A2365 was Km^R, sucrose-sensitive and secretion-deficient. The plasmids pTdB-OC (Amp^R) carrying *outC* gene coding for a cysteine substitution of interest were transformed into this strain. The cells were first grown on the GL plates with Amp. Then, the cells were grown overnight in LB without antibiotics and next in LB supplemented with sucrose to a final concentration 10%. The *outC* allele containing single cysteine substitution was exchanged for the chromosomal allele containing the *nptI-sacB-sacR* cartridge by selection for sucrose tolerance. The culture was subsequently diluted and plated onto GL without antibiotics. Next, the sensetivity of colonies to Amp and Kan was checked on replica plates. The resulting *D. dadantii* mutant strains should lose the plasmid (Amp^S) and *nptI-sacB-sacR* chromosomial cartridge (Kan^S). The desired point mutations were then checked by PCR using chromosomic DNA of corresponding *D. dadantii* mutant strain as template, and the

primers OutC (GCCAGAGCATGAATATCGTG) and ROutC (GAACTCCTGAATATCGGTTC). The *D. dadantii* mutant strains constructed are listed in Table. 2 and the secretion ability of the mutant strains was analyzed by complementation tests.

Table. 2: *D. dadantii* strains used in this thesis

Strain	Genotype/phenotype	Reference
A350	*rafR ganB*	Hugouvieux-Cotte-Pattat and Charaoui-Boukerzaza, 2009
A3556	*rafR ganB* Δ*outC*	Bouley *et al.*, 2001
A3558	*rafR ganB* Δ*outD*	Bouley *et al.*, 2001
A5210	*rafR ganB outC* (I113C)	This thesis
A5274	*rafR ganB outC* (V143C)	This thesis
A5176	*rafR ganB outC* (V144C)	This thesis
A5177	*rafR ganB outC* (L145C)	This thesis
A5211	*rafR ganB outC* (V153C)	This thesis
A5212	*rafR ganB outC* (L154C)	This thesis

III Biochemical methods

III.1 Complementation tests

To assess the secretion ability of the mutant *D. dadantii* strains, secretion of pectinases and cellulase was compared with that of the wild type strain. To test the functionality of the mutant OutC and OutD proteins, the *D. dadantii* Δ*outC* and Δ*outD* mutant strains respectively (Table. 2) were transformed with pTdB-OC or pTdB-OD plasmids carrying a corresponding *outC* or *outD* mutant gene. Secretion efficiency was estimated by both plate assays and immunoblotting assays.

The plate assays were performed on the solid medium containing M63 + glycerol + carboxymethyl cellulose (CMC) + $MgSO_4$, for cellulase activity and on solid medium containing M63 + glycerol + PGA, for pectate lyase activity. To estimate the cellulase secretion, after growth for 24 h at 30°C, plates were covered with a saturated solution of Congo red (0.2%) that binds to CMC. After washing with 1M NaCl, the colonies secreting cellulase were surrounded by a translucent yellow halo on a red background. To estimate the pectate lyase secretion, after growth for 24 h at 30°C, plates were covered with a saturated solution of copper acetate (10%). The colonies secreting pectate lyases are surrounded by a translucent halo on a blue background. The size of halo represents the secretion ability.

For immunoblotting assays, *D. dadantii* cells were grown at 28°C in LB supplemented with

galacturonate for variable time periods (12-16 hours) until the early stationary phase. Cells were pelleted by centrifugation at 10,000 g for 2 minutes, the supernatant was collected and cells were resuspended in the same volume of LB. The culture supernatants and cell suspensions were boiled with Laemmli sample buffer. Then, the proteins were separated by SDS-PAGE and revealed with antibodies generated against diverse pectate lyases secreted by Out system, namely PelB, PelD and PelI. Ratio of pectinases in the culture supernatant reflects efficiency of the secretion and hence functionality of the corresponding mutant OutC and OutD proteins.

III.2 GST copurification and pull-down assays

The principle of copurification and pull-down is shown in Fig. 71. GST fused to OutC derivative of interest was used as a bait protein and an OutD derivative fused to His was used as a prey protein. The GST-fused bait protein can be then captured by Glutathione Sepharose resin. If the two proteins interact with each other, the prey protein can also be co-purified.

III.2.1 GST copurification assay

For copurification assays, the bait and prey proteins were coexpressed in the same cell. The couples of GST-OutC and $OutD_{His}$ derivatives were coexpressed in *E. coli* BL21 (DE3) carrying one of the pGX-oC_{X-Y}-oD_{X-Y} plasmids (oC_{X-Y} and oD_{X-Y} for any OutC and OutD derivatives). Bacteria were grown in 100 ml LB. At an OD600 of ~0.5, IPTG was added to 1 mM. After 3 h of additional growth, the cells were pelleted by centrifugation for 8 min at 5000 g and frozen at -80°C. To perform copurification, the cells were resuspended in 2.5 ml of buffer TSE (50 mM Tris-HCl pH 8.0, 100 mM NaCl, 1 mM EDTA, 1 mM PMSF). After sonication, cell extracts were supplemented with Triton X-100 to 1% (v/v) and the final volume was adjusted to 3 ml. Then, cell extracts were incubated for 20 min at 12 rpm to solubilize the proteins. Unbroken cells were eliminated at 6000 g for 10 min and 1.5 ml of such cell lysate were added to 0.3 ml of Glutathione Sepharose which had been washed with water and equilibrated with TSE buffer supplemented with 1% (v/v) Triton X-100. After 1 h of incubation with mixing at 12 rpm and at 15°C, the resin was spun for 2 min at 1000 g, and then washed three times with 1 ml of TSE buffer supplemented with Triton X-100 to 1% (v/v). At this stage, the bound proteins could be eluted with Laemmli sample buffer, separated by SDS-PAGE and probed by immunoblotting with either OutD antibodies, or Ni-NTA conjugated with peroxidase, or Tetra-His-antibodies (Quiagen). Alternatively, the GST-fused protein could be released from GST by PreScission protease. To do this, the washed resin was supplemented with TSE buffer containing Triton X-100 1% (v/v) and PreScission protease (~ 40 u/ml). After an overnight incubation with mixing at

8 rpm and at 15°C, the supernatant containing the proteins of interest released from GST were collected and used for further analysis.

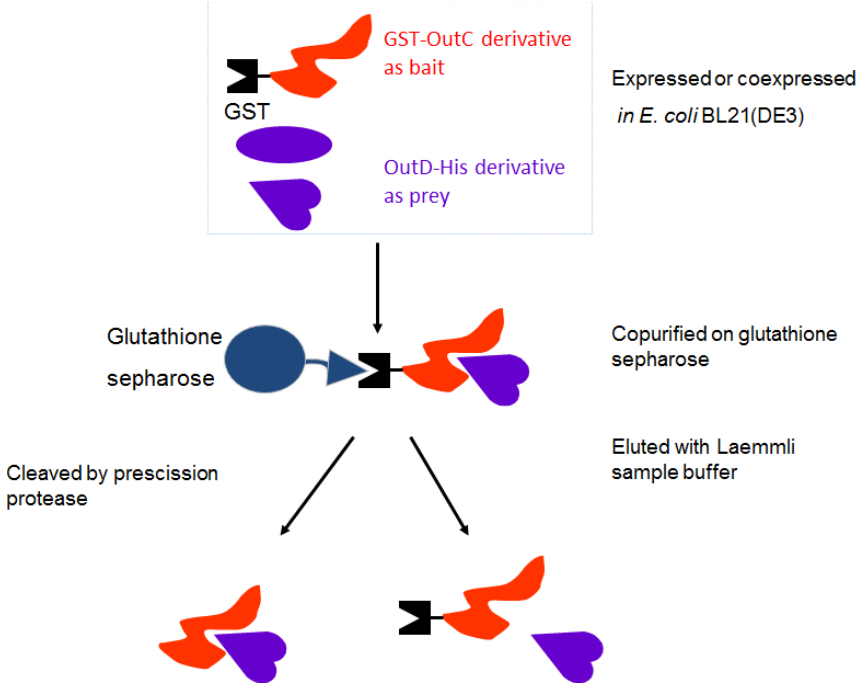

Fig. 71: Principle of copurification and pull-down.

III.2.2 GST pull-down assay

In contrast to copurification assay, in GST pull-down assay, the bait and prey proteins were expressed separately and the matrix consisting of GST-OutC derivative bound on Glutathione Sepharose has been prepared and checked in advance. The beads with bound GST-OutC derivatives or with GST alone used a negative control have been systematically checked by SDS-PAGE prior to the binding assay and then diluted if necessary with non-charged resin to reach a similar amount of various fusion proteins. Then, an equal amount of prey protein of interest ($OutD_{His}$ derivative) was loaded onto the resin with immobilized GST fusions, incubated for 1 h and then washed three times with TSE. The bound proteins were eluted with Laemmli sample buffer, separated by SDS-PAGE and probed by immunoblotting with either OutD antibodies, or Ni-NTA conjugated with peroxidase, or Tetra-His-antibodies (Quiagen).

III.3 Limited proteolysis

Limited proteolysis was carried out either with purified OutC and OutD derivatives or with copurified OutC-OutD complexes by using trypsin. 3 µl of trypsin at 0.1 mg/ml were added to 150 µl samples and incubated at 25 °C for various time periods (2, 5, 15, 30 and 60 min). Proteolysis was stopped by adding 3 µl of 100 mM PMSF. The samples were then analyzed by

Tricine SDS-PAGE (12%). The proteins were either stained with Coomassie G-250 or transferred to a PVDF membrane by electroblotting using Tris-borate buffer (50mM Tris and 50 mM boric acid) and then stained with Coomassie G-250. The bands of interest were cut off and subjected to N-terminal (Edman) analysis.

III.4 Disulfide cross-linking analysis

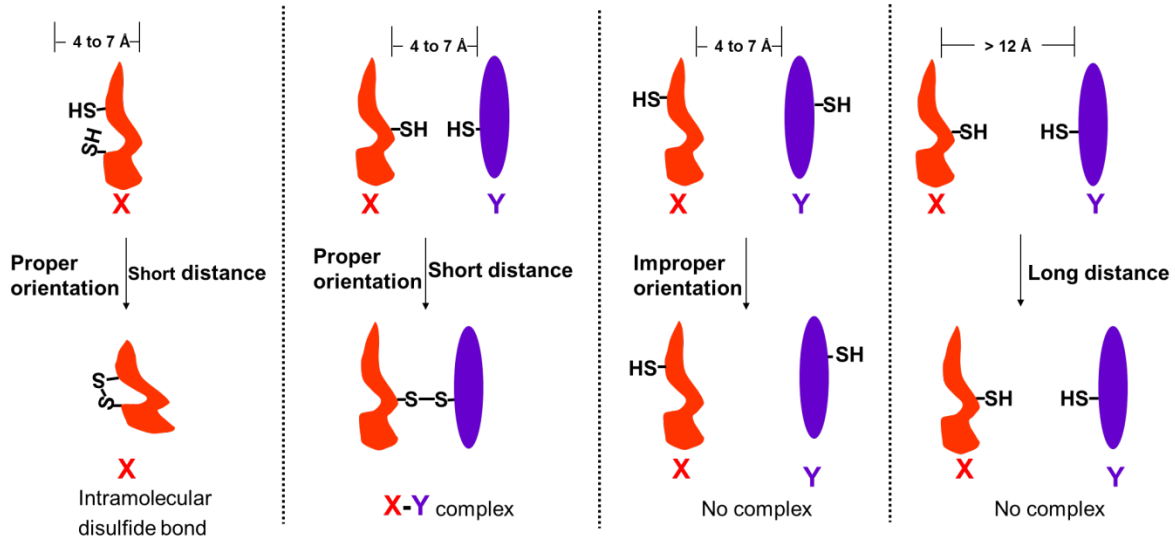

Fig. 72: Principle of cysteine disulfide cross-linking.

The principle of cysteine disulfide cross-linking is shown in Fig. 72. If the two introduced cysteine residues are in close proximity, the disulfide bond can be formed either spontaneously in an appropriate oxidative environment (e.g., the periplasm) or upon application of an oxidizing agent. The maximal distance found in proteins between α-carbons linked by disulfide bond is approximately 7 Å, with an average distance of 5-6 Å (Lynche and Koshland, 1991). This method allows therefore to estimate the proximity between the selected protein sites in the natural background (e.g., within the functional T2SS) and to identify sites involved in protein-protein interactions.

III.4.1 *In vivo* disulfide cross-linking analysis

We firstly performed oxidative disulfide cross-linking by coexpressing OutC and OutD mutant proteins carrying cysteine substitutions in *D. dadantii*. However, due to a high background noise detectable by western blot, it was often difficult to exploit these results. Therefore, more frequently, we employed such an analysis in *E. coli* by coexpressing cysteine variants of OutC and OutD from the same plasmid. To enable a proper targeting and assembly of OutD into the OM, the pilotin OutS was also coexpressed with OutC and OutD variants from pACT3-oS plasmid. Indeed, we considered that coexpression of OutC and OutD in *E. coli* can mimic some

OutC-OutD interaction within the functional T2SS. To assess the extent of disulfide cross-linking, spontaneous formation of disulfide bonds in steady-state cultures was examined. We considered that oxidizing environment of the periplasm is adequate to generate disulfide bonds between proximal residues during the bacterial growth. Indeed, induction of disulfide bonding by the addition of an external oxidant copper phenanthroline (CuP) increased the extent of cross-linking but significantly dropped its specificity.

More exactly, plasmids pTdB-oCoD that coexpress *outC* and *outD* coding for paired combinations of cysteine substitutions in OutC and OutD were transformed into *E. coli* NM522 cells bearing the pACT-oS plasmid. To test the effect of the secreted protein on disulfide cross-linking, pTPLB-oCoD plasmids coexpressing the pectate lyase PelB together with the paired combinations of cysteine substitutions in OutC and OutD were used instead of pTdB-oCoD that is lacking *pelB*. To assess the effect of the T2SS IM components OutL, OutM and OutE, the pK-ELM plasmid or the empty pBADIK vector were combined with pTdB-oCoD (or pTPLB-oCoD) and pACT-oS plasmids in the same *E. coli* NM522 cells. Bacteria were grown aerobically at 120 rpm for 14-15 h at 30°C in LB supplemented if necessary with 1 mM IPTG, 0.3 mg ml^{-1} arabinose and appropriate antibiotics. Cells from 1 ml culture were pelleted at 10,000 g for l min and washed with TBS buffer (50 mM Tris-HCl pH 7.5, 100 mM NaCl). Then, to block free thiol groups and prevent further disulfide bond formation, the cells were incubated in the same volume of 20 mM 2-iodoacetamide (IA) in TBS for an additional 30 min at 25°C. The cells were then pelleted, resuspended in 200 µl Laemmli sample buffer without 2-mercaptoethanol and lysed in boiling water for 10 min. The samples were then additionally incubated for 15 min at 37°C with benzonase (Sigma-Aldrich), separated by 10% SDS-PAGE and analyzed by immunoblotting with anti-OutC and anti-OutD antibodies.

III.4.2 Development of optimal conditions for *in vitro* disulfide cross-linking

The over-expression vectors pGX-oC_{60-272}-oD_{28-285} carrying various combinations of cysteine substitution in these OutC and OutD derivatives were constructed. The expression procedure was the same as in copurification assay described above. The cells were harvested by centrifugation and resuspended in 1.5 ml of TSE buffer supplemented with 1 mM PMSF. To search for optimal oxidation conditions favoring formation of the OutC-OutD complex, we firstly used different concentrations of the oxidative agent, copper phenanthroline (CuP). Once cells have been broken, the cell extracts were adjusted to 3 ml with TSE and then separated into 3 aliquots (A, B, C). In A and B, CuP was added at 0.25 mM and 1.25 mM, respectively, while C was used as a control. After incubation for 30 min at 12 rpm at 15°C, unbroken cells were eliminated by centrifugation

and the supernatants were loaded to 0.3 ml of Glutathione Sepharose which has been preliminarily equilibrated with TSE. The following procedures were the same as in an usual copurification. We found that the amounts of cross-linked products were increased in the presence of CuP but similarly at 0.25 mM and 1.25 mM. We subsequently probed the effect of 1.5 mM CuP as oxidizing agent on various steps of the purification process, this agent was either added: a) in the cell extract just after the cells were broken; or b) in the cell supernatants after elimination of unbroken cells by centrifugation; or c) in Glutathione Sepharose with bound GST fusion proteins; or d) in proteins released from the GST fusion by PreScission protease. The other procedures were the same as in an usual copurification. All the samples were analyzed by SDS-PAGE in non-reducing condition (without β-mercaptoethanol).

III.5 Cell fractionation

Subcellular fractionation was carried out on cells grown to exponential or early stationary phase (OD_{600} 1.0 to 1.4). Release of periplasmic proteins was performed by osmotic shock, and cell membrane fractionation was performed by sucrose gradient centrifugation, as described previously (Shevchik *et al*., 1996). After breaking the cells in a French press and removing the debris at 5000 g for 10 min, crude membrane fractions were isolated by centrifugation (200 000 g for 2 h). The pellet and the supernatant correspond to the membrane fraction and the soluble fraction respectively. The membranes were then solubilized in 20 mM HEPES-NaOH pH 7.2 containing 65% (W/V) sucrose, loaded at the bottom of a centrifugation tube and covered by a step-gradient in the same buffer containing continuous layers of sucrose (60 to 35%). The vesicles corresponding to the inner and outer membrane were separated by centrifugation at 200 000 g for 48 h. Fractions were collected from the bottom of the gradient and the presence of OutD was revealed by immunodetection after SDS-PAGE. The position of the OM porins was determined by staining of the gel and the position of the IM fractions was determined by assaying of NADH oxidase activity (Osborn *et al*., 1972) and immunodetection of the IMP TolA.

III.6 SDS-PAGE and immunoblotting

III.6.1 SDS-PAGE

SDS-PAGE was usually performed according to Laemmli (Laemmli, 1970). Protein samples were electrophoresed on 10%, 12% or 15% SDS-PAGE gels, depending on protein size. For analysis of disulfide cross-linking complexes, the samples were treated as indicated above (page 108); importantly, β-mercaptoethanol was absent in this case. After electrophoresis, proteins were either stained with Coomassie Brilliant Blue G-250 (CBB) or were analyzed by

immunoblotting. For CBB staining, the gels were soaked in stain solution (0.5% CBB, 10% v/v acetic acid and 40% v/v methanol) for half an hour, followed by destaining in 10% acetic acid until the background was destained completely. Two types of SDS-PAGE were used in this thesis, namely Tris-Glycine–SDS-PAGE (Laemmli, 1970) and Tris-Tricine–SDS-PAGE (Schägger, 2006). Tris-Glycine-SDS-PAGE was preferentially used for separation of proteins larger than 30 kDa, and Tris-Tricine-SDS-PAGE for proteins smaller than 20 kDa.

III.6.2 Immunoblotting (Western blot)

After electrophoretic separation by SDS-PAGE, proteins were transferred onto a PVDF membrane in a semi-dry apparatus. The membrane was then saturated in TBS containing 4% gelatine for 1 h at 30 °C and washed three times with TBS-T (TBS, 0.1% Tween 20). Then the membrane was incubated with the primary antibodies of interest diluted in TBS-T (1:6000 diluted anti-OutC, 1:3000 diluted anti-OutL, 1:4000 diluted anti-OutD, 1:6000 diluted anti-PelB, 1:10000 diluted anti-PelI, 1:4000 diluted anti-PelD and 1:6000 diluted anti-BlaM) for 1 h at room temperature. Non bound primary antibodies were removed by washing of the membrane with TBS-T (7 min, for 3 times). Secondary antibodies, anti-rabbit IgG, labeled with peroxidase and diluted 1/60000 in TBS-T, were then added. After incubation for 1 h at room temperature, the membrane was washed with TBS-T (7 min, for 3 times). Detection of peroxidase activity was performed using the ECL kit (GE Healthcare). The membrane was covered with substrate containing luminol. A light emitted as a result of oxidation of the substrate by peroxidase was captured by exposure of a film.

Results

Chapter I: Identification of the interaction regions between OutC and OutD

I.1 Preface

The outer membrane pore-forming secretin GspD and the inner membrane protein GspC are two key components of the type II secretion complex, involved in secretion specificity. GspC and GspD could interact to provide the structural and functional integrity of the secretion machinery across the two membranes of the Gram-negative bacteria (Lindeberg *et al*., 1996; Shevchik *et al*., 1997). However, there was no direct evidence which regions and sites of GspC and GspD are involved in the interaction. In this study, we examined the interaction between the secretin OutD and an inner membrane component OutC using both *in vitro* and *in vivo* approaches. We showed that a 20-residue peptide of OutC named OutCsip interacts with two distinct sites of OutD, one located in N0 domain and another overlapping N2-N3' domains and suggested an alternating mode of these interactions during the secretion process.

This study was mainly accomplished in our laboratory and complementary NMR experiments have been performed in the Lab. of Pr. R.W. Pickersgill (London University). The experimental results of Mr. Login (Ph.D thesis) showed that the N-terminal domain of OutD (residues 28-285) interacts with the non-PDZ periplasmic region of OutC (mainly corresponding to HR). In addition, he found that the N-terminal domain of OutD interacts with another region of OutC, the TMS of OutC or the region proximal to the TMS.

In this study, I participated in or completely performed the following parts of the work:

(1) The N-domain of OutD consists of four subdomains (N0 to N3). Thus, to identify the minimal regions of OutC and OutD involved in the interactions, I constructed certain truncated derivatives of OutC and OutD and corresponding coexpression vectors (an exhaustive list of the plasmids used in this study is present in the supplementary section, Table S1). Then, I used these derivatives in GST copurification assays to map the interaction regions within OutC and OutD (the section *"A short region of OutC interacts with the two distinct sites within the N-domain of OutD"* in the enclosed paper).

(2) I assessed the binding of OutCsip to two distinct sites of OutD and performed competition

binding assays with multiple protein derivatives (the section "*The two binding sites of the N-domain of OutD recognize different regions of OutCsip*" in the enclosed paper).

(3) I assessed the functional relevance of the OutCsip region in a complementation test with *E. chrysanthemi* Δ*outC* strain (the section "*A single amino acid substitution in the OutCsip region blocks secretion in E. chrysanthemi*" in the enclosed paper)

(4) I studied the effect of the V143S mutation on the OutC-OutD interaction in pull-down assays (the section "*The substitution V143S prevents interaction of OutCsip with* $OutD_{116–285}$" in the enclosed paper)

The details of these results are present as a part of the following article:

I.2 Article 1:

A 20-residue peptide of the inner membrane protein OutC mediates interaction with two distinct sites of the outer membrane secretin OutD and is essential for the functional type II secretion system in *Erwinia chrysanthemi*.

Chapter II: Structure-functional analysis of the HR domain of OutC

II.1 Preface

OutC (GspC) is one of the twelve core components of the T2SS. It is thought to be involved in both recognition of substrate and interaction with the outer-membrane secretin, OutD (GspD). OutC is a bitopic inner membrane protein. It consists of a short N-terminal cytoplasmic sequence, a single trans-membrane segment followed by two periplasmic regions: a so-called homology region (HR) and a C-terminal PDZ domain (Login and Shevchik, 2006). The PDZ domain is involved in secretion specificity but is not an essential module since it is absent or replaced by a coiled-coil domain in certain GspCs (Bouley *et al.*, 2001; Peabody *et al.*, 200). The crystal structure of the PDZ domain of GspC from *V. cholerae* and *D. dadantii* has been solved and suggested an unusual mechanism of substrate recognition (Korotkov *et al.*, 2006; Fries *et al.*, non-published). Neither the exact function of HR nor its structure are unknown; however it was shown to interact *in vitro* with the N-terminal region of the secretin GspD (see Chapters I and III). This chapter reports the solution structure of the HR domain of OutC and explores its interaction with the secretin. This structure was solved in collaboration with the team of Pr. R.W.Pickersgill from Queen Mary University of London. The HR domain adopts a β-sandwich-like fold consisting of two β-sheets each composed of three anti-parallel β-strands. This structure is strikingly similar to the periplasmic region of PilP, an inner membrane lipoprotein from the type IV pilus system highlighting the common evolutionary origin of these two systems. We elucidated an interaction between the HR domain of OutC and N0 domain of OutD ($\beta1^{HR}$-$\alpha2/\beta3^{N0}$) *in vitro* and demonstrated the importance of the interactions involving β1 of the HR domain *in vivo*. The biological relevance of these structural predictions was assessed by site directed mutagenesis followed by functional assays in *D. dadantii* and *in vivo* disulfide-bonding analysis.

In this study, I performed following experimental work:

(1) I assessed the biological relevance of highly conserved residues, which constitutes a hydrophobic core of the HR domain, by *in vivo* site directed mutagenesis and cysteine mediated cross-linking analysis (the section "*Several conserved residues form the hydrophobic core of HR*" in the enclosed paper)

(2) I explored the functional importance of HR residues involved in the HR-N0 interface

presumed by NMR experiments. To perform this analysis, I used alanine and cysteine site directed mutagenesis followed by functional assays in *D. dadantii* (the section "*Assessment of HR residues involved in HR-N0 interaction in vivo*" in the enclosed paper)

(3) I probed by *in vivo* disulfide cross-linking analysis the biological relevance of HR-N0 and N0-N1 interfaces predicted by structural studies (the section "*In vivo assessment of HR-N0 and N0-N1 interactions*" in the enclosed paper).

The details of these results are present as a part of the following article.

II.2 Article 2:

Solution structure of homology region (HR) domain of the type II secretion system.

Chapter III: Mapping of the critical interaction sites between OutC and OutD by *in vivo* disulfide-bonding analysis

III.1 Preface

The results presented in Chapter I (Article 1) revealed that a short segment of the HR domain of OutC, consisting of strands $\beta6^{HR}$ and $\beta7^{HR}$, interacts *in vitro* with two distinct sites of OutD, one located in the N0 domain and another overlapping the N2-N3' domains. Recent structural studies addressed this question by crystallographic and NMR analysis and presumed another mode of interaction (Chapter II (Article 2) and Korotkov *et al.*, 2011). The solution and the crystal HR/N0 interfaces both involve strand $\beta1^{HR}$ of HR but two different sites in N0, strands $\beta3^{N0}$ and $\beta1^{N0}$, respectively. To assess the functional relevance of these presumed interaction sites, we exploited these recent structural data and used cysteine mutagenesis and *in vivo* disulfide-bonding analysis to map the interactions between the HR domain of OutC and the periplasmic region of OutD in their native environment, within the T2SS of *D. dadantii*. The results suggest the presence of at least three distinct sites of interactions between the periplasmic domains of OutC and OutD, namely, 1) $\beta1^{HR}$-$\beta1^{N0}$, 2) $\beta7^{HR}$-$\beta2^{N0}$ and 3) $\beta7^{HR}$-$\beta10^{N2}$. The secretion substrate diminishes certain interactions and provokes an important rearrangement of the HR structure. The inner membrane components OutE/L/M differently affect various interaction sites, reinforcing ones but diminishing the others, suggesting a possible switching mechanism of their interaction in the course of secretion. Disulfide mapping shows that organization of GspD and GspC protomers is incompatible with rotational symmetry and suggests a radial symmetry of their organization within the T2SS.

I participated in all the aspects of this study. Moreover, I performed the most part of experimental work presented in this paper.

The details of these results are present in the following article.

III.2 Article 3:

Cysteine scanning mutagenesis and disulfide mapping analysis of the arrangement of GspC and GspD protomers within the T2SS

III.3 Un-published results and discussion

Disulfide cross-linking analysis of the HR domain of OutC revealed an unexpected behavior of the cysteine substitutions of residues located at the second β-sheet. The corresponding cysteine variants of OutC generated self-bonding patterns incoherent with the structure of this domain. Namely, cysteine substitutions of the buried L145 (β6) and L154 (β7) provoked an efficient self-bonding whereas the contiguous, but solvent exposed, V144 and V153 did not (Wang *et al*., submitted). Such a behavior could reflect an "inverted" orientation of the corresponding β-strands (β6 and β7) and probably the entire second β-sheet consisting of three anti-parallel β-strands (β5 to β7). Alternatively, it could not be completely excluded that substitution of the hydrophobic residues (Leu and Val) by nucleophilic Cys severely affected hydrophobic core of the HR domain and provoked such an aberrant behavior. Several evidences suggest a biological relevance of this phenomenon. First, such "inverted" cross-linking patterns were reinforced within the functional T2SS of *D. dadantii*. Second, the secreted protein PelB and the inner membrane components OutE/L/M generated a rather opposite effect on such an "inversion", suggesting that it could be functionally reversible. Third, cysteine substitutions of the hydrophobic residues located on the first β-sheet, V100 (strand β1) and I113 (strand β2) did not provoke an aberrant cross-linking indicating that substitutions of these hydrophobic residues are well tolerated. Nevertheless, to better understand this phenomenon, we performed some additional experiments.

The two β-sheets of the HR domain of OutC are connected together through several hydrophobic interactions, including the side chains of well-conserved Leu93, Leu97, Ile113 (the first β-sheet) and V143, Leu154 and Leu156 and semi-conserved Leu/Ile145, Ile/Leu/Val135 and Ile/Val138 (the second β-sheet) (Gu *et al*., 2011a). Consistent with the HR structure, double I113C/V143C substitution provoked an efficient intramolecular disulfide bond within OutC and fully arrested secretion, indicating that a covalent cross-linking of the two β-sheets of HR abolishes the protein function (Gu *et al*., 2011a). It should be noted that all the tested single cysteine variants of OutC (except for G99C) retained functional (Fig. 4A, lanes 2 to 9 and Wang *et al*., submitted). Unexpectedly, when we combined I113C (buried) with either V144C or V153C (both are solvent exposed), the corresponding double substitutions, I113C/V144C and I113C/V153C, were completely defective in secretion (Fig. III. N1A, lanes 8 and 9). On non-reducing gel, these two mutants migrated slightly faster than the wild-type OutC, indicating an efficient intramolecular disulfide bonding within HR (Fig. III. N1B, lane 3 and not shown). A certain amount of homodimer, which is usually formed by the single I113C mutant, was fully

disappeared in these double mutants, indicating that the sulfhydryl group of I113C was fully involved in a more proficient intramolecular disulfide bond with either V144C or V153C (Fig. III. N1B, compare lanes 2 with 3). These results are inconsistent with the HR structure where the side chains of V144 and V153 are solvent exposed and are not close to that of I113 (Fig. 1 in Wang *et al*., submitted). However, these data confirm the notion that, within the functional T2SS, the β6 and β7 strands of the HR domain could take an "inverted" orientation. Such intramolecular disulfide bonds were therefore formed between the "correctly" arranged buried side chain of I113C (β2) and those of V144C or V153C located at the "inverted" β-strands β6 and β7, respectively. In order to test a competition between "correct" and "inverted" side chains, we constructed the two triple OutC mutants, I113C/V143C/V153C and I113C/V144C/V153C. The former protein was fully non-functional and formed at least one intramolecular disulfide bond (Fig. III. N1A, lane 10 and Fig. III. N1B, lane 4). Notably, the homodimer usually formed by I113C was fully absent, indicating that its sulfhydryl was completely involved in the intramolecular bonding with either V143C or V153C. On the contrary, the triple I113C/V144C/V153C mutant became functional. It is remarkable since each of the corresponding double mutants (I113C/V144C and I113C/V153C) was completely nonfunctional (Fig. III. N1A, compare lanes 8 and 9 with 11). Notably, similar to single I113C variant, a certain amount of homodimer formed by I113C was detected with this triple mutant (Fig. III. N1B, compare lanes 2 and 5), indicating that sulfhydryl of I113C became available and was not involved in an intramolecular bonding with either V144C or V153C. We could provide a following explanation of these apparently puzzling results. In the triple I113C/V144C/V153C mutant, the solvent exposed side chains of V144C and V153C are close enough since located on neighboring β-strands (β6 and β7, respectively) and thus, efficiently form an intramolecular disulfide bond (V144C-V153C), which is compatible with the protein function. Consequently, the sulfhydryl of I113C becomes free and thus, could be partially engaged in an intermolecular bonding with the same group from the neighboring OutC protomer. Therefore, functionality of this triple mutant is improved in comparison with the corresponding double mutants. On the contrary, in the triple I113C/V143C/V153C mutant, I113C is fully engaged in a more proficient intramolecular bonding either with the buried V143C or with the solvent exposed V153C, which completely arrests the protein function. Moreover, these data show that multiple cysteine substitutions *per se* are well compatible with the functionality of OutC and thus, do not disturb folding of the HR domain.

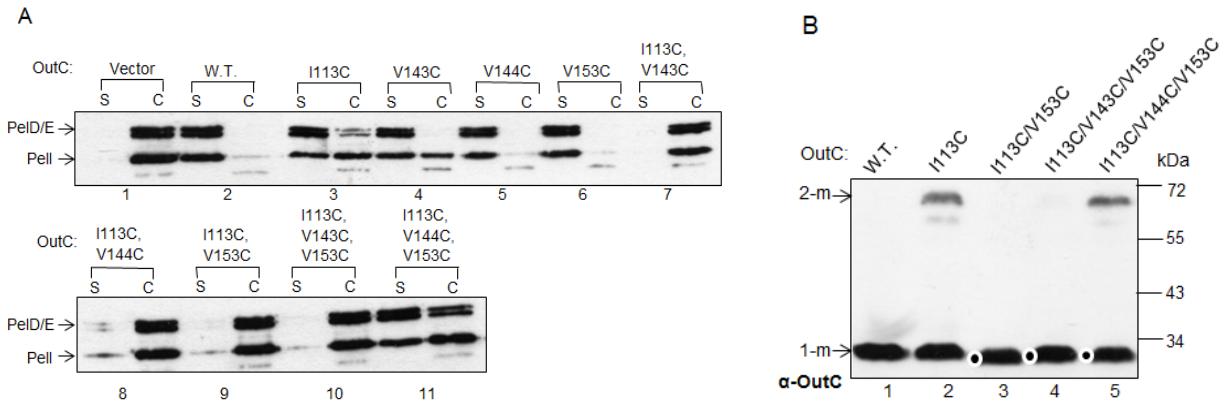

Fig. III: N1 Functional (A) and disulfide bond analysis of OutC variants carrying multiple cysteine substitutions within the T2SS of *D. dadantii*. (A) The secretion activity of OutC variants (indicated on top of gels) was estimated in a complementation assays with *D. dadantii* Δ*outC* strain A3556. Bacteria carrying a plasmid with OutC variants were grown to steady-state, then, culture supernatant (s) and cells (c) were separated and analyzed by immunoblotting with PelD and PelI-antibodies. The amount of secreted proteins (PelD, PelE and PelI) in the culture supernatant reflects secretion efficiency. (B) Disulfide-bonding analysis of the same OutC variants. Cells from the same cultures as in A were treated with iodoacetamide to block remaining free thiol groups and the extent of disulfide-bonding was assessed by non-reducing SDS-PAGE followed by immunoblotting with OutD-antibodies. A certain amount of homodimer characteristic for the thiol of I113C was only detected with OutCI113C and OutCI113C/V144C/V153C (As shown on Fig. 3B of the Article 3, homodimers formed by various cysteine variants of OutC have different and thus, characteristic, apparent molecular mass.) Double I113C/V153C and triple I113C/V143C/V153C and I113C/V144C/V153C variants (indicated by a dot) migrated slightly faster than the wild type OutC monomer, indicating formation of an intramolecular disulfide bond. Positions of monomers (1-m) and dimers (2-m) are indicated by arrowheads.

Chapter IV: Assessment of the secretin-pilotin interaction *in vivo*

IV.1 Preface

Secretins form oligomeric ring-like structures in the OM of Gram-negative bacteria, which facilitate the translocation of proteins and other macromolecular complexes across the OM. Besides the T2SS, the secretins are also present in the type III secretion and type IV pili systems and are involved in extrusion of the filamentous bacteriophages. Given the complexity and size of secretin assemblies, with molecular weights in the range between 0.5 and 1.0 MDa, it is not surprising that auxiliary proteins have been identified that are important for secretin targeting, oligomerization, insertion and proper assembly in the OM. A specialized class of small lipoproteins named pilotins plays these functions towards the cognate secretins. For example, in certain T2SSs, the pilotin GspS is necessary for the correct targeting and insertion of the secretin GspD into the OM. Although the pilotins from different export pathways are thought to perform roughly similar functions in the biogenesis of their cognate secretins, they appear to be unrelated in sequence and structure. Notably, the crystal structure of the pilotin MxiM from the T3SS of *Shigella flexneri* adopts a conical shape β-barrel structure interrupted by an α-helix (Okon *et al*., 2008), while the pilotins from the T4P of *Pseudomonas aeruginosa* and *Neisseria meningitidis* are composed of six tetratricopeptide repeats arranged as a superhelix (Koo *et al*., 2008; Trindade *et al*., 2008). This indicates that the pilotins from various export pathways could have somewhat different modes of function. No pilotin structure from the T2SS has been available until July 2011. To unravel the molecular mechanisms of OutS (GspS) action and its interaction with the secretin, we undertook a structure-functional analysis of the pilotin OutS from the T2SS of *D. dadantii*. Once again, this study was performed in collaboration with the team of Pr. R.W.Pickrsgill from Queen Mary University of London. The crystal structure of OutS that comprises an arrangement of four α-helices is profoundly different from the pilotins from the T3SS and T4P. We showed that OutS binds tightly to 18 residues close to the C-terminus of the secretin OutD causing this unstructured region to become helical on forming the complex. To assess the pilotin/secretin interaction *in vivo*, we constructed truncated and/or mutated variants of these proteins and performed a series of *in vivo* experiments. They confirm an essential role of the ultimate C-terminal sequence of OutD. Furthermore, we showed that the region upstream of this binding site is not required for targeting of the secretin but is essential for its function.

In this study, I constructed several OutD derivatives and examined their functionality and targeting to the OM by flotation sucrose gradient centrifugation (the section "*Assessment of the*

pilotin/secretin interaction in vivo" in this paper).

The details of these results are present as a part of the following article:

IV.2 Article 4:

Structural and functional insights into the pilotin-secretin complex of the type II secretion system.

Chapter V: Interaction between OutB and OutD

V.1 Introduction

The T2SS is composed of at least 12 core components which could be subdivided into three groups, i.e., 1) the OM pore forming secretin GspD, 2) the IM membrane components GspC-L-M-F and the ATPase GspE, 3) the pseudopilins GspG, H, I, J, K and prepilin peptidase GspO. Besides this conserved core of 12 proteins, in certain bacteria, some additional Gsp proteins are required for assembly of a functional T2S machinery. For example, an OM lipoprotein GspS named pilotin, is required for the correct targeting and insertion of the secretin into the OM in *Erwinia*, *Klebsiella* and some other bacteria; an IM protein with putative ATPase activity GspA, has been found in *E. coli* (Francetic and Pugsley, 1996; Francetic *et al.*, 2000), *Aeromonas* species (ExeA) and *Vibrio* species (EpsA) (Heidelberg *et al.*, 2000); an IM protein GspB has been described in *Klebsiella* species (PulB) (d'Enfert and Pugsley, 1989), *Erwinia* species (OutB) (Condemine *et al.*, 1992; Lindeberg *et al.*, 1996), *Aeromonas* species (ExeB) (Jahagirdar and Howard, 1994) and *Vibrio* species (EpsB) (Heidelberg *et al.*, 2000). In *Klebsiella* and *Erwinia* species, *gspB* gene is clustered with *gspS*, and an equivalent of *gspA* gene was not found in their chromosome. In *Aeromonads* and *Vibrios*, *gspB* forms an operon with *gspA*. Indeed, in *A. hydrophila*, GspA and GspB are found to form an IM complex that is required for an efficient secretion of aerolysin (Schoenhofen *et al.*, 1998). Further studies demonstrated that ExeAB complex is required for a correct localization and multimerization of the ExeD secretin in the OM (Ast *et al.*, 2002; Strozen *et al.*, 2011). In the absence of ExeAB, ExeD remains in the IM as a monomer. ExeA contains a putative peptidoglycan-binding motif, the interaction between ExeA and peptidoglycan may cause the periplasmic ExeAB domains to form a large multimers, possibly a ring-like structure on peptidoglycan. Such ring could be necessary for transport and assembly of the secretin multimer in the OM (Li *et al.*, 2010). In contrast to *Aeromonads*, where *gspAB* are absolutely required for the function of T2SS, in *Vibrios*, inactivation of *gspA* resulted in only minor reduction in secretion of T2SS substrates. However, the amount of secretin multimer was more significantly decreased in these mutants, indicating that although GspAB of *Vibrios* facilitate the assembly of the secretin, other yet unidentified factors may provide redundancy for secretin assembly (Strozen *et al.*, 2011). In many bacteria carrying a functional T2SS, no obvious GspAB homologues have been found and in some bacteria, such as *Erwinia* and *Klebsiella*, GspB but no GspA is present. In *K. oxytoca*, *pulB* mutation has no apparent effect on secretion (D'Enfert and Pugsley, 1989). In *E. chrysanthemi*, the absence of OutB results in the

reduction of secretion by 30% (Condemine *et al.*, 1992). An overproduction of OutD was shown to suppress the phenotype of an *outB* mutant (Condemine and Shevchik, 2000). Similar result was also found in *A. hydrophila* (Ast *et al.*, 2002). Overexpression of the secretin ExeD is sufficient to suppress the secretion defect of ExeAB mutant. In *E. coli*, cloning of the *gspAB* operon into the same plasmid with *gspC-O* caused a marked increase in GspG levels, which suggests that GspA and/or GspB might play a regulatory role (Francetic *et al.*, 2000). However, considering a significant sequence similarity between GspA/B of *Aeromonas*, *Vibrio* and *E. coli*, it seems unlikely that these proteins could play so different functions in these bacteria, i.e., peptidoglycan binding and secretin assembly in the first but regulation in the latter. Therefore, to date, the precise role of GspB in T2SS remains unclear.

OutB is an IMP with a deduced molecular mass of about 23.5 kDa, while with an apparent molecular mass of 29 kDa. This aberrant mobility could result from its amino acid composition (9% proline) (Condemine and Shevchik, 2000). Topological analysis revealed that OutB have a bitopic topology with the N-terminus anchored in the IM and a large C-terminal periplasmic domain. The similarity between ExeB and energy-transducing protein TonB led Schoenhofen *et al.* (1998) to suggest that ExeB could function with the putative ATPase ExeA to transduce metabolic energy to open the secretion pore. Interestingly, *V. vulnificus* encodes a 718 amino acids (aa) protein that contains a GspA domain within the N-terminal 530 aa of the protein and a GspB domain within the C-terminal 188 aa, which indicates that GspA and GspB really function together (Strozen *et al*., 2011). The periplasmic domain is well conserved between ExeB and OutB, suggesting that both proteins could play similar functions within respective T2SS, although GspA is apparently lacking in *E. chrysanthemi*. *outB* and *pulB* are clustered with *outS* and *pulS*, respectively, which indicates that these two proteins may collaborate to pilot the cognate secretin to the OM. Indeed, OutS binds tightly to 18 residues close to the C-terminus of the secretin to target and insert the secretin into the OM (Gu *et al.*, 2012a, accepted). In the absence of pilotin or S domain, the secretin miss-locates to the IM (Guilvout *et al.*, 2006; Gu *et al.*, 2012a, accepted). Several experiments have suggested an interaction between OutB and OutD (Condemine and Shevchik, 2000). In *E. chrysanthemi*, the presence of OutB stabilizes OutD. OutD expressed in *E. coli* can be partially protected from proteolytic degradation by the coexpression of OutB. OutB can be cross-linked with OutD by formaldehyde. However, there is no direct evidence on the interaction between GspB and GspD, and, the exact role of GspB in T2SS remains unclear.

In this chapter, we examined the interaction between the secretin OutD and OutB using *in*

vitro co-purification. To elucidate the role of OutB, we studied the effect of OutB on the interactions between the HR domain of OutC and the two distinct sites of OutD, one located in N0 domain and another overlapping N2-N3' domains.

V.2 Results

V.2.1 Effect of OutB on the interactions of OutC with two distinct sites of OutD

It seems reasonable to expect that certain protein/protein interactions between the T2SS components occur during the assembly of the system, while others take place in the functional machinery. These interactions may be either permanent or transient, and could induce conformational changes of proteins in the course of the secretion process. The fact that OutB and OutD stabilized each other indicates an interaction between OutB and OutD in the functional secretion machinery (Condemine and Shevchik, 2000). To test whether the interaction between OutB and OutD affects the interaction patterns between OutD and OutC, we constructed the plasmid pACT3 expressing either *outS* or *outS* with *outB* under the control of P*tac*. Then, pT7-6 plasmids coexpressing various combinations of cysteine variants of OutC and OutD (Table. V. 1) either coexpressed or not with PelB were introduced into *E. coli* NM522, which carry a pACT3 plasmid either with *outS* or *with outS* and *outB*. Therefore, we could test the effect of the secreted protein (PelB) and OutB on the extent of disulfide cross linking between various cysteine variants of OutC and OutD. Thus, we could estimate whether PelB and/or OutB interfere with the corresponding OutC-OutD interactions. Overnight cultures were harvested and treated as described in Materials and methods. The expression level of proteins was verified by immunoblotting and the cross-linked patterns with various gene combinations were assessed by non-reducing SDS-PAGE gel.

(1) Effect of OutB on the interaction of OutCsip and N0 of OutD

OutCsip region consists of two β strands (β6 and β7) located on HR domain. An efficient disulfide cross-linking between V153C (β7 strand) of HR and T53C (β2 strand) of N0 domain of OutD suggests that the β7 of HR is proximal to the β2 of N0 during the secretion process. However, no obvious cross-linked complex was detected between V144C (β6 strand) of HR and T53C (β2 strand) of N0, which indicates that these two positions are not juxtaposed *in vivo*. We showed that the interaction between these sites of OutC and OutD depend on the presence of other Out components (OutE/L/M) and the secreted protein (chapter III). We further tested whether the presence of OutB affects the extent of crosslinks between various cysteine variants

Table. V. 1: Plasmids employed in this chapter.

Plasmid	Relevant characteristic(s)	Reference
pT7-6	The Φ10 promoter of T7, Amp^R	Tabor and Richardson, 1985
pACT3	The tac promoter, Cm^R	Dykxhoorn *et al*., 1996
pACT3-oS	pACT3 carrying *outS* under P*tac*	Chapter III
pACT3-oSoB	pACT3 carrying *outS* and *outB* under P*tac*	This chapter
Vectors coexpressing OutC and OutD cysteine variants under the control of P*pelC*		
pTdB-oC$_{V144C}$-oD$_{T53C}$	*outC* (V144C) and *outD* (T53C)	Chapter III
pTdB-oC$_{V144C}$-oD$_{V232C}$	*outC* (V144C) and *outD* (V232C)	Chapter III
pTdB-oC$_{V144C}$-oD$_{VI271C}$	*outC* (V144C) and *outD* (V271C)	Chapter III
pTdB-oC$_{V153C}$-oD$_{T53C}$	*outC* (V153C) and *outD* (T53C)	Chapter III
pTdB-oC$_{V153C}$-oD$_{V232C}$	*outC* (V153C) and *outD* (V232C)	Chapter III
pTdB-oC$_{V153C}$-oD$_{V271C}$	*outC* (V153C) and *outD* (V271C)	Chapter III
Vectors coexpressing PelB with OutC and OutD cysteine variants under the control of P*pelC*		
pTPLB-oC$_{V144C}$-oD$_{T53C}$	*pelB* followed by *outC* (V144C) and *outD* (T53C)	Chapter III
pTPLB-oC$_{V144C}$-oD$_{V232C}$	*pelB* followed by *outC* (V144C) and *outD* (V232C)	Chapter III
pTPLB-oC$_{V144C}$-oD$_{V271C}$	*pelB* followed by *outC* (V144C) and *outD* (V271C)	Chapter III
pTPLB-oC$_{V153C}$-oD$_{T53C}$	*pelB* followed by *outC* (V153C) and *outD* (T53C)	Chapter III
pTPLB-oC$_{V153C}$-oD$_{V232C}$	*pelB* followed by *outC* (V153C) and *outD* (V232C)	Chapter III
pTPLB-oC$_{V153C}$-oD$_{V271C}$	*pelB* followed by *outC* (V153C) and *outD* (V271C)	Chapter III
Vectors coexpressing GST-OutC and OutDHis derivatives		
pGEX-6P-3	GST-fusion vector with PreScission protease cleavage site, Amp^R	GE Healthcare
pGX-oC$_{128-272}$-oD$_{28-285}$	*GST-outC* (aa 128 to 272) and *outD-6His* (aa 28 to 285)	Login *et al.*, 2010
pGX-oC$_{128-272}$-oD$_{28-112}$	*GST-outC* (aa 128 to 272) and *outD-6His* (aa 28 to 112)	Login *et al.*, 2010
pGX-oC$_{128-272}$-oD$_{116-285}$	*GST-outC* (aa 128 to 272) and *outD-6His* (aa 116 to 285)	Login *et al.*, 2010
pGX-oC$_{161-272}$-oD$_{28-285}$	*GST-outC* (aa 161 to 272) and *outD-6His* (aa 28 to 285)	Login *et al.*, 2010
pGX-oC$_{161-272}$-oD$_{28-112}$	*GST-outC* (aa 161 to 272) and *outD-6His* (aa 28 to 112)	Login *et al.*, 2010
pGX-oC$_{161-272}$-oD$_{116-285}$	*GST-outC* (aa 161 to 272) and *outD-6His* (aa 116 to 285)	Login *et al.*, 2010
Vectors coexpressing GST-OutB and OutDHis derivatives		
pGX-oB$_{112-220}$-oD$_{28-285}$	*GST-outB* (aa 112 to 220) and *outD-6His* (aa 28 to 285)	This chapter
pGX-oB$_{112-220}$-oD$_{28-112}$	*GST-outB* (aa 112 to 220) and *outD-6His* (aa 28 to 112)	This chapter
pGX-oB$_{112-220}$-oD$_{116-285}$	*GST-outB* (aa 112 to 220) and *outD-6His* (aa 116 to 285)	This chapter

Table. V. 2: Primers used in this chapter. Mutated or introduced bases are in bold.

Primer	Nucleotide sequence (5'→3')
OutB-BH-5'	**CTGGGATCC**CCCGCCAAATTGGTAACAG
OutB-XB-3'	**CGGAATTCCGGCTCTAGA**GCATGATGTGCAGTTGCTG

of OutC and OutD. We found that the presence of OutB slightly increased the amount of OutC-OutD complex between V153C (β7) of HR and T53C (β2) of N0 subdomain of OutD (Fig. V. 1. IA, lanes 5 and 7). However, OutB had no obvious effect on cross-linking between V144C (β6) of HR and T53C (β2) of N0 subdomain of OutD (Fig. V. 1. IA, lanes 1 and 3).

(2) Effect of OutB on the interaction of OutCsip and N2-N3' of OutD

An *in vivo* disulfide cross-linking analysis revealed that the second interacting site consisting of OutCsip and N2-N3' domain, such as V144C (β6 of HR) of OutC interacts with V271C (β12 of N3) of OutD while V153C (β7 of HR) of OutC interacts with V232C (β10 of N2) of OutD. This indicates that these domains (HR of OutC and N2 and N3' of OutD) are arranged in a manner such that β6 of OutC is more proximal to β12 of N3 of OutD whereas β7 of OutC is closer to β10 of N2. We therefore tested whether OutB affects these crosslinking patterns. We observed that the presence of OutB led to a substantial decrease in the formation of complex between V144C (β6 of HR) of OutC and V271C (β12 of N3) of OutD (Fig. V. 1. IIIA, lanes 1 and 3). However, the presence of OutB only slightly affected the formation of the complex between V153C (β7 of HR) of OutC and V271C (β12 of N3) of OutD (Fig. V. 1. IIIA, lanes 5 and 7). OutB had no obvious effect on the crosslinking ability between V144C (β6) and V153C (β7) of OutC and V232C (β10 of N2) of OutD (Fig. V. 1. IIA, lanes 1 and 3, 5 and 7).

Therefore, these experiments suggest that OutB differently affects the affinity of the two OutC-OutD interacting sites, slightly increasing the interaction between V153C (β7 of HR) and T53C (β2 of N0) but decreasing that between V144C (β6 of HR) and V271C (β12 of N3). This may result from the direct interaction of OutB with OutC or with OutD. Therefore, OutB could probably compete for the same interaction site(s) within OutC and OutD. Previous study suggested an interaction between OutB and OutD (Condemine and Shevchik, 2000). To provide a direct evidence for an interaction between OutB and OutD, we performed an *in vitro* copurification.

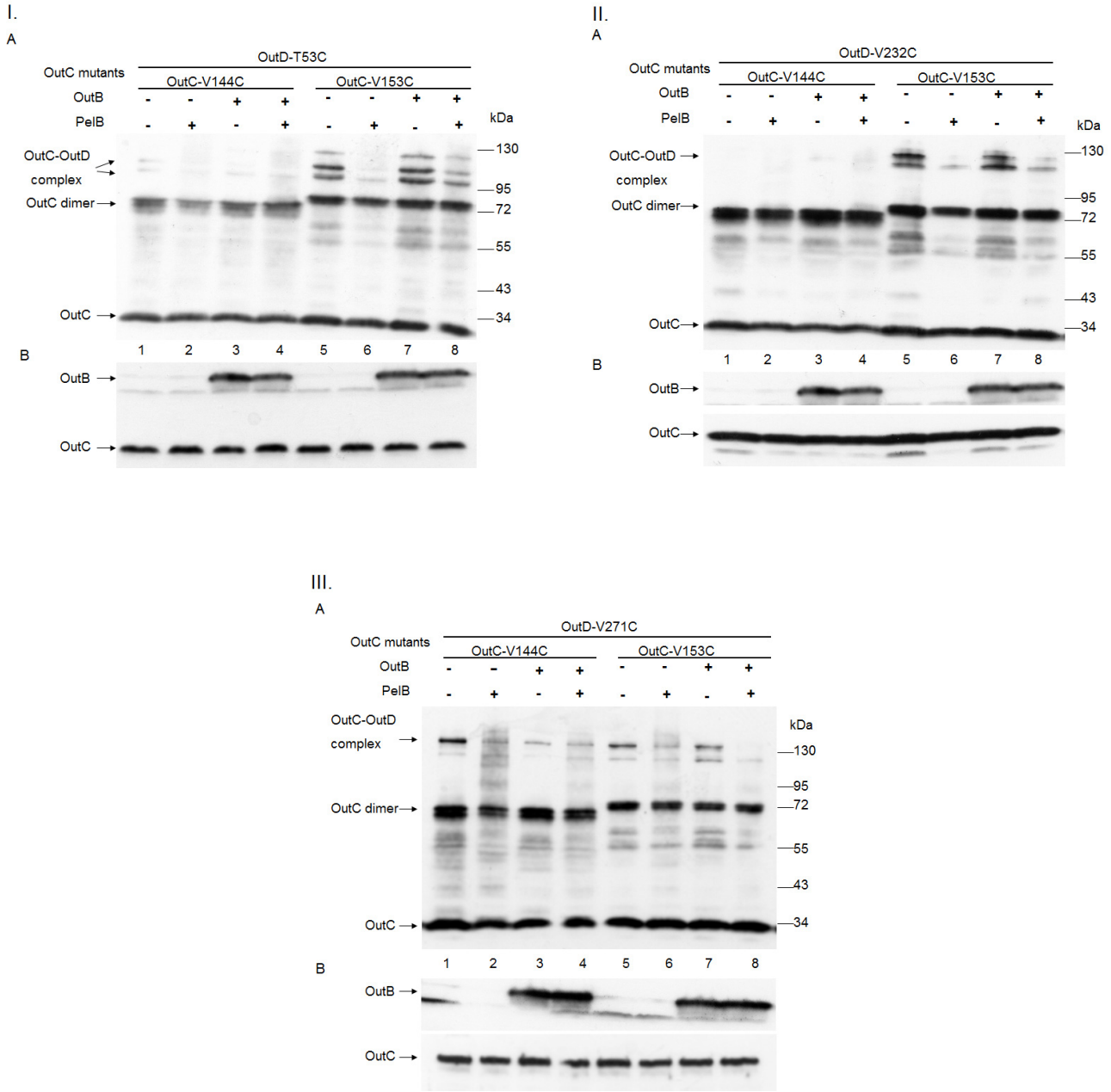

Fig. V. 1: The effect of OutB on the interactions between the HR of OutC and two distinct sites of OutD, N0 (I) and N2-N3' (II and III). *E. coli* NM522 cells expressing the indicated variants of OutC and OutD either alone or with PelB, or with OutB, or with PelB and OutB (indicated on top of the panels) were grown overnight and treated as described in Materials and methods to preserve spontaneously formed disulfide bonds. (A) The samples were separated by SDS-PAGE under non-reducing conditions (without β-mercaptoethanol) and probed with OutC-antibodies. (B) The samples were separated by SDS-PAGE under reducing condition (with β-mercaptoethanol) and either probed with OutB-antibodies or with OutC-antibodies to estimate the amounts of OutB and OutC variants. The deduced compositions of the immunoreactive species (OutC dimer and OutC-OutD complex) are indicated by arrows.

V.2.2 Mapping of the interaction site between OutB and OutD

OutB protects OutD from proteolytic degradation when the two proteins are coexpressed in *E. coli* (Condemine and Shevchik, 2000). This effect does not require the N-terminal portion of OutB. In addition, family sequence alignment shows that the N-terminal region of GspB is dissimilar while the C-terminal portion is much more conserved (Fig. V. 2). These indicate that C-terminal region of OutB which extends into the periplasm could play a similar function within GspBs, for example, they could be involved in the interaction with the periplasmic region of OutD. To test this hypothesis, the C-terminal region of OutB ($OutB_{112-220}$) was fused to GST and coexpressed with a His-tagged N-terminal region of OutD ($OutD_{28-285}$) from the same plasmid pGEX-6P-3. Then the two proteins were co-purified from the same whole cell extract by glutathione-affinity chromatography. In these experiments, GST-tagged OutB was bound to Glutathione Sepharose and used as a bait to catch other proteins that interact with OutB (e.g., OutD). Our previous results showed that $OutD_{28-285}$ bound efficiently to GST-$OutC_{128-272}$, but not to GST-$OutC_{161-272}$. We therefore used these two GST fusions as a positive and a negative control, respectively (Fig. V. 3 and Fig. V. 4A, lanes 1 and 3). In copurification assay, $OutD_{28-285}$ bound efficiently to GST-$OutC_{128-272}$ and to GST- $OutB_{112-220}$ (Fig. V. 4A, lanes 1 and 2), but not to GST-$OutC_{161-272}$ (Fig. V. 4A, lane 3). This indicates that the C-terminal region of OutB ($OutB_{112-220}$) interacts with the N-terminal region of OutD ($OutD_{28-285}$). To map the interaction site(s) within OutD, we employed two shorter OutD derivatives, $OutD_{28-112}$ and $OutD_{116-285}$, one consisting of the N0 domain and the other comprising the N1, N2 and the beginning of N3 domains (Fig. V. 3C). In copurification assay, we found that only $OutD_{28-112}$ (N0) bound to GST-$OutB_{112-220}$ (Fig. V. 4B, lane 5). This suggests that the C-domain of OutB ($OutB_{112-220}$) interacts with the N0 domain of OutD ($OutD_{28-112}$). Therefore, N0 domain of OutD interacts with two sites within HR domain of OutC (Chapter III) and the C-terminal domain of OutB. The competition experiments above (Fig. V. 1. IA) suggested that at least some of these interactions are compatible and even cooperative.

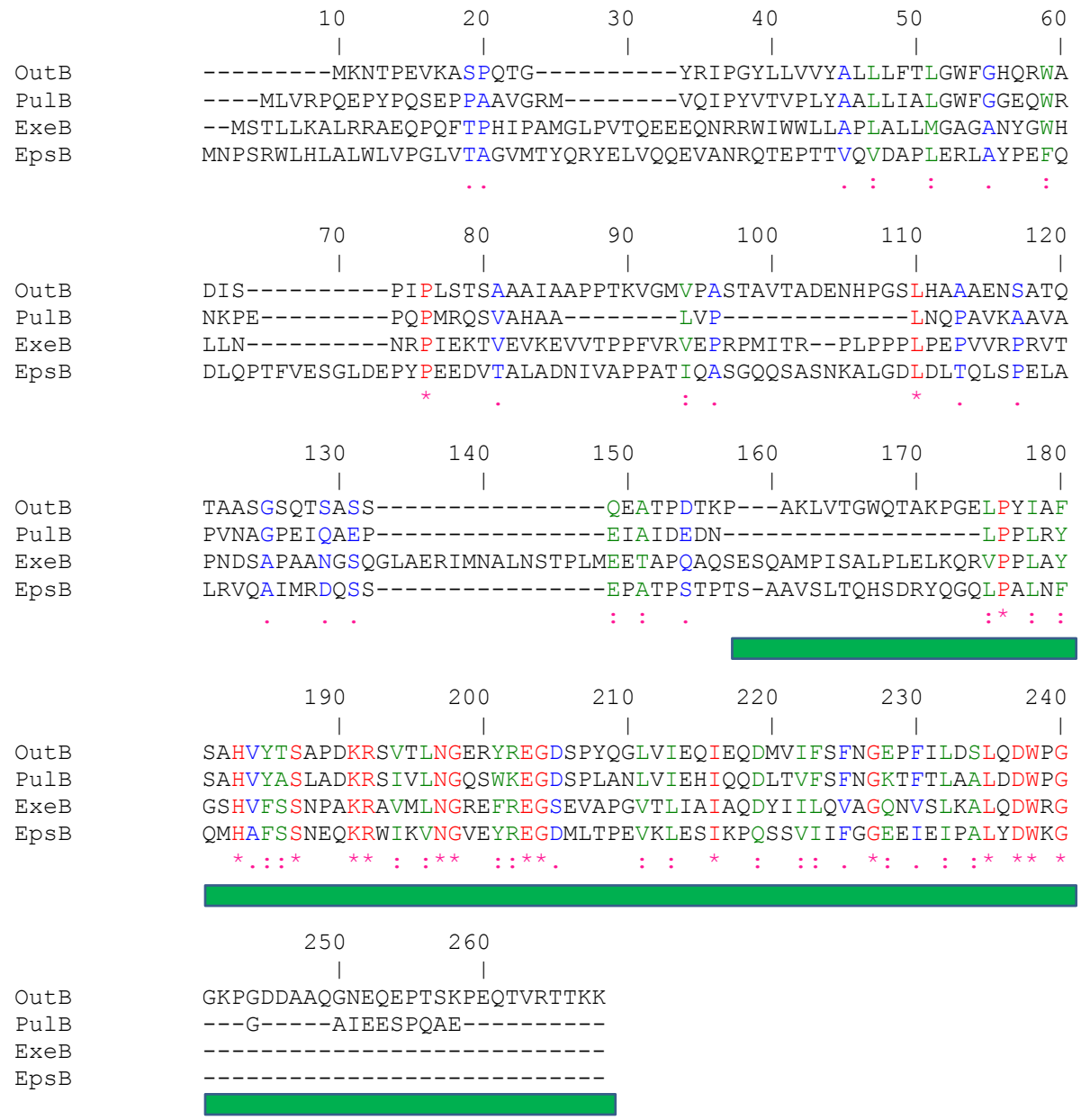

Fig. V. 2: Family sequence alignment of GspB proteins. OutB from *Erwinia chrysanthemi*, PulB from *Klebsiella oxytoca*, ExeB from *Aeromonas hydrophila* and EpsB from *Vibrio cholera* are aligned by ClustalW. Identical residues are in red, strongly similar and weakly similar residues are in green and blue respectively. The OutB region used in copurification assay is indicated by a green bar.

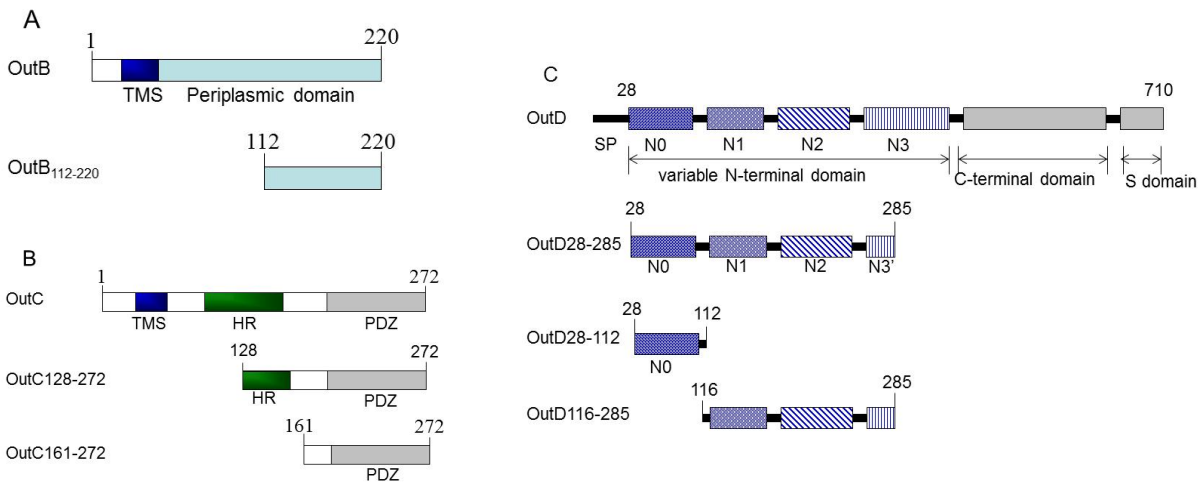

Fig. V. 3: Schematic diagrams of OutB (A), OutC (B) and OutD (C) and their truncated derivatives used in this chapter.

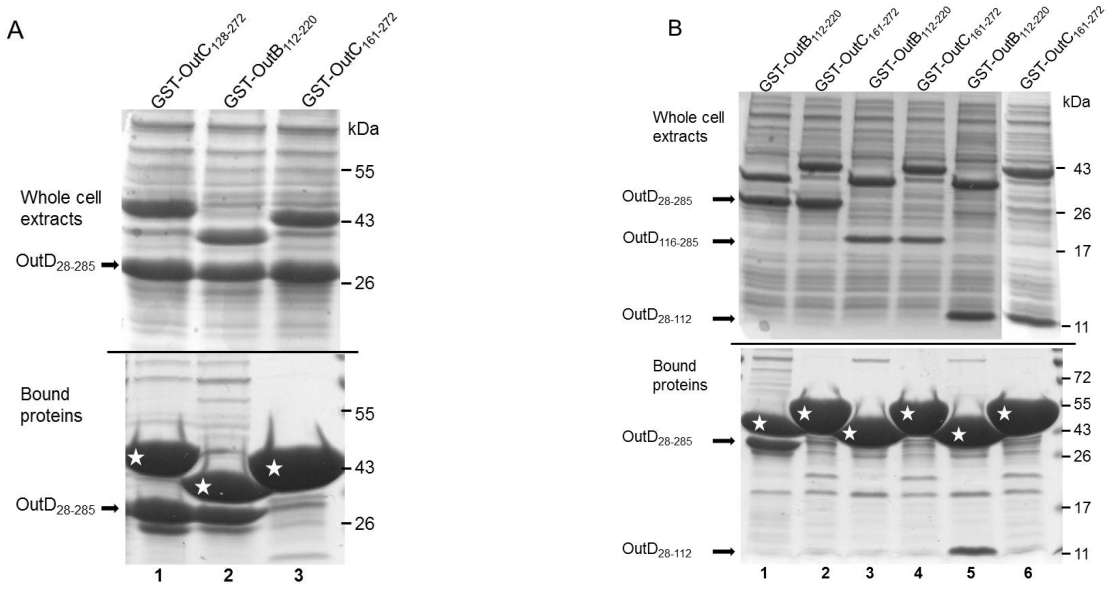

Fig. V. 4: Mapping the interaction region(s) between OutB and OutD. (A) C-terminal domain of OutB interacts with N-terminal domain of OutD. (B) C-terminal domain of OutB interacts with N0 subdomain of OutD. Whole-cell extracts of *E. coli* BL21 (DE3) coexpressing GST-OutB$_{112-220}$ or GST-OutC derivatives with OutD derivatives (indicated on top) were used in copurification assays on Glutathione Sepharose. Bound proteins were eluted with Laemmli sample buffer, separated by SDS-PAGE and then stained with Coomassie G250. GST-OutB$_{112-220}$ or GST-OutC derivatives are indicated by asterisks, OutD derivatives are indicated by arrows.

V.3 Discussion and conclusions

In bacteria that contain both *gspA* and *gspB*, e.g., *Aeromonads* and *Vibrios*, *gspA* and *gspB* are clustered into the same operon, which indicates that GspAB acts in partnership. Indeed, in *A. hydrophila*, ExeA and ExeB were shown to form a large heteromultimeric complex in the IM, which is required for a correct localization and multimerization of the ExeD secretin in the OM (Ast *et al.*, 2002; Strozen *et al.*, 2011). Moreover, in *V. vulnificus*, *gspA* and *gspB* genes are fused into the single gene. In the absence of GspAB complex, the secretion of aerolysin and assembly of the secretin multimer in *A. hydrophila* were abrogated (Ast *et al.*, 2002). However, deletion of *gspA* and *gspB* in *Vibrio* species had a minimal effect on the secretion while it decreased assembly of the secretin multimer. Further cross-complementation experiments confirmed that GspAB perform the same role in *Vibrios* as does in *Aeromonads*, although they are differently required for assembly of the functional secretion machinery. It was suggested that the C-terminal peptidoglycan-binding motif of GspA could be directly involved in the assembly of secretin in the OM. The interaction between GspA and peptidoglycan may result in the reorganization of the peptidoglycan meshwork to allow monomeric GspD subunits or the secretin multimer itself to pass through to reach the OM, or may possibly provide a scaffold for assembly of the secretin (Li *et al.*, 2010; Strozen *et al.*, 2011). The role of GspB in assembly of the secretin is not clear. GspB may fulfil the part of the pilotin role that GspS plays in *K. oxytoca and E. chrysanthemi*, since no obvious GspA homologue is present and *gspB* is clustered with *gspS* in these bacteria. These indicate that two proteins may collaborate to pilot the secretins to the OM. The GspB is not required for the T2SS secretion by the Pul system of *K. oxytoca* reconstructed in *E. coli*. However, it significantly improves secretion of *E. chrysanthemi* Out system. Thus, the role of GspB remains a puzzle.

Our *in vitro* and *in vivo* results have shown that a short peptide of OutC (OutCsip, 139-158) interacts with two distinct sites of OutD, one located in N0 subdomain and another overlapping N2-N3' subdomain (chapter I). Further cysteine scanning and disulfide cross-linking analysis confirmed these interactions *in vivo* and showed that the secreted protein and the other T2SS components (OutE/L/M) differently affect these interactions (Chapter III). These data suggest that various OutC-OutD interactions could correspond to various functional states of the secretion machinery. We proposed that during secretion process, certain T2SS components and/or substrates could affect differently the interactions between OutC and various sites of OutD, thus provoke a switch from one functional state to another. In Chapter III, we have examined the effects of secreted proteins and IM components OutE-L-M on the interactions

between OutC and various sites of OutD. In this study, we showed that OutB interacts directly with OutD and more precisely with N0 domain (Fig. V. 4). Such interaction may induce the conformational change of OutD and therefore affect the interactions between OutC and OutD. Alternatively, OutB could probably compete with OutC for the same interaction site(s) with OutD. Disulfide cross-linking analysis showed that the presence of OutB slightly increases the formation of OutC-OutD complex between V153C (β7) of OutC and T53C (β2) of N0 domain of OutD (Fig. V. 1A, lanes 5 and 7) whereas it decreases that between V144C (β6) of OutC and V271C (β12) of N3 domain of OutD. Disulfide cross-linking requires a close proximity and proper orientation of the two cysteine residues to allow formation of a disulfide bond between them. The presence of OutB increased the formation of OutC-D complex suggests a conformational change either in OutC or OutD or both that improve these interactions. Such a conformational change may occur via their direct interaction with OutB. Since no data suggests an interaction between OutC and OutB, we proposed that the conformational change occurs in OutD via an interaction between the periplasmic domain of OutB and the periplasmic domain of OutD. Indeed, copurification assays revealed an interaction between the periplasmic region of OutB ($OutB_{112-220}$) and N0 domain of OutD ($OutD_{28-112}$).

Together with *in vivo* disulfide cross-linking results (Fig. V. 1 .I), we showed that N0 domain of OutD interacts with both the HR domain of OutC and the periplasmic region of OutB. Moreover, our results indicated that these interactions are compatible and even cooperative since in the presence of OutB, the cross-linking between OutC (β7) and N0 domain (β2) becomes ever more pronounced, indicating a possible cooperative effect. Thus, different faces of N0 may be involved in interactions with HR and OutB.

The presence of OutB decreases the formation of the complex between OutC (β6) and N2-N3' (β12) of OutD (Fig. V. 1. III). The effect of OutB on this OutC-OutD interaction site seems to be indirect since no interaction were detected between OutB ($OutB_{112-220}$) and N1-N2-N3' of OutD ($OutD_{116-285}$) (Fig. V. 4B). Alternatively, OutB could probably compete with N2-N3' of OutD for binding to HR of OutC.

To examine whether HR of OutC and OutB bind to different sites of N0 domain of OutD and to test if the interactions between them are cooperative or competitive, the binding affinities of these three proteins should be assessed by using copurification competition assays. In this type of experiments, the binding of various OutD derivatives on GST-HR or GST-OutB matrixes could be affected (either increased or diminished by the presence of the third partner, either OutB or HR of OutC, respectively). It should also be noted that the effect of OutB on the $\beta1^{HR}$-$\beta1^{N0}$

interaction site was not examined in this work. This interface has been suggested by a recent structural study (Korotokov *et al*., 2011) and was recently assessed by cysteine bonding analysis (chapter III). It is therefore necessary to test the effect of OutB on this OutC-OutD interaction site. We showed that OutB diminished the interaction between HR and N2-N3' domains of OutD. Although no data indicates the interaction between OutC and OutB, we cannot exclude the possibility that OutB and N2-N3' of OutD compete for binding to HR of OutC. To examine this, a direct interaction between OutB and OutC should be assessed by using *in vitro* copurification. It should be also interesting to construct protein derivatives suitable for NMR or X-ray crystallography to determine the interface between the C-terminal of OutB and N0 domain of OutD.

Chapter VI: Construction of OutC and OutD protein derivatives suitable for structural analysis

VI.1 Introduction

The previous studies and this work demonstrated that the periplasmic regions of OutC and OutD interact together. To understand the molecular mechanisms of these interactions, we undertook structural studies of these proteins, notably, in collaboration with the team of Prof. R. Pickersgill from Queen Mary University. Previously, in collaboration with this team, the crystal structures of the pectate lyase PelL, pectin methylesterase PemA and the PDZ domain of OutC have been solved (Jenkins *et al*., 2001; 2004). Unfortunately, a similar crystal structure of the PDZ domain of OutC homologue, EpsC from *V. cholerae* had been published just before finishing our work (Korotkov *et al.*, 2006), which compromised the publication of our PDZ structure. When I started this thesis work, neither the atomic resolution structures of the periplasmic region of GspD and HR domain of OutC alone nor in complex were available. Since such data are essential to understand molecular organization and assembly of GspC and GspD within the T2SS, we also undertook to prepare OutC and OutD derivatives suitable for the X-ray crystallography and Nuclear Magnetic Resonance (NMR) analysis. Since during this thesis work, the crystal structures of certain periplasmic domain of GspD and GspC have been solved in parallel by another research team, it became necessary to readapt our strategy of the structural analysis of OutC and OutD. Therefore, some experimental approaches used to generate protein derivatives suitable for further structural analysis have been initiated and developed but stopped because they became obsolete.

X-ray crystallography and NMR are widely used techniques to determine structures of proteins. X-ray crystallography makes use of the diffraction pattern of X-rays which are shot through an object. The pattern is determined by the electron density within the crystal. The diffraction is the result of an interaction with the high energy X-rays and the electrons in the atom. X-ray crystallography requires the growth of protein crystals up to 1 mm in size from a highly purified protein source. Since crystal growth is an experimental technique and there exists no rules about the optimal conditions for a protein solution to result in a good protein crystal, preparing protein crystals suitable for structural analysis is currently the bottleneck in structure determination by this method. A pure (>97%) and homogeneous protein sample is crucial to successful crystallization attempt.

NMR is a technique to study biological macromolecules in solution and does not require the protein crystal. It is based on the fact that nuclei of atoms have magnetic properties that can be utilized to yield chemical information. In order to analyze the nuclear magnetic resonance data, it is important to find out the correspondence between chemical shifts and atoms. To avoid problems with overlapping peaks generated by the hydrogen atoms using homonuclear magnetic resonance, NMR heteronuclear (hydrogen/nitrogen or hydrogen/nitrogen/carbon) is most commonly used. The HSQC (heteronuclear single quantum correlation) is a heteronuclear NMR with isotopic labeling to N^{15} and HMQC (heteronuclear multiple quantum correlation) is NMR heteronuclear labeling with ^{15}N and C^{13} isotope.

Table. VI. 1: Plasmids employed in this chapter.

Plasmid	Relevant characteristic(s)	Reference
Vectors co-expressing GST-OutC and OutDHis derivatives		
pGX-oC$_{60-272}$-oD$_{28-285}$	pGEX-6P-3 carrying *GST-outC* (aa 60 to 272) followed by *outD-6His* (aa 28 to 285)	Chapter I
pGX-oC$_{60-272}$-oD$_{28-285}$ (G190C)	pGEX-6P-3 carrying *GST-outC* (aa 60 to 272) followed by *outD-6His* (aa 28 to 285 with G190C)	This chapter
pGX-oC$_{60-272(V143C)}$-oD$_{28-285}$ (G190C)	pGEX-6P-3 carrying *GST-outC* (aa 60 to 272 with V143C) followed by *outD-6His* (aa 28 to 285 with G190C)	This chapter
pGX-oC$_{60-272}$ $_{(V153C)}$-oD$_{28-285}$ (T53C)	pGEX-6P-3 carrying *GST-outC* (aa 60 to 272 with V153C) followed by *outD-6His* (aa 28 to 285 with T53C)	This chapter
Vectors GST-OutC or GST- OutDHis derivatives		
pGX-oC$_{60-272}$	pGEX-6P-3 carrying *GST-outC* (aa 60 to 272)	Login *et al.*, 2010
pET-oD$_{28-285}$	pET-20b(+) carrying *GST-outD-6His* (aa 28-285)	This chapter

Fig.VI. 1: The schematic diagrams of OutC (A) and OutD (B) and their truncated derivatives used in this chapter.

VI.2 Results

Since OutC and OutD are membrane proteins, they need the addition of detergents to be soluble in aqueous solution. In this case, membrane proteins form mixed micelles with detergents. Stoichiometry and properties of membrane proteins in such mixed micelles depend on the protein and detergent nature. The presence of detergents often interferes with regular

arrangements of the protein complexes in the crystal resulting in diffuse diffraction pattern. An alternative approach consists in using of only soluble regions of membrane proteins. Several soluble derivatives of OutC and OutD have been tested in previous study for crystallization trails, but failed to yield crystals (Login, Ph.D. thesis). A possible reason is that the presence of many flexible regions impairs crystallization. To bypass this problem, we have applied two strategies, i.e., limited proteolysis of large protein derivatives to find more stable domains and formation of covalently linked complexes, and at the final step, combination of these two approaches.

VI.2.1. Identification of stable OutC and OutD derivatives by limited proteolysis

Copurification assays showed that the periplasmic domain of OutD ($OutD_{28-285}$) is efficiently copurified with the periplasmic domain of OutC ($OutC_{60-272}$). This suggests formation of a complex between these two proteins. However, affinity of such a complex is too low, since the two proteins were then eluted as two separate peaks in gel filtration (Login *et al*., 2010, supplementary data). The interaction interface could be buried and therefore partially protected from proteolysis. To examine this hypothesis and to generate the derivatives of OutC and OutD suitable for a structural analysis, we employed limited proteolysis.

The vector expressing either GST-$OutC_{60-272}$ or GST-$OutD_{28-285}$ or coexpressing GST-$OutC_{60-272}$ together with $OutD_{28-285}$ (Table. VI. 1 and Fig. VI. 1) were transformed into *E. coli* BL21 (DE3) cells. The proteins were purified or copurified by affinity chromatography on Glutathione Sepharose (Materials and methods). Then we performed a limited proteolysis with trypsin of either purified $OutC_{60-272}$ or $OutD_{28-285}$ or a complex of these two protein derivatives (Materials and methods). Limited proteolysis assays revealed that $OutD_{28-285}$ alone appeared far more susceptible to proteolysis than $OutD_{28-285}$ in complex with $OutC_{60-272}$. These results suggested that $OutC_{60-272}$ can stabilize the structure of $OutD_{28-285}$ and prevent its degradation (data not shown). This implies that these two proteins interact with each other *in vitro*. Therefore, we used this phenomenon to identify the protein regions protected from proteolysis. Several relatively stable derivatives of OutC and OutD were obtained by limited proteolysis (Fig. VI. 2). The N-terminal (Edman) analysis was performed to identify the sequence of these derivatives. Certain of these derivatives have been characterized (Fig. VI. 3) and sent to our collaborators in London Univeristy for structural analysis.

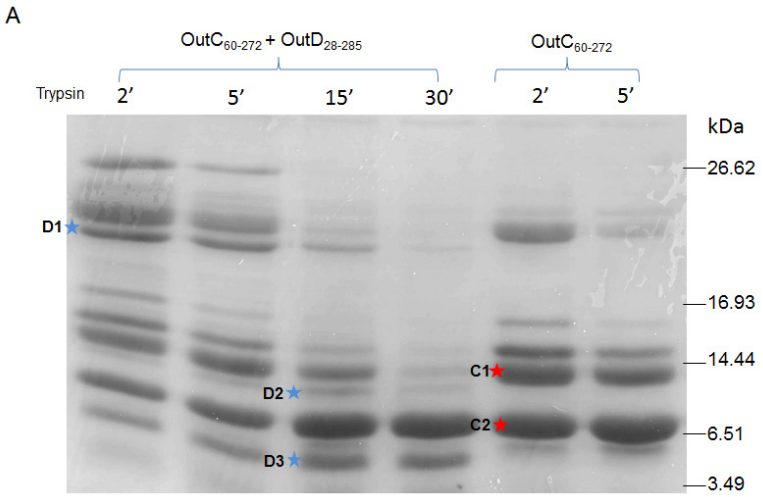

Fig. VI. 2: Generation of OutC and OutD fragments by limited proteolysis with trypsin. $OutC_{60-272}$ and $OutD_{28-285}$ were either coexpressed or $OutC_{60-272}$ was expressed alone (as indicated on top) and used in copurification assays on Glutathione Sepharose. Proteins were eluted with PreScision protease and then incubated for various periods time (indicated at the top of panels) with 2 µg/ml of trypsin. Samples were analysed by Tricine SDS-PAGE. The proteins were transferred to a PDVF membrane and then stained with Coomassie G250. The bands of interest (indicated by red star for OutC fragments and blue star for OutD fragments) were cut off and subjected to the N-terminal (Edman) analysis.

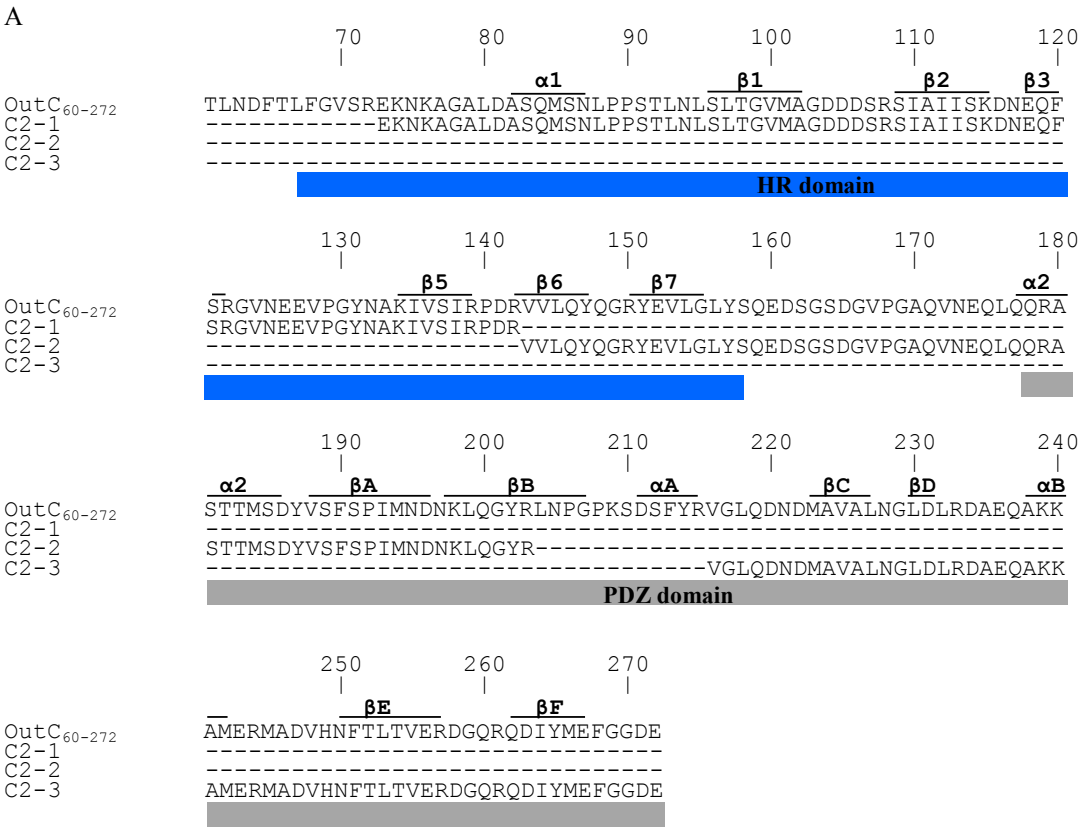

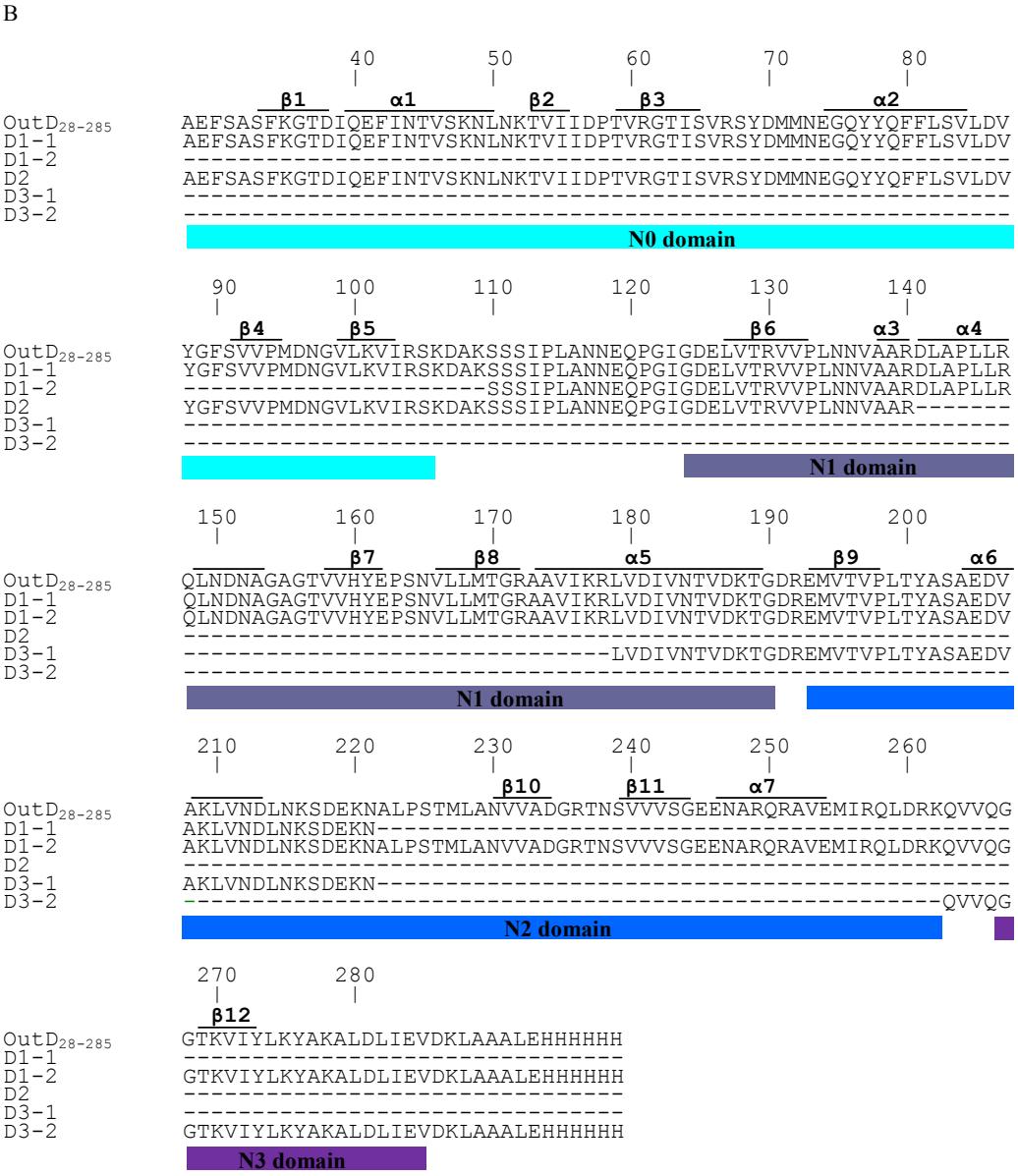

Fig. VI. 3: Sequence alignment of OutC (A) or OutD (B) and the fragments released by limited proteolysis with trypsin (Fig. VI. 2) whose sequences were determined by N-terminal (Edman) analysis. The C-termini of the fragments were deduced from their molecular weight by using trypsin cleavage sites. The sequence of fragment C1 was not obtained while several bands, i.e., C2, D1 and D3 correspond to more than one peptide. The secondary structure of HR is deduced from the recently solved 3D structure of OutC (Gu *et al.*, 2012b, reviewed) while that of PDZ is deduced from the 3D structure of OutC homologue, EpsC of *V. cholerae* (Korotkov *et al.*, 2006). The secondary structure of peri-OutD is deduced from the 3D structure of peri-GspD (Korotkov *et al.*, 2009a).

VI.2.2 Construction of OutC-OutD derivatives suitable for disulfide cross-linking

In another approach, we introduced the site-specific cysteine substitutions into the presumed interaction sites of OutC and OutD to obtain an OutC-OutD complex stabilized by an intermolecular disulfide bond. We suggested that OutC and OutD derivatives bound together via an intermolecular disulfide bond could be more stable and thus suitable for crystallography or NMR studies. Positions for such cysteine substitutions were suggested by our previous functional studies and *in vivo* disulfide cross-linking analysis (Chapter III).

(1) Construction of appropriate over-expression vectors

Functional analysis showed that V143S substitution in OutC blocks secretion in *D. dadantii*. Moreover, our *in vitro* copurification showed that V143S mutation prevents the interaction of OutCsip peptide with the N1-N3' region of OutD (Login *et al.*, 2010). This suggests that V143 of OutC could be directly involved in interaction with OutD. By a search for extragenic suppressor mutations, we found two point mutations in OutD, i.e., A174V and G190D, which partially restore secretion in *D. dadantii outCV143S* mutant (not published). The allele-specific suppression could indicate a direct interaction of these residues. In addition, sequence alignment showed that G190 is highly conserved residue. Thus, cysteine residues were firstly introduced by site-directed mutagenesis in place of V143 of OutC and G190 of OutD in the expression vector pGX-oC$_{60\text{-}272}$-oD$_{28\text{-}285}$.

(2) Disulfide cross-linking *in vitro*

GST-OutC$_{60\text{-}272}$ and OutD$_{28\text{-}285}$ carrying V143C and G190C substitutions in OutC and OutD, respectively, were coexpressed in *E. coli* BL21 (DE3) and whole cell extracts were used to co-purify the OutC-OutD cross-linked species. We firstly tested the formation of spontaneously formed corss-linked products. A certain amount of OutD homodimer was detected whereas only little OutC homodimer and OutC-OutD heterodimer was found (Fig. VI. 4). To improve the formation of disulfide bound complexes, we applied an external oxidant, copper phenanthroline (CuP) which increases oxidation potential of the medium. After sonication, cell extracts were incubated with different concentrations of CuP and then the proteins of interest were copurified

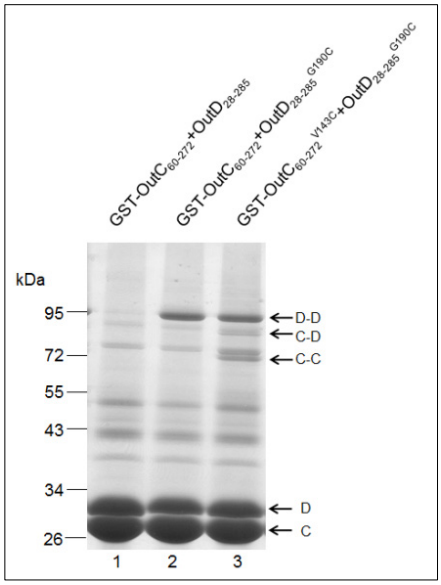

Fig. VI. 4: Analysis of the spontaneous disulfide bond formation *in vitro*. V143C and G190C substitutions were introduced in GST-$OutC_{60-272}$ and $OutD_{28-285}$, respectively (indicated on top of panels). Proteins were coexpressed and whole cell extracts were used in copurification assays on Glutathione Sepharose and then eluted with PreScision protease. The eluted proteins were separated by SDS-PAGE under non-reducing conditions and then stained with Coomassie G250. D-D: cross-linked $OutD_{28-285}$ homodimer, C-D: cross-linked OutC-OutD heterodimer, C-C: $OutC_{60-272}$ homodimer. The nature of these complexes has been revealed by immunoblotting with OutC- and OutD- antibodies (Fig. VI. 6B).

on Glutathione Agarose as usually (Materials and methods). The results show that the amounts of cross-linked homodimer OutC-OutC and heterodimer OutC-OutD were increased in the presence of CuP (Fig. VI. 5A lane 2 and 3). However, the amount of OutD-OutD homodimer was decreased (Fig.VI. 5A, lane 1). The nature of these cross-linked complexes was established by immunoblotting with antibodies against OutC and OutD (Fig. VI. 6B). Variation of the concentration of the oxidative agent from 0.25 mM to 1.25 mM did not apparently affect the extent of disulfide cross-linking (Fig. VI. 5A, lane 2 and 3). The amount of the complexes eluted with PreScision protease was still not sufficient for further purification. Further analysis showed that an abundant amount of cross-linked complexes still bound to the resin after elution with the PreScision protease (Fig. VI. 5A, II - to fully release the bound proteins, the resin was treated with Laemmli sample buffer).

We subsequently examined whether application of the oxidative agent on the other steps of copurification process is more efficient and generates a higher amount of disulfide complexes. Therefore, 1.5 mM CuP was applied of various steps of the copurification process (Materials and methods and Fig. VI. 5B). The results clearly show that using of the oxidative agent at the final step of the copurification assay was much more efficient (Fig. VI. 5B, lane 4). Homodimer of OutC was the major cross-linked product while homodimers of OutD and heterodimers OutC-OutD were less abundant. Nevertheless, the amounts of all these complexes seem to be sufficient to envisage their further purification by ion-exchange and/or hydrophobic-interaction chromatography. In an attempt to perform this, we assessed the solubility of these protein complexes by their precipitation/solubilization with ammonium sulfate (Fig. VI. 6A). The results show that contrary to OutD-OutD dimer, OutC-OutD and OutC-OutC complexes

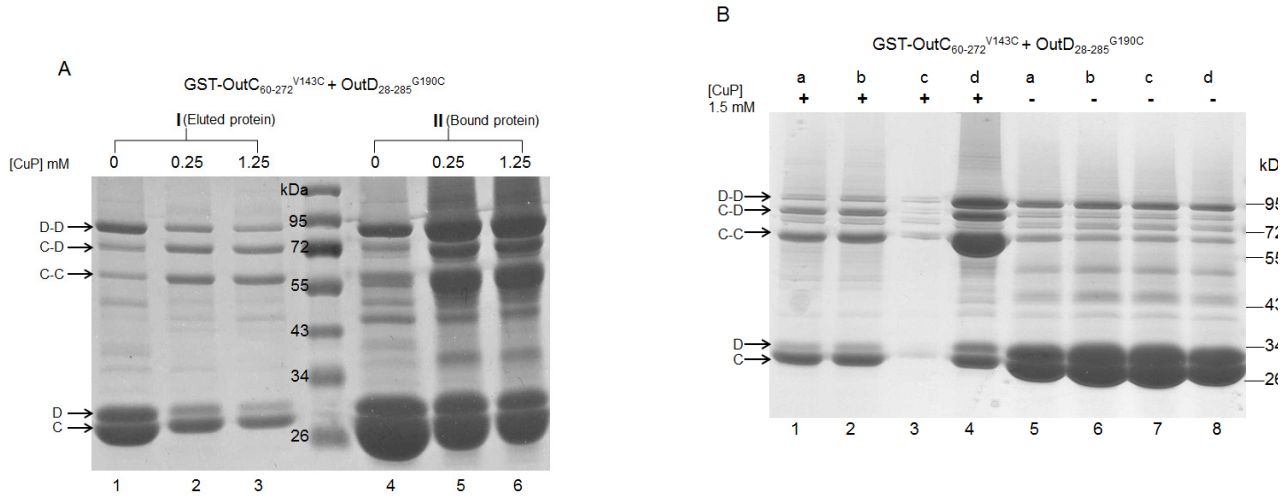

Fig. VI. 5: Development of optimal conditions for disulfide cross-linking *in vitro*. (A) Effect of copper phenanthroline (CuP) concentration on the formation of OutC-D complexes. Indicated concentrations of CuP were added to cell extracts, incubated for 20 min and then the proteins were purified on Glutathione Sepharose and eluted with PreScision protease (panel I). The proteins remain bound to the resin were then eluted with Laemmli sample buffer without β-mercaptoethanol (panel II). (B) Effect of CuP on formation of OutC-D complexes on different steps of purification process. CuP (1.5 mM) was added either to the whole cell extract (a), or soluble cell fraction (b), or resin with bound GST fusion proteins (c), or proteins eluted from the resin with PreScision protease (d).

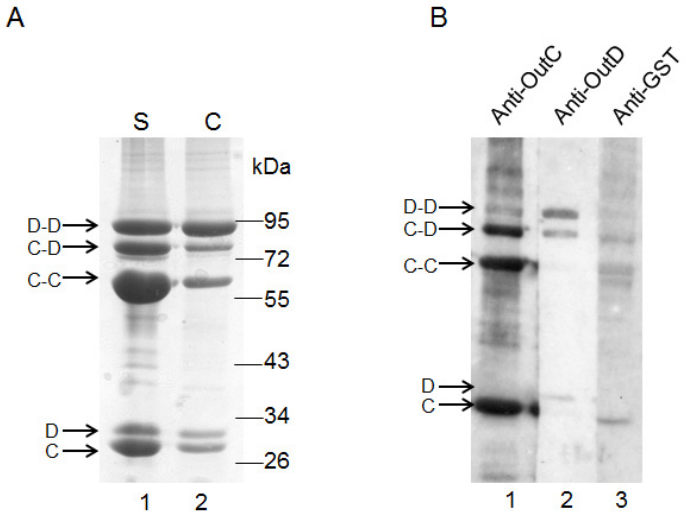

Fig. VI. 6: Solubility assays of the cross-linked OutC-OutD complexes. (A) $OutC_{60-272}^{V143C}$ and $OutD_{28-285}^{G190C}$ proteins were copurified on Glutathione Sepharose and treated with CuP as above (Fig. VI. 5B, lane 4). Then the proteins were precipitated with ammonium sulfate (90%) and resolubilized in the elution buffer to appreciate their suitability for further purification steps. S: the soluble fraction, C: the insoluble fraction. (B) Nature of cross-linked complexes was assessed by immunoblotting with ani-OutC (lane 1), anti-OutD (lane 2) and anti-GST (lane 3) antibodies.

remained well soluble after precipitation by ammonium sulfate (Fig. VI. 6A) and thus are well compatible with further purification by hydrophobic-interaction chromatography. However, this axe has not been continued, since *in vivo* cysteine bonding analysis (which has been performed in parallel, chapter III) revealed that this combination of cysteine variants OutCV143C/OutDG190C generates only trace amounts of OutC-OutD complexes within the functional T2SS and thus is not biologically relevant.

In vivo disulfide cross-linking analysis pointed out some other prominent combinations of cysteine variants of OutC and OutD. Namely, it showed that OutC V153C was efficiently cross-linked with OutD T53C (Chapter III), which suggests that this OutC/OutD interface is functionally relevant. We therefore introduced V153C and T53C substitutions in the expression vector pGEX-o$C_{60\text{-}272}$-o$D_{28\text{-}285}$ and then examined the formation of the corresponding OutC-OutD complex stabilized by a disulfide bond. We found a huge amount of OutD homodimer but only traces of OutC-OutD heterodimer (Fig. VI. 7). This suggests that these OutC and OutD derivatives do not take a proper mutual arrangement *in vitro*, which prevents an efficient OutC-OutD disulfide bonding.

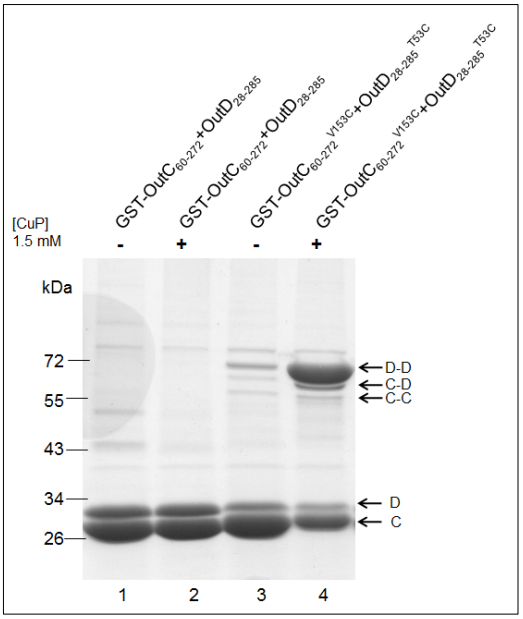

Fig. VI. 7: *In vitro* cysteine bonding analysis between $OutC_{60\text{-}272}^{V153C}$ and $OutD_{28\text{-}285}^{T53C}$. The eluted proteins were either treated with CuP (+) or not (-), separated by SDS-PAGE under non-reducing conditions and then stained with Coomassie G250. D-D: cross-linked $OutD_{28\text{-}285}$ homodimer, C-D: cross-linked OutC-OutD heterodimer, C-C: $OutC_{60\text{-}272}$ homodimer.

VI.3 Discussion and conclusions

OutC and OutD are two core components of the *D. dadantii* T2SS. Our *in vitro* (Chapter I) and *in vivo* (Chapter III) results showed that the HR domain of OutC interacts with at least three distinct sites of OutD. These interactions could correspond to various functional states of the secretion system. Structural characterization of the corresponding OutC-OutD complexes is essential to reveal molecular mechanisms of these interactions and understand the function and

assembly of these proteins within the T2S machinery. In this chapter, we tried to construct the OutC and OutD derivatives suitable for structural analysis by using two complementary approaches. Firstly, we constructed a vector coexpressing GST-$OutC_{60-272}$-$OutD_{28-285}$ and used it in copurification assay. $OutD_{28-285}$ was copurified efficiently with $OutC_{60-272}$, which indicated that the two proteins interact *in vitro*. To remove the flexible regions and generate stable OutC and OutD derivatives, we performed limited proteolysis of copurified proteins. The sequences of these derivatives have been determined by the N-terminal (Edman) analysis (Fig. VI. 3). Using these data and results of copurification assay, several folded OutC and OutD derivatives were constructed and sent to our collaborators in London University for NMR and crystallization trials. In parallel, our collaborators identified a stable folded region corresponding to residues 77-172 of OutC, which gave more clear NMR signals and was used for further structural analysis. We therefore stopped further construction and analysis of the OutC and OutD derivatives by limited proteolysis. Recently, the 3D structure of HR domain of OutC (aa 77-172) and the structure of HR domain of OutC in complex with N0 subdomain of OutD (aa 28-112) have been solved by NMR (Chapter II). We largely exploited these structural data together with the structure of N-terminal domain of GspD in ETEC (Korotkov *et al.*, 2009a) to perform cysteine scanning mutagenesis and *in vivo* disulfide bonding analysis in order to map the OutC-OutD interaction sites.

In another approach, we tried to generate stable derivatives of OutC and OutD cross-linked together by an intermolecular disulfide bond. Positions suitable for such disulfide cross-linking were indicated by *in vivo* disulfide bonding analysis that has been performed in parallel (Chapter III). However, such a comprehensive *in vivo* analysis took a long time and we have started the *in vitro* cross-linking approach before the completed results of the corresponding *in vivo* analysis was available. Indeed, many technical approaches have been used with OutCV143C and OutDG190C variants in order to purify these derivatives bound by an intermolecular disulfide. However, subsequent *in vivo* assays (chapter III) showed that the corresponding disulfide bonding is poorly relevant *in vivo*. Therefore, biological significance of such a complex would be rather low. Nevertheless, multiple practical approaches employed in the course of this study could be useful in the future to generate and purify cross-linked complexes of some other protein derivatives.

Using of another couple of cysteine variants of OutC and OutD, V153C and T53C, respectively, was not successful either. In this case, homodimer of the corresponding OutD derivative was the main cross-linking product while OutC-OutD heterodimer was faintly

detectable, which compromised its further purification. A probable explanation is that an appropriate conformation and/or mutual arrangement of OutC and OutD are necessary for V153C and T53C becoming proximal enough to form a disulfide bond. Such conditions could occur within the functional T2SS but are not fulfilled when the isolated periplasmic regions of OutC and OutD are assembled *in vitro*. In any case, in the used *in vitro* conditions, T53C is mainly involved in the OutD-OutD interface and is not accessible for an interaction with V153 of OutC. These results even if negative are rather well compatible with the *in vivo* disulfide-bonding analysis (Chapter III). Indeed, the latter suggested that the OutC-OutD interactions are not formed through static interfaces, since the same sites of OutC and OutD are often involved in self-interactions with the equivalent sites of neighboring protomers (i.e., homodimerization of OutDT53C) and in an interaction with another protein partner (i.e., OutCV153C-OutDT53C complex). The *in vivo* disulfide-bonding analysis also showed that extent of OutC-OutD cross-linking was rather low in comparison with that of self-bonding of the corresponding OutC and OutD variants. This suggests that self-interactions of OutC and OutD protomers are more prevalent and could constitute initial or "basal" interactions within the secretion machine while the OutC-OutD contacts are transient and loose. Thus, the interactions representative of the "stand by" state of the system would generate more efficient cross-linking than the transient but functionally important contacts.

Recently, the interfaces between HR of GspC/OutC and N0 of GspD/OutD have been revealed both by NMR and X-ray crystallography (Chapter II and Gu *et al.*, 2012b; Korotkov *et al.*, 2011a). In these studies, isolated domains of these two proteins have been used. In the latter study, the structure of the complex has been stabilized by using specific nanobodies. Our recent *in vivo* disulfide bonding analysis suggests that the corresponding interface is functionally relevant. It should be interesting to generate corresponding derivatives of OutC and OutD carrying appropriate cysteine substitutions and probe the efficiency of their disulfide cross-linking *in vitro* and try to purify such a complex. This would allow to test a general feasibility of this approach.

General conclusions and perspectives

The enterobacterium *Dickeya dadantii* (ex. *Erwinia chrysanthemi*) causes soft-rot disease of various plants. The tissue maceration results from the degradation of the pectin of plant cell walls by pectinolytic enzymes. These pectinases are secreted by the type II secretion system, named Out. The Out system consists of 14 proteins, OutB to OutM and OutS. This thesis focuses on the functional and structural characterization of the two core components of the system OutC and OutD, and molecular analysis of the interaction between them.

The first axis of this thesis is to understand structure-function relationships between OutC and OutD and characterize their interaction sites.

In the first part (Chapter I), we used truncation analysis of OutC and OutD to map the minimal regions involved in OutC-OutD interaction. This work employed pull-down assays and mutagenesis analysis, and followed the previous study realized in the laboratory (Mr. Login, Ph.D. thesis). Together with the previous results, we showed that a 20-residue peptide named OutCsip (secretin interacting peptide, residues 139-158) interacts *in vitro* with two distinct sites of the N-terminal (periplasmic) region of OutD: one located in the N0 subdomain and another overlapping the N2-N3' subdomains. We found that two distinct regions of OutD interact either with the same site or with two partially overlapping sites located within OutCsip segment. Moreover, the binding of one interacting region (N0 of OutD) to OutCsip increases the binding of the other interacting region (N2-N3' of OutD). Conversely, the binding of N2-N3' to OutCsip reduces the binding of N0 to OutCsip. Mutagenesis analysis shows that OutCsip is critical for the function of the T2SS. A single substitution, V143S, located within OutCsip prevents its interaction with N2-N3' and fully inactivates the T2SS. The thesis of Mr. Login showed that the N0 subdomain of OutD interacts also with a second binding site within OutC located in the region proximal to the transmembrane segment. We thus suggest that successive interactions between these distinct regions of OutC and OutD may have functional importance in switching the secretion machine.

To better understand molecular mechanisms that govern OutC-OutD interactions, we performed structural analysis of OutC and of OutC-OutD interactions by NMR in collaboration with the team of Prof. Pickersgill from Queen Mary University of London (Chapter II). The solution structure showed that the HR domain of OutC adopts a β-sandwich-like fold constituted by two β-sheets, each composed of three antiparallel β-strands. The two β-sheets are connected

together through several conserved hydrophobic interactions, notably, I113-V143 couple. This has been further confirmed by *in vivo* cysteine bonding analysis. The solution structure of the complex formed by the HR domain of OutC and N0 domain of OutD suggested that the HR/N0 interface involves a pair of antiparallel β strands, β1 of HR and β3 of N0. However, *in vivo* cysteine bonding analysis detected only low amounts of the corresponding OutC-OutD complex. This suggests that N0/HR interface presumed by the NMR experiments is not biologically relevant. Alternatively, an optimal arrangement of residues or the distance adequate for disulfide formation was not achieved. Single cysteine substitution of G99 on β1 of HR, and I64 and S65 on β3 of N0 provoked homodimerization of the mutant OutC and OutD, respectively, which suggests that in the functional T2SS, neighboring HR domains of OutC and neighboring N0 domains of OutD could interact via the β1 strand and β3 strand, respectively. We further assessed by disulfide bonding analysis the mutual arrangement of N0 and N1 domains of OutD within the functional T2SS. We showed that the crystal interface suggested by the recent structural study (Korotkov *et al*., 2009) consisting of β3 of N0 and β6 of N1 is functionally relevant.

Recent crystal structure of $GspC^{HR}$-$GspD^{N0-N1}$ complex (Korotkov *et al.*, 2011b) revealed that the corresponding interface includes an antiparallel arrangement of strand β1 of $GspC^{HR}$ and strand β1 of $GspD^{N0}$. To assess its biological relevance in the functional secretion system and to probe the other putative HR/OutD interfaces suggested by the previous *in vitro* study (Login *et al*., 2010), we performed *in vivo* cysteine scanning and disulfide cross-linking analysis (Chapter III). At least three distinct GspC-GspD interactions were detected, namely 1) $\beta1^{HR}$-$\beta1^{N0}$, 2) $\beta7^{HR}$-$\beta2^{N0}$, 3) $\beta7^{HR}$- $\beta10^{N2}$. None of these interactions is formed through static interfaces since the same sites are also involved in self-interactions with equivalent neighboring domains. Disulfide self-bonding of critical interaction sites abolishes the secretion implying a transient nature of these interactions. The secretion substrate diminishes certain interactions and provokes an important rearrangement of the HR^{GspC} structure. The inner membrane components OutE/L/M differently affect various interaction sites, reinforcing ones but diminishing the others, suggesting a possible switching mechanism of their interaction in the course of secretion. Disulfide mapping shows that organization of GspD and GspC protomers is incompatible with rotational symmetry and suggests a radial symmetry of their organization within the T2SS.

The second axis of this thesis is to study the mechanism of the targeting and assembly of the secretin OutD in the outer membrane. Two auxiliary proteins, i.e., OutB and OutS are involved in this process. Firstly, we undertook structure-function analysis of OutS and OutS-OutD complex (Chapter IV). This study revealed that the OutS structure is very different from that of

the T3SS (MxiM) or T4P (PilW). The OutS structure comprises four α-helices which is the remarkable insertion of one α-helical hairpin into a second open α-helical hairpin with bent final helix. Both *in vitro* and *in vivo* results showed that the pilotin OutS binds tightly to 18 residues close to the C-terminus of the secretin causing this unstructured region to become helical on binding to the pilotin. Furthermore, our *in vivo* results showed that the pilotin OutS can also interact with the region upstream of this binding site, which is not required for targeting, but is required for the secretin function in the T2SS. These results are coherent with the data from the pilotin PulS of *K. oxytoca* that were recently published (Nickerson *et al*., 2011; Tosi *et al*., 2011).

The role of the second auxiliary protein OutB in the targeting and assembly of the secretin remains less evident. Our study (Chapter V), notably *in vitro* copurification assay showed a direct interaction between the periplasmic domain of OutB and the N0 domain of OutD. Moreover, the presence of OutB differently alters the affinity of the HR domain of OutC towards two sites of OutD, N0 and N2-N3. These data presume a complex interplay between various domains of OutD, OutC and OutB.

Thus, our results suggest the existence of two distinct interfaces between $OutD^{N0}$/$OutC^{HR}$, one involving the strand β1 of N0 and the strand β1 of HR and another including the strand β2 of N0 and the strands β6 and β7 of HR. We showed that the latter site of HR is also implicated in the interaction with the N2-N3' domains of OutD. In addition, the two mentioned sites of HR as well as several sites within the periplasmic domains of OutD are also involved in the self-interactions with an equivalent neighboring domain (in Fig. 73 panels A and B, these self-interactions are indicated by the dots of same color). These data together with the other recent research findings allow us to propose an improved model of the type II secretion system (Fig. 73C). OutC could be organized in dodecamer with C6 symmetry and neighboring protomers can interact via $\beta1^{HR}$-$\beta1^{HR}$ interface (indicated by pink dots, Fig. 73A). The OutD dodecamer could also be organized with a C6 symmetry (via $\beta2^{N0}$-$\beta2^{N0}$, $\beta10^{N2}$-$\beta10^{N2}$and $\beta11^{N2}$-$\beta11^{N2}$) (indicated by orange dots, Fig. 73B). The dodecamer of OutC surrounds the periplasmic portion of the OutD dodecamer (Fig. 73B) through twelve OutC/OutD heterodimeric interactions via the first β sheet of HR and β1 of OutD in standby state. OutC and OutD could be important for secreted proteins recognition and capture them within the large periplasmic vestibule of OutD. The presence of the secreted proteins could provoke an "inverted" orientation of the second β sheet of HR and reinforce homodimerization of OutC through this "inverted" interface (indicated by orange dots, Fig. 73A). On the other hand, the secreted proteins could diminish the self-interactions of neighboring N0 domains of OutD via $\beta2^{N0}$-$\beta2^{N0}$ but increase those through $\beta1^{N0}$-$\beta1^{N0}$ (indicated by orange and

mangeta dots, respectively, Fig. 73B). A decreasing of $\beta1^{HR}$-$\beta1^{HR}$ self-contact

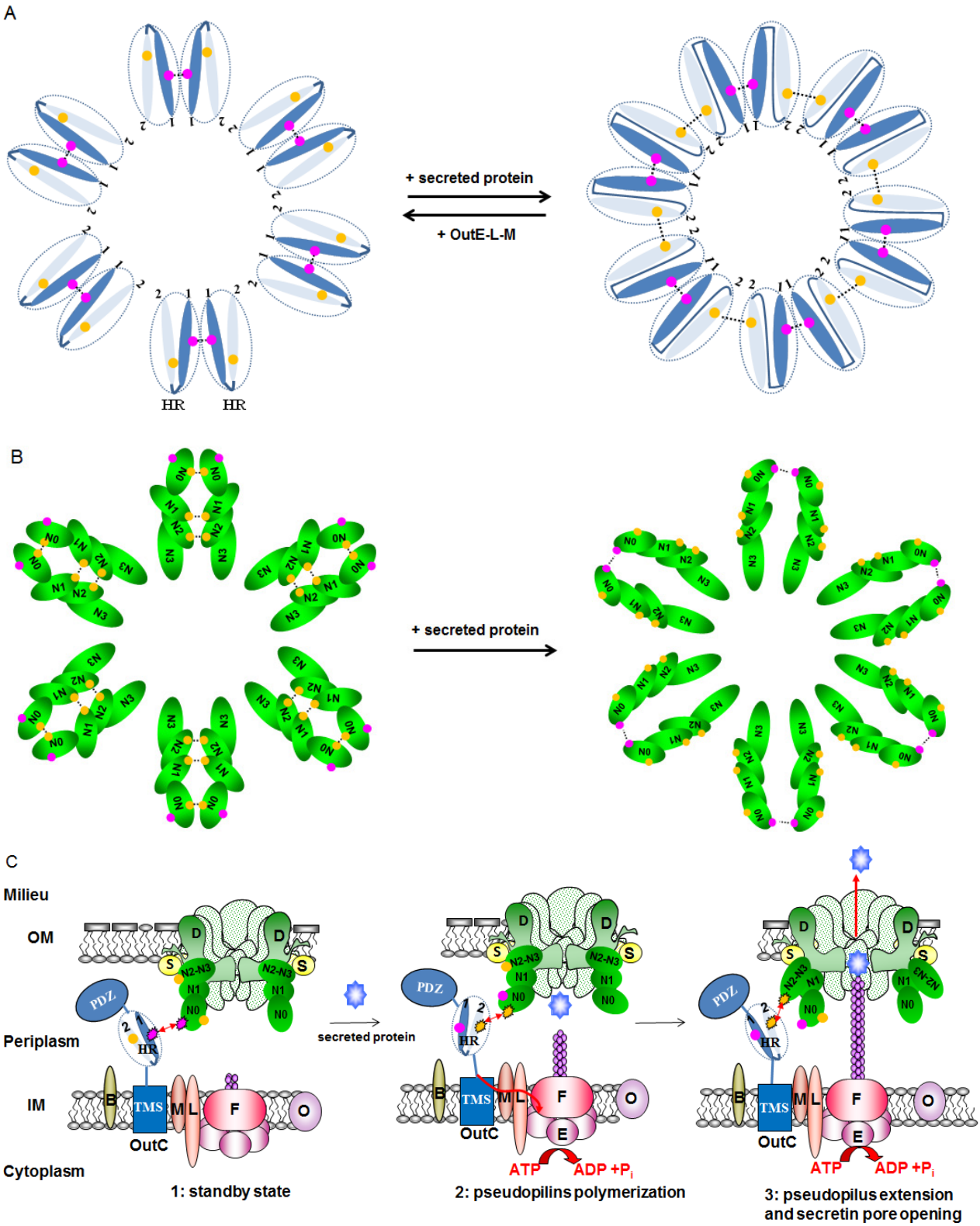

Fig. 73: Proposed models. (A) A model of a dodecameric ring with C6 symmetry formed by HR domains of OutC. The HR domain comprises two β-sheets which are represented by dark blue indicated 1 consisting of β1, β2 and β3, and light blue indicated 2 consisting of β5, β6 and β7, respectively. The two distinct sites involving in homodimerization are represented by orange and magenta dots. The homodimerization of HR the first β-

sheet (left) (magenta dots) may correspond to the standby state of the T2SS. The presence of the secreted protein reinforces homodimerization of OutC through an "inverted" interface (orange dots) formed by the second β-sheet (right) while the IM components OutE-L-M produced an opposite effect. (B) A model of a dodecameric ring of the periplasmic region of OutD with C6 symmetry. The sites involved in homodimerization are represented by dots. Two distinct self-interacting sites of N0 are indicated by orange and magenta dots. The presence of the secreted protein provokes the rearrangement of OutD protomers within dodecameric complex. (C) Model of *D. dadantii* Out secreton. For better simplicity, only the interactions between one molecule of OutC and OutD are shown. The successive interactions between distinct sites of the periplasmic regions of OutC and OutD may correspond to different step in the course of secretion. The same colors as in pannels A and B are used to show the sites in HR, N0 and N2 involved in both homo- and hetero-interaction s (A, B and C).

between neighboring HR domains (Fig. 73A right panel) could constitute a signal that would be transferred via the interactions of OutC with the inner membrane components OutM and OutL, and finally to the ATPase OutE and stimulates the hydrolysis of ATP to provide energy for polymerization of pseudopilins. The extension of pseudopilus could act as piston to push exoprotein through the secretin pore. Simultaneously, the interaction between OutC and OutL-M induce the conformation change of OutC which reinforces homodimerization of OutC via $\beta1^{HR}$-$\beta1^{HR}$ interface and weakens the affinity of $\beta1^{HR}$ to $\beta1^{N0}$ while increase the affinity of $\beta7^{HR}$ to $\beta2^{N0}$ (Fig. 73C, middle panel). Then, (by yet unknown mechanism) the latter interaction between HR and N0 (via $\beta7^{HR}$-$\beta2^{N0}$) would be replaced by the interaction of HR with the other interaction site located in N2-N3' ($\beta7^{HR}$-$\beta10^{N2}$) (Fig. 73C, right panel). This interaction could trigger a conformation change in the secretin that causes opening of the periplasmic gate. Upon opening of the secretin pore, the extending pseudopilus may push the exoprotein through the opened gate and serve as a plug to prevent channel leakage. How the GspD periplasmic gate closes, and the pseudopilus retracts and/or disassembles to reset the system remain to be elucidated. Understanding of this mechanism requires elucidating of the functions and interactions of other components of the secretion system.

To give a perspective of this work, the following studies should be performed. These studies will allow to a better understand of the assembly and mechanism of the T2SS.

i) The exact function of OutB should be elucidated. Our results (Chapter V) showed that the periplasmic domain of OutB ($OutB_{112-220}$) interacts with N0 domain of OutD. Cysteine cross-linking analysis indicates that the two distinct sites of N0, i.e., located at strands β1 (F34C) and β2 (T53C), respectively are involved in interaction with strands β1 (G99C) and β7 (153C) of HR, respectively (Chapter III). We have showed that the presence of OutB increases the formation of cross-linked complexes between

OutC V153C (strand β7 of HR) and OutD T53C (strand β2 of N0), indicating a certain cooperation between OutB/N0 and the latter HR/N0 interaction. The effect of OutB on another HR/N0 interacting site including of β1 of HR and β1 of N0 should be examined and the affinity of HR of OutC and OutB to N0 of OutD should be compared using copurification (pull-down) assay. We also showed that OutB decreases the interaction between V144C (β6) of HR and V271C (β12) of N3. Although no data indicates the interaction between OutC and OutB, we cannot exclude the possibility that OutB and N3 of OutD compete for binding to the same site of HR domain of OutC. To probe this idea, a direct interaction between OutB and OutC should be examined. The structure determination of the periplasmic domain of OutB (either by NMR or X-ray crystallography) is in progress in collaboration with the team of Prof. Pickersgill from Queen Mary University of London. This work will allow to confirm the interaction between the periplasmic domain of OutB and N0 domain of OutD and reveal the molecular mechanism of this interaction.

ii) The precise interaction sites between secreted protein and OutC and OutD, respectively, should be determined. Our results showed that the presence of secreted protein differently alters homodimerization via various sites of the periplasmic regions of OutC and OutD and affects the interaction between OutC and OutD. To explain the latter phenomenon, we firstly suggested that the interaction between a secreted protein and the PDZ domain of OutC changes the conformation of HR that weakens the affinity of OutC to OutD. However, a secreted protein CelZ, whose secretion is PDZ independent, gives the same effect on the interactions between OutC and OutD as PelB. Thus, the secreted protein may probably interact with some other region(s) of OutC or/and OutD. To map the precise interaction regions, multiple complementary approaches could be employed: a) NMR experiments to study *in vitro* interactions between various domains of OutC and OutD and the secreted protein. Most of these protein derivatives suitable for such type of study have been constructed in the course of this thesis; b) experiments employing bacterial two-hybrid assay to study equivalent interactions between various OutC, OutD domains and secreted proteins *in vivo*; c) another approach using site directed *in vivo* photo-cross linking. Indeed, the two latter approaches are currently exploited in the laboratory.

iii) The interaction between OutD and the IM components OutL and OutM should be examined. Our results showed that the presence of OutE-L-M differently alters the

cross-linking patterns of various OutC-OutD interacting sites. These effects may be due to the direct interaction between OutC and OutL-M, Indeed, we showed a strong effect of OutE-L-M on OutC homodimerization, indicating an interaction between them. However, we could not exclude that these effect may also due to the direct interactions between OutD and OutL-M. Indeed, the thesis of Mr. Login showed that the periplasmic domain of OutM interacts with the periplasmic domain of OutD (Login, Ph.D. thesis).

iv) The precise stoichiometry of Out proteins should be determined. The actual representation of the T2SS suggests that the secretin GspD could form a dodecameric ring in the OM. The secretion ATPase GspE is suggested to be a hexamer and associates with the T2SS through forming a 1:1 complex with the cytoplasmic domain of GspL, which indicates a hexameric arrangement of GspL. The relative *in vivo* stoichiometry between pseudopilins has been estimated to be 16 (GspG):1(GspH):1(GspI):4(GspJ). The stoichiometry of the other T2SS components remains unknown. Although we proposed that OutC and OutD could form a 1:1 complex in the functional T2SS, we cannot exclude the other possibility, e.g., 1:2 or 2:1 ratio between OutC and OutD. To determine the stoichiometry of OutC and OutD, we could use immunodetection to estimate the relative amount of these proteins within the functional T2SS. The purified OutC and OutD proteins could be used as control to determine the concentration of these proteins in *D. dadantii* cells. Fluorescence fluctuation spectroscopy could be also used to quantify the stoichiometry of protein complexes in living cells via analysis of brightness. The brightness provides a spectroscopic marker for observing protein interactions and their stoichiometry directly inside cells.

References

Aas, F.E., Winther-Larsen, H.C., Wolfgang, M., Frye, S., Løvold, C., Roos, N. *et al. (2007)* Substitutions in the N-terminal alpha helical spine of *Neisseria gonorrhoeae* pilin affect type IV pilus assembly, dynamics and associated functions. *Mol Microbiol*. **63:** 69-85.

Abbott, D.W. and Boraston, A.B. (2008) Structural biology of pectin degradation by Enterobacteriaceae. *Microbiol Mol Biol Rev* **72:** 301-16.

Abendroth, J., Bagdasarian, M., Sandkvist, M. and Hol, W.G.J. (2004a) The structure of the cytoplasmic domain of EpsL, an inner membrane component of the type II secretion system of *Vibrio cholerae*: an unusual member of the actin-like ATPase superfamily. *J Mol Biol* **344:** 619-33.

Abendroth, J., Rice, A.E., McLuskey, K., Bagdasarian, M. and Hol, W.G.J. (2004b) The crystal structure of the periplasmic domain of the type II secretion system protein EpsM from *Vibrio cholerae*: the simplest version of the ferredoxin fold. *J Mol Biol* **338:** 585-96.

Abendroth, J., Murphy, P., Sandkvist, M., Bagdasarian, M. and Hol, W.G.J. (2005) The X-ray structure of the type II secretion system complex formed by the N-terminal domain of EpsE and the cytoplasmic domain of EpsL of *Vibrio cholerae*. *J Mol Biol* **348:** 845-55.

Abendroth, J., Mitchell, D.D., Korotkov, K.V., Johnson, T.L., Kreger, A., Sandkvist, M. *et al.* (2009a) The three-dimensional structure of the cytoplasmic domains of EpsF from the type 2 secretion system of *Vibrio cholerae*. *J Struct Biol* **166:** 303-15.

Abendroth, J., Kreger, A. C. and Hol, W.G.J. (2009b) The dimer formed by the periplasmic domain of EpsL from the Type 2 Secretion System of *Vibrio parahaemolyticus*. *J Struct Biol* **168:** 313-22.

Akama, H., Matsuura, T., Kashiwagi, S., Yoneyama, H., Narita, S., Tsukihara, T. *et al.* (2004) Crystal structure of the membrane fusion protein, MexA, of the multidrug transporter in *Pseudomonas aeruginosa*. *J Biol Chem* **279:** 25939-42.

Alami, M., Lüke, I., Deitermann, S., Eisner, G., Koch, H.G., Brunner, J. *et al.* (2003) Differential interactions between a twin-arginine signal peptide and its translocase in *Escherichia coli*. *Mol Cell* **12:** 937-46.

Alphonse, S., Durand, E., Douzi, B., Waegele, B., Darbon, H., Filloux, A. *et al.* (2010) Structure of the *Pseudomonas aeruginosa* XcpT pseudopilin, a major component of the type II secretion system. *J Struct Biol* **169:** 75-80.

Alvarez-Martinez, C.E. and Christie, P.J. (2009) Biological diversity of prokaryotic type IV secretion system. *Microbiol Mol Biol Rev* **73:** 775-808.

Aly, K.A. and Baron, C. (2007) The VirB5 protein localizes to the T-pilus tips in *Agrobacterium tumefaciens*. Microbiology **153:** 3766-3775.

Andersen, C., Koronakis, E., Bokma, E., Eswaran, J., Humphreys, D., Hughes, C. *et al.* (2002) Transition to the open state of the TolC periplasmic tunnel entrance. *Proc Natl Acad Sci USA* **99:** 11103-8.

Angelini, S., Boy, D., Schiltz, E. and Koch, H.G. (2006) Membrane binding of the bacterial signal recognition particle receptor involves two distinct binding sites. *J Cell Biol* **174:** 715-24.

Anwari, K., Poggio, S., Perry, A., Gatsos, X., Ramarathinam, S.H., Williamson, N.A. *et al.* (2010) A modular BAM complex in the outer membrane of the alpha-proteobacterium *PLoS One*. **5:** 1-8 (e8619).

Arechaga, I., Pena, A., Zunzunegui, S., del Carmen Fernandez-Alonso, M., Rivas, G. and de la Cruz, F. (2008) ATPase activity and oligomeric state of TrwK, the VirB4 homologue of the plasmid R388 type IV secretion system. *J Bacteriol* **190:** 5472-9.

Arnold, R., Jehl, A. and Rattei, T. (2010) Targeting effectors: the molecular recognition of Type III secreted proteins. *Microbes Infect* **12:** 346-58.

Arts, J., de Groot, A., Ball, G., Durand, E., Khattabi, M.E., Filloux, A. *et al.* (2007) Interaction domains in the *Pseudomonas aeruginosa* type II secretory apparatus component XcpS (GspF). *Microbiology* **153:** 1582-1592.

Aschtgen, M.S., Bernard, C.S., De Bentzmann, S., Lloubes, R. and Cascales, E. (2008) SciN is an outer membrane lipoprotein required for type VI secretion in enteroaggregative. *Escherichia coli*. *J Bacteriol* **190:** 7523-7531.

Ast, V.M., Schoenhofen, I.C., Langen, G.R., Stratilo, C.W., Chamberlain, M.D. and Howard, S.P. (2002) Expression of the ExeAB complex of *Aeromonas hydrophila* is required for the localization and assembly of the ExeD secretion port multimer. *Mol Microbiol* **44:** 217-31.

Ayers, M., Sampaleanu, L.M., Tammam, S., Koo, J., Harvey, H., Howell, P.L. *et al.* (2009) PilM/N/O/P proteins form an inner membrane complex that affects the stability of the *Pseudomonas aeruginosa* type IV pilus secretin. *J Mol Biol* **394:** 128-42.

Ayers, M., Howell, P.L. and Burrows, L.L. (2010) Architecture of the type II secretion and type IV pilus machineries. *Future Microbiol* **5:** 1203-18.

Balasingham, S.V., Collins, R.F., Assalkhou, R., Homberset, H., Frye, S.A., Derrick, J.P. *et al.* (2007) Interactions between the lipoprotein PilP and the secretin PilQ in *Neisseria meningitidis*. *J Bacteriol* **189**: 5716-27.

Banta, L.M., Kerr, J.E., Cascales, E., Giuliano, M.E., Bailey, M.E., McKay, C. *et al.* (2011) An *Agrobacterium* VirB10 mutation conferring a type IV secretion system gating defect. *J Bacteriol* **193:** 2566-74.

Baud, C., Hodak, H., Willery, E., Drobecq, H., Locht, C., Jamin, M. *et al.* (2009) Role of DegP for two-partner secretion in *Bordetella*. *Mol Microbiol* **74:** 315-29.

Bechtluft, P., van Leeuwen, R.G., Tyreman, M., Tomkiewicz, D., Nouwen, N., Tepper, H.L., Driessen, A.J. *et al.* (2007) Direct observation of chaperone-induced changes in a protein folding pathway. *Science* **318:** 1458-61.

Behrendt, J., Lindenstrauss, U. and Brüser, T. (2007) The TatBC complex formation suppresses a modular TatB-multimerization in *Escherichia coli*. **581:** 4085-90.

Berks, B.C., Palmer, T. and Sargent, F. (2005) Protein targeting by the bacterial twin-arginine translocation (Tat) pathway. *Curr Opin Microbiol* **8:** 174-181.

Bitter, W., Koster, M., Latijnhouwers, M., de Cock, H. and Tommassen, J. (1998) Formation of oligomeric rings by XcpQ and PilQ, which are involved in protein transport across the outer membrane of *Pseudomonas aeruginosa*. *Mol Microbiol* **27:** 209-19.

Bingle, L.E., Bailey, C.M. and Pallen, M.J. (2008) Type VI secretion: a beginner's guide. *Curr Opin Microbiol* **11:** 3-8.

Blaylock, B., Sorg, J.A. and Schneewind, O. (2008) *Yersinia enterocolitica* type III secretion of YopR requires a structure in its mRNA. *Mol Microbiol* **70:** 1210-22.

Bleves, S., Voulhoux, R., Michel, G., Lazdunski, A., Tommassen, J. and Filloux, A. (1998) The secretion apparatus of *Pseudomonas aeruginosa*: identification of a fifth pseudopilin, XcpX (GspK family). *Mol Microbiol* **27:** 31-40.

Bleves, S., Gérard-Vincent, M., Lazdunski, A. and Filloux, A. (1999) Structure-function analysis of XcpP, a component involved in general secretory pathway-dependent protein secretion in Pseudomonas aeruginosa. *J Bacteriol* **181:** 4012-9.

Bleves, S, Viarre, V., Salacha, R., Michel, G.P., Filloux, A. and Voulhoux, R. (2010) Protein secretion systems in *Pseudomonas aeruginosa*: A wealth of pathogenic weapons. *Int J Med Microbiol* **300:** 534-43.

Blight, M.A. and Holland, I.B. (1994) Heterologous protein secretion and the versatile *Escherichia coli* haemolysin translocator. *Trends Biotechnol* **12:** 450-5.

Blocker, A., Jouihri, N., Larquet, E., Gounon, P., Ebel, F., Parsot, C. *et al.* (2001) Structure and composition of the *Shigella flexneri* 'needle complex', a part of its type III secreton. *Mol Microbiol* **39:** 652-33.

Blocker, A., Komoriya, K. and Aizawa, S. (2003) Type III secretion systems and bacterial flagella: insights into their function from structural similarities. *Proc Natl Acad Sci USA* **100:** 3027-30.

Blot, N., Berrier, C., Hugouvieux-Cotte-Pattat, N., Ghazi, A. and Condemine, G. (2002) The oligogalacturonate-specific porin KdgM of *Erwinia chrysanthemi* belongs to a new porin family. *J Biol Chem* **277:** 7936-44.

Bolwell, G.P. and Wojtaszek, P. (1997) Mechanisms for the generation of reactive oxygen species in plant defence-a broad perspective. *Physiol Mol Plant Pathol* **51:** 347-366.

Bos, MP., Robert, V. and Tommassen, J. (2007) Functioning of outer membrane protein assembly factor Omp85 requires a single POTRA domain. *EMBO Rep* **8:** 1149-54.

Bönemann, G., Pietrosiuk, A., Diemand, A., Zentgraf, H. and Mogk, A. (2009) Remodelling of VipA/VipB tubules by ClpV-mediated threading is crucial for type VI protein secretion. *EMBO J* **28:** 315-25.

Bönemann, G., Pietrosiuk, A. and Mogk, A. (2010) Tubules and donuts: a type VI secretion story. *Mol Microbiol* **76:** 815-21.

Bortoli-German, I., Brun, E., Py, B., Chippaux, M. and Barras, F. (1994) Periplasmic disulphide bond formation is essential for cellulase secretion by the plant pathogen *Erwinia chrysanthemi*. *Mol Microbiol* **11:** 545-53.

Bose, N., Payne, S.M. and Taylor, R.K. (2002) Type 4 pilus biogenesis and type II-mediated protein secretion by *Vibrio cholerae* occur independently of the TonB-facilitated proton motive force. *J Bacteriol* **184:** 2305-9.

Bose, N. and Taylor, R.K. (2005) Identification of a TcpC-TcpQ outer membrane complex involved in the biogenesis of the toxin-coregulated pilus of Vibrio cholerae. *J. Bacteriol* **187:** 2225-32.

Bouley, J., Condemine, G. and Shevchik, V. E. (2001) The PDZ domain of OutC and the N-terminal region of OutD determine the secretion specificity of the type II out pathway of *Erwinia chrysanthemi*. *J Mol Biol* **308:** 205-19.

Boyer, M.H., Cami, B., Chambost, J.P., Magnan, M. and Cattanéo, J. (1987) Characterization of a new endoglucanase from *Erwinia chrysanthemi*. *Eur J Biochem* **162:** 311-6.

Boyer, F., Fichant, G., Berthod, J., Vandenbrouck, Y. and Attree, I. (2009) Dissecting the bacterial type VI secretion system by a genome wide in silico analysis: what can be learned from available microbial genomic resources? *BMC Genomics* **10:** 1-14.

Brenman, J.E., Christopherson, K.S., Craven, S.E., McGee, A.W. and Bredt, D.S. (1996) Cloning and characterization of postsynaptic density 93, a nitric oxide synthase interacting protein. *J Neurosci* **16:** 7407-15.

Breukink, K., Kusters, R. and De Kruijff, B. (1992) In vitro studies on the folding characteristics of the *Escherichia coli* precursor protein prePhoE. Evidence that SecB prevents the precursor from aggregating by forming a functional complex. *Eur J Biochem* **208:** 419-25.

Brillet, K., Journet, L., Célia, H., Paulus, L., Stahl, A., Pattus, F. *et al.* (2007) A beta strand lock exchange for signal transduction in TonB-dependent transducers on the basis of a common structural motif. *Structure* **15:** 1383-91.

Buddelmeijer, N., Francetic, O. and Pugsley, A.P. (2006) Green fluorescent chimeras indicate nonpolar localization of pullulanase secreton components PulL and PulM. *J Bacteriol* **188:** 2928-35.

Buddelmeijer, N., Krehenbrink, M., Pecorari, F. and Pugsley, A. P. (2009) Type II secretion system secretin PulD localizes in clusters in the Escherichia coli outer membrane. *J Bacteriol* **191:** 161-8.

Burghout, P., Beckers, F., de Wit, E., van Boxtel, R., Cornelis, G.R., Tommassen, J. *et al.* (2004a) Role of the pilot protein YscW in the biogenesis of the YscC secretin in *Yersinia enterocolitica*. *J Bacteriol* **186:** 5366-75.

Burghout, P., van Boxtel, R., Van Gelder, P., Ringler, P., Müller, S.A., Tommassen, J. *et al.* (2004b) Structure and electrophysiological properties of the YscC secretin from the type III secretion system of *Yersinia enterocolitica*. *J Bacteriol* **186:** 4645-54.

Burkhard, P., Stetefeld, J. and Strelkov S.V. (2001) Coiled coils: a highly versatile protein folding motif. *Trends Cell Biol* **11:** 82-8.

Burkholder, W.H., MacFadden, L.H. and Dimock, A.H. (1953) A bacterial blight of chrysanthemums. *Phytopathology* **43:** 522-5.

Burkhardt, J., Vonck, J. and Averhoff, B. (2011) Structure and function of PilQ, a secretin of the DNA transporter from the thermophilic bacterium *Thermus thermophilus HB27*. *J Biol Chem* **286:** 9977-84.

Caffall, K.H. and Mohnen, D. (2009) The structure, function and biosynthesis of plant cell wall pectic polysaccharides. *Carbohydr Res* **344:** 1879-900.

Camberg, J.L., Johnson, T.L., Patrick, M., Abendroth, J., Hol, W.G.J. and Sandkvist, M. (2007) Synergistic stimulation of EpsE ATP hydrolysis by EpsL and acidic phospholipids. *EMBO J* **26:** 19-27.

Campos, M., Nilges, M., Cisneros, D. A. and Francetic, O. (2010) Detailed structural and assembly model of the type II secretion pilus from sparse data. *Proc Natl Acad Sci USA* **107:** 13081-6.

Campos, M., Francetic, O. and Nilges, M. (2011) Modeling pilus structures from sparse data. *J Struct Biol* **173:** 436-44.

Carbonnelle, E., Hélaine, S., Prouvensier, L., Nassif, X. and Pelicic, V. (2005) Type IV pilus biogenesis in Neisseria meningitidis: PilW is involved in a step occurring after pilus assembly, essential for fibre stability and function. *Mol Microbiol* **55:** 54-64.

Cascales, E. and Christie, P.J. (2004) Definition of a bacterial type IV secretion pathway for a DNA substrate. *Science*, **304:** 1170-3.

Cascales, E. (2008) The type VI secretion toolkit. *EMBO Rep* **9:** 735-41.

Cescau, S., Debarbieux, L. and Wandersman, C. (2007) Probing the in vivo dynamics of type I protein secretion complex association through sensitivity to detergents. *J Bacteriol* **189:**1496-504.

Chami, M., Guilvout, I., Gregorini, M., Rémigy, H. W., Müller, S.A., Valerio, M. et al (2005) Structural insights into the secretin PulD and its trypsin-resistant core. *J Biol Chem* **280:** 37732-41.

Chandran, V., Fronzes, R., Duquerrory, S., Cronin, N., Navaza, J. and Waksman, G. (2009) Structure of the outer membrane complex of a type IV secretion system. *Nature* **462:** 1011-5.

Chapon, V., Simpson, H.D., Morelli, X., Brun, E. and Barras, F. (2000) Alteration of a single tryptophan residue of the cellulose-binding domain blocks secretion of the *Erwinia chrysanthemi* Cel5 cellulase (ex-EGZ) via the type II system. *J Mol Biol* **303:** 117-23.

Chapon, V., Czjzek, M., EI Hassouni, M., Py, B., Juy, M. and Barras, F. (2001) Type II protein secretion in gram-negative pathogenic bacteria: the study of the structure/secretion relationships of the cellulase Cel5 (formerly EGZ) from *Erwinia chrysanthemi*. *J Mol Biol* **310:** 1055-66.

Chen, Y., Shiue, S.J., Huang, C.W., Chang, J.L., Chien, Y.L., Hu, N.T. *et al.* (2005) Structure and function of the XpsE N-terminal domain, an essential component of the Xanthomonas campestris type II secretion system. *J Biol Chem* **280:** 42356-63.

Chevalier, N., Moser, M., Koch, H.G., Schimz, K.L., Willery, E., Locht, C. *et al.* (2004) Membrane targeting of a bacterial virulence factor harbouring an extended signal peptide. *J Mol Microbiol Biotechnol* **8:** 7-

18.
Chiang, P., Habash, M. and Burrows, L.L. (2005) Disparate subcellular localization patterns of *Pseudomonas aeruginosa* Type IV pilus ATPase involved in twitching motility. *J Bacteriol* **187:** 829-39.
Christie, P.J., Atmakuri, K., Krishnamoorthy, V., Jakubowski, S. and Cascales, E. (2005) Biogenesis, architecture and function of bacterial type IV secretion systems. *Annu Rev Microbiol* **59:** 451-85.
Cianciotto, N.P. (2005) Type II secretion: a protein secretion system for all seasons. *Trends Microbiol* **13:** 581-8.
Clantin, B., Hodak, H., Willery, E., Locht, C., Jacob-Dubuisson, F. and Villeret, V. (2004) The crystal structure of filamentous hemagglutinin secretion domain and its implications for the two-partner secretion pathway. *Proc Natl Acad Sci USA* **101:** 6194-9.
Clantin, B., Delattre, A.S., Rucktooa, P., Saint, N., Meli, A.C., Locht, C. *et al.* (2007) Structure of the membrane protein FhaC: a membrane of the Omp85-TpsB transporter superfamily. *Science* **317:** 957-61.
Collins, R.F., Davidsen, L., Derrick, J.P., Ford, R.C. and Tønjum, T. (2001) Analysis of the PilQ secretin from *Neisseria meningitidis* by transmission electron microscopy reveals a dodecameric quaternary structure. *J Bacteriol* **183:** 3825-32.
Collins, R.F., Ford, R.C., Kitmitto, A., Olsen, R.O., Tønjum, T. and Derrick, J.P. (2003) Three-dimensional structure of the *Neisseria meningitidis* secretin PilQ determined from negative-stain transmission electron microscopy. *J Bacteriol* **185:** 2611-7.
Collins, R.F., Frye, S.A., Kitmitto, A., Ford, R.C., Tønjum, T. and Derrick, J.P. (2004) Structure of the *Neisseria meningitidis* outer membrane PilQ secretin complex at 12 Å resolution. *J Biol Chem* **279:** 39750-6.
Collin, S., Guilvout, I., Chami, M. and Pugsley, A.P. (2007) YaeT-independent multimerization and outer membrane association of secretin PulD. *Mol Microbiol* **64:** 1350-1357.
Collin, S., Guilvout, I., Nickerson, N.N. and Pugsley, A.P. (2011) Sorting of an integral outer membrane protein via the lipoprotein-specific Lol pathway and a dedicated lipoprotein pilotin. *Mol Microbiol* **80:** 655-65.
Condemine, G., Dorel, C., Cotte-Pattat, N. H. and Robert-Baudouy, J. (1992) Some of the out genes involved in the secretion of pectate lyases in *Erwinia chrysanthemi* are regulated by kdgR. *Mol Microbiol* **6:** 3199-3211.
Condemine, G. and Shevchik, V.E. (2000) Overproduction of the secretin OutD suppresses the secretion defect of an *Erwinia chrysanthemi* OutB mutant. *Microbiology* **146:** 639-47.
Condemine, G. and Ghazi, A. (2007) Differential regulation of two oligogalacturonate outer membrane channels, KdgN and KdgM, of *Dickeya dadantii* (*Erwinia chrysanthemi*). *J Bacteriol* **189:** 5955-5962.
Cornelis, G.R. (2006) The type III secretion injectisome. *Nat Rev Microbiol* **4:** 811-25.
Cotter, S.E., Surana, N.K. and St Geme, J.W.R. (2005) Trimeric autotransporters: a distinct subfamily of autotransporter proteins. *Trends Microbiol* **13:** 199-205.
Craig, L., Pique, M.E. and Tainer, J.A. (2004) Type IV pilus structure and bacterial pathogenicity. *Nat Rev Microbiol* **2:** 363-78.
Craig, L., Volkmann, N., Arvai, A. S., Pique, M. E., Yeager, M., Egelman, E.H. *et al.* (2006) Type IV pilus structure by cryo-electron microscopy and crystallography: implications for pilus assembly and functions. *Mol Cell* **23:** 651-62.
Craig, L. and Li, J. (2008) Type IV pili: paradoxes in form and function. *Curr Opin Struct Biol* **18:** 267-77.
Crane, J.M., Suo, Y., Lilly, A.A., Mao, C., Hubbell, W.L. and Randall, L.L. (2006) Sites of interaction of a precursor polypeptide on the export chaperone SecB mapped by site-directed spin labeling. *J Mol Biol* **363:** 63-74.
Creze, C., Castang, S., Derivery, E., Haser, R., Hugouvieux-Cotte-Pattat, N., Shevchik, V.E. and Gouet, P. (2008) The crystal structure of pectate lyase peli from soft rot pathogen *Erwinia chrysanthemi* in complex with its substrate. *J Biol Chem* **283:** 18260-8.
Dabney-Smith, C., Mori, H. and Cline, K. (2006) Oligomers of Tha4 organize at the thylakoid Tat translocase during protein transport. *J Biol Chem* **281:** 5476-83.
Dacheux, D., Goure, J., Chabert, J., Usson, Y. and Attree, I. (2001) Pore-forming activity of type III system-secreted proteins leads to oncosis of *Pseudomonas aeruginosa*-infected macrophages. *Mol Microbiol* **40:** 76-85.
Dalbey, R.E., Wang, P. and Kuhn, A. (2011) Assembly of bacterial inner membrane proteins. *Annu Rev Biochem* **80:** 167-81.
Daniel, R.A., Noirot-Gros, M.F., Noirot, P. and Errington, J. (2006) Multiple interactions between the transmembrane division proteins of Bacillus subtilis and the role of FtsL instability in divisome assembly. *J Bacteriol* **188**: 7396-404.
Dautin, N. and Bernstein, H.D. (2007) Protein secretion in gram-negative bacteria via the autotransporter pathway. *Annu Rev Microbiol* **61:** 89-112.

Deane, J.E., Roversi, P., Cordes, F.S., Johnson, S., Kenjale, R., Daniell, S. *et al.* (2006) Molecular model of a type III secretion system needle: impliactions for host-cell sensing. *Pro Natl Acad Sci USA* **103:** 12529-33.

DebRoy, S., Thilmony, R., Kwack, Y.B., Nomura, K. and He, S.Y. (2004) A family of conserved bacterial effectors inhibits salicylic acid-mediated basal immunity and promotes disease necrosis in plants. *Proc Natl Acad Sci USA* **101:** 9927-32.

de Gier, J.W., Valent, Q.A., Von Heijine, G. and Luirink, J. (1997) The E. coli SRP: preferences of a targeting factor. *FEBS Lett* **408:** 1-4.

de Groot, A., Filloux, A. and Tommassen, J. (1991) Conservation of xcp genes, involved in the two-step protein secretion process, in different Pseudomonas species and other gram-negative bacteria. *Mol Gen Genet* **229:** 278-84.

de Groot, A., Koster, M., Gérard-Vincent, M., Gerritse, G., Lazdunski, A., Tommassen, J. *et al.* (2001) Exchange of Xcp (Gsp) secretion machineries between Pseudomonas aeruginosa and Pseudomonas alcaligenes: species specificity unrelated to substrate recognition. *J Bacteriol* **183:** 959-967.

de Keyzer, J., van der Does, C. and Driessen, A.J. (2003) The bacterial translocase: a dynamic protein channel complex. *Cell Mol Life Sci* **60:** 2034-52.

Delattre, A.S., Saint, N., Clantin, B., Willery, E., Lippens, G., Locht, C. *et al.* (2011) Substrate recognition by the POTRA domains of TpsB transporter FhaC. *Mol Microbiol* **81:** 99-112.

Delepelaire, P. and Wandersman, C. (1990) Protein secretion in gram-negative bacteria. The extracellular metalloprotease B from *Erwinia chrysanthemi* contains a C-terminal secretion signal analogous to that of *Escherichia coli* alpha-hemolysin. *J Biol Chem* **265:**17118-25.

Delepelaire, P. (2004) Type I secretion in gram-negative bacteria. *Biochim Biophys Acta* **1694:** 149-61.

Demchick, P. and Koch, A.L. (1996) The permeability of the wall fabric of Escherichia coli and Bacillus subtilis. *J Bacteriol* **178:** 768-73.

D'Enfert, C., Ryter, A. and Pugsley, A.P. (1987) Cloning and expression in *Escherichia coli* of the *Klebsiella pneumoniae* genes for production, surface localization and secrtion of the lipoprotein pullulanase. *EMBO* J **14:** 157-60.

Desvaux, M., Parham, N.J. and Henderson, I.R. (2004) Type V protein secretion: simplicity gone awry? *Curr Issues Mol Biol* **6:** 111-24.

Desvaux, M., Hébraud, M., Talon, R. and Henderson, I. R. (2009) Secretion and subcellular localizations of bacterial proteins: a semantic awareness issue. *Trends Microbiol* **17:** 139-45.

Dev, I.K. and Ray, P.H. (1984) Rapid assay and purification of a unique signal peptidase that processes the prolipoprotein from *Escherichia coli* B. *J Biol Chem* **259:** 11114-20.

Diepold, A., Amstutz, M., Abel, S., Sorg, I., Jenal, U. and Cornelis, G.R. (2010) Deciphering the assembly of the Yersinia type III secretion injectisome. *EMBO J* **29:** 1928-40.

Doerrler, W.T. and Raetz, C.R. (2005) Loss of outer membrane proteins without inhibition of lipid export in an *Escherichia coli* YaeT mutant. *J Biol Chem* **280:** 27679-87.

Douet, V., Loiseau, L., Barras, F. and Py, B. (2004) Systematic analysis, by the yeast two-hybrid, of protein interaction between components of the type II secretory machinery of *Erwinia chrysanthemi*. *Res Microbiol* **155:** 71-5.

Douzi, B., Durand, E., Bernard, C., Alphonse, S., Cambillau, C., Filloux, A., Tegoni, M. and Voulhoux, R. (2009) The XcpV/GspI pseudopilin has a central role in the assembly of a quaternary complex within the T2SS pseudopilus. *J Biol Chem* **284:** 34580-89.

Drake, S.L., Sandstedt, S.A. and Koomey, M. (1997) PilP, a pilus biogenesis lipoprotein in *Neisseria gonorrhoeae*, affects expression of PilQ as a high-molecular-mass multimer. *Mol Microbiol* **23:** 657-68.

Driessen, A.J. and Nouwen, N. (2008) Protein translocation across the bacterial cytoplasmic membrane. *Annu Rev Biochem* **77:** 643-67.

du Plessis, D.J., Nouwen, N. and Driessen, A.J. (2011) The Sec translocase. *Biochim Biophys Acta*. **1808:** 851-65.

Durand, E., Bernadac, A., Ball, G., Lazdunski, A., Sturgis, J. N. and Filloux, A. (2003) Type II protein secretion in *Pseudomonas aeruginosa*: the pseudopilus is a multifibrillar and adhesive structure. *J Bacteriol* **185:** 2749-58.

Durand, E., Michel, G., Voulhoux, R., Kürner, J., Bernadac, A. and Filloux, A. (2005) XcpX controls biogenesis of the *Pseudomonas aeruginosa* XcpT-containing pseudopilus. *J Biol Chem* **280:** 31378-89.

Durand, E., Verger, D., Toste Rêgo, A., Chandran, V., Meng, G., Fronzes, R. *et al.* (2009) Structural biology of bacterial secretion systems in Gram-negative pathogens-potential for new drug targets. *Infect Disord Drug Targets* **9:** 518-47.

Durand, E., Oomen, C. and Waksman, G. (2010) Biochemical dissection of the ATPase TraB, the VirB4 homologue of the *Escherichia coli* pKM101 conjugation machinery. *J Bacteriol* **192:** 2315-23.

Durand, E., Alphonse, S., Brochier-Armanet, C., Ball, G., Douzi, B., Filloux, A. *et al.* (2011) The assembly mode of the pseudopilus: a hallmark to distinguish a novel secretion system subtype. *J Biol Chem* **286:**

24407-16.
Egea, P.F., Shan, S.O., Napetschnig, J., Savage, D.F., Walter, P. and Stroud, R.M. (2004) Substrate twinning activates the signal recognition particle and its receptor. *Nature* **427:** 215-21.
Eisenbrandt, R., Kalkum, M., Lai, E.M., Lurz, R., Kado, C.I. and Lanka, E. (1999) Conjugative pili of IncP plasmids and the Ti plasmid Tpilus are composed of cyclic subunits. *J Biol Chem* **274:** 22548-55.
Emsley, P., Charles, I.G., Fairweather, N.F. and Isaacs, N.W. (1996) Structure of Bordetella pertussis virulence factor P.69 pertactin. *Nature* **381:** 90-2.
Enderle, P.J. and Farwell, M.A. (1998) Electroporation of freshly plated *Escherichia coli* and *Pseudomonas aeruginosa* cells. *Biotechniques* **25:** 954-58.
Enninga, J. and Rosenshine, I. (2009) Imaging the assembly, structure and activity of type III secretion systems. *Cell Microbiol* **11:** 1462-70.
Enos-Berlage, J.L., Guvener, Z.T., Keenan, C.E. and McCarter, L.L (2005) Genetic determinants of biofilm development of opaque and translucent *Vibrio parahaemolyticus*. *Mol Microbiol* **55:** 1160-82.
Erhardt, M., Namba, K. and Hughes, K.T. (2010) Bacterial nanomachines: the flagellum and type III injectisome. *Cold Spring Harb Perspect Biol* **2:** 1-22 (a000299).
Facey, S.J. and Kuhn, A. (2010) Biogenesis of bacterial inner-membrane proteins. *Cell Mol Life Sci* **67:** 2343-62.
Fardini, Y., Trotereau, J., Bottreau, E., Souchard, C., Velge, P. and Virlogeux-Payant. (2009) Investigation of the role of the BAM complex and SurA chaperone in outer-membrane protein biogenesis and type III secretion system expression in *Salmonella*. *Microbiology* **155:** 1613-22.
Faudry, E., Vernier, G., Neumann, E., Forge, V. and Attree, I. (2006) Synergistic pore formation by type III toxin translocators of *Pseudomonas aeruginosa***. 45:** 8117-23.
Federici, L., Du, D., Walas, F., Matsumura, H., Fernandez-Recio, J., McKeegan, K.S. *et al.* (2005) The crystal structure of the outer membrane protein VceC from the bacterial pathogen vibrio cholerae at 18 Å resolution. *J Biol Chem* **280:** 15307-14.
Ferguson, A.D., Amezcua, C.A., Halabi, N.M., Chelliah, Y., Rosen, M.K., Ranganathna, R. *et al.* (2007) Signal transduction pathway of TonB-dependent transporters. *Proc Natl Acad Sci USA* **104:** 513-18.
Ferrandez, Y. and Condemine, G. (2008) Novel mechanism of outer membrane targeting of proteins in Gram-negative bacteria. *Mol Microbiol* **69:** 1349-57.
Fetsch, E.E. and Davidson, A.L. (2002) Vanadate-catalyzed phtocleavage of the signture motif of an ATP-binding cassette (ABC) transporter. *Proc Natl Sci USA* **99:** 9685-90.
Filloux, A. (2004) The underlying mechanisms of type II protein secretion. *Biochim Biophys Acta* **1694:** 163-179.
Filloux, A. (2011) Protein secretion system in Pseudomonas aeruginosa: an essay on diversity, evolution and function. *Front Microbiol* **2:** 1-21 (155).
Francetic, O. and Pugsley, A.P. (1996) The cryptic general secretory pathway (gsp) operon of *Escherichia coli* K-12 encodes functional proteins. *J Bacteriol* **178:** 3544-9.
Francetic, O., Belin, D., Badaut, C. and Pugsley, A.P. (2000) Expression of the endogenous type II secretion pathway in Escherichia coli leads to chitinase secretion. *EMBO J* **19:** 6697-703.
Francetic, O. and Pugsley, A.P. (2005) Towards the identification of type II secretion signals in a nonacylated variant of pullulanase from *Klebsiella oxytoca*. *J Bacteriol* 187: 7045-55.
Francetic, O., Buddelmeijer, N., Lewenza, S., Kumamoto, C.A. and Pugsley, A.P. (2007) Signal recognition particle-dependent inner membrane targeting of the PulG pseudopilin component of a type II secretion system. *J Bacteriol* **189:** 1783-93.
Franza, T., Mahé, B. and Expert, D. (2005) *Erwinia chrysanthemi* requires a second iron transport route dependent of the siderophore achromobactin for extracellular growth and plant infection. *Mol Microbiol* **55:** 261-75.
Fries, M., Ihrig, J., Brocklehurst, K., Shevchik, V. E. and Pickersgill, R. W. (2007) Molecular basis of the activity of the phytopathogen pectin methylesterase. *EMBO J* **26:** 3879-87.
Fronzes, R., Schäfer, E., Wang, L., Saibil, H.R., Orlova, E.V. and Waksman, G. (2009) Structure of a type IV secretion system core complex. *Science* **323:** 266-8.
Forest, K.T. (2008) The type II secretion arrowhead: The structure of GspI-GspJ-GspK. *Nat Struct Mol Biol* **15:** 428-30.
Gatsos, X., Perry, A.J., Anwari, K., Dolezal, P., Wolynec, P.P., Likic, V.A. *et al.* (2008) Protein secretion and outer membrane assembly in *Alphaproteobacteria*. *FEMS Microbiol Rev* **32:** 995-1009.
Genin, S. and Boucher, C.A. (1994) A superfamily of proteins involved in different secretion pathways in gram-negative bacteria: modular structure and specificity of the N-terminal domain. *Mol Gen Genet* **243:** 112-8.
Gérard-Vincent, M., Robert, V., Ball, G., Bleves, S., Michel, G.P., Lazdunski, A. *et al.* (2002) Identification of XcpP domains that confer functionality and specificity to the *Pseudomonas aeruginosa* type II secretion apparatus. *Mol Microbiol* **44:** 1651-65.

Gerlach, R.G. and Hensel, M. (2007) Protein secretion systems and adhesins: the molecular armory of Gram-negative pathogens. *Int J Med Microbiol* **297:** 401-15.

Giltner, C.L., Habash, M. and Burrows, L.L. (2010) *Pseudomonas aeruginosa* minor pilins are incorporated into type IV pili. *J Mol Biol* **398:** 444-61.

Glasner, J.D., Yang, C.H., Reverchon, S., Hugouvieux-Cotte-Pattat, N., Condemine, G., Bohin, J.P. *et al.* (2011) Genome sequence of the plant-pathogenic bacterium Dickeya dadantii 3937. *J Bacteriol* **193:** 2076-7.

Golovanov, A.P., Balasingham, S., Tzitzilonis, C., Goult, B.T., Lian, L.Y., Homberset, H. *et al.* (2006) The solution structure of a domain from the *Neisseria meningitidis* lipoprotein PilP reveals a new beta-sandwich fold. *J Mol Biol* **364:** 186-95.

Gomis-Rüth, F.X., Moncalian, G., Pérez-Luque, R., Gonzalez, A., Cabezon, E., de la Cruz, F. *et al.* (2001) The bacterial conjugation protein TrwB resembles ring helicases and F1-ATPase. *Nature* **409:** 637-41.

Goure, J., Broz, P., Attree, O., Cornelis, G.R. and Attree, I. (2005) Protective anti-V antibodies inhibit Pseudomonas and Yersinia translocon assembly within host membranes. *J Infect Dis* **192:** 218-25.

Greene, N.P., Porcelli, I., Buchanan, G., Hicks, M.G., Schermann, S.M., Palmer, T. *et al.* (2007) Cysteine scanning mutagenesis and disulfide mapping studies of the TatA component of the bacterial twin arginine translocase. *J Biol Chem* **282:** 23937-45.

Guilvout, I., Hardie, K.R., Sauvonnet, N. and Pugsley, A.P. (1999) Genetic dissection of the outer membrane secretin PulD: are there distinct domains for multimerization and secretion specificity? *J Bacteriol* **181:** 7212-20.

Guilvout, I., Chami, M., Engel, A., Pugsley, A.P. and Bayan, N. (2006) Bacterial outer membrane secretin PulD assembles and inserts into the inner membrane in the absence of its pilotin. *EMBO J* **25:** 5241-9.

Guilvout, I., Chami, M., Berrier, C., Ghazi, A., Engel, A., Pugsley, A.P. *et al.* (2008) In vitro multimerization and membrane insertion of bacterial outer membrane secretin PulD. *J Mol Biol* **382:** 13-23.

Guilvout, I., Nickerson, N.N., Chami, M. and Pugsley, A.P. (2011) Multimerization-defective variants of dodecameric secretin PulD. *Res Microbiol* **162:** 180-90.

Gralnick, J. A., Vali, H., Lies, D. P. and Newman, D. K. (2006) Extracellular respiration of dimethyl sulfoxide by *Shewanella oneidensis* strain MR-1. *Proc Natl Acad Sci USA* **103:** 4669-4674.

Gray, M.D., Bagdasarian, M., Hol, W.G. and Sandkvist, M. (2011) In vivo cross-linking of EpsG to EpsL suggests a role for EpsL as an ATPase-pseudopilin coupling protein in the Type II secretion system of *Vibrio cholerae*. *Mol Microbiol* **79:** 786-98.

Gyimesi, G., Ramachandran, S., Kota, P., Dokholyan, N.V., Sarkadi, B. and Hegedus, T. (2011) ATP hydrolysis at one of the two sites in ABC transporters initiates transport related conformational transitions. *Biochim Biophys Acta* **12:** 2954-64.

Hachani, A., Lossi, N.S., Hamilton, A., Jones, C., Bleves, S., Albesa-Jové, D. *et al.* (2011) Type VI secretion system in *Pseudomonas aeruginosa*: secretion and multimerization of VgrG proteins. *J Biol Chem* **286:** 12317-27.

Hager, A.J., Bolton, D.L., Pelletier, M.R., Brittnacher, M.J., Gallagher, L.A., Kaul, R. *et al.* (2006) Type IV pili-mediated secretion modulates Francisella virulence. *Mol Microbiol* **62:** 227-37.

Han, X., Kennan, R.M., Parker, D., Davies, J.K. and Rood, J.I. (2007) Type IV fimbrial biogenesis is required for protease secretion and natural transformation in *Dichelobacter nodosus*. *J Bacteriol* **189:** 5022-33.

Harris, B.Z. and Lim, W.A. (2001) Mechanism and role of PDZ domains in signaling complex assembly. *J Cell Sci* **114:** 3219-31.

Hassan, S. and Hugouvieux-Cotte-Pattat, N. (2011) Identification of two feruloyl esterases in *Dickeya dadantii* 3937 and induction of the major feruloyl esterase and of pectate lyases by ferulic acid. *J Bacteriol* **193:** 963-70.

Hatzixanthis, K., Palmer, T., Sargent, F. (2003) A subset of bacterial inner membrane proteins integrated by the twin-arginine translocase. *Mol Microbiol* **49:** 1377-90.

Hauben, L., Morre, E.R.B., Vauterin, L., Steenackers, M., Mergaert, J., Verdonck, L. *et al.* (1998) Phylogenetic position of phytopathogens within the Enterobacteriaceae. *Syst Appl Microbiol* **21:** 384-397.

Hazes, B. and Frost, L.S. (2008) Towards a systems biology approach to study type II/IV secretion systems. *Biochim Biophys Act* **1778:** 1839-50.

He, S.Y., Lindeberg, M., Chatterjee, A.K. and Collmer, A. (1991) Cloned *Erwinia chrysanthemi* out genes enable *Escherichia coli* to selectively secrete a diverse family of heterologous proteins to its milieu. *Proc Natl Acad Sci USA* **88:** 1079-83.

Heidelberg, J.F., Eisen,J.A., Nelson, W.C., Clayton, R.A., Gwinn, M.L., Dodson, R.J. *et al.* (2000) DNA sequence of both chromosomesof the cholera pathogen *Vibrio cholerae*. *Nature* **406:** 477-83.

Heuck, A., Schleiffer, A., Clausen, T. (2011) Augmenting β-augmentation: structural basis of how BamB binds BamA and may support folding of outer membrane proteins. *J Mol Biol* **406:** 659-66.

Hicks, M.G., de Leeuw, E., Porcelli, I., Buchanan, G., Berks, B.C. and Palmer, T. (2003) The Escherichia coli twin-arginine translocase: conserved residues of TatA and TatB family components involved in protein transport. *FEBS Lett* **539:** 61-7.

Hicks, M.G., Lee, P.A., Georgiou, G., Berks, B.C. and Palmer, T. (2005) Positive selection for loss-of-function tat mutations identifies critical residues required for TatA activity. *J Bacteriol* **187:** 2920-25.

Hillier, B.J., Christopherson, K.S., Prehoda, K.E., Bredt, D.S. and Lim, W.A. (1999) Unexpected modes of PDZ domain scaffolding revealed by structure of nNOS-syntrophin complex. *Science* **284:** 812-15.

Hirst, T.R. and Holmgren, J. (1987) Conformation of protein secreted across bacterial outer membranes: a study of enterotoxin translocation from *Vibrio cholerae*. *Proc NatI Acad Sci USA* **84:** 7418-22.

Hodak, H. and Jacob-Dubuisson, F. (2007) Current challenges in autotransport and two-partner protein secretion pathways. *Res Microbiol* **158:**631-7.

Hodgkinson, J.L., Horsley, A., Stabat, D., Simon, M., Johnson. S., da Fonseca, P.C.A. *et al.* (2009) Three-dimensional reconstruction of the *Shigella* T3SS transmembrane regions reveals 12-fold symmetry and novel features throughout. *Nat Struct Mol Biol* **16:** 477-85.

Holland, I.B., Schmitt, L. and Young, J. (2005) Type I protein secretion in bacteria, the ABC-transporter dependent pathway. *Mol Membr Biol* **22:** 29-39.

Hollenstein, K., Frei, D.C. and Locher, K.P. (2007) Structure of an ABC transporter in complex with its binding protein. *Nature* **446:** 213-6.

Holzapfel, E., Eisner, G., Alami, M., Barrett, C.M., Buchanan, G., Lüke, I. *et al.* (2007) The entire N-terminal half of TatC is involved in twin-arginine precursor binding. *Biochemistry* **46:** 2892-8.

Howard, S.P., Gebhart, C., Langen, G.R., Li, G. and Strozen, T.G. (2006) Interactions between peptidoglycan and the ExeAB complex during assembly of the type II secretin of *Aeromonas hydrophila*. *Mol Microbiol* **59:** 1062-72.

Hugouvieux-Cotte-Pattat, N. and Reverchon, S. (2001) Two transporters, TogT and TogMNAB, are responsible for oligogalacturonide uptake in *Erwinia chrysanthemi 3937*. *Mol Microbiol* **41:** 1125-32.

Hugouvieux-Cotte-Pattat, N., Shevchik, V.E. and Nasser, W. (2002) PehN, a polygalacturonase homologue with a low hydrolase activity, is coregulated with the other *Erwinia chrysanthemi* polygalacturonases. *J Bacteriol* **184:** 2664-73.

Hugouvieux-Cotte-Pattat, N., and Charaoui-Boukerzaza S. (2009) Catabolism of raffinose, sucrose, and melibiose in *Erwinia chrysanthemi* 3937. *J Bacteriol* **191:** 6960-6967.

Hung, A.Y. and Sheng, M. (2002) PDZ domains: structural modules for protein complex assembly. *J Biol Chem* **277:** 5699-702.

Hunt, J.F., Weinkauf, S., Henry, L., Fak, J.J., McNicholas, P., Oliver, D.B. *et al.* (2002) Nucleotide control of interdomain interactions in the conformational reaction cycle of SecA. *Science* **297:** 2018-26.

Ide, T., Laarmann, S., Greune, L., Schillers, H., Oberleithner, H. and Schmidt, M.A. (2001) Characterization of translocation pores inserted into plasma membranes by type III-secreted Esp proteins of enteropathogenic *Escherichia coli*. *Cell Microbiol* **3:** 669-679.

Ieva, R. and Bernstein, H.D. (2009) Interaction of an autotransporter passenger domain with BamA during its translocation across the bacterial outer membrane. *Proc Natl Acad Sci USA* **106:** 19120-5.

Inaba, K. (2009) Disulfide bond formation system in *Escherichia coli*. *J Biochem* **146:** 591-7.

Ito, Y., Kanamaru, K., Taniguchi, N., Miyamoto, S., Tokuda, H. (2006) A novel ligand bound ABC transporter, LolCDE, provides insights into the molecular mechanisms underlying membrane detachment of bacterial lipoproteins. *Mol Microbiol* **62:** 1064-75.

Izoré, T., Job, V. and Dessen, A. (2011) Biogenesis, regulation and targeting of the type III secretion system. *Structure* **19:** 603-12.

Jacob-Dubuisson, F., Fernandez, R. and Coutte, L. (2004) Protein secretion through autotransporter and two-partner pathways. *Biochim Biophys Acta* **1694:** 235-57.

Jain, S., Moscicka, K.B., Bos, M.P., Pachulec, E., Stuart, M.C., Keegstra, W. *et al.* (2011) Structural characterization of outer membrane components of the type IV pili system in pathogenic *Neisseria*. *PLoS One* **6:** 1-11 (e16624).

Jahagirdar, R. and Howard, S.P. (1994) Isolation and characterization of a second exe operon required for extracellular protein secretion in *Aeromonas hydrophila*. *J Bacteriol* **176:** 6819-26.

Jani, A.J. and Cotter, P.A. (2010) Type VI secretion: not just for pathogenesis anymore. *Cell Host Microbe* **8:** 2-6.

Jakubowski, S.J., Krishnamoorthy, V., Cascales, E. and Christie, P.J. (2004) *Agrobacterium tumefaciens* VirB6 domains direct the ordered export of a DNA substrate through a type IV secretion system. J Mol Biol **341:** 961-77.

Jeleń, F., Oleksy, A., Smietana, K. and Otlewski, J. (2003) PDZ domains-common players in the cell signaling. *Acta Biochim Pol* **50:** 985-1017.

Jenkins, J., Shevchik, V.E., Hugouvieux-Cotte-Pattat, N. and Pickersgill RW. (2004) The crystal structure of pectate lyase Pel9A from *Erwinia chrysanthemi*. *J Biol Chem* **279:** 9139-45.

Jobichen, C., Chakraborty, S., Li, M., Zheng, J., Joseph, L., Mok, Y.K. *et al.* (2010) Structural basis for the secretion of EvpC: a key type VI secretion system protein form *Edwardsiella tarda*. *PLoS One* 5: 1-10 (e12910).

Johnson, T.L., Abendroth, J., Hol, W.G. and Sandkvist, M. (2006) Type II secretion: from structure to function. *FEMS Microbiol Lett* **255:** 175-86.

Johnson, T.L., Scott, M.E. and Sandkvist, M. (2007) Mapping critical interactive sites within the periplasmic domain of the *Vibrio cholerae* type II secretion protein EpsM. *J Bacteriol* **189:** 9082-9.

Journet, L., Agrain, C., Broz, P. and Cornelis, G.R. (2003) The needle length of bacterial injectisomes is determined by a molecular ruler. *Science* **302:** 1757-60.

Junker, M., Schuster, C.C., McDonnell, A.V., Sorg, K.A., Finn, M.C., Berger, B. *et al.* (2006) Pertactin β-helix folding mechanism suggests common themes for the secretion and folding of autotransporter proteins. *Proc Natl Acad Sci USA* **103:** 4918-23.

Kajava, A.V. and Steven, A.C. (2006) The turn of the screw: variations of the abundant beta-solenoid motif in passenger domains of Type V secretory proteins. *J Struct Biol* **155:** 306-15.

Kanamaru, S. (2009) Structural similarity of tailed phages and pathogenic bacterial secretion systems. *Proc Natl Acad Sci USA* **106:** 4067-8.

Karuppiah, V., Derrick, J.P. (2011). Structure of the PilM-PilN, inner membrane Type IV pilus biogenesis complex from *Thermus thermophilus*. *J Biol Chem* **286:** 24434-42.

Kaufmann, A., Manting , E.H., Veenendaal, A.K., Driessen, A.J. and van der Does, C. (1999) Cysteine-directed cross-linking demonstrates that helix 3 of SecE is close to helix 2 of SecY and helix 3 of a neighboring SecE. *Biochemistry* **38:** 9115-25.

Kazemi-Pour, N., Condemine, G. and Hugouvieux-Cotte-Pattat, N. (2004) The secretome of the plant pathogenic bacterium *Erwinia chrysanthemi*. *Proteomics* **4:** 3177-86.

Kenjale, R., Wilson, J., Zenk, S.F., Saurya, S., Picking, W.L., Picking, W.D. *et al.* (2005) The needle component of the type III secretion of Shigella regulates the activity of the secretion apparatus. *J Biol Chem* **280:** 42929-37.

Kihara, A., Akiyama, Y. and Ito, K. (1995) FtsH is required for proteolytic elimination of uncomplexed forms of SecY, an essential protein translocase. *Pro Natl Acad Sci USA* **92:**4532-6.

Kim, S., Malinverni, J.C., Sliz, P., Silhavy, T.J., Harrison, S.C. and Kahne, D. (2007) Structure and function of an essential component of the outer membrane protein assembly machine. *Science* **317:** 961-4.

Kim, K.H. and Paetzel, M. (2011) Crystal structure of Escherichia coli BamB, a lipoprotein component of the β-barrel assembly machinery complex. *J Mol Biol* **406:** 667-78.

Kimbrough, T.G. and Miller, S.I. (2002) Assembly of the type III secretion needle complex of *Salmonella typhimurium*. *Microbes Infect/Institut Pasteur* **4:** 75-82.

Kirn, T.J., Lafferty, M.J., Sandoe, C.M. and Taylor, R.K. (2000) Delineation of pilin domains required for bacterial association into microcolonies and intestinal colonization by *Vibrio cholerae*. *Mol Microbiol* **35:** 896-910.

Knoblauch, N.T, Rüdiger, S., Schönfeld, H.J., Driessen, A.J., Schneider-Mergener, J. and Bukau, B. (1999) Substrate specificity of the SecB chaperone. *J Biol Chem* **274:** 34219-25.

Knowles, T.J., Jeeves, M., Bobat, S., Dancea, F., McClelland, D., Palmer, T. *et al.* (2008) Fold and function of polypeptide transport-associated domains responsible for delivering unfolded proteins to membranes. *Mol Microbiol* **68:** 1216-27.

Knowles, T.J., Scott-Tucker, A., Overduin, M. and Henderson, I.R. (2009) Membrane protein architects: the role of the BAM complex in outer membrane protein assembly. *Nat Rev Microbiol* **7:** 206-14.

Kol, S., Majczak, W., Heerlien, R. van der Berg, J.P., Nouwen, N. and Driessen, A.J. (2009) Subunit a of the F(1)F(0) ATP synthase requires YidC and SecYEG form membrane insertion. *J Mol Biol* **390:** 893-901.

Köhler, R., Schäfer, K., Müller, S., Vignon, G., Diederichs, K., Philippsen, A. *et al.* (2004) Structure and assembly of the pseudopilin PulG. *Mol Microbiol* **54:** 647-64.

Koo, J., Tammam, S., Ku, S.Y., Sampaleanu, L.M., Burrows, L.L. and Howell, P.L. (2008) PilF is an outer membrane lipoprotein required for multimerization and localization of the *Pseudomonas aeruginosa* Type IV pilus secretin. *J Bacteriol* **190:** 6961-9.

Koronakis, V., Sharff, A., Koronakis, E., Luisi, B. and Hughes, C. (2000) Crystal structure of the bacterial membrane protein TolC central to multidrug efflux and protein export. *Nature* **405:** 914-9.

Korotkov, K.V., Krumm, B., Bagdasarian, M. and Hol, W.G.J. (2006) Structural and functional studies of EpsC, a crucial component of the type 2 secretion system from *Vibrio cholerae*. *J Mol Biol* **363:** 311-21.

Korotkov, K.V. and Hol, W.G.J. (2008) Structure of the GspK-GspI-GspJ complex from the enterotoxigenic *Escherichia coli* type 2 secretion system. *Nat Struct Mol Biol* **15:** 462-8.

Korotkov, K.V., Pardon, E., Steyaert, J. and Hol, W.G.J. (2009a) Crystal structure of the N-terminal domain of the secretin GspD from ETEC determined with the assistance of a nanobody. *Structure* **17:** 255-65.

Korotkov, K.V., Gray, M.D., Kreger, A., Turley, S., Sandkvist, M. and Hol, W.G.J. (2009b) Calcium is

essential for the major pseudopilin in the type 2 secretion system. *J Biol Chem* **284:** 25466-70.
Korotkov, K.V., Gonen, T. and Hol, W.G.J. (2011a) Secretins: dynamic channels for protein transport across membranes. *Trends Biochem Sci* **36:** 433-43.
Korotkov, K.V., Johnson, T.L., Jobling, M.G., Pruneda, J., Pardon, E., Héroux, A. *et al.* (2011b) Structural and functional studies on the interaction of GspC and GspD in the type II secretion system. *PLoS Pathog* **7:** 1-14 (e1002228).
Krause, S., Barcena, M., Pansegrau, W., Lurz, R., Carazo, J.M. and Lanka, E. (2000) Sequence-related protein export NTPase encoded by the conjugative transfer region of RP4 and by the cag pathogenicity island of helicobacter pylori share similar hexameric ring structures. *Proc Natl Acad Sci USA* **97:** 3067-72.
Kreutzenbeck, P., Kröger, C., Lausberg, F., Blaudeck, N., Sprenger, G.A. and Freudl, R. (2007) *Escherichia coli* twin arginine (Tat) mutant translocases possessing relaxed signal peptide recognition specificities. *J Biol Chem* **282:** 7903-11.
Kuhn, A., Stuart, R., Henry, R. and Dalbey, R.E. (2003) The Alb3/Oxa1/YidC protein family: membrane-localized chaperones facilitating membrane protein insertion? *Trends Cell Biol* **13:** 510-6.
Kuhn, P., Weiche, B., Sturm, L., Sommer, E., Drepper, F., Warscheid, B. *et al.* (2011) The bacterial SRP receptor, SecA and the ribosome use overlapping binding sites on the SecY translocon. *Traffic* **12:** 563-78.
Kuo, W.W., Kuo, H.W., Cheng, C.C., Lai, H.L. and Chen, L.Y. (2005) Roles of the minor pseudopilins, XpsH, XpsI and XpsJ, in the formation of XpsG-containing pseudopilus in *Xanthomonas campestris pv. campestris*. *J Biomed Sci* **12:** 587-99.
Kusters, I. and Driessen, A.J. (2011) SecA, a remarkable nanomachine. *Cell Mol Life Sci* **68:** 2053-66.
Laatu, M. and Condemine, G. (2003) Rhamnogalacturonate lyase RhiE is secreted by the out system in *Erwinia chrysanthemi*. *J Bacteriol* **185:** 1642-9.
Laemmli, U.K. (1970) Cleavage of structural proteins during assembly of the head of bacteriophage T4. *Nature* **227:** 680-5.
La Pointe, C. F. and Taylor, R. K. (2000) The type 4 prepilin peptidases comprise a novel family of aspartic acid proteases. *J Biol Chem* **275:** 1502-10.
Lam, A.Y., Pardon, E., Korotkov, K.V., Hol, W.G.J. and Steyaert, J. (2009) Nanobody-aided structure determination of the EpsI:EpsJ pseudopilin heterodimer from Vibrio vulnificus. *J Struct Biol* **166:** 8-15.
Lazar Adler, N.R., Stevens, J.M., Stevens, M.P. and Galyov, E.E. (2011) Autotransporters and their role in the virulence of *Burkholderia pseudomallei* and *Burkholderia mallei*. *Front Microbiol* **2:** 1-7 (151).
Laurent, F., Kotoujansky, A., Labesse, G. and Bertheau, Y. (1993) Characterization and overexpression of the pem gene encoding pectin methylesterase of *Erwinia chrysanthemi* strain 3937. *Gene* **131:** 17-25.
Lee, H.M., Wang, K.C., Liu, Y.L., Yew, H.Y., Chen, L.Y., Leu *et al.* (2000), Association of the cytoplasmic membrane protein XpsN with the outer membrane protein XpsD in the type II protein secretion apparatus of *Xanthomonas campestris pv. campestris*. *J Bacteriol* **182:** 1549-57.
Lee, H.M., Tyan, S.W., Leu, W.M., Chen, L.Y., Chen, D.C. and Hu, N.T. (2001) Involvement of the XpsN protein in formation of the XpsL-XpsM complex in *Xanthomonas campestris pv. campestris* type II secretion apparatus. *J Bacteriol* **183:** 528-35.
Lee, H.M., Chen, J.R., Lee, H.L., Leu, W.M., Chen, L.Y. and Hu, N.T. (2004) Functional dissection of the XpsN (GspC) protein of the *Xanthomonas campestris pv. campestris* type II secretion machinery. *J Bacteriol* **186:** 2946-55.
Lee, M.S., Chen, L.Y., Leu, W.M., Shiau, R.J. and Hu, N.T. (2005) Associations of the major pseudopilin XpsG with XpsN (GspC) and secretin XpsD of *Xanthomonas campestris pv. campestris* type II secretion apparatus revealed by cross-linking analysis. *J Biol Chem* **280:** 4585-91.
Lee, P.A., Tullman-Ercek, D. and Georgiou, G. (2006) The bacterial twin-arginine translocation pathway. *Annu Rev Microbiol* **60:** 373-95.
Lehr, U., Schütz, M., Oberhettinger, P., Ruiz-Perez, F., Donald, J.W., Palmer, T. *et al.* (2010) C-terminal amino acid residues of the trimeric autotransporter adhesin YadA of Yersinia enterocolitica are decisive for its recognition and assembly by BamA. *Mol Microbiol* **78:** 932-46.
Leiman, P.G., Basler, M., Ramagopal, U.A., Bonanno, J.B., Sauder, J.M., Pukatzki, S. *et al.* (2009) Type VI secretion apparatus and phage tail-associated protein complexes share a common evolutionary origin. *Proc Natl Acad Sci USA* **106:**4154-9.
Létoffé, S. and Wandersman, S. (1992) Secretion of CyaA-PrtB and HlyA-PrtB fusion proteins in *Escherichia coli*: involvement of the glycine-rich repeat domain *of Erwinia chrysanthemi* protease B. *J Bacteriol* **174:** 4920-7.
Lewenza, S., Vidal-Ingigliardi, D. and Pugsley, A.P. (2006) Direct visualization of red fluorescent lipoproteins indicates conservation of the membrane sorting rules in the family Enterobacteriaceae. *J Bacteriol* **188:** 3516-24.
Li, G. and Howard, S. P. (2010) ExeA binds to peptidoglycan and forms a multimer for assembly of the type

II secretion apparatus in *Aeromonas hydrophila*. *Mol Microbiol* **76:** 772-81.
Lietzke, S.E., Yoder, M.D., Keen, N.T. and Jurnak, F. (1994) The three-dimensional structure of pectate lyase E, a plant virulence factor from *Erwinia chrysanthemi*. *Plant Physiol* **106:** 849-62.
Lill, R., Dowhan, W. and Wickner, W. (1990) The ATPase activity of SecA is regulated by acidic phospholipids, SecY and the leader and mature domains of precursor proteins. *Cell* **60:** 271-80.
Lindeberg, M., Salmond, G.P.C. and Collmer, A. (1996) Complementation of deletion mutants in a cloned functional cluster of *Erwinia chrysanthemi out* genes with *Erwinia carotovora out* homologues reveals OutC and OutD as candidate gatekeepers of species-specific secretion of proteins via the type II pathway. *Mol Microbiol* **20:** 175-90.
Lindeberg, M., Boyd, C.M., Keen, N.T. and Collmer, A. (1998) External loops at the C terminus of *Erwinia chrysanthemi* pectate lyase C are required for species-specific secretion through the out type II pathway. *J Bacteriol* **180:** 1431-7.
Lobedanz, S., Bokma, E., Symmons, M.F., Koronakis, E., Hughes, C. and Koronakis, V. (2007) A periplasmic coiled-coil interface underlying TolC recruitment and the assembly of bacterial drug efflux pumps. *Proc Natl Acad Sci USA* **104:** 4612-7.
Login, F.H. and Shevchik, V.E. (2006) The single transmembrane segment drives self-assembly of OutC and the formation of a functional type II secretion system in *Erwinia chrysanthemi. J Biol Chem* 281: 33152-62.
Login, F.H. (2007) Etude fonctionnelle et structurale de la protéine OutC, un composant du système de sécretion de type II de la bactérie phytopathogène *Erwinia chrysanthemi*. Thèse. Université Claude Bernard Lyon 1.
Login, F.H., Fries, M., Wang, X., Pickersgill, R. W. and Shevchik, V. E. (2010) A 20-residue peptide of the inner membrane protein OutC mediates interaction with two distinct sites of the outer membrane secretin OutD and is essential for the functional type II secretion system in *Erwinia chrysanthemi*. *Mol Microbiol* **76:** 944-55.
Lossi, N.S., Dajani, R., Freemont, P. and Filloux, A. (2011) Structure-function analysis of HsiF, a gp25-like component of the type VI secretion system in *Pseudomonas aeruginosa*. *Microbiology* (in press).
Lu, H.M. and Lory, S. (1996) A specific targeting domain in mature exotoxin A is required for its extracellular secretion from *Pseudomonas aeruginosa*. *EMBO J* **15:** 429-36.
Lybarger, S.R., Johnson, T.L., Gray, M.D., Sikora, A.E. and Sandkvist, M. (2009) Docking and assembly of the type II secretion complex of Vibrio cholerae. *J Bacteriol* **191:** 3149-61.
Lynch, B.A. and Koshland, D.E. Jr. (1991) Disulfide cross-linking studies of the transmembrane regions of the aspartate sensory receptor of *Escherichia coli*. *Proc. Natl Acad. Sci. USA*, **88:** 10402-6.
Lyskowski, A., Leo, J.C. and Goldman, A. (2011) Structure and biology of trimeric autotransporter adhesins. *Adv Exp Med Biol* **725:** 143-58.
Ma, L.S., Lin, J.S. and Lai, E.M. (2009b) An IcmF family protein, ImpLM, is an integral inner membrane protein interacting with ImpKL and its walker a motif is required for type VI secretion system-mediated Hcp secretion in Agrobacterium tumefaciens. *J Bacteriol* **191:** 4316-29.
Manting, E.H., van der Does, C., Remigy, H., Engel, A. and Driessen, A.J.M. (2000) SecYEG assembles into a tetramer to form the active protein translocation channel. *EMBO J* **19:** 852-61.
Masi, M. and Wandersman, C. (2010) Multiple signals direct the assembly and function of a type I secretion system. *J Bacteriol* **192:** 3861-9.
Matteï, P.J., Faudry, E., Job, V., Izoré, T., Attree, I. and Dessen, A. (2011) Membrane targeting and pore formation by the type III secretion system translocon. *FEBS J* **278:** 414-26.
Maurer, C., Panahandeh, S., Jungkamp, A.C., Moser, M. and Müller, M. (2010) TatB Functions as an Oligomeric Binding Site for Folded Tat Precursor Proteins. *Mol Biol Cell* **21:** 4151-61.
McDevitt, C.A., Buchanan, G., Sargent, F., Palmer, T. and Berks, B.C. (2006) Subunit composition and in vivo substrate-binding characteristics of Escherichia coli Tat protein complexes expressed at native levels. *FEBS J* **273:** 5656-68.
Meng, G., Surana, N.K., St Geme, J.W 3rd. and Waksman, G. (2006) Structure of the outer membrane translocator domain of the Haemophilus influenzae Hia trimeric autotransporter. *EMBO J* **25:** 2297-304.
Michel, G., Bleves, S., Ball, G., Lazdunski, A. and Filloux, A. (1998) Mutual stabilization of the XcpZ and XcpY components of the secretory apparatus in *Pseudomonas aeruginosa*. *Microbiology* **144:** 3379-86.
Michel, G.P.F., Durand, E. and Filloux, A. (2007) XphA/XqhA, a novel GspCD subunit for type II secretion in *Pseudomonas aeruginosa*. *J Bacteriol* **189:** 3776-83.
Mikolosko, J., Bobyk, k., Zgurskaya, H.I. and Ghosh, P. (2006) Conformational flexibility in the multidrug efflux system protein AcrA. *Structure* **14:** 577-87.
Misra, R. (2007) First glimpse of the crystal structure of YaeT's POTRA domains. *ACS chem Biol* **2:** 649-651.

Mitra, K., Schaffitzel, C., Shaikh, T., Tama, F., Jenni, S., Brooks III *et al.* (2005) Structure of the *E. coli* protein-conducting channel bound to a translating ribosome. *Nature* **438:** 318-24.

Mogensen, J.E. and Otzen, D.E. (2005) Interactions between folding factors and bacterial outer membrane proteins. *Mol Microbiol* **57:** 326-46.

Morand, P.C., Bille, E., Morelle, S., Eugène, E., Beretti, J.L., Wolfgang, M. *et al.* (2004) Type IV pilus retraction in pathogenic *Neisseria* is regulated by the PilC proteins. *EMBO J* **23:** 2009-17.

Moraes, T.F., Spreter, T. and Strynadka, N.C. (2008) Piecing together the type III injectisome of bacterial pathogens. *Curr Opin Struct Biol* **18:** 258-66.

Mougous, J.D., Cuff, M.E., Raunser, S., Shen, A., Zhou, M., Gifford, C.A. *et al.* (2006) A virulence locus of Pseudomonas aeruginosa encodes a protein secretion apparatus. *Science*, **312:** 1526-30.

Mudrak, B. and Kuehn, M.J. (2010) Specificity of the type II secretion systems of enterotoxigenic *Escherichia coli* and *Vivrio cholerae* for heat-labile enterotoxin and cholera toxin. *J Bacteriol* **192:** 1902-11.

Mueller, C.A., Broz, P. and Cornelis, G.R. (2008) The type III secretion system tip complex and translocon. *Mol Microbiol* **68:** 1085-95.

Müller, M., Koch, H.G., Beck, K. and Schäfer, U. (2001) Protein traffic in bacteria: multiple routes from the ribosome to and across the membrane. *Prog Nucleic Acid Res Mol Biol* **66:** 107-57.

Müller, M. (2005) Twin-arginine-specific protein export in *Escherichia coli*. *Res Microbiol* **156:** 131-6.

Nagamori, S., Nishiyama, K. and Tokuda, H. (2002) Membrane topology inversion of SecG detected by labeling with a membrane-impermeable sulfhydryl reagent that causes a close association of SecG with SecA. *J Biochem* **132:** 629-34.

Nakamoto, H. and Bardwell, J.C. (2004) Catalysis of disulfide bond formation and isomerization in the *Esherichia coli* periplasm. *Biochim Biophys Acta* **1694:** 111-9.

Narita, S. and Tokuda, H. (2007) Amino acids at positions 3 and 4 determine the membrane specificity of *Pseudomonas aeruginosa* lipoproteins. *J Biol Chem* **282:** 13372-8.

Nasser, W., Shevchik, V. E. and Hugouvieux-Cotte-Pattat, N. (1999) Analysis of three clustered polygalacturonase genes in *Erwinia chrysanthemi* 3937 revealed an anti-repressor function for the PecS regulator. *Mol Microbiol* **34:** 641-50.

Natale, P., Brüser, T. and Driessen, A.J.M. (2008) Sec- and Tat-mediated protein secretion across the bacterial cytoplasmic membrane-distinct translocases and mechanisms. *Biochim Biophys Acta* **1778:** 1735-56.

Nickerson, N.N., Tosi, T., Dessen, A., Baron, B., Raynal, B., England, P. *et al.* (2011). Outer membrane targeting of secretin PulD relies on disordered domain recognition by a dedicated chaperone. *J Biol Chem* **286:** 38833-43.

Nguyen, H.A., Kaneko, J. and Kamio, Y. (2002) Temperature-dependant production of carotovoricin Er and pectin lyase in phytopathogenic *Erwinia carotovora* subsp. carotovora Er. *Biosci Biotech Biochem*. **66:** 444-7.

Noinaj, N., Guillier, M., Barnard, T.J. and Buchanan, S.K. (2010) TonB-dependent transporters: regulation, structure and function. *Annu Rev Microbiol* **64:** 43-60.

Norman, C., Vidal, S. and Palva, E.T. (1999) Oligogalacturonide-mediated induction of gene involved in jasmonic acid synthesis in response to the cell-wall-degrading enzymes of the plant pathogen *Erwinia carotovora*. *Mol Plant Microbe Interact* **12:** 640-4.

Nouwen, N., Ranson, N., Saibil, H., Wolpensinger, B., Engel, A., Ghazi, A. *et al.* (1999) Secretin PulD: association with pilot PulS, structure and ion-conducting channel formation. *Proc Natl Acad Sci USA* **96:** 8173-7.

Nouwen, N., Stahlberg, H., Pugsley, A. P. and Engel, A. (2000) Domain structure of secretin PulD revealed by limited proteolysis and electron microscopy. *EMBO J* **19:** 2229-36.

Nouwen, N. and Driessen, A.J. (2002) SecDFyajC forms a heterotetrameric complex with YidC. *Mol Microbiol* **44:** 1397-405.

Nudlemen, E., Wall, D. and Kaiser, D. (2006). Polar assembly of the type IV pilus secretin in *Myxicoccus xanthus*. *Mol Microbiol* **60:** 16-29.

Nummelin, H., Merckel, M.C., Leo, J.C., Lankinen, H., Skurnik, M. and Goldman, A. (2004) The *Yersinia* adhesin YadA collagen-binding domain structure is a novel left-handed parallel β-roll. *EMBO J* **23:** 701-11.

Oates, J., Barrett, C.M. L., Barnett, J.P., Byrne, K.G., Bolhuis, A. and Robinson, C. (2005) The Escherichia coli twin-arginine translocation apparatus incorporates a distinct form of TatABC complex, spectrum of modular TatA complexes and minor TatAB complex. *J Mol Biol* **346**: 295-305.

Obsborn, M. J., Gander, J. E., Parisi, E. and Garson, J. (1972) Mechanism of assembly of the outer membrane of *Salmonella typhimurium*. *J Biol Chem* **247:** 3962-72.

Okinaka, Y., Yang, C.H., Perna, N. T. and Keen, N.T. (2002) Microarray profiling of Erwinia chrysanthemi 3937 genes that are regulated during plant infection. *Mol Plant Microbe Interact* **15:** 619-29.

Okon, M., Moraes, T.F., Lario, P.I., Creagh, A.L., Haynes, C.A., Strynadka, N.C. and Mclntosh, L.P (2008) Structural characterization of the type-III pilot-secretin complex from *Shigella flexneri*. *Structure* **16:** 1544-54.

Oomen, C.J., Van Ulsen, P., Van Gelder, P., Feijen, M., Tommassen, J. and Gros, P (2004) Structure of the translocator domain of a bacterial autotransporter. *EMBO J* **23:**1257-66.

Opalka, N., Beckmann, R., Boisset, N., Simon, M.N., Russel, M. and Darst, S.A. (2003) Structure of the filamentous phage pIV multimer by cryo-electron microscopy. *J Mol Biol* **325:** 461-70.

Orriss, G.L., Tarry, M.J., Ize, B., Sargent, F., Lea, S.M., Palmer, T., Berks, B.C. (2007) TatBC, TatB and TatC form structurally autonomous units within the twin arginine protein transport system of *Escherichia coli*. *FEBS Lett* **581:** 4091-7.

Osborne, A.R., Clemons, W.M., Jr and Rapoport, T.A. (2004) A large conformational change of the translocation ATPase SecA. *Proc Natl Acad Sci USA* **101:** 10937-42.

Otto, B.R., Sijbrandi, R., Luirink, J., Oudega, B., Heddle, J.G., Mizutani, K. *et al.* (2005) Crystal structure of hemoglobin protease, a heme binding autotransporter protein form pathogenic *Escherichia coli*. *J Biol Chem* **280:** 17339-45.

Palacios, J.L., Zaror, I., Martinez, P., Uribe, F., Opazo, P., Socias, T. *et al.* (2001) Subset of hybrid eukaryotic proteins is exported by the type I secretion system of *Erwinia chrysanthemi*. *J Bacteriol* **183:** 1346-58.

Palmer, T., Sargent, F. and Berks, B.C. (2005) Export of complex cofactor-containing proteins by the bacterial Tat pathway. *Trends Microbiol* **13:** 175-80.

Palomäki, T., Pickersgill, R., Riekki, R., Romantschuk, M. and Saarilahti, H.T. (2002) A putative three-dimensional targeting motif of polygalacturonase (PehA), a protein secreted through the type II (GSP) pathway in *Erwinia carotovora*. *Mol Microbiol* **43:** 585-96.

Papanikolau, Y., Papadovasilaki, M., Ravelli, R.B., McCarthy, A.A., Cusack, S., Economou, A. *et al.* (2007) Structure of dimeric SecA, the *Escherichia coli* preprotein translocase motor. *J Mol Biol* **366:** 1545-57.

Patrick, M., Korotkov, K.V., Hol, W.G., Sandkvist, M. (2011) Oligomerization of EpsE coordinates residues from multiple subunits to facilitate ATPase activity. *J Biol Chem* **286:** 10378-86.

Peabody, C.R., Chung, Y.J., Yen, M.R., Vidal-Ingigliardi, D., Pugsley, A.P. and Saier, M.H. (2003) Type II protein secretion and its relationship to bacterial type IV pili and archaeal flagella. *Microbiology* **149:** 3051-72.

Pei, X.Y., Hinchliffe, P., Symmons, M.F., Koronakis, E., Benz, R., Hughes, C. and Koronakis, V. (2011) Structures of sequential open states in a symmetrical opening transition of the TolC exit duct. *Proc Natl Acad Sci USA* **108:** 2112-7.

Pelicic, V. (2008) Type IV pili: e pluribus unum? *Mol Microbiol* **68 :** 827-37.

Peng, Q., Yang, S.H., Charkowski, A.O., Yap, M.N., Steeber, D.A., Keen, N.T., *et al*. (2006) Population behavior analysis of dspE and pelD regulation in *Erwinia chrysanthemi 3937*. *Mol Plant Microbe Interact* **19:** 451-7.

Pérombelon, M.C.M. and Kelman, A. (1980) Ecology of soft rot erwinias. *Ann. Rev. Phytopathol*. **18:** 361-387.

Pérombelon, M.C.M., Lumb, V.M. and Zutra, D. (1987) Pathogenicty of soft rot erwinias to potato plants in Scotland and Israel. *J Appl Bacteriol*. **63:** 73-84.

Pérombelon, M.C.M. and Salmond, G.P.C. (1995) Bacterial soft rots. in pathogenesis and host specificity in plant diseases, Vol.1. Prokaryotes (Singh, U.S., Singh, R.P and Kohmoto, K., eds), pp. 1-20. Oxford, UK: pergamon.

Pickersgill, R., Smith, D., Worboys, K. and Jenkins, J. (1998) Crystal structure of polygalacturonase from *Erwinia carotovora ssp. carotovora. J Biol Chem* **273:** 24660-4.

Plé, S., Job, V., Dessen, A. and Attree, I. (2010) Cochaperone interactions in export of the type III needle component PscF of Pseudomonas aeruginosa. *J Bacteriol* **192:** 3801-8.

Planet, P.J., Kachlany, S.C., DeSalle, R. and Figurski, D.H. (2001) Phylogeny of genes for secretion NTPases: identification of the widespread tadA subfamily and development of a diagnostic key for gene classification. *Proc Natl Acad Sci USA* **98:** 2503-8.

Possot, O.M. and Pugsley, A.P. (1997) The conserved tetracysteine motif in the general secretory pathway component PulE is required for efficient pullulanase secretion. *Gene* **192:** 45-50.

Possot, O.M., Gérard-Vincent, M. and Pugsley, A.P. (1999) Membrane association and multimerization of secreton component pulC. *J Bacteriol* **181:** 4004-11.

Possot, O.M., Vignon, G., Bomchil, N., Ebel, F. and Pugsley, A.P. (2000) Multiple interactions between pullulanase secreton components involved in stabilization and cytoplasmic membrane association of PulE. *J Bacteriol* **182:** 2142-52.

Poyraz, O., Schmidt, H., Seidel, K., Delissen, F., Ader, C., Tenenboim, H. *et al.* (2010) Protein refolding is required for assembly of the type three secretion needle. *Nat Struct Mol Biol* **17:** 788-92.

Procko, E., O'Mara, M.L., Bennett, W.F.D., Tieleman, D.P. and Gaudet, R. (2009) The mechanism of ABC

transporters: general lessons from structural and functional studies of an antigenic peptide transporter. *FASEB J* **23:** 1287-302.

Pugsley, A.P. (1993) The complete general secretory pathway in gram-negative bacteria. *Microbiol Rev* **57:** 50-108.

Pukatzki, S., Ma, A.T., Revel, A.T., Sturtevant, D. and Mekalanos, J.J. (2007) Type VI secretion system translocates a phage tail spike-like protein into target cells where it cross-links actin. *Proc Natl Acad Sci USA* **104:** 15508-13.

Pukatzki, S., McAuley, S.B. and Miyata, S.T. (2009) The type VI secretion system: translocation of effectors and effector-domains. *Curr Opin Microbiol* **12:** 11-7.

Py, B., Loiseau, L. and Barras, F. (1999) Assembly of the type II secretion machinery of *Erwinia chrysanthemi*: direct interaction and associated conformational change between OutE, the putative ATP-binding component and the membrane protein OutL. *J Mol Biol* **289:** 659-70.

Py, B., Chippaux, M. and Barras, F. (1993) Mutagenesis of cellulase EGZ for studying the general protein secretory pathway in *Erwinia chrysanthemi*. *Mol Microbiol* **7:** 785-93.

Py, B., Loiseau, L. and Barras, F. (2001) An inner membrane platform in the type II secretion machinery of Gram-negative bacteria. *EMBO Rep* **2:** 244-8.

Pugsley, A.P. (1992) Translocation of a folded protein across the outer membrane in *Escherichia coli*. *Proc Natl Acad Sci USA* **89:** 12058-62.

Pugsley, A.P., Bayan, N. and Sauvonnet, N. (2001) Disulfide bond formation in secreton component PulK provides a possible explanation for the role of DsbA in pullulanase secretion. *J Bacteriol* **183:** 1312-9.

Rabel, C., Grahn, A.M., Lurz, R. and Lanka, E. (2003) The VirB4 family of proposed traffic nucleoside triphosphatases: common motifs in plasmid RP4 TrbE are essential for conjugation and phage adsorption. *J Bacteriol* **185:** 1045-58.

Randall, L.L., Hardy, S.J., Topping, T.B., Smith, V.F., Bruce, J.E. and Smith, R.D. (1998) The interaction between the chaperone SecB and its ligands: evidence for multiple subsites for binding. *Protein Sci* **7:** 2384-90.

Randall, L.L. and Hardy, S.J. (2002) SecB, one small chaperone in the complex milieu of the cell. *Cell Mol Life Sci* **59:**1617-23.

Randall, L.L. and Henzl, M.T. (2010) Direct identification of the site of binding on the chaperone SecB for the amino terminus of the translocon motor SecA. *Protein Sci* **19:** 1173-9.

Reeves, P.J., Douglas, P. and Salmond, G.P. (1994) beta-Lactamase topology probe analysis of the OutO NMePhe peptidase and six other Out protein components of the *Erwinia carotovora* general secretion pathway apparatus. *Mol Microbiol* **12:** 445-57.

Remaut, H. and Waksman, G. (2006) Protein-protein interaction through beta-strand addition. *Trends Biochem Sci* **31:** 436-44.

Reichow, S.L., Korotkov, K.V., Hol, W.G. and Gonen, T. (2010) Structure of the cholera toxin secretion channel in its closed state. *Nat Struct Mol Biol*. **17:** 1226-32.

Reichow, S.L., Korotkov, K.V., Gonen, M., Sun, J., Delarosa, R.J., Hol, W.G. *et al.* (2011) The binding of cholera toxin to the periplasmic vestibule of the type II secretion channel. *Channels (Austin)* **5:** 215-8.

Rico, A.I., Garcia-Ovalle, M., Mingorance, J. and Vincent, M. (2004) Role of two essential domains of *Escherichia coli* FtsA in localizsation and progression of the division ring. *Mol Microbiol* **53:** 1359-1371.

Ried, J.L. and Collmer, A. (1987) An *nptI-sacB-sacR* cartridge for constructing directed, unmarked mutations in Gram-negative bacteria by marker exchange-eviction mutagenesis. *Gene*, **57:** 239-46.

Robert, V., Hayes, F., Lazdunski, A. and Michel, G.P.F. (2002) Identification of XcpZ domains required for assembly of the secreton of *Pseudomonas aeruginosa*. *J Bacteriol* **184:** 1779-82.

Robert, V., Filloux, A. and Michel, G.P.F. (2005) Role of XcpP in the functionality of the Pseudomonas aeruginosa secreton. *Res Microbiol* **156:** 880-6.

Robert, V., Volokhina, E.B., Senf, F., Bos, M.P., Van Gelder, P. and Tommassen, J. (2006) Assembly factor Omp85 recognizes its outer membrane protein substrates by a species-specific C-terminal moti. *PLoS Biol* **4:** 1984-95.

Robert-Baudouy, J., Nasser, W., Condemine, G., Reverchon, S., Shevchik, V.E. and Hugouvieux-Cotte-Pattat, N. (2000) Pectic enzymes of *Erwinia chrysanthemi*, regulation and role in pathogenesis. *Plant-Microbe Interact* **5:** 221-269.

Robien, M.A., Krumm, B.E., Sandkvist, M. and Hol, W.G.J. (2003) Crystal structure of the extracellular protein secretion NTPase EpsE of *Vibrio cholerae*. *J Mol Biol* **333:** 657-74.

Robinson, C., Matos, C.F., Beck, D., Ren, C., Lawrence, J., Vasisht, N. *et al.* (2011) Transport and proofreading of proteins by the twin-arginine translocation (Tat) system in bacteria. *Biochim Biophys Acta* **1808:** 876-84.

Rodrigue, A., Chanal, A., Beck, K., Müller, M., Wu, L.F. (1999) Co-translocation of a periplasmic

enzyme complex by a hitchhiker mechanism through the bacterial tat pathway. *J Biol Chem* **274:** 13223-8.

Ruiz-Perze, F., Henderson, I.R., Leyton, D.L., Rossiter, A.E., Zhang, Y. and Nataro, J.P. (2009) Roles of periplasmic chaperone proteins in the biogenesis of serine protease autotransporters of Enterobacteriaceae. *J Bacteriol* **191:** 6571-83.

Sambrook, J., Fritsch, E.F. and Maniatis, T. (1989) Molecular Cloning: A Laboratory Manual. Cold Spring Harbor, NY: Cold Spring Harbor Laboratory Press.

Samson, R., Legendre, J. B., Christen, R., Saux, M. F.L., Achouak, W. and Gardan, L. (2005) Transfer of Pectobacterium chrysanthemi (Burkholder *et al.* 1953) Brenner *et al.* 1973 and *Brenneria paradisiaca* to the genus *Dickeya* gen. nov. as *Dickeya chrysanthemi* comb. nov. and *Dickeya paradisiaca* comb. nov. and delineation of four novel species, *Dickeya dadantii* sp. nov., *Dickeya dianthicola* sp. nov., *Dickeya dieffenbachiae* sp. nov. and *Dickeya zeae* sp. nov. *Int J Syst Evol Microbiol* **55:** 1415-27.

Sampaleanu, L.M., Bonanno, J.B., Ayers, M., Koo, J., Tammam, S., Burley, S.K. *et al.* (2009) Periplasmic domains of *Pseudomonas aeruginosa* PilN and PilO form a stable heterodimeric complex. *J Mol Biol* **394:** 143-59.

Samuelson, J.C., Chen, M., Jiang, F., Möller, I., Wiedmann, M., Kuhn, A. *et al.* (2000) YidC mediates membrane protein insertion in bacteria. *Nature* **406:** 637-41.

Sankaran, K. and Wu, H.C. (1994) Lipid modification of bacterial prolipoprotein. Transfer of diacylglyceryl moiety from phosphatidylglycerol. *J Biol Chem* **269:** 19701-6.

Sandkvist, M., Hough, L.P., Bagdasarian, M.M. and Bagdasarian, M. (1999) Direct interaction of the EpsL and EpsM proteins of the general secretion apparatus in *Vibrio cholerae*. *J Bacteriol* **181:** 3129-35.

Sandkvist, M. (2001) Type II secretion and pathogenesis. *Infect Immun* **69:** 3523-35.

Sandoval, C.M., Baker, S.L., Jansen, K., Metzner, S.I. and Sousa, M.C. (2011) Crystal structure of BamD: an essential component of the β-Barrel assembly machinery of gram-negative bacteria. *J Mol Biol* **409:** 348-57.

Sargent, F., Gohlke, U., De Leeuw, E., Stanley, N.R., Palmer, T., Saibil, H.R. *et al.* (2001) Purified components of the *Escherichia coli* Tat protein transport system form a double-layered ring structure. *Eur J Biochem* **268:** 3361-7.

Sauri, A., Soprova, Z., Wickström, D., De Gier, J.W., van der Schors, R.C., Smit, A.B. *et al.* (2009) The Bam (Omp85) complex is involved in secretion of the autotransporter haemoglobin protease. *Microbiology*, **155:** 3982-91.

Sauvonnet, N. and Pugsley, A.P. (1996) Identification of two regions of *Klebsiella oxytoca* pullulanase that together are capable of promoting beta-lactamase secretion by the general secretory pathway. *Mol Microbiol* **22:** 1-7.

Sauvonnet, N., Vignon, G., Pugsley, A.P. and Gounon, P. (2000) Pilus formation and protein secretion by the same machinery in *Escherichia coli*. *EMBO J* **19:** 2221-28.

Savvides, S.N., Yeo, H.J., Beck, M.R., Blaesing, F., Lurz, R., Lanka, E. *et al.* (2003) VirB11 ATPase are dynamic hexameric assemblies: new insights into bacterial type IV secretion. *EMBO J* **22:** 1969-80.

Schägge, H. (2006) Tricine–SDS-PAGE. *Nature Protocols* **1:** 16-22.

Schaffitzel, C., Oswald, M., Berger, I., Ishikawa, T., Abrahams, J.P., Koerten, H.K. *et al.* (2006) Structure of the *E. coli* signal recognition particle bound to a translating ribosome. *Nature* **444:** 503-6.

Scheuring, J., Braun, N., Nothdurft, L., Stumpf, M., Veenendaal, A.K., Kol, S. *et al.* (2005) The oligomeric distribution of SecYEG is altered by SecA and translocation ligands. *J Mol Biol* **354:** 258-71.

Schmidt, S.A., Bieber, D., Ramer, S.W., Hwang, J., Wu, C.Y. and Schoolnik, G. (2001) Structure-function analysis of BfpB, a secretin-like protein encoded by the bundle-forming-pilus operon of enteropathogenic *Escherichia coli*. *J Bacteriol* **183:** 4848-59.

Schoehn, G., Di Guilmi, A.M., Lemaire, D., Attree, I., Weissenhorn, W. and Dessen, A. (2003) Oligomerization of type III secretion proteins PopB and PopD precedes pore formation in Pseudomonas. *EMBO J* **22:** 4957-67.

Schoenhofen, I.C., Stratilo, C. and Howard, S.P. (1998) An ExeAB complex in the type II secretion pathway of Aeromonas hydrophila: effect of ATP-binding cassette mutations on complex formation and function. *Mol Microbiol* **29:** 1237-47.

Schoenhofen, I.C., Li, G., Strozen, T.G. and Howard, S.P. (2005) Purification and characterization of the N-terminal domain of ExeA: a novel ATPase involved in the type II secretion pathway of *Aeromonas hydrophila*. *J Bacteriol* **187:** 6370-78.

Schraidt, O., Lefebre, M.D., Brunner, M.J., Schmied, W.H., Schmidt, A., Radics, J. *et al.* (2010) Topology and organization of the *Salmonella typhimurium* type III secretion needle complex components. *PloS Pathog* **6:** 1-12 (e1000824).

Schraidt, O. and Marlovits, T.C. (2011) Three-dimensional model of Salmonella's needle complex at subnanometer resolution. *Science* **331:** 1192-5.

Schulein, R., Guye, P., Rhomberg, T.A., Schmid, M.C., Schroder, G., Vergunst, A.C. et al. (2005) A bipartite signal mediates the transfer of type IV secretion substrates of *Bartonella henselae* into human cells. *Proc Natl Acad Sci USA* **102:** 856-61.

Schwarz, S., Hood, R.D. and Mougous, J.D. (2010) What is type VI secretion doing in all those bugs? *Trends Microbiol* **18:** 531-7.

Scott, M.E., Dossani, Z.Y. and Sandkvist, M. (2001) Directed polar secretion of protease from single cells of Vibrio cholerae via the type II secretion pathway. *Proc Natl Acad Sci USA* **98:**13978-83.

Serek, J., Bauer-Manz, G., Struhalla, G., van den Berg, L., Kiefer, D., Dalbey, R. *et al.* (2004) *Escherichia coli* YidC is a membrane insertase for Sec-independent proteins. *EMBO J* **23:** 294-301.

Sexton, J.A., Miller, J.L., Yoneda, A., Kehl-Fie, T.E. and Vogel, J.P. (2004) Legionella pneumophila DotU and IcmF are required for stability of the Dot/Icm complex. *Infect Immun* **72:** 5983-92.

Sharma, V., Arockiasamy, A., Ronning, D.R., Savva, C.G., Holzenburg, A., Braunstein, M. *et al.* (2003) Crystal structure of Mycobacterium tuberculosis SecA, a preprotein translocating ATPase. *Pro Natl Acad Sci USA* **100:** 2243-8.

Shevchik, V.E., Bortoli-German I., Robert-Baudouy, J., Robinet, S., Barras, F. and Condemine G. (1995) Differential effect of dsbA and dsbC mutations on extracellular enzyme secretion in *Erwinia chrysanthemi*. *Mol Microbiol* **16:** 745-53.

Shevchik, V.E., Condemine, G., Cotte-Pattat, N.H. and Robert-Baudouy, J. (1996) Characterization of pectin methylesterase B, an outer membrane lipoprotein of *Erwinia chrysanthemi* 3937. *Mol Microbiol* **19:** 455-66.

Shevchik, V.E., Robert-Baudouy, J. and Condemine, G. (1997) Specific interaction between OutD, an Erwinia chrysanthemi outer membrane protein of the general secretory pathway and secreted proteins. *EMBO J* **16:** 3007-16

Shevchik, V.E. and Hugouvieux-Cotte-Pattat, N (1997) Identification of a bacterial pectin acetyl esterase in *Erwinia chrysanthemi* 3937. *Mol Microbiol* **24:** 1285-301.

Shevchik, V.E. and Condemine, G. (1998) Functional characterization of the *Erwinia chrysanthemi* OutS protein, an element of a type II secretion system. *Microbiology* **144:** 3219-28.

Shevchik, V.E., Kester, H.C., Benen, J.A., Visser, J., Robert-Baudouy, J. and Hugouvieux-Cotte-Pattat, N. (1999a) Characterization of the exopolygalacturonate lyase PelX of *Erwinia chrysanthemi* 3937. *J Bacteriol* **181:** 1652-63.

Shevchik, V.E., Condemine, G., Robert-Baudouy, J. and Hugouvieux-Cotte-Pattat, N. (1999b) The exopolygalacturonate lyase PelW and the oligogalacturonate lyase Ogl, two cytoplasmic enzymes of pectin catabolism in *Erwinia chrysanthemi* 3937. *J Bacteriol* **181:** 3912-9.

Shevchik, V.E. and Hugouvieux-Cotte-Pattat, N (2003) PaeX, a second pectin acetylesterase of *Erwinia chrysanthemi* 3937. *J Bacteriol* **185:** 3091-100.

Shiue, S.J., Kao, K.M., Leu, W.M., Chen, L.Y., Chan, N.L. and Hu, N.T. (2006) XpsE oligomerization triggered by ATP binding, not hydrolysis, leads to its association with XpsL. *EMBO J* **25:** 1426-35.

Shiue, S.J., Chien, I.L., Chan, N.L., Leu, W.M. and Hu, N.T. (2007) Mutation of a key residue in the type II secretion system ATPase uncouples ATP hydrolysis from protein translocation. *Mol Microbiol* **65:** 401-12.

Sklar, J.G., Wu, T., Gronenberg, L.S., Malinverni, J.C., Kahne, D. and Silhavy, T.J. (2007a) Lipoprotein SmpA is a component of the YaeT complex that assembles outer membrane proteins in *Escherichia coli*. *Proc Natl Acad Sci USA* **104:**6400-5.

Sklar, J.G., Wu, T., Kahne, D. and Silhavy, T.J. (2007b) Defining the roles of the periplasmic chaperones SurA, Skp and DegP in *Escherichia coli*. *Genes Dev* **21:** 2473-84.

Shruthi, H., Anand, P., Murugan, V. and Sankaran, K. (2010) Twin arginine translocase pathway and fast-folding lipoprotein biosynthesis in *E. coli*: interesting implications and applications. *Mol Biosyst* **6:** 999-1007.

Sorg, I., Wagner, S., Amstutz, M., Muller, S.A., Broz, P., Lussi, Y. *et al.* (2007) YscU recognizes translocators as export substrates of the *Yersinia* injectisome. *EMBO J* **26:** 3015-24.

Spagnuolo, J., Opalka, N., Wen, W.X., Gagic, D., Chabaud, E., Bellini, P. *et al.* (2010) Identification of the gate regions in the primary structure of the secretin pIV. *Mol Microbiol* **76:** 133-50.

Spreter, T., Yip, C.K., Sanowar, S., André. I., Kimbrough, T.G., Vuckovic, M. *et al.* (2009) A conserved structural motif mediates formation of the periplasmic rings in the type III secretion system. *Nat Struct Mol Biol* **16:** 468-76.

Strauch, E.M. and Georgiou, G. (2007) *Escherichia coli* tatC mutations that suppress defective twin-arginine transporter signal peptides. *J Mol Biol* **374:** 283-91.

Strom, M.S. and Lory, S. (1993) structure-function and biogenesis of the type IV pili. *Annu Rev Microbiol* **47:** 565-96.

Strozen, T.G., Stanley, H., Gu, Y., Boyd, J., Bagdasarian, M., Sandkvist, M. *et al.* (2011) Involvement of the GspAB complex in assembly of the type II secretion system secretin of *Aeromonas* and *Vibrio*

species. *J Bacteriol* **193:** 2322-31.
Symmons, M.F., Bokma, E., Koronakis, E., Hughes, C. and Koronakis, V. (2009) The assembled structure of a complete tripartite bacterial multidrug efflux pump. *Proc Natl Acad Sci USA* **106:** 7173-8.
Tamano, K., Aizawa, S., Katayama, E., Nonaka, T., Imajoh-Ohmi, S., Kuwae, A. *et al.* (2000) Supramolecular structure of the Shigella type III secretion machinery: the needle part is changeable in length and essential for delivery of effectors. *EMBO J* **19:** 3876-87.
Tanaka, S.Y., Narita, S. and Tokuda, H. (2007) Characterization of the *Pseudomonas aeruginosa* Lol system as a lipoprotein sorting mechanism. *J Biol Chem* **282:** 13379-84.
Tato, I., Matilla, I., Arechaga, I., Zunzunegui, S., de la Cruz, F. and Cabezon, E. (2007) The ATPase activity of the DNA transporter TrwB is modulated by protein TrwA: implications for a common assembly mechanism of DNA translocating motors. *J Biol Chem* **282:** 25569-76.
Terradot, L., Bayliss, R., Oomen, C., Leonard, G.A., Baron, C. and Waksman, G. (2005) Structure of two core subunits of the bacterial type IV secretion system, VirB8 from *Brucella suis* and ComB10 from *Helicobacterpylori*. *Proc Natl Acad Sci USA* **102:** 4596-601.
Thomas, J. D., Reeves, P.J. and Salmond, G.P. (1997) The general secretion pathway of *Erwinia carotovora subsp*. *carotovora*: analysis of the membrane topology of OutC and OutF. *Microbiology* **143:**713-20.
Thomas, L.M., Doan, C.N., Oliver, R.L. and Yoder, M.D. (2002) Structure of pectate lyase A: comparison to other isoforms. *Acta Crystallogr D Biol Crystallogr* **58:** 1008-15.
Tommassen, J. (2010) Assembly of outer-membrane proteins in bacteria and mitochondria. *Microbiology* **156:** 2587-96.
Tomkiewicz, D., Nouwen, N. and Driessen, A.J. (2008) Kinetics and energetics of the translocation of maltose binding protein folding mutants. *J Mol Biol* **377:** 83-90.
Tokuda, H. and Matsuyama, S. (2004) Sorting of lipoproteins to the outer membrane in *E. coli*. *Biochim Biophys Acta* **1694:** IN1-9.
Toth, I.K., Bell, K.S., Holeva, M.C. and Birch, P.R. (2003) Soft rot erwiniae: from genes to genomes. *Mol Plant Pathol* **4:** 17-30.
Toth, I.K., Pritchard, L. and Birch, P.R.J. (2006) Comparative genomics reveals what makes an enterobacterial plant pathogen. *Annu Rev Phytopathol* **44:** 305-36.
Toth, I.K., van der Wolf, J.M., Saddler, G., Lojkowska, E., Hélias, V., Pirhonen, M. *et al.* (2011) Dickeya species: an emerging problem for potato production in Europe. *Plant Pathol*. **60:** 385-99.
Trindade, M.B., Job, V., Contreras-Martel C., Pelicic, V. and Dessen, A (2008) Structure of a widely conserved type IV pilus biogenesis factor that affects the stability of secretin multimers. *J Mol Biol* **378:** 1031-9.
Tsai, R.T., Leu, W.M., Chen, L.Y. and Hu, N.T. (2002) A reversibly dissociable ternary complex formed by XpsL, XpsM and XpsN of the *Xanthomonas campestris pv. campestris* type II secretion apparatus. *Biochem J* **367:** 865-71.
Tsukazaki, T., Mori, H., Echizen, Y., Ishitani, R., Fukai, S., Tanaka, T. *et al.* (2011) Structure and function of a membrane component SecDF that enhances protein export. *Nature* **474:** 235-8.
Tullman-Ercek, D., DeLisa, M.P., Kawarasaki, Y., Iranpour, P., Ribnicky, B., Palmer, T. *et al.* (2007) Export pathway selectivity of *Escherichia coli* twin arginine translocation signal peptides. *J Biol Chem*. **282:** 8309-16.
Tuteja, R. (2005) Type I signal peptidase: an overview. *Arch Biochem Biophys* **441:** 107-11.
Tziatzios, C., Schubert, D., Lotz, M., Gundogan, D., Betz, H., Schägger, H. *et al.* (2004) The bacterial protein-translocation complex: SecYEG dimers associate with one or two SecA molecules. *J Mol Biol* **340:** 513-24.
Urban, A., Leipelt, M., Eggert, T. and Jaeger, K.E. (2001) DsbA and DsbC affect extracellular enzyme formation in *Psudomonas aeruginosa*. *J Bacteriol* **183:** 587-96.
Van den Ent, F. and Löwe, J. (2000) Crystal structure of the cell division protein FtsA from *Thermotoga maritima*. *EMBO J* **19:** 5300-7.
van der Sluis, E.O., van der Vries, E., Berrelkamp, G., Nouwen, N. and Driessen, A.J. (2006) Topologically fixed SecG is fully functional. *J Bacteriol* **188:** 1188-90.
van Ulsen, P. and Tommassen, J. (2006) Protein secretion and secreted proteins in pathogenic *Neisseriaceae*. *FEMS Microbiol Rev* **30:** 292-319.
van Ulsen, P. (2011) Protein folding in bacterial adhesion: secretion and folding of classical monomeic autotransporters. *Adv Exp Med Biol* **715:** 125-42.
Valverde, R., Edwards, L. and Regan, L. (2008) Structure and function of KH domains. *FEBS J* **275:** 2712-26.
Vassylyev, D.G., Mori, H., Vassylyeva, M.N., Tsukazaki, T., Kimura,Y., Tahirov , T.H. *et al.* (2006) Crystal structure of the translocation ATPase SecA from Thermus Thermophilus reveals a parallel, head-to-head dimer. *J Mol Biol* **364:** 248-58.
Veenendaal, A.K., van der Does, C. and Driessen, A.J. (2001) Mapping the sites of interaction between

SecY and SecE by cysteine scanning mutagenesis. *J Biol Chem* **276:** 32559-66.
Veenendaal, A.K., van der Does, C. and Driessen, A.J. (2002) The core of the bacterial translocase harbors a tilted transmembrane segment 3 of SecE. *J Biol Chem* **277:** 36640-5.
Viarre, V., Cascales, E., Ball, G., Michel G.P., Filloux, A. and Voulhoux, R. (2009) HxcQ liposecretin is self-piloted to the outer membrane by its N-terminal lipid anchor. *J Biol Chem* **284:** 33815-23.
Vignon, G., Köhler, R., Larquet, E., Giroux, S., Prévost, M.C., Roux, P. *et al.* (2003) Type IV-like pili formed by the type II secreton: specificity, composition, bundling, polar localization and surface presentation of peptides. *J Bacteriol* **185:** 3416-28.
Volokhina, E.B., Beckers, F., Tommassen, J. and Bos, M.P. (2009) The beta-barrel outer membrane protein assembly complex of Neisseria meningitidis. *J Bacteriol* **191:** 7074-85.
von Heijne, G. (2006) Membrane-protein topology. *Nat Rev Mol Cell Biol* **7:** 909-18.
Voulhoux, R., Ball, G., Ize, B., Vasil, M.L., Lazdunski, A., Wu, L.F. *et al.* (2001) Involvement of the twin-arginine translocation system in protein secretion via the type II pathway. *EMBO J* **20:** 6735-41.
Voulhoux, R., Bos, M. P., Geurtsen, J., Mols, M. and Tommassen, J. (2003) Role of a highly conserved bacterial protein in outer membrane protein assembly. *Science* **299:** 262-65.
Vuong, P., Bennion, D., Mantei, J., Frost, D. and Misra, R. (2008) Analysis of YfgL and YaeT interactions through bioinformatics, mutagenesis and biochemistry. *J Bacteriol* **190:** 1507-17.
Wallden, K., Rivera-Calzada, A. and Waksman, G. (2010) Type IV secretion systems: versatility and diversity in function. *Cell Microbiol* **12:** 1203-12.
Wagner, S., Sorg, I., Degiacomi, M., Journet, L., Dal Peraro, M. and Cornelis, G.R. (2009) The helical content of the YscP molecular ruler determines the length of the Yersinia injectisome. *Mol Microbiol* **71:** 692-701.
Wagner, S., Königsmaier, L., Lara-Tejero, M., Lefebre, M., Marlovits, T.C. and Galan, J.E. (2010) Organization and coordinated assembly of the type III secretion export apparatus. *Proc Natl Acad Sci USA* **107:** 17745-50.
Waksman, G. and Fronzes, R. (2010) Molecular architecture of bacterial type IV secretion systems. *Trends Biochem Sci* **35:** 691-8.
Waldee, E.L. (1945) Comparative studies of some peritrichous phytopathogenic bacteria. *Iowa State J Sci* **19:** 435-84.
Watson, A.A., Alm, R.A. and Mattick, J.S. (1996) Identification of a gene, pilF, required for type 4 fimbrial biogenesis and twitching motility in *Pseudomonas aeruginosa*. *Gene* **180:** 49-56.
Werner, J. and Misra, R. (2005) YaeT (Omp85) affects the assembly of lipid-dependent and lipid-independent outer membrane proteins of Escherichia coli. *Mol Microbiol* **57:** 1450-9.
Willats, W.G., McCartney, L., Mackie, W. and Knox, J.P. (2001) Pectin: cell biology and prospects for functional analysis. *Plant Mol Biol* **47:** 9-27.
Winterfeld, S., Imhof, N., Roos, T., Bär, G., Kuhn, A. and Gerken, U. (2009) Substrate-induced conformational change of the Escherichia coli membrane insertase YidC. *Biochemistry* **48:** 6684-91.
Worrall, L.J., Lameignere, E. and Strynadka, N.C. (2011) Structural overview of the bacterial injectisome. *Curr Opin Microbiol* **14:** 3-8.
Wu, T., Malinverni, J., Ruiz, N., Kim, S., Silhavy, T.J. and Kahne, D. (2005) Identification of a multicomponent complex required for outer membrane biogenesis in *Escherichia coli*. *Cell* **121:** 235-245. Xu, Y., Sim, S.H., Nam, K.H., Jin, X.L., Kim, H.M., Hwang, K.Y. *et al.* (2009) Crystal structure of the periplasmic region of MacB, a noncanonic ABC transporter. *Biochemistry* **48:** 5218-25.
Xu, Y., Sim, S.H., Song, S., Piao, S., Kim, H.M., Jin, X.L. *et al.* (2010) The tip region of the MacA alpha-hairpin is important for the binding to TolC to the Escherichia coli MacAB-TolC pump. *Biochem Biophys Res Commun*. **394:** 962-5.
Yanez, M.E., Korotkov, K.V., Abendroth, J. and Hol, W.G.J. (2008a) The crystal structure of a binary complex of two pseudopilins: EpsI and EpsJ from the type 2 secretion system of *Vibrio vulnificus*. *J Mol Biol* **375:** 471-86.
Yanez, M.E., Korotkov, K.V., Abendroth, J. and Hol, W.G.J. (2008b) Structure of the minor pseudopilin EpsH from the Type 2 secretion system of *Vibrio cholerae*. *J Mol Biol* **377:** 91-103.
Yen, M.R., Peabod, C.R., Partovi, S.M., Zhai, Y., Tseng, Y.H. and Saier, M.H (2002) Protein-translocating outer membrane porins of Gram-negative bacteria. *Biochim Biophys Acta* **1562:** 6-31.
Yeo, H.J., Savvides, S.N., Herr, A.B., Lanka, E. and Waksman, G. (2000) Crystal structure of the hexameric traffic ATPase of the helicobacter pylori type IV secretion system. *Mol Cell* **6:** 1461-72.
Yeo, H.J., Yuan, Q., Beck, M.R., Baron, C. and Waksman, G. (2003) Structural and functional characterization of the VirB5 protein from the type IV secretion system encoded by the conjugative plasmid pKM101. *Proc Natl Acad Sci USA* **100:** 15947-52.
Yeo, H.J., Cotter, S.E., Laarmann, S., Juehne, T., St Geme III J.W. and Waksman, G. (2004) Structural basis for host recognition by the Haemophilus influenzae Hia autotransporter. *EMBO J* **23:** 1245-56.
Yeo, H.J., Yokoyama, T., Walkiewicz, K., Kim, Y., Grass, S. and Geme, J,W 3rd. (2007) The structure of the

Haemophilus influenzae HMW1 pro-piece reveals a structural domain essential for bacterial two-partner secretion. *J Biol Chem* **282:** 31076-84.

Yoder, M.D., Lietzke, S.E. and Jurnak, F (1993) Unusual structural features in the parallel beta-helix in pectate lyases. *Structure* **15:** 241-51.

Young, J.M., Dye, D.W., Bradbury, J.F., Panagopoulos, C.G. and Robbs, C.F. (1978) A proposed nomenclature and classification for plant-pathogenic bacteria. *N Z J Agric Res* **21:** 153-77.

Yum, S., Xu, Y., Piao, S., Sim, S.H., Kim, H.M., Jo, W.S. *et al.* (2009) Crystal structure of the periplasmic component of a tripartite macrolide-specific efflux pump. *J Mol Biol* **387:** 1286-97.

Zaitseva, J., Jenewein, S., Wiedenmann, A., Benabdelhak, H., Holland, I.B. and Schmitt, L. (2005a) Functional characterization and ATP-induced dimerization of the isolated ABC-domain of the haemolysin B transporter. *Biochemistry* **44:** 9680-90.

Zaitseva, J., Jenewein, S., Oswald, C., Jumpertz, T., Holland, I.B. and Schmitt, L. (2005b) A molecular understanding of the catalytic cycle of the nucleotide-binding domain of the ABC transporter HlyB. *Biochem Soc Trans* **33:** 990-5.

Zaitseva, J., Oswald, C., Jumpertz, T., Jenewein, S., Wiedenmann, A., Holland *et al.* (2006) A structural analysis of asymmetry required for catalytic activity of an ABC-ATPase domain dimer. *EMBO J* **25:** 3432-43.

Zheng, J., Ho, B. and Mekalanos, J.J. (2011) Genetic analysis of anti-amoebae and anti-bacterial activities of the type VI secretion system in *Vibrio cholerae*. *PloS One* **6:** 1-12 (e23876).

Zhou, J. and Xu, Z. (2005) The structural view of bacterial translocation-specific chaperone SecB: implications for function. *Mol Microbiol* **58**: 349-57.

Zhou, S., Yomano, L.P., Saleh, A.Z., Davis, F.C., Aldrich, H.C. and Ingram, L.O. (1999) Enhancement of expression and apparent secretion of *Erwinia chrysanthemi* endoglucanase (encoded by celZ) in *Escherichia coli* B. *Appl Environ Microbiol* **65:** 2439-45.

Zhou, S. and Ingram, L.O. (2000) Synergistic hydrolysis of carboxymethyl cellulose and acid-swollen cellulose by two endoglucanases (CelZ and CelY) from *Erwinia chrysanthemi*. *J Bacteriol* **182:** 5676-82.

Zimmer, J., Nam, Y. and Rapoport, T.A. (2008) Structure of a complex of the ATPase SecA and the protein-translocation channel. *Nature* **455:** 936-43.

Zipfel, C., Robatzek, S., Navarro, L., Oakeley, E.J., Jones, J.D., Felix, G. and Boller, T. (2004) Bacterial disease resistance in Arabidopsis through flagellin perception. *Nature* **428:** 764-7.

Yang, C.H., Gavilanes-Ruiz, M., Okinaka, Y., Vedel, R., Berthuy, I., Boccara, M. *et al.* (2002) hrp genes of *Erwinia chrysanthemi* 3937 are important virulence factors. *Mol Plant Microbe interact* **15:** 472-80.